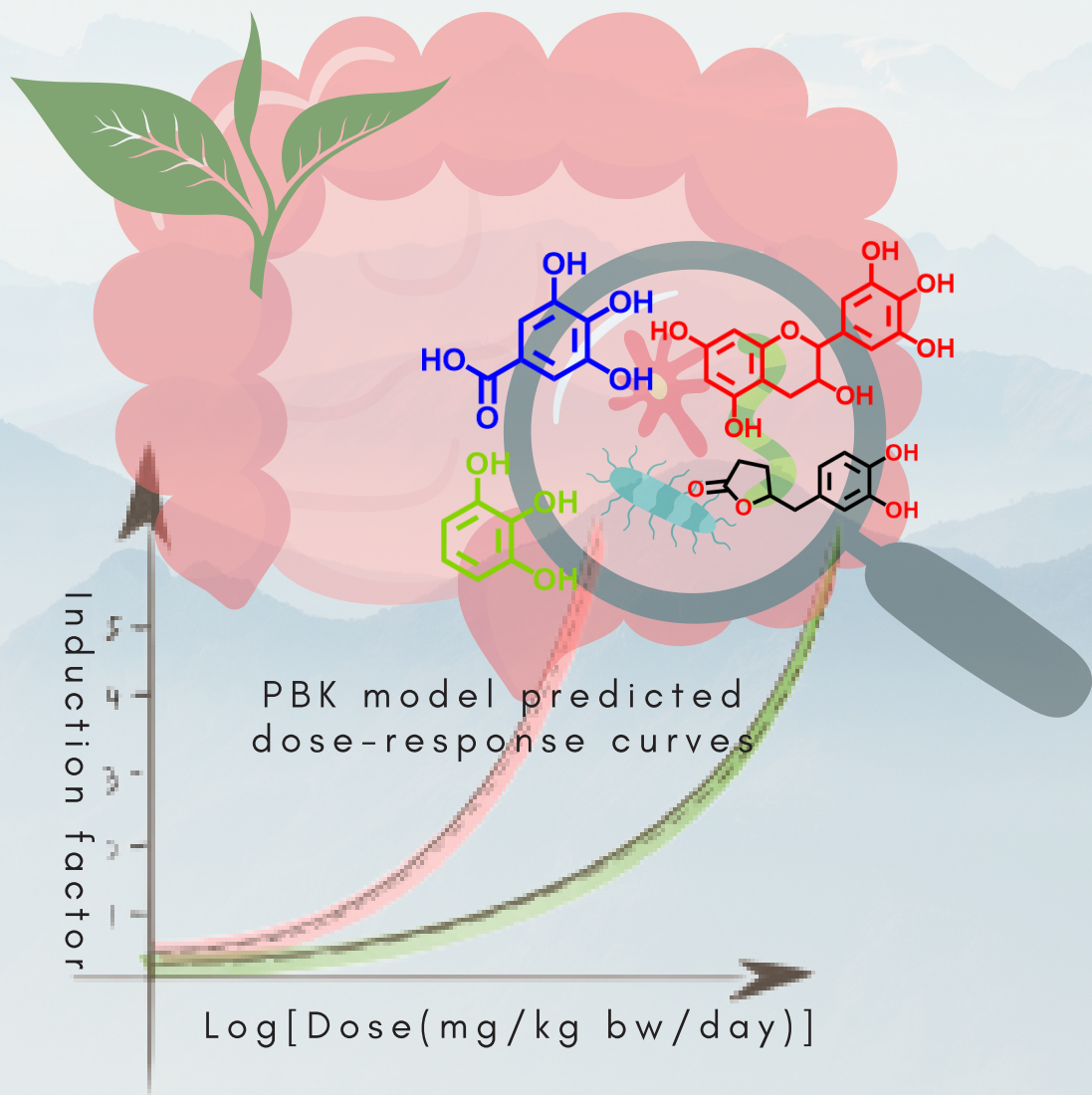# Influence of human intestinal microbial metabolism on the induction of Nrf2 signaling by green tea catechins as characterized by new approach methodologies (NAMs)

PBK model predicted dose-response curves

OH
OH
HO
OH
O

OH
OH
HO
OH
OH
O
OH

OH
OH
OH

O
O
OH
OH

Induction factor

5
4
3
2
1

Log[Dose(mg/kg bw/day)]

Chen Liu

刘臣

Propositions

1. Gut microbial metabolites of green tea catechins contribute to their biological effects.

(this thesis)

2. Physiologically based kinetic (PBK) modelling combined with in vitro bioassays can elucidate the in vivo effects of green tea catechins without the need for animal or human intervention studies.

(this thesis)

3. Transgenic crops provide an effective way to reduce the application of chemical pesticides.

4. The COVID-19 pandemic reduces the anthropogenic disturbances of both wildlife and environment.

5. Unconditional support from the family paves the way for a PhD degree.

6. Do not be scared of starting in a new field as self-learning should be a lifetime activity.

Propositions belonging to the thesis, entitled

Influence of human intestinal microbial metabolism on the induction of Nrf2 signaling by green tea catechins as characterized by new approach methodologies (NAMs)

Chen Liu

Wageningen, 17 June 2022

Influence of human intestinal microbial metabolism on the induction of Nrf2 signaling by green tea catechins as characterized by new approach methodologies (NAMs)

Chen Liu

Thesis committee

Promotor

Prof. Dr I.M.C.M Rietjens
Professor of Toxicology
Wageningen University & Research

Co-promotor

Dr Jacques Vervoort
Associate Professor, Laboratory of Biochemistry
Wageningen University & Research

Other members

Prof. Dr J.Keijer, Wageningen University & Research
Dr G.J.E.J. Hooiveld, Wageningen University & Research
Prof. Dr G. Williamson, Monash University, Melbourne, Australia
Prof. Dr G.R.M.M Haenen, Maastricht University

Influence of human intestinal microbial metabolism on the induction of Nrf2 signaling by green tea catechins as characterized by new approach methodologies (NAMs)

Chen Liu

Thesis

submitted in fulfilment of the requirements for the degree of doctor

at Wageningen University

by the authority of the Rector Magnificus,

Prof. Dr A.P.J. Mol,

in the presence of the

Thesis Committee appointed by the Academic Board

to be defended in public

on Friday 17 June 2022

at 11 a.m. in the Omnia Auditorium.

Table of Contents

Chapter 1

General introduction

1.1 Introduction and aim of the present thesis

Green tea is mainly manufactured from buds and leaves of *Camellia sinensis*. It originated in China and has been spread worldwide, becoming one of the most popular beverages that is welcomed both by Asian and Western cultures nowadays.[1] Typical processing steps during green tea production consist of partial withering, steaming, rolling, drying and the final firing, in which the steaming step is of importance for maintaining the flavan-3-ols content of green tea.[2] The high temperature during steaming inactivates the enzymatic activity of polyphenol oxidase and peroxidase thus preventing the oxidation of monomeric flavan-3-ols.[3-4] The chemical composition of green tea is complicated, consisting of polyphenols, proteins (enzymes), amino acids, carbohydrates, lipids, vitamins, sterols, caffeine, minerals, volatiles, etc.[2] Among all these constituents the polyphenolic compounds are dominant, comprising 30 - 42% of the dry weight of the leaves. Especially flavan-3-ols (catechins) are the representative polyphenols in green tea, accounting for up to 30% of the total dry weight.[3-5] The main catechins found in green tea are (-)-epigallocatechin gallate (EGCG), (-)-epigallocatechin (EGC), (-)-epicatechin gallate (ECG) and (-)-epicatechin (EC) (Figure 1).[4, 6] EGCG is the most abundant catechin, making up 48 - 55% of the total catechin constituents.[7] To illustrate this major contribution of EGCG, Figure 2 presents a chromatogram from a green tea water extract.
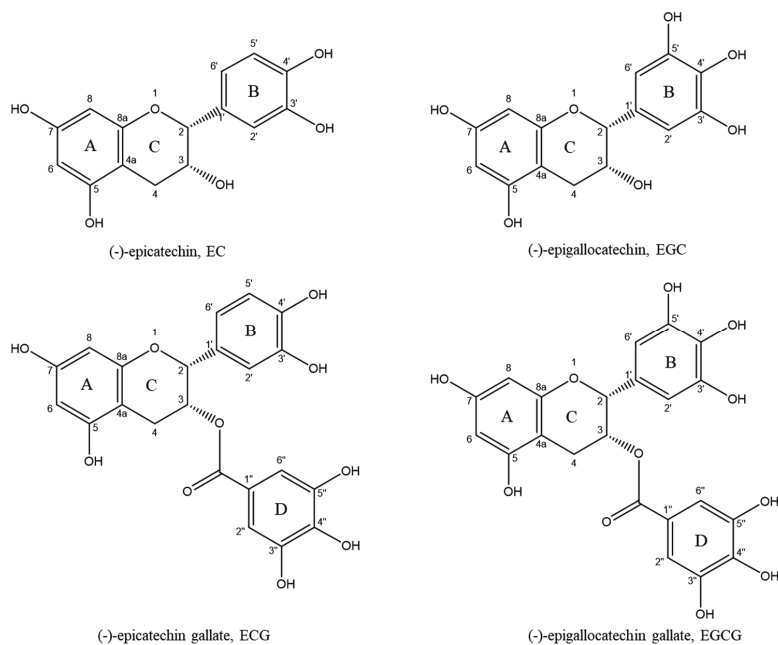

Figure 1. Chemical structures of the principal catechins in green tea (*Camellia sinensis*).

Daily intake of catechins via consumption of green tea has been associated with various health benefits, such as reduced risk of cardiovascular diseases, and anti-diabetes and anti-cancer effects.[8-10] However, the bioavailability of catechins is general low.[3] After ingestion of green tea or green tea catechins, only a small portion of the catechins is directly absorbed in the small intestinal tract while the majority reaches the large intestine where it is degraded by intestinal microbiota.[11-12] The bioavailability and resulting plasma concentrations of the microbial metabolites formed in the large intestine are often higher than those of the parent compounds, suggesting a potential role for these microbial catechin metabolites in the biological activities associated with green tea (catechins) consumption.[13-14]

The possible modes of actions underlying the health-promoting effects of catechins are mostly studied using either *in vitro* cell-based models or *in vivo* laboratory animal studies. The former often overlook the potential contribution of metabolites which may also induce biological activities, and especially the metabolic capacity of the intestinal microbiome is generally entirely ignored. Despite its non-human nature, the intestinal microbiome plays an important role in the health of the human host, among others by metabolizing xenobiotic substances and thereby changing host exposure to those xenobiotics and their metabolites.[15-16] Furthermore, *in vivo* studies using laboratory animals are considered costly, time-consuming, unethical, and not always adequately representing the human physiological situation.[17] Therefore, developing a combined *in vitro* and physiologically based kinetic (PBK) modelling approach that includes gut microbial metabolism could provide a novel tool to characterize the microbial metabolism of tea catechins *in vivo*, e.g. include the microbial metabolism of flavan-3-ols in the colon, and predict systemic exposure of the host to both the parent compound and its metabolites.[18]

The aim of the present thesis was to obtain better insights into human intestinal microbiota-mediated conversion of model green tea catechins, including the intra- and inter-individual variability, by using an *in vitro* anaerobic fecal incubation model, and to identify the activity of the formed microbial metabolites in the activation of Nrf2-EpRE-mediated gene expression a potential mode of action underlying the beneficial health effects. Furthermore, the thesis also aimed to build a PBK model including gut microbial metabolism for the most abundant and bioactive catechin, EGCG, and to use a PBK modelling-based reverse dosimetry approach to extrapolate the *in vitro* concentration-response curve from U2OS-Nrf2 CALUX reporter gene assays to *in vivo* dose-response curves for Nrf2 activation in human. This latter strategy will provide a new approach methodology (NAM) to evaluate whether at realistic daily intake levels Nrf2 mediated health effects are to be expected without the need for a human intervention study.
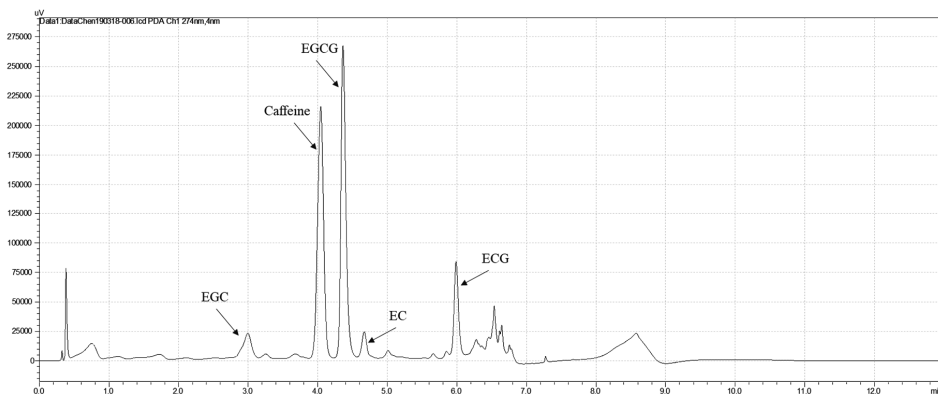
Figure 2. UHPLC chromatograms of green tea water extracts.

1.2 The model compounds of the present thesis: green tea catechins

As mentioned above, the most abundant constituent in green tea leaves are catechins, especially EC, that represents approximately 6.4% of the total catechins; EGC (19% approximately); ECG (13.6% approximately); and EGCG (59% approximately).[2] Figure 1. already showed the chemical structures of the four catechins. These catechins share a similar C_6-C_3-C_6 diphenylpropanoid skeleton, also known as a backbone comprising an A ring and a B ring that are connected by a heterocyclic C ring (Figure 1). EC has an ortho-dihydroxyl group at the 3' and 4' position of the B-ring, and a hydroxyl group at the 3 position on the C ring. EGC differs from EC in that it has three hydroxyl groups at the 3', 4', and 5' positions of the B ring. ECG and EGCG are ester derivatives of EC and EGC, respectively, formed through gallate moiety esterification at the hydroxyl moiety of carbon 3 on the C ring (Figure 1).

1.3 Modulation of Kelch-like ECH-associated protein 1/Nuclear factor E2-related factor 2 (Keap1/Nrf2) system by green tea catechins

Green tea has been considered a traditional Chinese medicine and a healthful beverage since ancient times.[1] Nowadays, green tea catechins have become one of the most promising dietary supplements.[19] Various health-promoting effects have been ascribed to green tea catechins, such as antioxidant, antimutagenic, anticarcinogenic, anti-hypertensive activities, reduced risk of cardiovascular disease, solar ultraviolet protection, antibacterial and antiviral effects, etc.[6, 20-24] The modes of action behind these beneficial effects can be complicated and have not been fully elucidated, although the Kelch-like ECH-associated protein 1/Nuclear factor E2-related factor 2 (Keap1/Nrf2) regulatory network has been reported to play a role.[25-26] The Keap1/Nrf2 system

and its different modes of regulation, especially its regulation by catechins, will be introduced in the following section.

1.3.1 Keap1/Nrf2 regulatory system

1.3.1.1 Nrf2

The antioxidant response element (ARE) also known as the electrophile response element (EpRE) often locates at the promoter region of antioxidant genes and detoxification genes. Nrf2 was firstly confirmed by Itoch et al. to be an essential transcription factor for ARE/EpRE that mediates phase 2 enzyme expression in 1997.[27] Since then, it opened a door in toxicology which attracts continuous attention from researchers all over the world for discovering the regulatory mechanisms of numerous defensive and adaptive biological process.

Nrf2 is a 605- amino acid protein encoded by the gene nuclear factor, erythroid 2 like 2 (Nfe2l2). It belongs to the Cap "n" collar (CNC) subfamily of basic region leucine zipper (bZIP) transcription factors together with nuclear factor erythroid-derived 2 (Nfe2), Nrf1, Nrf3, Bach1 and Bach2.[26, 28-30] Nrf2 comprises seven conservative Nrf2-ECH domains, namely Neh1 - Neh7, with each have distinct roles (Figure 3A). The conserved Neh1 domain consists of CNC and bZIP regions which facilitate DNA binding and dimerization with small musculoaponeurotic fibrosarcoma proteins (sMAF). The Neh2 domain also has two highly conservative amino acid sequences, namely DLG and ETGE motifs, who play important roles in binding with Keap1 and subsequent ubiquitination and proteasomal degradation of Nrf2 proteins. Thus, the Neh2 is also known as the Keap1 interacting degron of Nrf2. Neh3, Neh4 and Neh5 are transactivation domains with Neh3 locating in the C terminal of the Nrf2 protein. They are able to bind with different transcriptional components to mediate transactivation, with especially the adjacent Neh4 and Neh5 contributing more. Neh6, in contrast to Neh2, is a Keap1 independent degron of Nrf2. It has two conserved amino acid domains, i.e., DSAPGS and DSGIS, which contain serine residues. The phosphorylation of especially these serine residues facilitates the proteasomal degradation of Nrf2. Neh7 could repress Nrf2 transactivation by interacting with retinoic X receptor alpha (RXRα).[25-26, 31]

1.3.1.2 Keap1

Keap1 contains 624 amino acids making up five domains: two amino terminal regions (NTR and CTR), a Broad-complex, Tramtrack, Bric-a-brac (BTB) dimerization domain, a cysteine-rich intervening region (IVR) and six repeated Kelch domains.[31] The BTB is the site of Keap1

homodimerization through which the Keap1 homodimer forms. It also contributes to the interaction of the Cullin3 (Cul3)-based ubiquitin E3 ligase complex with IVR. The Kelch repeats together with CTR regulate Keap1 binding with Nrf2 at the Neh2 domain.[25, 31-32] The organization of the human Keap1 protein is depicted in Figure 3B.
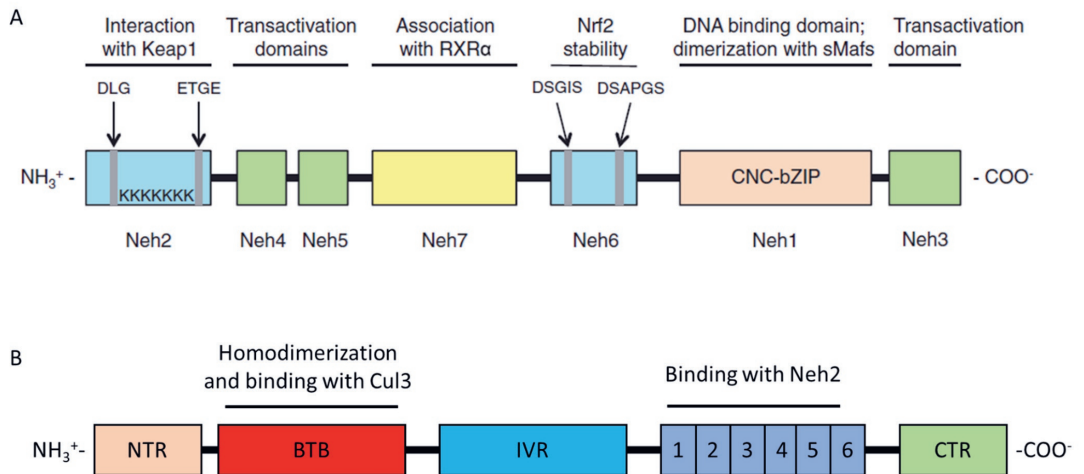

Figure 3. Domains of the human Nrf2 (A) and Keap1 (B) proteins. Adapted from Tonelli et al. (2018)[25]

1.3.2 Mechanism of Keap1/Nrf2 pathway activation

Under basal condition, the abundance of Nrf2 protein within cells is strictly regulated by Keap1. In the cytoplasm, the Keap1 homodimer binds to Nrf2 at its DLG and ETGE sequences in the Neh2 domain. The Keap1 homodimer then acts as a bridge between Nrf2 and the Cul3 based ubiquitin E3 ligase via forming a Keap1-Cul3 complex which is responsible for the continuous polyubiquitylation of Nrf2 and its sequent proteasomal degradation.[26, 33] Although under homeostasis Nrf2 is synthesized it is sequestered by the Keap1 homodimer for degradation. Thus, its half-life is quite short, approximately 10 to 30 minutes, which explains the low basal quantity and activity of Nrf2.[25] However, under perturbed conditions, i.e., exposure to electrophiles or reactive oxygen species (ROS), some key cysteine residues of Keap1 are oxidized and/or conjugated, causing the inactivation of Keap1 and dissociation of the Keap1/Nrf2 complex.[25] As a result the synthesised Nrf2 is no longer ubiquitylated by Cul3 E3 ligase and thus no longer degraded by proteasomal degradation. More Nrf2 is accumulated in the cytoplasm which facilitates its nuclear translocation. Besides the Keap1-dependent regulation of Nrf2 stabilization, PI3K-AKT signalling activation (Keap1-independed Nrf2 activation) can also release Nrf2 from proteasomal degradation via inhibition of GSK-3β.[32] The

inhibition of GSK-3β reduces Nrf2 phosphorylation which derepresses it from β-TrCP-Cul1-dependent degradation in the nucleus.[32]

After Nrf2 translocation into the nucleus, it binds to sMaf proteins, e.g., MafF, MafK and MafG, to form a heterodimer. This heterodimerization is necessary as a study has proved that silencing of MafG abolished the Nrf2 activation effects.[34] The sMaf-Nrf2 complex binds to the ARE/EpRE at the upstream regulatory region of a battery of cytoprotective genes, which activates their transcription. These cytoprotective genes include, but are not limited to, NADPH quinone dehydrogenase 1 (Nqo1), glutamate-cysteine ligase (Gcl), glutathione S-transferase (Gst), heme oxygenase 1 (Hmox1), etc.[35] Figure 4 shows a general schematic diagram of Keap1/Nrf2 signalling pathway activation.

1.3.3 Beneficial effects of green tea catechins via Keap1/Nrf2 pathway activation

Several green tea catechins are reported to be capable of inducing the Keap1/Nrf2 activation to strengthen cellular defense systems.[36-37] Especially for EGCG it has been reported that its antioxidant and detoxifying abilities are at least partially due to its potency in triggering the activation of Nrf2 mediated gene expression.[38] After been transported into cells, catechins can form quinone metabolites. Quinones are able to either directly inactivate Keap1 or oxidize intracellular GSH which results in transient oxidative stress and causes oxidation or modification of the thiol groups at Keap1.[38-39] Therefore, Nrf2 protein is dissociated from the Keap1 homodimer and translocates into the nucleus where it forms a heterodimer with sMaf proteins and binds to the ARE/EpRE to transcribe a wide array of cytoprotective genes.[26] In one study using both wild type mice and Nrf2-deficient mice, the detoxification enzymes, Gcl, Hmox-1, and γ-glutamyltransferase 1 (GGT1) were only found upregulated after EGCG administration in wild type mice.[40] In another study, the Nrf2 nuclear translocation was stimulated by provoking the PI3K-AKT pathway in EGCG treated HepG2 cells.[41] As a result, the expression of antioxidant enzymes, e.g., HMOX-1 and NQO1 was induced. While this phenomenon was not seen in Nrf2 knockdown cells. In consistence with *in vitro* results, the authors also found that an EGCG supplement significantly ameliorated oxidative stress via induction of the Keap1/Nrf2 pathway in C57BL/6J male mice.[41] Moreover, EGCG is also reported to attenuate diabetic nephropathy via induction of the Nrf2 pathway. Sun and colleagues discovered that diabetes-induced renal oxidative damage, fibrosis, inflammation and albuminuria in C57Bl/6J mice were significantly prevented by subcutaneously injecting EGCG while deletion of the Nrf2 gene led to a complete abrogation of these protective effects.[42]

Besides EGCG, other model green tea catechins appeared also able to exert protective effects through Nrf2 activation. For instance, Huang et al. proved that EC protects rats from monocrotaline (MCT) induced liver oxidative injury via activating Nrf2-mediated cytoprotective genes expression.[43] They found for instance that upon administration of 40 mg/kg EC, the levels Nrf2 together with those of Gst, Gclc, Gclm, Nqo1 and Hmox-1 in MCT exposed rats could be recovered to a homeostatic level.[43] Chiou and colleges found that ECG could disrupt the Keap-Nrf2 complex and thus induce the expression of Homx-1 and cellular glutathione (GSH) levels which were responsible for the attenuation of lipopolysaccharide (LPS)-induced inflammatory mediator expression and intracellular ROS levels in RAW 264.7 cells.[44] There are very limited publications reporting the Nrf2 mediated gene expression stimulated by EGC. In one study conducted by Ogborne et al., EGC was able to increase both transcriptional and translational levels of Hmox-1 in human monocytic THP-12 cells. However, other Nrf2-regualted genes, i.e., Nqo1, Gcl and ferritin were barely affected by EGC exposure.[37]
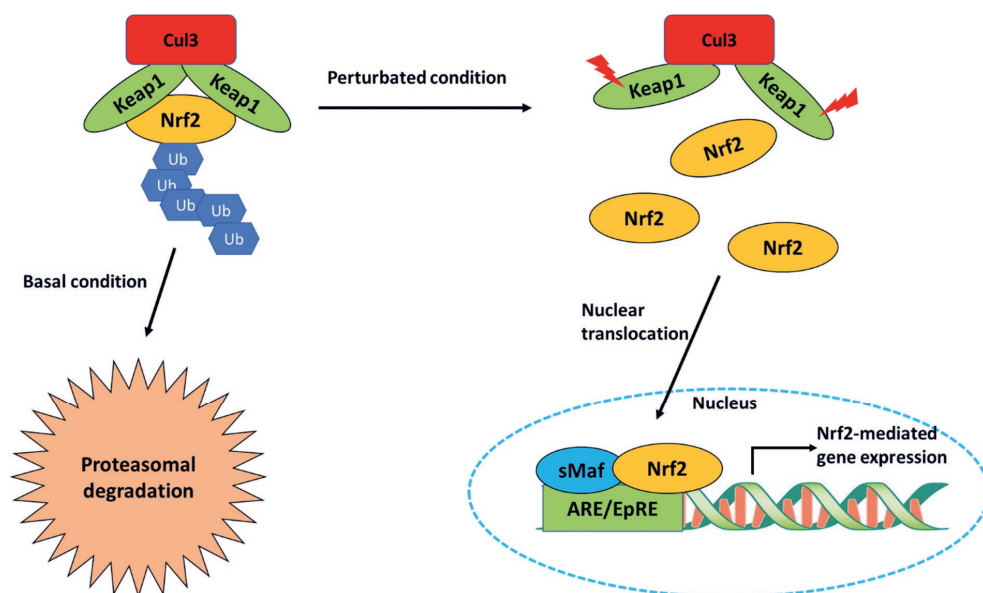
Figure 4. Mechanism of Nrf2 signalling pathway activation.

1.4 Metabolism of green tea catechins

Despite the fact that the daily intake of polyphenols is ten times than that of vitamin C and 100 times that of vitamin E,[45] the overall bioavailability of polyphenols is considered to be lower than 10%,[46] resulting in plasma concentrations of catechins to be more than 50 times lower than those of vitamin C and more than 20 times lower than those of vitamin E.[47-48] EC is recognized

as a well-absorbed catechin but still only about 20 - 30% of the intake is absorbed directly in the small gastrointestinal tract and passed into systemic circulations.[48] When EC is ingested, the metabolism already starts at the proximal gastrointestinal tract. Conjugation takes place in the enterocytes which produces several structurally-related (-)-epicatechin metabolites (SREMs) including especially 3'-*O*-methyl-(-)-epicatechin-5-sulfate, (-)-epicatechin-3'-*O*-glucuronide and (-)-epicatechin-3'-*O*-sulfate.[48] These SREMs can be directly passed on to the systemic circulation (indicated by the short T_{max} which was 1.0 ± 0.1 h).[48] Meanwhile a large amount of unabsorbed EC (~ 70% of intake) reaches the large intestine where it is subject to extensive degradation by intestinal microbiota.[16, 48-49] Compared to the non-galloylated tea catechin EC, the galloylated ECG and EGCG have a very poor bioavailability, amounting to less than 1% of total oral intake.[50] Barely no conjugated ECG and EGCG have been detected in biological fluids.[51-52] For example, EGCG was detected almost all in free form in plasma in several studies.[51, 53-54]

Thus, the majority of orally ingested green tea catechins is passed on to the colon (including catechins excreted via bile) where they are subject to extensive microbial metabolism. A diversity of microbiota inhabits the large intestine, providing the capability of catalysing various reactions. These reactions include for example hydrolysis of glycosides, sulfates, lactones, esters, etc., and reduction, decarboxylation, demethylation.[3] As a result, the unabsorbed tea catechin conjugates are first deconjugated and subsequently, together with other unabsorbed aglycones, further degraded by the intestine microflora. For the galloylated tea catechins, namely ECG and EGCG, the microbial conversion starts with the rapid degalloylation by microbial esterases which produces EC and EGC, respectively. Gallic acid (GA) is formed upon hydrolysis of both these parent compounds, and is further decarboxylated to give rise to pyrogallol (PG). PG can be converted further to molecules including catechol, butyric acid and acetic acid.[11, 55] Meanwhile, in EC and EGC, the 1-2 bond in the heterocyclic C-ring is prone to reductive cleavage, giving rise to diphenylpropanols. Further A-ring fission, lactonization, dehydroxylation, decarboxylation and beta-oxidation catalysed by the gut microbiome results in the formation of phenyl-γ-valerolactones and various smaller phenolic acids, which are more readily absorbed.[3, 51-52, 56] The proposed microbial metabolic pathway of green tea catechins is presented in Figure 5.

The extensive metabolism of green tea catechins improves both the overall bioavailability of the parent catechins in the form of their metabolites and may at the same time contribute to the physiological bioactivities that are attributed to the parent compound. For instance, Ottaviani et

al. quantified 48 h urine excretion from human volunteers upon oral administration of EC. They found that urinary excretion accounted for EC metabolites at a level corresponding to 89% of the ingested EC, among which the EC microbial metabolites, including 5 carbon side-chain ring fission metabolites (5C-RFMs, e.g., phenyl valerolactones and phenyl valeric acids) made up the largest portion, amounting to 42% of the total EC ingested.[48] In another study, 20 healthy volunteers were served 400 mL of ready-to-drink green tea and their urine and plasma samples were collected and analysed. The researchers concluded that when colonic ring fission metabolites of tea catechins (amounting to 39% of the amount of catechins ingested) are taken into account, the bioavailability of these flavan-3-ols is more promising than previously observed.[57]

Given the systemic bioavailability of the microbial catechin metabolites, the biological activities of these metabolites are of interest. For example, one of the major microflora-derived catechin metabolites, 5-(3',4'-dihydroxyphenyl)-γ-valerolactone (3,4-diHPV), was reported to be able to inhibit NO production and iNOS expression in RAW 264.7 cells, suggesting potential anti-inflammatory activity.[58] In another study, Chen et al. found that the C-ring cleavage metabolite, 1-(3',4'-dihydroxyphenyl)-3-(2'',4'',6''-trihydroxyphenyl)-2-propanol (3,4-diHPP-2-ol), exerted a 2- and 1.8-times higher antioxidant activity than its parent compounds catechin and epicatechin, respectively.[14] Therefore, the various physiological effects that were previously ascribed to green tea catechins may be at least partially be due to the formation of a wide range of metabolites resulting either from conjugation in the liver and intestinal cells or from microbial metabolism in the colon.

Figure 5. Proposed microbial metabolism pathway of green tea catechins.

1.5 Intestinal microbiota and intra- and inter-individual differences

As outlined in the preceding section, it is increasingly realized that the intestinal microbiota plays a crucial role in the physiology and biological effects of tea catechins. Thus, it is of importance to shortly introduce the gut microbiome, and the factors that contribute to its variation and potential impact on human health.

1.5.1 Gut microbiota and its functions

Gut microbiota refers to the collection of eukarya, archaea and bacteria that colonise the GI tract. It is estimated that more than 100 trillion of microbes inhabit the human intestine, which encompasses an around 10 times higher number of bacterial cells than the number of human cells.[59] With the help of high throughput sequencing techniques, it has been elucidated that Bacteroidetes, Firmicutes, Actinobacteria, Proteobacteria and Tenericutes are the predominant bacterial phyla in human gut, with the first two phyla being dominant. Other bacterial phyla such as Fusobacteria, Verrucomicrobia, Saccharibacteri are generally detected in minor abundance.[60-62] Though many studies suggest the existences of a core gut microbiota which consists of the most prevalent bacterial phylotypes with essential roles in the microbial ecological community, it is still difficult to make solid conclusions as there also appear to exist large inter-individual differences in microbiota compositions.[60, 63]

Due to the immense genomic content and wide range of catalytic abilities of gut microbiota, a wide range of physiological effects are at least partially influenced by this external "organ". A healthy gut microbiota ecosystem benefits the host physiological state via, for example, facilitating nutrient extraction, instructing innate immunity, protecting against pathogens, regulating epithelial development, etc.[61] Some different populations of bacteria may be able to perform similar functions. For instance, the short chain fatty acid (SCFA) acetate can be produced by most intestinal anaerobes.[64] The same holds for the degalloylation of galloylated green tea catechins, which also seems not to require certain specific phenotypes.[11] On the other hand, it is also recognized that certain biotransformations of food ingredients or drugs need specific microbes. For example, Eubacterium SDG-2, Lactobacillus plantarum, Eggerthella lenta, and Adlercreutzia equolifaciens are the only bacteria reported so far to be capable of producing the metabolite diphenylpropan-2-ol from epicatechins (or catechins).[65-67] The first two belong to the phylum Firmicutes and the latter two to the phylum Actinobacteria. Under this perspective, the determination of the functional core microbiome, instead of determination of the microbiota composition only at the microbial organism level, could be a more meaningful and feasible alternative strategy.[60]

1.5.2 Factors shaping the variations of human gut microbes

Stable gut microbial composition is one of the most important indicators of a healthy host. However, some internal and extern factors could affect this stable status of gut microbiota. For instance, age can be quite an influential factor driving the changes of host microbiota composition. The microbes of a new born infant are largely affected by the mode of birth and the mother's gut microbiota.[68] The gut microbiota of natural laboured infants are initially

colonized by organisms from the maternal vagina.[69] In contrast, in cesarean delivered infants the intestine is mostly colonized by the maternal skin flora.[69-70] Over the first 3 to 5 years of shifting, the child's gut microbiota increases in diversity and stability, and evolves towards an adult-like configuration.[68, 71] Odamaki et al. conducted a study using fecal samples from 367 healthy subjects over a wide age range, 0 – 104 years, and they concluded that the transition from infant to centenarian was accompanied by distinctive bacterial co-abundance group dominance, with a significant abundance of Bacteroides, Clostridiaceae, Eubacterium, Bifidobacterium and Lachnospiraceae. Moreover, Megamonas and Peptoniphilus co-abundance groups were relatively enriched in the elderly.[68]

Diet can be another important factor that contributes to the microbial diversity and composition. For instance, it is wildly accepted that a diet rich in fruits, fibres and vegetables is in favour of the diversity of the gut microbiome.[72] Compared to infant formula, breast milk contains human milk oligosaccharides providing a selective growth advantage for Bifidobacterium sp.[73] Higher abundance of Bacteroides was associated with a western diet rich in animal protein, sugar and starch.[74] Moreover, EGCG treatment has been reported to be able to act as a prebiotic which selectively promoted the abundance of beneficial bacteria, e.g., Bacteroides, Christensenellaceae and Bifidobacterium, while it reduced the pathogenic bacteria, e.g., Fusobacterium varium, Bilophila, and Enterobacteriaceae.[75]

Besides, genetics is another factor driving the differences in human gut microbiota. However, conclusions based on this factor are still unclear since normally different populations not only possess genetic differences but are also under different environmental exposures, such as sanitation levels, frequency of using antibiotics and diet. To better illustrate the associations between different factors and gut microbiota requires expanded studies that sample large populations and control the confounding factors.[60]

1.5.3 Intra- and inter-individual differences in microbial metabolism of green tea catechins

Owing to the differences in age, gender, ethnic factors, lifestyle and diet, human microbial composition is known to vary substantially among people, which in turn could cause inter-individual differences in gut microbial metabolism of polyphenols. Researchers are trying to define certain metabolic phenotypes (aka metabotypes) to characterize subjects that possess distinct microbial-derived metabolic profiles. For instance, Mena et al. analysed the urinary profile of green tea metabolites from 11 subjects who consumed green tea extract daily for eight

weeks.[76] They putatively proposed three metabotypes which were characterised by the different proportions of four important microbial metabolites of green tea catechins, namely trihydroxyphenyl-γ-valerolactones, dihydroxyphenyl-γ-valerolactones, mon-hydroxyphenyl-γ-valerolactones and hydroxyphenyl propionic acid, quantified in urine samples from different volunteers.[76-77] Ottaviani and colleagues conducted another human intervention study with eight participants consuming an EC-containing drink. They also found striking inter-individual differences in both urinary and plasma metabolic profiles of EC microbial metabolites. For example, 3.6- and 3.2-fold differences in colon derived 5 carbon side chain ring fission metabolites were detected in the plasma and urine of volunteers. Moreover, the lower molecular weight microbial 3/1-carbon-side chain ring fission metabolites (e.g., phenylpropanoic acids, phenylacetic acids and phenylbenzoic acids) presented a much more substantial variation (9-fold).[16, 48] This was likely due to the higher number of conversion steps required for producing the lower molecular weight metabolites, which probably requires involvement of more types of bacteria which increased the chance of observing larger inter-individual differences.

In addition to these *in vivo* studies, it can be anticipated that *in vitro* studies using fecal anaerobic incubation models could provide useful alternatives to study colonic metabolism and potential inter-individual differences of microbial metabolism, an approach tested in the current thesis (Chapter 2 to 4). Several research groups around the world are developing and using the so called simulator of the human intestinal microbial ecosystem (SHIME) to simulate the entire human gastrointestinal system, in which human fecal materials are inoculated, thus enabling the establishment of a microbial population that resembles human GI tract.[78-79] For instance, Li et al. discovered significant interindividual variability in metabolic efficiency of (+)-catechin microbial metabolism among 12 tested donor microbiota by using the SHIME model.[80]

In contrast to the well-accepted existence of inter-individual differences in human microbiota composition and resulting metabotypes, the intra-individual differences in human microbial metabolism are often ignored or considered not evident. This may be the case because the microbiota composition is considered to be relatively stable within healthy individuals.[81-82] However, to what extent the intra-individual differences of microbiota composition can cause differences in the metabolic pattern of conversion of catechins still needs to be unveiled.

1.6 Proteomics used in studies on the bioactivity of green tea catechins

When studying the mode of action of beneficial/protective properties of green tea catechins, many studies were trying to elucidate changes in the levels of certain proteins in cells/tissue

after tea catechin exposure. This was normally done by either ELISA or Western blot.[83-86] However, the numbers of proteins that could be measured in these experiments are often restricted. On the other hand, the proteomics technologies offer a comparatively high-throughput way to study the large number of proteins in cells or tissues, which can be extremely complex, exceedingly dynamic, and largely defines cellular behaviour and function.[87]

1.6.1 Proteomics workflow in the present thesis

Proteomics is an advanced large-scale technique used to identify and characterize global protein expression.[88] Compared to other detection techniques, mass spectrometry (MS) provides better efficiency and sensitivity, facilitating the direct analysis of proteins and multiprotein complexes involved in biological responses and regulatory mechanisms, including the Keap1/Nrf2-mediated regulatory network that is of interest for studies in the present thesis.

The current thesis applied a bottom-up proteomics workflow (Figure 6).[89] Either colonic cells or hepatic cells were exposed *in vitro* to green tea catechins or some of their selected microbial metabolites for 24 hours. Subsequently, proteins from the cells were collected, quantified and digested to peptides using trypsin. Then those peptide mixtures were separated by nano-LC (nano-liquid chromatography) and identified by a mass spectrometer. The resulting peptide identifications were subsequently mapped to proteins and subjected to downstream bioinformatical analysis for extracting biological meanings.

1.6.2 Downstream bioinformatical analysis

Given that proteomics is able to identify and quantify thousands of proteins, providing so called "big data", data processing and interpretation can be complicated. Therefore, it is necessary to build an efficient and comprehensive downstream data processing pipeline to fully address the biological activity and cellular mechanisms in cells or tissues reflected by the proteomics data.[90]

Before bridging quantitative protein data and protein interactions or signalling networks, it is important to define the differentially expressed proteins (DEPs). DEPs are usually derived from proteins meeting two criteria which are: (1) showing a fold change (usually compared to a control group) less and greater than a certain fold (in different research areas the fold could vary) and (2) a P-value for the fold change of less than 0.05 (or more stringent: 0.01). In the present study the DEPs from exposure treatments of cells with green tea catechins or their selected microbial metabolites were characterized based on a fold change less than 0.8 or greater than 1.2 and a P-value less than 0.05.

After obtaining the DEPs from different treatments, enrichment analysis can be performed to identify proteins that are overrepresented in the predefined dataset of interest. Gene Ontology (GO) enrichment is one the most widely used enrichment analyses. It is a technique for interpreting certain sets of genes and to assign the genes to predefined groups (GO terms) depending on their function characteristics.[90-91] GO terms are divided into three categories, namely Molecular Function (MF), Cellular Component (CC) and Biological Process (BP). Commonly used GO enrichment tools include Gorilla, Blast2GO, DAVID and STRING, etc.[92-95]

Besides, GO enrichment analysis, including analysis on regulatory pathways enriched in DEPs, is also of importance to understand cellular mechanisms. Thereby, pathway enrichments based on databases such as KEGG, PANTHER, and/or Reactome are often performed. Publicly available online tools are including DAVID, STRING, Metascape, ect.[94-96] Additionally, to explore further the relationship between proteins of interest within the cellular environment, the network biology (also known as systems biology) is worth investigating.[97] Protein-protein interaction (PPI) networks represent one of the proteomics-based network biology tools. PPI networks describe physical interactions between proteins, taking place to mediate the assembly of proteins into protein complexes, or e.g., mediating signalling/regulation and transport events in the cell.[98] The STRING database is one of the most commonly used tools to do PPI networks analysis.[95]

Finally, the results of the aforementioned analysis are visualized, e.g., by R, Cytoscape or more user-friendly webtools such as Bioinformatics (http://www.bioinformatics.com.cn/). This is how quantitative protein data from proteomics datasets can be used to reconstruct protein interactions and regulatory signalling networks, and to ultimately interpret the biological meanings.[90]
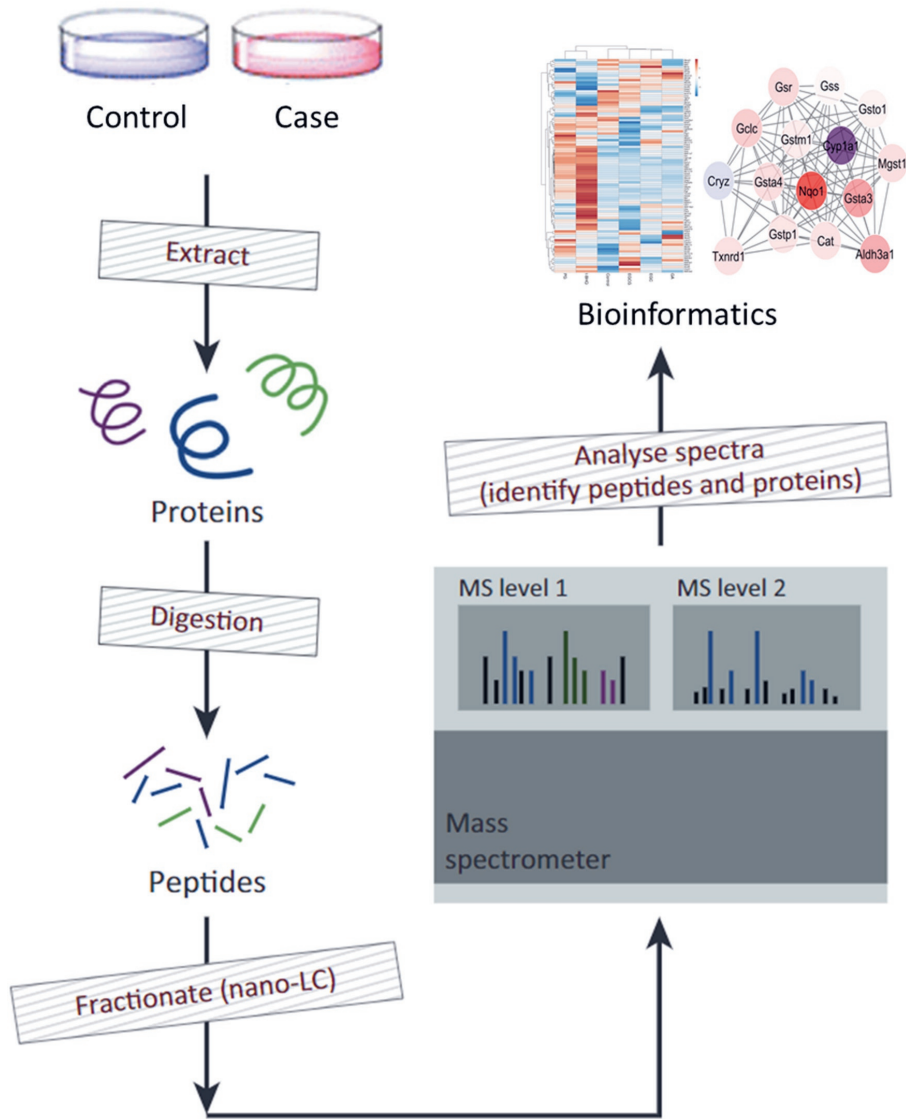
Figure 6. Bottom up proteomics workflow. Adapted from Ahmad and Lamond (2014).[89]

1.7 Use of physiologically based kinetic (PBK) modeling to study absorption, distribution, metabolism, and excretion (ADME) of green tea catechins

The studies of bioactivity of green tea catechins often need elucidation of ADME characteristics of these chemicals and their metabolites in the human body. However, sometimes data from human studies are difficult or even impossible to obtain. Therefore, investigations are often

carried out in laboratory animal models or *in vitro* cellular models. However, this brings other issues, namely how to obtain adequate extrapolation from the *in vitro* to the *in vivo* situation, from high-dose levels to physiological relevant low-dose levels and from laboratory animal models to humans. Moreover, the potential intra- and inter-individual differences of humans are of importance.[99] PBK models are able to facilitate these types of extrapolations and provide an alternative approach for non-animal based testing strategies.[18, 99]

1.7.1 Physiologically based kinetic (PBK) modeling

PBK modelling is a mathematical modelling technique for predicting the ADME of chemicals in humans or other animal species based on three kinds of parameters, namely physiological and anatomical parameters, physicochemical parameters and kinetic parameters. In general, PBK modelling includes six steps: (1) definition of the conceptual model, (2) translation into a mathematical model, (3) definition of the parameters, (4) solving the model equations, (5) evaluation/validation of the model performance and (6) making predictions.[18, 99] In the first step, it is important to define the organs/compartments that are relevant for the ADME characteristics of the compound of interest and its biological effects. Figure 7 presents the conceptual model developed in the present thesis for EGCG, with sub-models for its microbial metabolites gallic acid (GA) and pyrogallol. The separated compartments comprise small intestine lumen, small intestine tissue, large intestine lumen (for intestinal microbial metabolism), liver, fat, kidney and blood. All rest tissues are lumped into either a rapidly perfused tissue compartment or a slowly perfused tissue compartment. Then mathematical equations for each compartment can be defined with the three types of parameters mentioned above. Subsequently, by using software such as Berkeley Madonna, Simcyp, NONMEM and /or MATLAB, the mathematical equations can be solved. Afterwards, to evaluate how well the PBK model performs, *in vivo* data from literature can be used for comparison with PBK model predicted results. If the PBK model predicts well it can be used to make predictions on, e.g., concentrations of the compound or its metabolites in organs of interest over time at different dose levels.
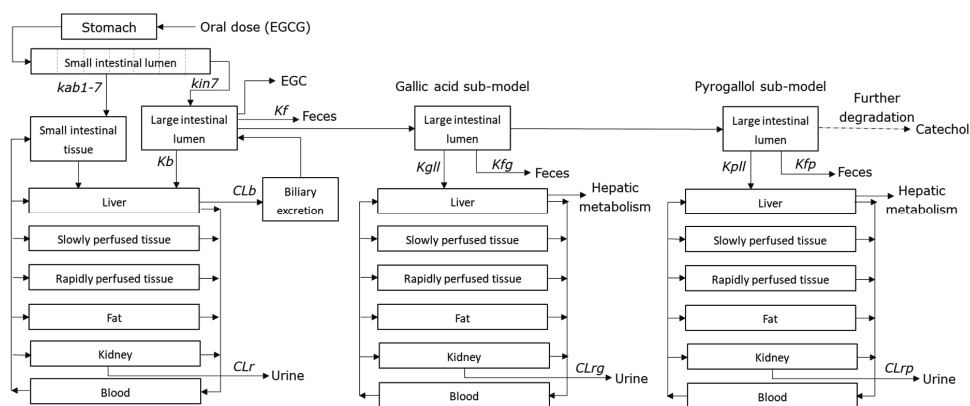
Figure 7. Schematic representation of the conceptual PBK model for EGCG with sub-models for the microbial metabolites gallic acid and pyrogallol developed in the present thesis.

1.7.2 PBK modelling-based reverse dosimetry

An important application of PBK modelling is PBK modelling-based reverse dosimetry, which extrapolates *in vitro* concentration-response curves to *in vivo* dose-response curves, thereby enabling quantitative *in vitro* to *in vivo* extrapolation (QIVIVE).[18, 99] Figure 8 shows a typical schematic representation of the PBK modelling-based reverse dosimetry approach for translating *in vitro* concentration-response curves (derived from e.g., a cellular based assay) into *in vivo* dose-response curves for species of interest including humans. To study the Nrf2-pathway activation activity (mechanism of cellular defence and detoxification) of EGCG and its major microbial metabolites, such as GA and pyrogallol, the CALUX reporter gene assay was performed using U2OS-Nrf2 cells. For the reverse dosimetry, the *in vitro* concentrations of EGCG and its microbial metabolites are set equal to blood levels in the PBK model and by using the PBK model in reverse order, the dose level needed to obtain those concentrations can be calculated. It is of note that the reverse dosimetry has to be based on the free form (unbound fraction) of the compound of interest both in the *in vitro* and *in vivo* condition.

With the generated *in vivo* dose-response curve from the PBK modelling-based reverse dosimetry approach, a point of departure (POD) for risk assessment can be defined. Especially for toxic chemicals, a no observed adverse effect level (NOAEL), a lowest observed adverse effect level (LOAEL) or the benchmark dose (BMD) or its lower confidence limit (BMDL) are the most commonly used PODs for the risk assessment or safety evaluation.[100] For prediction of the beneficial effects of green tea catechin EGCG and its microbial metabolites, the benchmark dose that causes 10% effect above background (BMD$_{10}$) or its lower bound

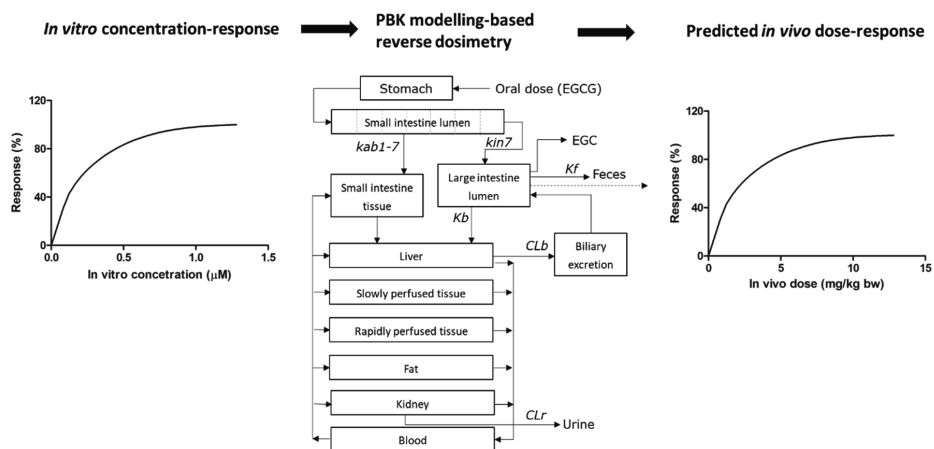confidence limit (BMDL$_{10}$) can also be derived and subsequently compared to estimated intake levels.

Figure 8. Schematic representation of the PBK modelling-based reverse dosimetry approach for extrapolation of *in vitro* concentration-response curves into *in vivo* dose-response curves.

1.8 Thesis overview

As described in the beginning of this chapter, the aim of the present thesis was to obtain better insights into human intestinal microbiota-mediated conversion of model green tea catechins, including the intra- and inter-individual variability, and to identify the activity of the formed microbial metabolites in the activation of Nrf2-EpRE-mediated gene expression. Furthermore, the thesis also aimed to build a PBK model including gut microbial metabolism for the most abundant and bioactive catechin, EGCG, and to use a PBK modelling-based reverse dosimetry approach to extrapolate *in vitro* concentration-response curves obtained in the Nrf2 CALUX reporter gene assay to *in vivo* dose-response curves in humans.

The present thesis comprises the following seven chapters:

Chapter 1 started with a brief introduction of the background and aims of the present thesis followed by an overview of the major green tea catechins. It then introduced the beneficial effects of green tea catechins focusing on the activation of the Keap1/Nrf2 signalling pathway. The structure of the Keap1/Nrf2 system was described and the mechanisms of action of its activation were also illustrated. Subsequently, the metabolism of green tea catechins was explained, including especially the role of the colonic metabolism, and the potential intra- and inter-individual variations in this metabolism by the colonic microbiota were introduced.

Furthermore, the proteomics technologies that were used in the present thesis were also described. Finally, the chapter introduced the PBK modelling and how to use it in a new approach methodology (NAM) for reverse dosimetry to translate *in vitro* concentration response curves into *in vivo* dose response curves.

In **Chapter 2**, the time-dependent microbial conversion of the green tea catechin EC was characterized using an *in vitro* anaerobic fecal incubation model. Moreover, the potential inter-individual differences in the human intestinal microbial metabolism of EC were studied using fecal inocula from 24 healthy donors. Quantitative microbiota characterization in these fecal samples was achieved by 16S rRNA analysis, and correlations between specific microbial phylotypes and formation of certain metabolites were established.

In **Chapter 3**, anaerobic human fecal incubations were performed to characterize the microbial metabolism of the most abundant green tea catechin, EGCG, including inter-individual variability in the metabolic profiles. Spearman correlations between specific microbial genera types/phylotypes and formation of major metabolites were established. The activity of the formed colonic metabolites in the activation of Nrf2-EpRE-mediated gene expression was tested by the EpRE-LUX reporter gene assay.

In **Chapter 4**, the intra- and inter-individual differences in the gut microbial metabolism of EC were characterized and compared by using anaerobic human fecal incubations. The Nrf2 signalling pathway activation by EC and its major colonic metabolite, 3,4-diHPV, was studied using the U2OS-Nrf2 CALUX reporter gene assay. Subsequently, the protein expression profiles of EC or 3,4-diHPV treated Caco-2 and Hepa1c1c7 cells were studied with the help of label-free proteomics. Bioinformatical analysis was carried out to interpret the biological consequences after exposure. Finally, RT-qPCR was performed to corroborate the results of the proteomics data.

In **Chapter 5**, the ability to activate the Nrf2 signalling pathway was tested for EGCG, EGC and their major colonic metabolites GA and pyrogallol using the U2OS-Nrf2 CALUX reporter gene assay. Based on the results from Chapter 4, Hepa1c1c7 cells were chosen as the *in vitro* cellular model to study the protein expression profile after exposure to above-mentioned four compounds via label-free proteomics analysis. The Nrf2-activator t-BHQ was included for comparison. Bioinformatical analysis was carried out to interpret the biological consequences of the exposure. Finally, RT-qPCR was performed to corroborate the results of the proteomics data.

In **Chapter 6**, a human PBK model was developed for EGCG, with sub-models for its major microbial metabolites GA and pyrogallol. The model allows comparison of the predicted internal concentrations of EGCG, GA and pyrogallol to the concentrations able to induce Nrf2 signalling pathway activation *in vitro*. It also allows the translation of the obtained *in vitro* concentration-response curves from U2OS-Nrf2 CALUX reporter gene assay to *in vivo* dose-response curves, and comparison of these data to estimated daily intake levels.

Finally, in **Chapter 7**, the main findings of the previous chapters were put together in an integrated discussion, and further recommendations/possibilities for future research were explored.

References

1.   Zhou, Y.; Huang, W.; Liu, X.; Cao, W.; Wang, D.; Liu, X.; Pang, Y.; Wen, S.; Zhang, X., Interannual variation and exposure risk assessment of lead in brick tea in Hubei, China. *Science of The Total Environment* **2020,** *745*, 141004.

2.   Cabrera, C.; Artacho, R.; Giménez, R., Beneficial effects of green tea—a review. *Journal of the American College of Nutrition* **2006,** *25* (2), 79-99.

3.   Liu, Z.; Bruins, M. E.; Ni, L.; Vincken, J.-P., Green and black tea phenolics: Bioavailability, transformation by colonic microbiota, and modulation of colonic microbiota. *Journal of Agricultural and Food Chemistry* **2018,** *66* (32), 8469-8477.

4.   Chacko, S. M.; Thambi, P. T.; Kuttan, R.; Nishigaki, I., Beneficial effects of green tea: a literature review. *Chinese medicine* **2010,** *5* (1), 1-9.

5.   Graham, H. N., Green tea composition, consumption, and polyphenol chemistry. *Preventive medicine* **1992,** *21* (3), 334-350.

6.   Musial, C.; Kuban-Jankowska, A.; Gorska-Ponikowska, M., Beneficial properties of green tea catechins. *International journal of molecular sciences* **2020,** *21* (5), 1744.

7.   Shahidi, F., Antioxidants in food and food antioxidants. *Food/nahrung* **2000,** *44* (3), 158-163.

8.   Higdon, J. V.; Frei, B., Tea catechins and polyphenols: health effects, metabolism, and antioxidant functions. *Critical Reviews in Food Science and Nutrition* **2003**.

9.   Xing, L.; Zhang, H.; Qi, R.; Tsao, R.; Mine, Y., Recent advances in the understanding of the health benefits and molecular mechanisms associated with green tea polyphenols. *Journal of agricultural and food chemistry* **2019,** *67* (4), 1029-1043.

10.   Kochman, J.; Jakubczyk, K.; Antoniewicz, J.; Mruk, H.; Janda, K., Health benefits and chemical composition of matcha green tea: A review. *Molecules* **2021,** *26* (1), 85.

11.   Liu, C.; Vervoort, J.; van den Elzen, J.; Beekmann, K.; Baccaro, M.; de Haan, L.; Rietjens, I. M., Interindividual Differences in Human In Vitro Intestinal Microbial Conversion of Green Tea (-)-Epigallocatechin-3-O-Gallate and Consequences for Activation of Nrf2 Mediated Gene Expression. *Molecular Nutrition & Food Research* **2021,** *65* (2), 2000934.

12.   van ͗t Slot, G.; Humpf, H.-U., Degradation and metabolism of catechin, epigallocatechin-3-gallate (EGCG), and related compounds by the intestinal microbiota in the pig cecum model. *Journal of agricultural and food chemistry* **2009,** *57* (17), 8041-8048.

13.   Gonthier, M.-P.; Cheynier, V.; Donovan, J. L.; Manach, C.; Morand, C.; Mila, I.; Lapierre, C.; Rémésy, C.; Scalbert, A., Microbial aromatic acid metabolites formed in the gut account for a major fraction of the polyphenols excreted in urine of rats fed red wine polyphenols. *The Journal of nutrition* **2003,** *133* (2), 461-467.

14.   Chen, W.; Zhu, X.; Lu, Q.; Zhang, L.; Wang, X.; Liu, R., C-ring cleavage metabolites of catechin and epicatechin enhanced antioxidant activities through intestinal microbiota. *Food Research International* **2020,** *135*, 109271.

15.   Hara-Terawaki, A.; Takagaki, A.; Kobayashi, H.; Nanjo, F., Inhibitory activity of catechin metabolites produced by intestinal microbiota on proliferation of HeLa cells. *Biological and Pharmaceutical Bulletin* **2017,** *40* (8), 1331-1335.

16.   Borges, G.; Ottaviani, J. I.; van der Hooft, J. J.; Schroeter, H.; Crozier, A., Absorption, metabolism, distribution and excretion of (−)-epicatechin: A review of recent findings. *Molecular Aspects of Medicine* **2018,** *61*, 18-30.

17.   Estudante, M.; Morais, J. G.; Soveral, G.; Benet, L. Z., Intestinal drug transporters: an overview. *Advanced drug delivery reviews* **2013,** *65* (10), 1340-1356.

18.   Louisse, J.; Beekmann, K.; Rietjens, I. M., Use of physiologically based kinetic modeling-based reverse dosimetry to predict in vivo toxicity from in vitro data. *Chemical research in toxicology* **2017,** *30* (1), 114-125.

19.   Dekant, W.; Fujii, K.; Shibata, E.; Morita, O.; Shimotoyodome, A., Safety assessment of green tea based beverages and dried green tea extracts as nutritional supplements. *Toxicology letters* **2017,** *277*, 104-108.

20.   Bernatoniene, J.; Kopustinskiene, D. M., The role of catechins in cellular responses to oxidative stress. *Molecules* **2018,** *23* (4), 965.

21.   Xu, J.; Xu, Z.; Zheng, W., A review of the antiviral role of green tea catechins. *Molecules* **2017,** *22* (8), 1337.

22.   Butt, M. S.; Ahmad, R. S.; Sultan, M. T.; Qayyum, M. M. N.; Naz, A., Green tea and anticancer perspectives: updates from last decade. *Critical reviews in food science and nutrition* **2015,** *55* (6), 792-805.

23.   Velayutham, P.; Babu, A.; Liu, D., Green tea catechins and cardiovascular health: an update. *Current medicinal chemistry* **2008,** *15* (18), 1840.

24.   Onakpoya, I.; Spencer, E.; Heneghan, C.; Thompson, M., The effect of green tea on blood pressure and lipid profile: a systematic review and meta-analysis of randomized clinical trials. *Nutrition, Metabolism and Cardiovascular Diseases* **2014,** *24* (8), 823-836.

25.   Tonelli, C.; Chio, I. I. C.; Tuveson, D. A., Transcriptional regulation by Nrf2. *Antioxidants & redox signaling* **2018,** *29* (17), 1727-1745.

26.   Yamamoto, M.; Kensler, T. W.; Motohashi, H., The KEAP1-NRF2 system: a thiol-based sensor-effector apparatus for maintaining redox homeostasis. *Physiological reviews* **2018,** *98* (3), 1169-1203.

27.   Itoh, K.; Chiba, T.; Takahashi, S.; Ishii, T.; Igarashi, K.; Katoh, Y.; Oyake, T.; Hayashi, N.; Satoh, K.; Hatayama, I., An Nrf2/small Maf heterodimer mediates the induction of phase II detoxifying enzyme genes through antioxidant response elements. *Biochemical and biophysical research communications* **1997,** *236* (2), 313-322.

28.   Cho, H.-Y.; Jedlicka, A. E.; Reddy, S. P.; Zhang, L.-Y.; Kensler, T. W.; Kleeberger, S. R., Linkage analysis of susceptibility to hyperoxia: Nrf2 is a candidate gene. *American Journal of Respiratory Cell and Molecular Biology* **2002,** *26* (1), 42-51.

29.   Itoh, K.; Igarashi, K.; Hayashi, N.; Nishizawa, M.; Yamamoto, M., Cloning and characterization of a novel erythroid cell-derived CNC family transcription factor heterodimerizing with the small Maf family proteins. *Molecular and cellular biology* **1995,** *15* (8), 4184-4193.

30.   Kobayashi, A.; Ito, E.; Toki, T.; Kogame, K.; Takahashi, S.; Igarashi, K.; Hayashi, N.; Yamamoto, M., Molecular cloning and functional characterization of a new Cap'n'collar family transcription factor Nrf3. *Journal of Biological Chemistry* **1999,** *274* (10), 6443-6452.

31.   Leung, C.-H.; Zhang, J.-T.; Yang, G.-J.; Liu, H.; Han, Q.-B.; Ma, D.-L., Emerging Screening Approaches in the development of Nrf2–Keap1 protein–protein interaction inhibitors. *International journal of molecular sciences* **2019,** *20* (18), 4445.

32.   He, F.; Ru, X.; Wen, T., NRF2, a transcription factor for stress response and beyond. *International journal of molecular sciences* **2020,** *21* (13), 4777.

33.   Baird, L.; Yamamoto, M., The molecular mechanisms regulating the KEAP1-NRF2 pathway. *Molecular and cellular biology* **2020,** *40* (13), e00099-20.

34.   Wakabayashi, N.; Itoh, K.; Wakabayashi, J.; Motohashi, H.; Noda, S.; Takahashi, S.; Imakado, S.; Kotsuji, T.; Otsuka, F.; Roop, D. R., Keap1-null mutation leads to postnatal lethality due to constitutive Nrf2 activation. *Nature genetics* **2003,** *35* (3), 238-245.

35.   Suzuki, T.; Motohashi, H.; Yamamoto, M., Toward clinical application of the Keap1–Nrf2 pathway. *Trends in pharmacological sciences* **2013,** *34* (6), 340-346.

36.   Muzolf-Panek, M.; Gliszczyńska-Świgło, A.; de Haan, L.; Aarts, J. M.; Szymusiak, H.; Vervoort, J. M.; Tyrakowska, B.; Rietjens, I. M., Role of catechin quinones in the induction of EpRE-mediated gene expression. *Chemical research in toxicology* **2008,** *21* (12), 2352-2360.

37.   Ogborne, R. M.; Rushworth, S. A.; O'Connell, M. A., Epigallocatechin activates haem oxygenase-1 expression via protein kinase Cδ and Nrf2. *Biochemical and biophysical research communications* **2008,** *373* (4), 584-588.

38.   Na, H.-K.; Surh, Y.-J., Modulation of Nrf2-mediated antioxidant and detoxifying enzyme induction by the green tea polyphenol EGCG. *Food and Chemical Toxicology* **2008,** *46* (4), 1271-1278.

39.   Lee-Hilz, Y. Y.; Boerboom, A.-M. J.; Westphal, A. H.; van Berkel, W. J.; Aarts, J. M.; Rietjens, I. M., Pro-oxidant activity of flavonoids induces EpRE-mediated gene expression. *Chemical research in toxicology* **2006,** *19* (11), 1499-1505.

40.   Shen, G.; Xu, C.; Hu, R.; Jain, M. R.; Nair, S.; Lin, W.; Yang, C. S.; Chan, J. Y.; Kong, A.-N. T., Comparison of (−)-epigallocatechin-3-gallate elicited liver and small intestine gene expression profiles between C57BL/6J mice and C57BL/6J/Nrf2 (−/−) mice. *Pharmaceutical research* **2005,** *22* (11), 1805-1820.

41.   Mi, Y.; Zhang, W.; Tian, H.; Li, R.; Huang, S.; Li, X.; Qi, G.; Liu, X., EGCG evokes Nrf2 nuclear translocation and dampens PTP1B expression to ameliorate metabolic misalignment under insulin resistance condition. *Food & function* **2018,** *9* (3), 1510-1523.

42.   Sun, W.; Liu, X.; Zhang, H.; Song, Y.; Li, T.; Liu, X.; Liu, Y.; Guo, L.; Wang, F.; Yang, T., Epigallocatechin gallate upregulates NRF2 to prevent diabetic nephropathy via disabling KEAP1. *Free Radical Biology and Medicine* **2017,** *108*, 840-857.

43.   Huang, Z.; Jing, X.; Sheng, Y.; Zhang, J.; Hao, Z.; Wang, Z.; Ji, L., (-)-Epicatechin attenuates hepatic sinusoidal obstruction syndrome by inhibiting liver oxidative and inflammatory injury. *Redox biology* **2019,** *22*, 101117.

44.   Chiou, Y.-S.; Huang, Q.; Ho, C.-T.; Wang, Y.-J.; Pan, M.-H., Directly interact with Keap1 and LPS is involved in the anti-inflammatory mechanisms of (-)-epicatechin-3-gallate in LPS-induced macrophages and endotoxemia. *Free Radical Biology and Medicine* **2016,** *94*, 1-16.

45.   Scalbert, A.; Johnson, I. T.; Saltmarsh, M., Polyphenols: antioxidants and beyond. *The American journal of clinical nutrition* **2005,** *81* (1), 215S-217S.

46.   Clifford, M., Diet-derived phenols in plasma and tissues and their implications for health. *Planta medica* **2004,** *70* (12), 1103-1114.

47.   Schwedhelm, E.; Maas, R.; Troost, R.; Böger, R. H., Clinical pharmacokinetics of antioxidants and their impact on systemic oxidative stress. *Clinical pharmacokinetics* **2003,** *42* (5), 437-459.

48.   Ottaviani, J. I.; Borges, G.; Momma, T. Y.; Spencer, J. P.; Keen, C. L.; Crozier, A.; Schroeter, H., The metabolome of [2-14 C](−)-epicatechin in humans: implications for the assessment of efficacy, safety and mechanisms of action of polyphenolic bioactives. *Scientific reports* **2016,** *6* (1), 1-10.

49.   Qu, Z.; Liu, A.; Li, P.; Liu, C.; Xiao, W.; Huang, J.; Liu, Z.; Zhang, S., Advances in physiological functions and mechanisms of (−)-epicatechin. *Critical reviews in food science and nutrition* **2021,** *61* (2), 211-233.

50.   Nakagawa, K.; Miyazawa, T., Chemiluminescence–high-performance liquid chromatographic determination of tea catechin, (−)-epigallocatechin 3-gallate, at picomole levels in rat and human plasma. *Analytical biochemistry* **1997,** *248* (1), 41-49.

51.   Monagas, M.; Urpi-Sarda, M.; Sánchez-Patán, F.; Llorach, R.; Garrido, I.; Gómez-Cordovés, C.; Andres-Lacueva, C.; Bartolomé, B., Insights into the metabolism and microbial biotransformation of dietary flavan-3-ols and the bioactivity of their metabolites. *Food & function* **2010,** *1* (3), 233-253.

52.   Kohri, T.; Suzuki, M.; Nanjo, F., Identification of metabolites of (−)-epicatechin gallate and their metabolic fate in the rat. *Journal of Agricultural and Food Chemistry* **2003,** *51* (18), 5561-5566.

53.   Narumi, K.; Sonoda, J.-I.; Shiotani, K.; Shigeru, M.; Shibata, M.; Kawachi, A.; Tomishige, E.; Sato, K.; Motoya, T., Simultaneous detection of green tea catechins and gallic acid in human serum after ingestion of green tea tablets using ion-pair high-performance liquid chromatography with electrochemical detection. *Journal of Chromatography B* **2014,** *945*, 147-153.

54.   Chow, H. S.; Cai, Y.; Alberts, D. S.; Hakim, I.; Dorr, R.; Shahi, F.; Crowell, J. A.; Yang, C. S.; Hara, Y., Phase I pharmacokinetic study of tea polyphenols following single-dose administration of epigallocatechin gallate and polyphenon E. *Cancer Epidemiology and Prevention Biomarkers* **2001,** *10* (1), 53-58.

55.   Gross, G.; Jacobs, D. M.; Peters, S.; Possemiers, S.; van Duynhoven, J.; Vaughan, E. E.; Van de Wiele, T., In vitro bioconversion of polyphenols from black tea and red wine/grape juice by human intestinal microbiota displays strong interindividual variability. *Journal of agricultural and food chemistry* **2010,** *58* (18), 10236-10246.

56.   Kohri, T.; Matsumoto, N.; Yamakawa, M.; Suzuki, M.; Nanjo, F.; Hara, Y.; Oku, N., Metabolic fate of (−)-[4-3H] epigallocatechin gallate in rats after oral administration. *Journal of agricultural and food chemistry* **2001,** *49* (8), 4102-4112.

57.   Del Rio, D.; Calani, L.; Cordero, C.; Salvatore, S.; Pellegrini, N.; Brighenti, F., Bioavailability and catabolism of green tea flavan-3-ols in humans. *Nutrition* **2010,** *26* (11-12), 1110-1116.

58.   Uhlenhut, K.; Högger, P., Facilitated cellular uptake and suppression of inducible nitric oxide synthase by a metabolite of maritime pine bark extract (Pycnogenol). *Free Radical Biology and Medicine* **2012,** *53* (2), 305-313.

59.   Thursby, E.; Juge, N., Introduction to the human gut microbiota. *Biochemical Journal* **2017,** *474* (11), 1823-1836.

60.   Lozupone, C. A.; Stombaugh, J. I.; Gordon, J. I.; Jansson, J. K.; Knight, R., Diversity, stability and resilience of the human gut microbiota. *Nature* **2012,** *489* (7415), 220-230.

61.   Eckburg, P. B.; Bik, E. M.; Bernstein, C. N.; Purdom, E.; Dethlefsen, L.; Sargent, M.; Gill, S. R.; Nelson, K. E.; Relman, D. A., Diversity of the human intestinal microbial flora. *science* **2005,** *308* (5728), 1635-1638.

62.   Almeida, A.; Mitchell, A. L.; Boland, M.; Forster, S. C.; Gloor, G. B.; Tarkowska, A.; Lawley, T. D.; Finn, R. D., A new genomic blueprint of the human gut microbiota. *Nature* **2019,** *568* (7753), 499-504.

63.   Falony, G.; Joossens, M.; Vieira-Silva, S.; Wang, J.; Darzi, Y.; Faust, K.; Kurilshikov, A.; Bonder, M. J.; Valles-Colomer, M.; Vandeputte, D., Population-level analysis of gut microbiome variation. *Science* **2016,** *352* (6285), 560-564.

64.   Louis, P.; Flint, H. J., Formation of propionate and butyrate by the human colonic microbiota. *Environmental microbiology* **2017,** *19* (1), 29-41.

65.   Kutschera, M.; Engst, W.; Blaut, M.; Braune, A., Isolation of catechin‐converting human intestinal bacteria. *Journal of applied microbiology* **2011,** *111* (1), 165-175.

66.   Takagaki, A.; Nanjo, F., Bioconversion of (−)-epicatechin,(+)-epicatechin,(−)-catechin, and (+)-catechin by (−)-epigallocatechin-metabolizing bacteria. *Biological and Pharmaceutical Bulletin* **2015,** *38* (5), 789-794.

67.   Sanchez-Patan, F.; Tabasco, R.; Monagas, M.; Requena, T.; Pelaez, C.; Moreno-Arribas, M. V.; Bartolome, B., Capability of Lactobacillus plantarum IFPL935 to catabolize flavan-3-ol compounds and complex phenolic extracts. *Journal of agricultural and food chemistry* **2012,** *60* (29), 7142-7151.

68.   Odamaki, T.; Kato, K.; Sugahara, H.; Hashikura, N.; Takahashi, S.; Xiao, J.-z., Abe, F.; Osawa, R., Age-related changes in gut microbiota composition from newborn to centenarian: a cross-sectional study. *BMC microbiology* **2016,** *16* (1), 1-12.

69.   Mackie, R. I.; Sghir, A.; Gaskins, H. R., Developmental microbial ecology of the neonatal gastrointestinal tract. *The American journal of clinical nutrition* **1999,** *69* (5), 1035s-1045s.

70.   Dominguez-Bello, M. G.; Costello, E. K.; Contreras, M.; Magris, M.; Hidalgo, G.; Fierer, N.; Knight, R., Delivery mode shapes the acquisition and structure of the initial microbiota across multiple body habitats in newborns. *Proceedings of the National Academy of Sciences* **2010,** *107* (26), 11971-11975.

71.   Cheng, J.; Ringel-Kulka, T.; Heikamp-de Jong, I.; Ringel, Y.; Carroll, I.; de Vos, W. M.; Salojärvi, J.; Satokari, R., Discordant temporal development of bacterial phyla and the emergence of core in the fecal microbiota of young children. *The ISME journal* **2016,** *10* (4), 1002-1014.

72.   Laitinen, K.; Mokkala, K., Overall dietary quality relates to gut microbiota diversity and abundance. *International journal of molecular sciences* **2019,** *20* (8), 1835.

73.   Zivkovic, A. M.; German, J. B.; Lebrilla, C. B.; Mills, D. A., Human milk glycobiome and its impact on the infant gastrointestinal microbiota. *Proceedings of the National Academy of Sciences* **2011,** *108* (Supplement 1), 4653-4658.

74.   Wu, G. D.; Chen, J.; Hoffmann, C.; Bittinger, K.; Chen, Y.-Y.; Keilbaugh, S. A.; Bewtra, M.; Knights, D.; Walters, W. A.; Knight, R., Linking long-term dietary patterns with gut microbial enterotypes. *Science* **2011,** *334* (6052), 105-108.

75.   Liu, Z.; de Bruijn, W. J.; Bruins, M. E.; Vincken, J.-P., Reciprocal interactions between epigallocatechin-3-gallate (EGCG) and human gut microbiota in vitro. *Journal of Agricultural and Food Chemistry* **2020,** *68* (36), 9804-9815.

76.   Mena, P.; Ludwig, I. A.; Tomatis, V. B.; Acharjee, A.; Calani, L.; Rosi, A.; Brighenti, F.; Ray, S.; Griffin, J. L.; Bluck, L. J., Inter-individual variability in the production of flavan-3-ol colonic metabolites: Preliminary elucidation of urinary metabotypes. *European journal of nutrition* **2019,** *58* (4), 1529-1543.

77.   Mena, P.; Bresciani, L.; Brindani, N.; Ludwig, I. A.; Pereira-Caro, G.; Angelino, D.; Llorach, R.; Calani, L.; Brighenti, F.; Clifford, M. N., Phenyl-γ-valerolactones and phenylvaleric acids, the main colonic metabolites of flavan-3-ols: Synthesis, analysis, bioavailability, and bioactivity. *Natural product reports* **2019,** *36* (5), 714-752.

78.   Wu, T.; Grootaert, C.; Pitart, J.; Vidovic, N. K.; Kamiloglu, S.; Possemiers, S.; Glibetic, M.; Smagghe, G.; Raes, K.; Van de Wiele, T., Aronia (Aronia melanocarpa) polyphenols modulate the microbial community in a Simulator of the Human Intestinal Microbial Ecosystem (SHIME) and decrease secretion of proinflammatory markers in a Caco‑2/endothelial cell coculture model. *Molecular nutrition & food research* **2018,** *62* (22), 1800607.

79.   Koper, J. E.; Loonen, L. M.; Wells, J. M.; Troise, A. D.; Capuano, E.; Fogliano, V., Polyphenols and tryptophan metabolites activate the aryl hydrocarbon receptor in an in vitro model of colonic fermentation. *Molecular nutrition & food research* **2019,** *63* (3), 1800722.

80.   Li, Q.; Van Herreweghen, F.; De Mey, M.; Goeminne, G.; Van de Wiele, T., The Donor-Dependent and Colon-Region-Dependent Metabolism of (+)-Catechin by Colonic Microbiota in the Simulator of the Human Intestinal Microbial Ecosystem. *Molecules* **2022,** *27* (1), 73.

81.   Bäckhed, F.; Fraser, C. M.; Ringel, Y.; Sanders, M. E.; Sartor, R. B.; Sherman, P. M.; Versalovic, J.; Young, V.; Finlay, B. B., Defining a healthy human gut microbiome: current concepts, future directions, and clinical applications. *Cell host & microbe* **2012,** *12* (5), 611-622.

82.   Fassarella, M.; Blaak, E. E.; Penders, J.; Nauta, A.; Smidt, H.; Zoetendal, E. G., Gut microbiome stability and resilience: elucidating the response to perturbations in order to modulate gut health. *Gut* **2021,** *70* (3), 595-605.

83.   Wang, D.; Zhang, M.; Wang, T.; Liu, T.; Guo, Y.; Granato, D., Green tea polyphenols mitigate the plant lectins-induced liver inflammation and immunological reaction in C57BL/6 mice via NLRP3 and Nrf2 signaling pathways. *Food and Chemical Toxicology* **2020,** *144*, 111576.

84.   Zhang, Y.-P.; Yang, X.-Q.; Yu, D.-K.; Xiao, H.-Y.; Du, J.-R., Nrf2 signalling pathway and autophagy impact on the preventive effect of green tea extract against alcohol-induced liver injury. *Journal of Pharmacy and Pharmacology* **2021,** *73* (7), 986-995.

85.   Zhao, Y.; Liu, X.; Fu, X.; Mo, Z.; Jiang, Y.; Yan, Y., Protective effects of epigallocatechin gallate against ischemia reperfusion injury in rat skeletal muscle via activating Nrf2/HO-1 signaling pathway. *Life sciences* **2019,** *239*, 117014.

86.   Hagiu, A.; Attin, T.; Schmidlin, P. R.; Ramenzoni, L. L., Dose-dependent green tea effect on decrease of inflammation in human oral gingival epithelial keratinocytes: in vitro study. *Clinical oral investigations* **2020,** *24* (7), 2375-2383.

87.   Yarmush, M. L.; Jayaraman, A., Advances in proteomic technologies. *Annual review of biomedical engineering* **2002,** *4* (1), 349-373.

88.   Suhre, K.; McCarthy, M. I.; Schwenk, J. M., Genetics meets proteomics: perspectives for large population-based studies. *Nature Reviews Genetics* **2021,** *22* (1), 19-37.

89.   Ahmad, Y.; Lamond, A. I., A perspective on proteomics in cell biology. *Trends in cell biology* **2014,** *24* (4), 257-264.

90.   Chen, C.; Hou, J.; Tanner, J. J.; Cheng, J., Bioinformatics methods for mass spectrometry-based proteomics data analysis. *International journal of molecular sciences* **2020,** *21* (8), 2873.

91.   The Gene Ontology resource: enriching a GOld mine. *Nucleic Acids Research* **2021,** *49* (D1), D325-D334.

92.   Eden, E.; Navon, R.; Steinfeld, I.; Lipson, D.; Yakhini, Z., GOrilla: a tool for discovery and visualization of enriched GO terms in ranked gene lists. *BMC bioinformatics* **2009,** *10* (1), 1-7.

93.   Conesa, A.; Götz, S.; García-Gómez, J. M.; Terol, J.; Talón, M.; Robles, M., Blast2GO: a universal tool for annotation, visualization and analysis in functional genomics research. *Bioinformatics* **2005,** *21* (18), 3674-3676.

94.   Huang, D. W.; Sherman, B. T.; Tan, Q.; Kir, J.; Liu, D.; Bryant, D.; Guo, Y.; Stephens, R.; Baseler, M. W.; Lane, H. C., DAVID Bioinformatics Resources: expanded annotation database and novel algorithms to better extract biology from large gene lists. *Nucleic acids research* **2007,** *35* (suppl_2), W169-W175.

95.   Mering, C. v.; Huynen, M.; Jaeggi, D.; Schmidt, S.; Bork, P.; Snel, B., STRING: a database of predicted functional associations between proteins. *Nucleic acids research* **2003,** *31* (1), 258-261.

96.   Zhou, Y.; Zhou, B.; Pache, L.; Chang, M.; Khodabakhshi, A. H.; Tanaseichuk, O.; Benner, C.; Chanda, S. K., Metascape provides a biologist-oriented resource for the analysis of systems-level datasets. *Nature communications* **2019,** *10* (1), 1-10.

97.   Palsson, B. Ø., *Systems biology: properties of reconstructed networks*. Cambridge university press: 2006.

98.   Castrillo, J. I.; Pir, P.; Oliver, S. G., Yeast Systems Biology: towards a systems understanding of regulation of eukaryotic networks in complex diseases and biotechnology. In *Handbook of Systems Biology*, Elsevier: 2013; pp 343-365.

99.   Rietjens, I. M.; Louisse, J.; Punt, A., Tutorial on physiologically based kinetic modeling in molecular nutrition and food research. *Molecular nutrition & food research* **2011,** *55* (6), 941-956.

100.   Johnson, G.; Soeteman-Hernández, L.; Gollapudi, B.; Bodger, O.; Dearfield, K.; Heflich, R.; Hixon, J.; Lovell, D.; MacGregor, J.; Pottenger, L., Derivation of point of departure (PoD) estimates in genetic toxicology studies and their potential applications in risk assessment. *Environmental and molecular mutagenesis* **2014,** *55* (8), 609-623.

2

Chapter 2

Interindividual differences in human intestinal microbial conversion of (-)-epicatechin to bioactive phenolic compounds

Chen Liu, Jacques Vervoort, Karsten Beekmann, Marta Baccaro, Lenny Kamelia, Sebas Wesseling, Ivonne M.C.M. Rietjens

Abstract

To quantify interindividual differences in human intestinal microbial metabolism of the (-)-epicatechin (EC), *in vitro* anaerobic incubations with fecal inocula from 24 healthy donors were conducted. EC derived colonic microbial metabolites were qualitatively and quantitively analyzed by liquid chromatograph triple quadrupole mass spectrometry (LC-TQ-MS) and liquid chromatograph time-of-flight mass spectrometry (LC-TOF-MS). Quantitative microbiota characterization was achieved by 16S rRNA analysis. Results obtained show 1-(3',4'-dihydroxyphenyl)-3-(2'',4'',6''-trihydroxyphenyl)-2-propanol (3,4-diHPP-2-ol) and 5-(3',4'-dihydroxyphenyl)-γ-valerolactone (3,4-diHPV) to be key intermediate microbial metabolites of EC and also revealed substantial interindividual differences in both the rate of EC conversion and the time-dependent EC metabolite pattern. Furthermore, substantial differences in microbiota composition among different individuals were detected. Correlations between specific microbial phylotypes and formation of certain metabolites were established. It is concluded that interindividual differences in the intestinal microbial metabolism of EC may contribute to interindividual differences in potential health effects of EC-abundant dietary foods or drinks.

Keywords: (-)-epicatechin; phenyl-γ-valerolactones; microbiota; microbial metabolism; inter-individual differences

1. Introduction

EC is one of the important dietary catechins that belongs to the group of flavan-3-ols and widely exists in plant-based foods, e.g., cocoa, apple, green tea, berries, chocolates, grape seeds, etc.[1-3] The ingestion of these EC-rich foods are often reported to be associated with beneficial health effects, including anti-inflammatory, cardioprotective, anti-cancer activities, etc.[4-7] However, the bioavailability of catechins has been reported to be low due to the fact that upon ingestion in the small intestine only a limited amount of the parent compounds will be absorbed with subsequent phase II biotransformation reactions, i.e., conjugated in glucuronidation, methylation, and/or sulfation reactions.[8-9] A substantial part of the catechins is known to be passed on to the large intestine, where they are subject to intense microbial metabolism to form a battery of smaller phenolic molecules.[10-11] For example, although EC possesses the highest bioavailability among other major catechins, e.g., (-)-epigallocatechin (EGC), (-)-epicatechin-3-*O*-gallate (ECG) and (-)-epigallocatechin-3-*O*-gallate (EGCG), still only about 20% of intake was reported to pass into the systemic circulation via absorption in the small intestine, while over 70% of the ingested EC appeared to end up in the systemic circulation in the form of colonic phenolic metabolites.[11-12] These intestinal microbial metabolites thus contribute substantially to the systemic metabolites of EC.[13]

An overview of the major metabolic pathways in the potential intestinal microbial degradation of EC is presented in **Figure 1**. Given the many potential metabolites that can be formed and the substantial differences in the interindividual composition of the human microbiota,[14-15] the microbial metabolic routes of EC may be expected to show interindividual differences, which have not been characterized so far.[9] Additionally, knowledge on the microbiota-mediated conversion of catechins is limited.
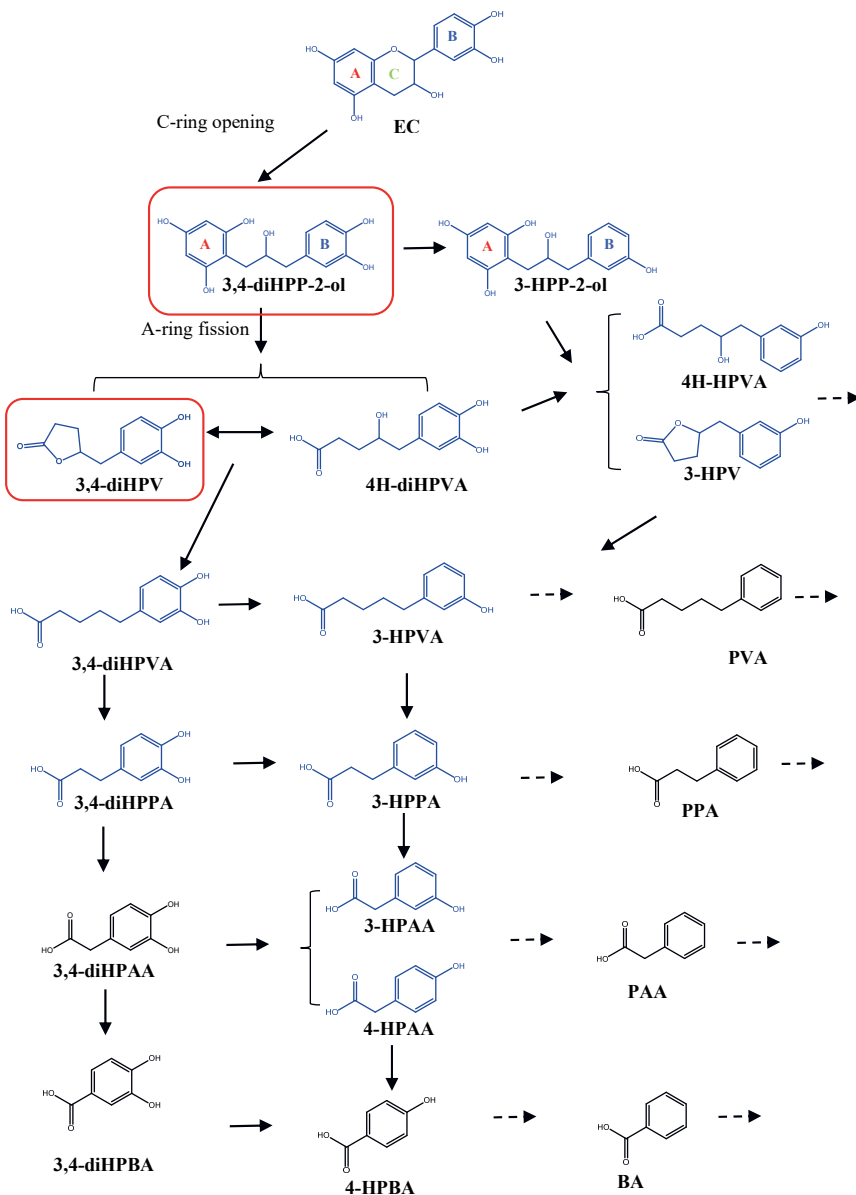
Figure 1. Proposed pathways for the colonic metabolism of EC. Structures in blue-color were detected in the present study. The chemicals in the red boxes (i.e., 1-(3',4'-dihydroxyphenyl)-3-(2'',4'',6''-trihydroxyphenyl)-2-propanol (3,4-diHPP-2-ol), 5-(3',4'-dihydroxyphenyl)-γ-valerolactone (3,4-diHPV)) were the major metabolites formed in the time-depend *in vitro* fecal incubation.

The aim of the present study was to obtain insight into the potential interindividual human differences in this intestinal microbial metabolism of EC. This insight will also contribute to a better understanding of the causal relationship between EC intake and potential beneficial effects since it has been hypothesized that these are due to the microbial metabolites of EC.[16-18]

2. Materials and Methods

2.1 Chemicals and reagents.

EC, catechol, gallic acid, 3'-hydroxyphenylacetic acid (3-HPAA), 4'-hydroxyphenylacetic acid (4-HPAA), 3-(3'-hydroxyphenyl)propionic acid (3-HPPA), 3-(3',4'-dihydroxyphenyl)propionic acid (3,4-diHPPA), 5-(3'-hydroxyphenyl)valeric acid (3-HPVA), 5-(3',4'-dihydroxyphenyl)valeric acid (3,4-diHPVA) and glycerol were purchased from Sigma-Aldrich (Zwijndrecht, The Netherlands). 5-(3'-hydroxyphenyl)-γ-valerolactone (3-HPV) and 5-(3',4'-dihydroxyphenyl)-γ-valerolactone (3,4-diHPV) were purchased from Enamine (Kyiv, Ukraine). Methanol and acetonitrile (ACN) were obtained from Biosolve BV (Valkenswaard, The Netherlands). Phosphate buffer saline (PBS) was purchased from Gibco (Paisley, UK). Acetic acid was ordered from Merck KGaA (Darmstadt, Germany) and formic acid was purchased from VWR CHEMICA (Amsterdam, The Netherlands).

2.2 Fecal slurry preparation

Feces were collected from 24 healthy individuals without dietary restrictions. They were of different gender, age, and ethnicity. All of them had not taken antibiotics for at least 3 months prior to the study. After volunteers' donations, fecal samples were collected and weighed, and then immediately transferred to the anaerobic operating chamber BACTRON300 (Cornelius, USA) with an atmosphere of 85% N_2, 10% CO_2, and 5% H_2 within 5 minutes. Subsequently, fecal samples were diluted with an anaerobic solution of 10% (v/v) glycerol in PBS to obtain a final fecal concentration of 20% (w/v). Samples were filtered in Para-Pak SpinCon tubes (New Hampshire, USA) by centrifugation (21,500 g for 5 minutes at 4 °C) to remove the larger particles and the resulting fecal suspension was collected and aliquoted. A pooled sample was obtained by mixing equal volumes of the first 14 fecal suspensions and subsequently aliquoted. All the above-mentioned steps were carried out under anaerobic conditions. In the end, all samples were stored at -80 °C until use. The effect of freezing, storing and thawing on the microbial metabolism of EC by the fecal samples was tested and shown not to significantly affect the activity (**Figure S1** in Supporting Information). The experimental protocol was

approved not to require further evaluation by the Medical Ethical Reviewing Committee of Wageningen University (METC-WU) based on Dutch Medical Research Involving Human Subjects Act. All participants gave their written consent.

2.3 Fecal batch-culture incubation

The experiments were performed in 1.5 mL Eppendorf tubes containing 39.5 µL anaerobic PBS, 10 µL of the fecal slurries (final fecal concentration: 40 mg/mL) and 0.5 µL EC (added from a 100 times concentrated stock solution in methanol; final concentration 100 µM) or methanol as control (referred to as "negative control"). The final concentration of 100 µM EC allows detection of the substrate and its metabolites without affecting the microbiota.[19] Incubations of EC without fecal slurries were included as blank control. All fecal incubations were carried out in the BACTRON300 anaerobic chamber with an atmosphere of 85% N_2, 10% CO_2, and 5% H_2 at 37 °C. Aliquots of fermented fecal samples (50µL) were collected after 0, 1, 2, 3, 4, 5, 6, and 24 h of incubation and the reaction was terminated by adding 1 volume of ice-cold methanol. For studies on interindividual differences, a timepoint of 2 h was selected. Subsequently, samples were put on ice for at least 15 minutes, followed by centrifugation at 21,500 g for 15 minutes at 4 °C to precipitate proteins, microorganisms, etc. The supernatant of each sample was collected and stored immediately at -80 °C until LC-TQ-MS and LC-TOF-MS analysis. The incubation of each individual and pooled fecal sample was performed in triplicate.

2.4 LC-TQ-MS analysis

A Shimadzu LC-TQ-MS 8045 was used to quantify the concentration of EC and its metabolites. This equipment consisted of an ultra high-performance liquid chromatography system coupled to a tandem triple quadrupole mass spectrometer containing an ESI source ('s- Hertogenbosch, The Netherland). The ESI source was operated in negative ion mode, and fragment ions *m/z* were obtained. Chromatographic separation was performed on a Waters Acquity UPLC® BEH C18 column (2.1 × 50 mm; 1.7 µm) at 40 °C. Solvent A was composed of water : acetic acid (999 : 1, v/v), and solvent B was methanol absolute. The eluents were delivered at a flow rate of 0.4 mL/min and the following gradient was used: 0 - 0.5 min: 5% B, 0.5 - 5 min: 5 - 25% B, 5 - 6 min: 25 - 100% B, 6 - 7 min: 100% B, 7 - 8 min: 100 - 5% B, 8 - 13 min: 5% B. The ESI parameters were as follows: nebulizing gas flow, 3.0 L/min; drying gas flow and heating gas flow, 10.0 L/min; interface temperature, 300 °C; desolvation temperature, 250 °C; heat block temperature, 400 °C. Chromatographic peaks were identified by comparison of the retention time and the ion values of the samples with those of the commercial authentic standards. The

identification information for EC and its potential colonic metabolites is summarized in **Table 1**. These compounds were included in the triple quadrupole based on several *in vitro* and *in vivo* studies reporting their formation.[3, 8-9, 11, 20-22] To quantify the metabolites formed during *in vitro* incubations, a set of mixed authentic standards were used to build calibration curves as appropriate using fourteen concentrations ranging between 0.01 μM and 50 μM (the area of peak against the concentration was obtained to define the linear regression equation). To guarantee the accuracy of each quantification, a set of calibrators to define the calibration curve was included in each measurement series. Concentrations of formed metabolites were calculated correcting for values of parallel negative controls incubated without EC. Each experimental replicate was corrected with the mean value of 3 negative controls obtained for the respective fecal sample.

2.5 LC-TOF-MS analysis

An Agilent 1200 series high-performance liquid chromatography system coupled with a Bruker micrOTOF was applied to qualitatively and quantitively detect 3,4-diHPP-2-ol, 1-(3'-hydroxyphenyl)-3-(2'',4'',6''-trihydroxyphenyl)-2-propanol (3-HPP-2-ol), 4-hydroxy-5-(3',4'-dihydroxyphenyl)-valeric acid (4H-diHPVA) and 4-hydroxy-5-(3'-hydroxyphenyl)-valeric acid (4H-HPVA). Chromatographic separation was performed on the same column as used in the LC-TQ-MS analysis. Solvent A was composed of water : formic acid (999 : 1, v/v) and solvent B was ACN : water (999 : 1, v/v). The eluents were delivered at a flow rate of 0.2 mL/min and the following gradient was used: 0 - 2.5 min: 100% A, 2.5 - 40 min: 0 - 40% B, 40 - 45 min: 40 - 100% B, 45 - 50 min: 100% B, 50 – 55 min: 100 - 0% B, 55 - 90 min: 100% A. The mass detection was operated in negative mode. Relative retention time and M-H value were used to identify these three EC colonic metabolites. Specifically, molecules such as 3,4-diHPP-2-ol, 3-HPP-2-ol and 4H-diHPVA have high M-H values (i.e., 291.09, 275.09 and 225.08) which are unique in the EC microbial conversion pathway. Furthermore, their time-dependent formations (e.g., the first two metabolites were largely detected at early hours of incubation) were taken into consideration. Additionally, chemical standards used in LC-TQ-MS were also analyzed in LC-TOF-MS, which helped to distinguish compounds sharing the same M-H values. For example, although 4H-HPVA and 3,4-diHPVA share the same M-H value in negative mode, the measurement of the 3,4-diHPVA standard in LC-TOF-MS ensured the unequivocal identification of both 3,4-diHPVA and 4H-HPVA. Altogether, this approach and the combination of LC-TQ-MS and LC-TOF-MS ensured the unequivocal identification of also those metabolites for which standards were not available. The quantification was carried out

through the calibration curves of EC (for quantifications of 3,4-diHPP-2-ol and 3-HPP-2-ol) or 3,4-diHPV (for quantifications of 4H-diHPVA and 4H-HPVA). Detailed identification information is summarized in **Table 1**.

2.6 Microbial taxonomic profiling and total bacterial load

Aliquots of all 24 fecal samples were sent to an accredited commercial laboratory (IMGM Laboratories GmbH, Martinsried, Germany) for DNA extraction, PCR, library preparation, and sequencing. Additionally, quantification of the bacterial load was carried out by real-time qPCR. PCR products were generated by amplification using 16S V3-V4 primers (F-NXT-Bakt-341F: 5'-CCTACGGGNGGCWGCAG-3' and R-NXT-Bakt-805R: 5'-GACTACHVGGGTATCTAATCC-3'). During an index PCR, barcodes for multiplexed sequencing were introduced using overhang tags. A sequencing library was prepared from barcoded PCR products and sequenced on the Illumina® MiSeq next generation sequencing system (Illumina® Inc.). Signals were processed to *.fastq-files and the resulting 2×250 bp reads were demultiplexed. Microbiota identification was carried out by clustering the operational taxonomic units (OTU).

2.7 Data analysis

Metabolic profile data acquisition and processing were carried out using Labsolutions software in the LC-TQ-MS system and HyStar software in the LC-TOF-MS system. Graphics were drawn by using Graphpad Prism 8.2 (San Diego, USA). ChemDraw 18.0 (PerkinElmer, Waltham, USA) was used to draw chemical structures. Results are shown as mean ± standard deviation (SD). Subsequently, principal component analysis (PCA) was applied to study the differences and relatedness of metabolic profiles following fecal incubations of EC (at t = 2 h) between different individuals. Using this approach, the multivariate metabolic profile data derived from interindividual fecal incubations were summarized, simplified, and then transformed into a smaller dataset called principal components (PCs) of PCA. In addition to PCA, a following heatmap to visualize the hierarchic clustering of different individuals, based on their metabolic profiles and EC residual, was also done. Both PCA and heatmap development were done using XLSTAT (Addinsoft, New York, USA). Spearman's rank correlation coefficients ρ $(-1 \leq \rho \leq 1)$ were calculated between the concentration of the 6 most relevant metabolites present after 2 hours of incubation and the relative abundance of the phyla (range between 0 - 100%). To display the correlations, a heatmap was constructed. Statistically significant correlation was tested by Student t-test (p < 0.05).

3. Results

## 3.1 LC-TQ-MS and LC-TOF-MS based identification of colonic metabolites of EC

Upon time-dependent incubation of EC with fecal samples, various metabolites were formed. These metabolites were identified and quantified based on chromatography of standard reference compounds, coupled with mass spectrometric fragmentation patterns. The analytical details of the LC-TQ-MS and LC-TOF-MS based detection of EC and its potential colonic metabolites are summarized in **Table 1**. In total, along the 8-hour incubation time, 12 metabolites, of which the chemical structures are highlighted in **Figure 1** in blue-color, were observed. These metabolites were 3,4-diHPP-2-ol, 3-HPP-2-ol, 4H-diHPVA, 3,4-diHPV, 4H-HPVA, 3-HPV, 3,4-diHPVA, 3-HPVA, 3,4-diHPPA, 3-HPPA, 3-HPAA and 4-HPAA.

Table 1. LC-TQ-MS and LC-TOF-MS Identification of EC and its Potential Colonic Metabolites, based on Relative Retention Time and MS (or MS Fragmentation) Values

Analytical platform	Chemical	Parent ion (m/z)	Product ion (m/z)	Collision energy [1]	Retention time
LC-TQ-MS	EC	289.1	245.10, 109.10, 203.00	14, 25, 18	5.72
	3,4-diHPVA	209.0	135.10, 191.05, 122.10	18, 15, 21	7.60
	3,4-diHPV	207.1	163.05, 122.15, 161.10	16, 21, 21	5.00
	3-HPVA	193.1	106.15, 149.05, 175.05	23, 17, 15	7.88
	3-HPV	191.1	147.05, 102.90, 135.00	8, 15, 15	6.93
	3,4-diHPPA	181.1	137.10, 59.00, 109.00	14, 17, 15	3.95
	3-HPPA	165.1	121.20, 106.10, 119.15	13, 22, 16	6.33
	3-HPAA	151.0	107.10, 65.00	12, 25	4.30
	4-HPAA	151.0	107.10, 79.15, 93.20	10, 20, 22	3.82
	Catechol	109.2	90.95, 81.10, 53.15	22, 21, 20	1.85
LC-TOF-MS	3,4-diHPP-2-ol	291.09	\	\	19.6
	3-HPP-2-ol	275.09	\	\	23.1
	4H-diHPVA	225.08	\	\	15.7
	4H-HPVA	209.08	\	\	15.2

Quantification was achieved via calibration curves made using commercially available reference compounds, except for 3,4-diHPP-2-ol, 3-HPP-2-ol, 4H-diHPVA and 4H-HPVA for which authentic references were not available. For these compounds, quantification was achieved using the calibration curves of EC for the first two and of 3,4-diHPV for the last two, based on their structural similarity. However, the amount of 4H-HPVA observed appeared to be below the levels required for quantification. The limit of detection (LOD) and the limit of

quantification (LOQ) of these compounds were listed in **Table S1** in Supporting Information. **Figure 2** presents the metabolite concentrations detected at increasing time of incubation with pooled fecal samples. Concentrations of metabolites formed were calculated, including a correction for the amounts detected in corresponding negative controls incubated without adding EC. Six polyphenols were detected in the negative controls albeit in limited amounts (generally < 11.5% of total mass recovery) (**Figure S2** in Supporting Information). The results obtained result in total molar mass recoveries that ranged between 82.9% to 112.9%, being somewhat lower at the later time points (**Table 2**). Comparison of the time-dependent metabolite profiles reveals similar patterns with 3,4-diHPP-2-ol being the first (detectable) and most abundant metabolite formed within the first 2 hours of incubation, representing more than 70% of the initial amount of EC. Upon prolonged incubation, its relative abundance dropped to 23.7 ± 10.4% of EC equivalents at 3 h while this metabolite was no longer detected at and beyond 4 h incubation. On the contrary, 3,4-diHPV was detected in large amount at later timepoints (3 - 6 h) and appeared to be the dominant metabolite in the metabolite patterns at and beyond 3 hours of incubation. Its relative abundance appeared to be relatively constant from 3 h to 6 h, ranging between 45.0% to 49.2% of the total metabolite pattern. In blank control incubations where EC was incubated without fecal slurries, no metabolite formation was observed, and EC was stable with an average mass recovery at all incubation time points of 95.3%. (**Figure S4** in Supporting Information).
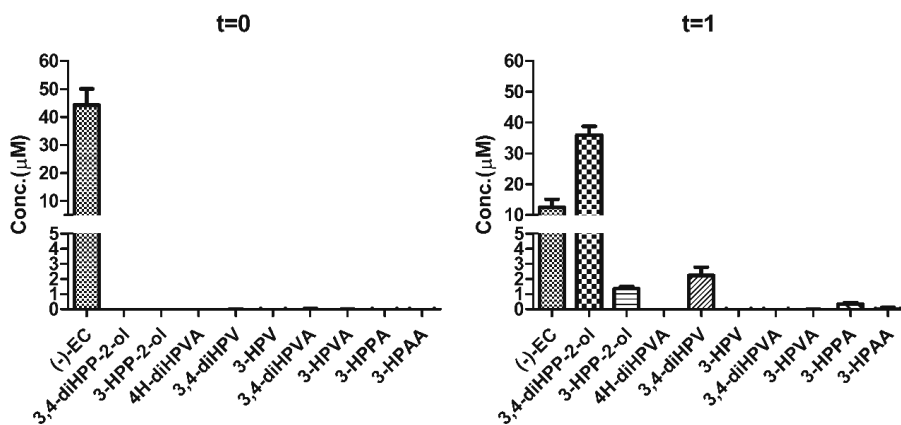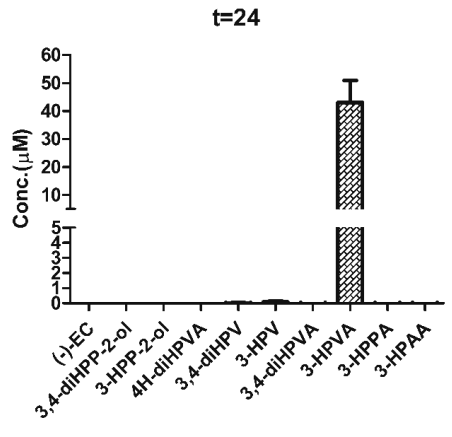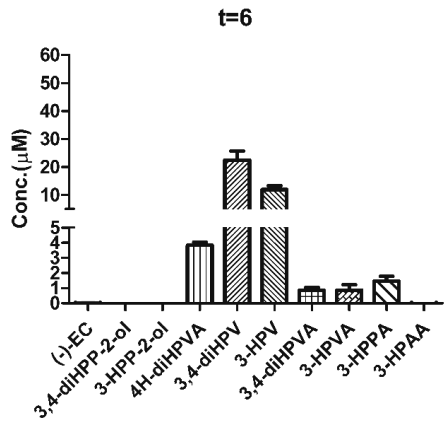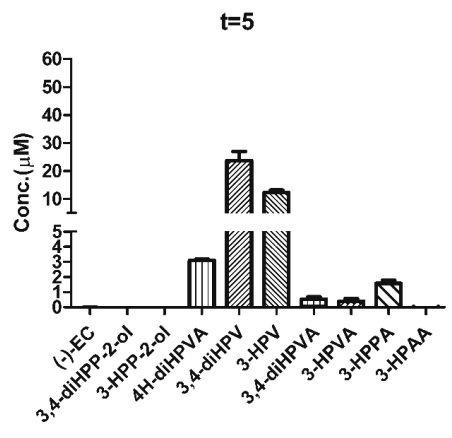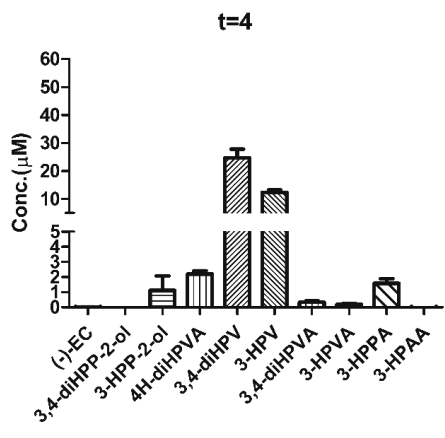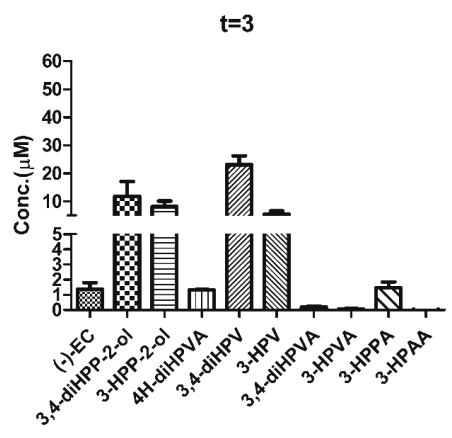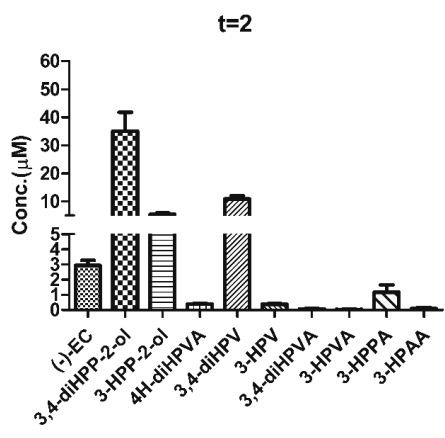
Figure 2. Time-dependent quantitative analysis of EC and its microbial metabolites formed during 24 hours of anaerobic incubation with a pooled fecal sample from fourteen donors. Results are shown as mean ± SD from three independent incubations.

Table 2. Molar Mass Recoveries for EC and its Colonic Metabolites (%) during 24 Hours of Anaerobic Incubation with a Pooled Faecal Sample from Fourteen Donors. Results are Shown as Mean ± SD from Three Independent Incubations.

Chemical	0 (h)	1 (h)	2 (h)	3 (h)	4 (h)	5 (h)	6 (h)	24 (h)
EC[a]	88.54 ± 11.51	24.92 ± 5.21	5.86 ± 0.68	2.74 ± 0.86	0.04 ± 0.03	0.01 ± 0.01	0.03 ± 0.03	n.d. [c]
3,4-diHPP-2-ol[b]	n.d.	71.92 ± 5.61	70.13 ± 13.47	23.74 ± 10.42	n.d.	n.d.	n.d.	n.d.
3-HPP-2-ol[b]	n.d.	2.72 ± 0.27	10.86 ± 0.84	16.32 ± 3.89	2.22 ± 1.93	n.d.	n.d.	n.d.
4H-diHPVA[b]	n.d.	n.d.	0.79 ± 0.10	2.64 ± 0.04	4.39 ± 0.42	6.20 ± 0.14	7.68 ± 0.39	n.d.
3,4-diHPV[a]	n.d.	4.48 ± 1.08	21.78 ± 2.19	46.19 ± 6.37	49.19 ± 6.48	47.48 ± 6.37	45.01 ± 6.25	0.04 ± 0.08
3-HPV[a]	n.d.	n.d.	0.75 ± 0.12	11.03 ± 2.15	24.68 ± 1.62	24.51 ± 1.80	23.76 ± 2.75	0.17 ± 0.14
3,4-diHPVA[a]	n.d.	n.d.	0.14 ± 0.07	0.39 ± 0.10	0.68 ± 0.16	1.08 ± 0.29	1.69 ± 0.40	n.d.
3-HPVA[a]	n.d.	0.02 ± 0.02	0.06 ± 0.06	0.09 ± 0.09	0.36 ± 0.18	0.79 ± 0.34	1.73 ± 0.71	86.14 ± 15.61
3-HPPA[a]	n.d.	0.66 ± 0.22	2.34 ± 0.95	2.94 ± 0.75	3.14 ± 0.65	3.16 ± 0.40	2.95 ± 0.62	n.d.
3-HPAA[a]	n.d.	0.03 ± 0.23	0.16 ± 0.18	n.d.	n.d.	n.d.	n.d.	n.d.
Total	88.54	104.75	112.88	106.08	84.70	83.23	82.85	86.35

(a) qualitatively and quantitatively detected by LC-TQ-MS

(b) qualitatively and quantitatively detected by LC-TOF-MS

(c) Not detected.

3.2 Comparison of EC *in vitro* metabolite profiles to reported *in vivo* plasma or urinary EC metabolite data

To enable evaluation of the *in vitro* metabolite profiles obtained, the human intestinal microbial metabolite patterns obtained in the anaerobic fecal incubations in the present study were compared to available literature data on EC metabolite patterns in human plasma and urine upon oral dosing.[8, 11] Wiese et al. (2015) reported that after ingestion of EC by six volunteers, four major microbial metabolites could be identified in the pharmacological kinetic course in human plasma samples including: 4-HPAA, ferulic acid, 3,4-diHPV, and 4H-diHPVA.[8] In the fecal incubations, three of these four metabolites were detected i.e., 3,4-diHPV, 4H-diHPVA, 4-HPAA, with the latter being present in trace amounts only. The formation of ferulic acid takes place in the liver and kidney,[9] hence it was not targeted in the *in vitro* incubation. Ottaviani et al. (2016) reported time-dependent EC urinary metabolites from eight volunteers after intake of the ^{14}C-EC test drink. They reported that about 70% of ingested EC was absorbed in the large

intestine.[11] In both studies, 3,4-diHPV conjugates were the most abundant EC metabolites. **Figure 3** presents a comparison of the time-dependent relative abundance of 3,4-diHPV formed in the *in vitro* fecal incubation model and in the *in vivo* plasma and urinary metabolite patterns (summing up unconjugated and conjugated forms) after the ingestion of EC. Similar kinetics were observed. Moreover, the total excretion of 3,4-diHPV conjugates accounted for 53.5% of the total EC that passed into the large intestine, which is comparable with the large and stable amount (45.0 - 49.2% of total metabolite pattern) produced in the *in vitro* fecal incubations.
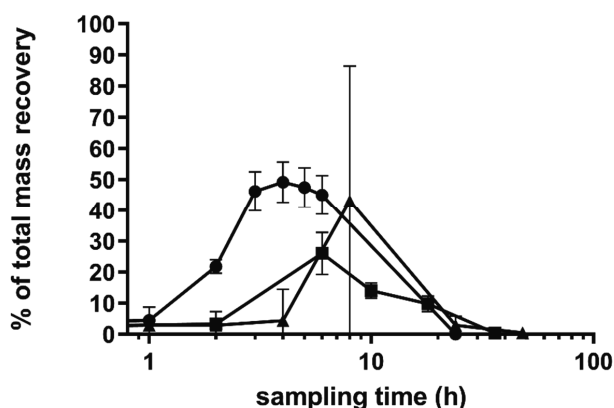

Figure 3. Comparison of EC microbial metabolite 3,4-diHPV from *in vivo* human urine samples (square, Ottaviani et al., 2016), human plasma samples (triangle, Wiese et al., 2015) and the *in vitro* data from the present study (circle).

3.3 Interindividual differences of EC bioconversion by human colonic microbiota

Based on the results obtained for the time-dependent *in vitro* microbial EC conversion in incubations with a pooled fecal sample, a period of 2 hours was selected to quantify potential human interindividual differences in EC intestinal microbial metabolism. This time point was selected as still residual EC was present while also showing substantial metabolite formation. At 1 h, limited colonic metabolites were detected, while at 3 h, the residual EC was limited (less than 3% of the original amount). Furthermore, the number of colonic metabolites detected at t = 3 h is the same as at t = 2 h. **Figure 4** provides an overview of the metabolite profiles detected after 2 hours incubation of EC with fecal slurries from 24 individual human donors. Phenolic compounds quantified in different individuals in the negative controls are presented in **Figure S3** in the Supporting Information. All phenolics were present in the negative controls at levels

< 12.8% of total mass recovery with the exception of 3-HPPA (82.5% of total mass recovery) in individual 3 and 3,4-diHPPA (22.5% of total mass recovery) in individual 5. Data from **Figure 4** clearly elucidate that the metabolite patterns obtained upon 2 h incubation with the fecal slurries from different individuals show marked differences in terms of both the types and amounts of metabolites formed as well as in the level of EC conversion. For instance, in the incubations with fecal slurry from individuals 8 and 16, 23.0 and 14.8 µM of EC (46.1% and 29.6% of the amount added) remained, respectively, while in incubations with fecal slurry from individuals 10 and 22 this amounted to less than 1 µM (< 1.3%) of EC (0.3 and 0.6 µM, respectively). Meanwhile, also substantial differences were observed for the major metabolite 3,4-diHPV. For instance, 26.9 µM (53.8% of original EC equivalents) of 3,4-diHPV was formed by individual 10, while only 1.8 µM (3.5% of original EC equivalents) was detected in incubations with fecal slurry from individual 1 and none for individual 8. On the basis of the data obtained, it can be concluded that the amount of residual EC after the first 2 hours of incubation differed up to 76.7-fold (calculated by using the highest EC residual from individual 8, i.e., 23.0 µM, divided by the lowest EC residual from individual 10, i.e., 0.3 µM) between the 24 individuals (**Figure 4**). It appears that individuals 8 and 16 can be classified as slow EC metabolizers (< 70.4% EC conversion within the first 2 hours) and the other individuals were defined as fast EC metabolizers (> 88.7% EC conversion within the first 2 hours). Setting 3,4-diHPV as the biomarker of EC colonic microbial bioconversion, individuals 3, 10 and 17 can be classified as fast 3,4-diHPV producers (> 47.3% of original EC equivalents of 3,4-diHPV formed within the first 2 hours). Individual 22 was detected to form the highest level of 3-HPV (17.5% of original EC equivalents) among others, which is likely due to the fast dehydroxylation of 3,4-diHPV. The other individuals showed lower formation of 3,4-diHPV either because of a relatively low EC clearance rate (individuals 8 and 16) or due to the accumulation of the precursor 3,4-diHPP-2-ol.

Besides differences in the rate of metabolic conversion also the types of metabolites observed in the metabolite profiles formed by the different individuals varied from one another. For example, besides EC, only 3,4-diHPP-2-ol was detected in incubations with fecal slurry from individual 8, while 11 different metabolites were observed in incubation with individuals 1 and 7. Additionally, for individual 5, only dihydroxyphenols were detected in the metabolic profile which may indicate this individual is in favor of producing dihydroxyphenolics rather than monohydroxyphenolics. Moreover, unlike most individuals, individual 9 tended to produce 3-

HPP-2-ol (60.2% of original EC equivalents) rather than 3,4-diHPP-2-ol (14.9% of original EC equivalents).
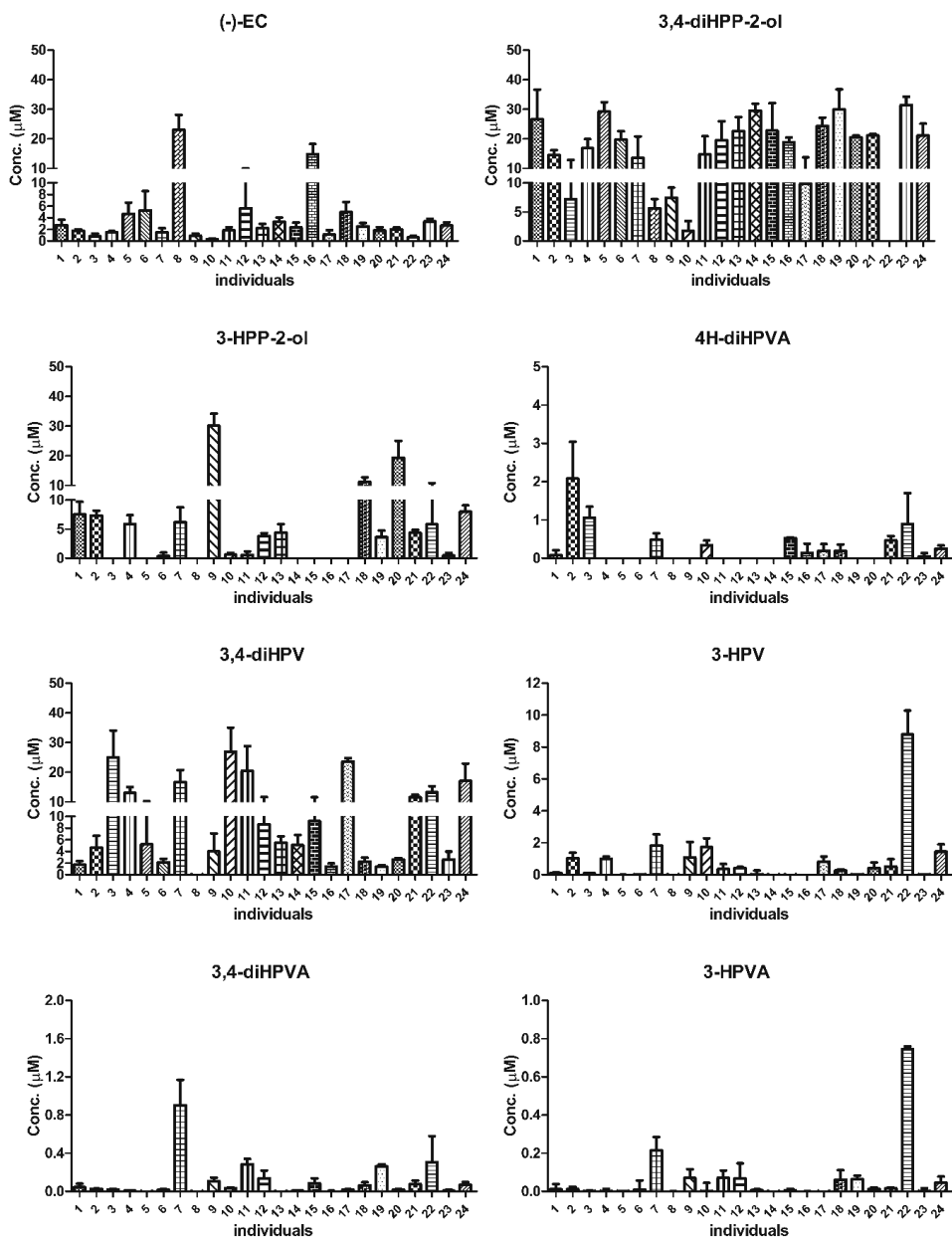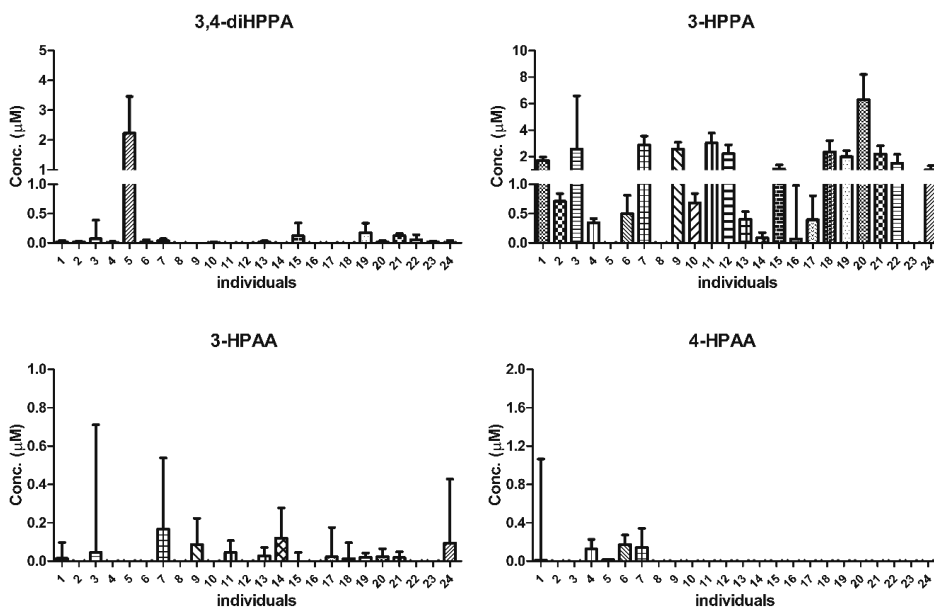
Figure 4. EC metabolite patterns formed in incubations with fecal slurries from 24 individuals at 2 h. Molar mass recoveries for EC and its colonic metabolites of each individual ranged from 53.3% to 103.1% (**Figure S7** in supporting information).

3.4 Class signatures of metabolic profiles and hierarchic clustering of 24 individuals

To further evaluate the interindividual differences in the intestinal microbial metabolic patterns and the possible existence of metabotypes among the 24 individuals, a PCA analysis was performed. The quantified amounts of the residual EC and all the 11 metabolites detected at t = 2 h (**Figure 4**) were used as data input for XLSTAT. The PCA results thus obtained revealed that only 43.8% of all variance in the metabolite patterns could be explained by 2 PCs (i.e., PC1 and PC2; **Figure S5** in Supporting Information). For a further evaluation, the quantified amounts of the residual EC and only its six major metabolites detected at t = 2 h, were used to define the multivariate dataset for the PCA analysis. These six major metabolites included 3,4-diHPP-2-ol, 3-HPP-2-ol, 3,4-diHPV, 3-HPV, 3-HPVA and 3-HPPA. The PCA analysis thus obtained (**Figure 5**) could explain 62.2% of the variation in the metabolite profiles using only 2 PCs (PC1 and PC2). PC1 accounts for the largest possible variance in the dataset (38.3%), where PC2 captures 23.9% of the remaining variation. In order to visualize the hierarchic clustering of different individuals based on their metabolic profiles, a heatmap was produced

(**Figure 6**). From the heatmap, it appears that individuals 18, 1 and 19 cluster together mainly due to the similar amounts of residual EC and 3,4-diHPP-2-ol in their metabolite patterns at 2 hours incubation, while the individuals 23, 5 and 14 cluster together because of similar amounts in these two compounds as well. In the PCA biplot, these individuals also locate close to one another driven by these similar metabolite levels. Individuals 9 and 20 cluster together and clearly separated from the other individuals, both in the PCA plot as well as in the heatmap, due to substantially higher amounts of 3-HPP-2-ol and 3-HPPA formed. Individual 22 was fully separated from other individuals both in the PCA plot and the heatmap mainly because of a high level of 3-HPV. Furthermore, individuals 8 and 16 cluster together in the heatmap because of the high residual amount of EC in line with their earlier identification as slow metabolizers. Individuals 10 and 17 cluster together, also clearly separated from the other individuals in the heatmap and PCA plot because of the substantially higher level of 3,4-diHPV in the metabolite profile at 2 hours incubation time.
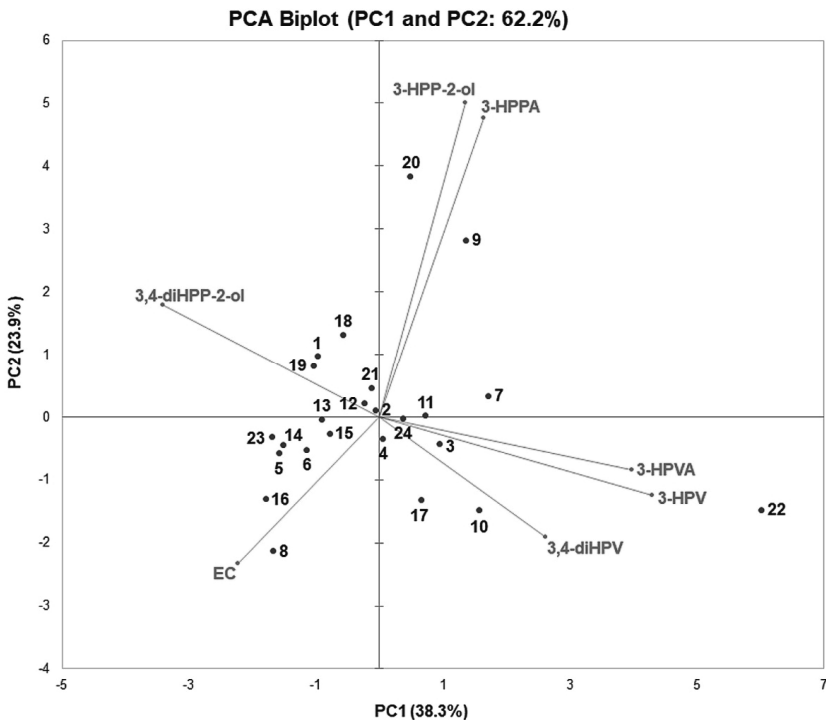

Figure 5. PCA based on the concentration of residual EC and the six major EC microbial metabolites present in incubations with fecal slurries from 24 individuals at 2 h.

Figure 6. Hierarchic clustering illustrated by heatmap composed based on the concentration of residual EC and the six major EC microbial metabolites present in incubations with fecal slurries from 24 individuals at 2 h.
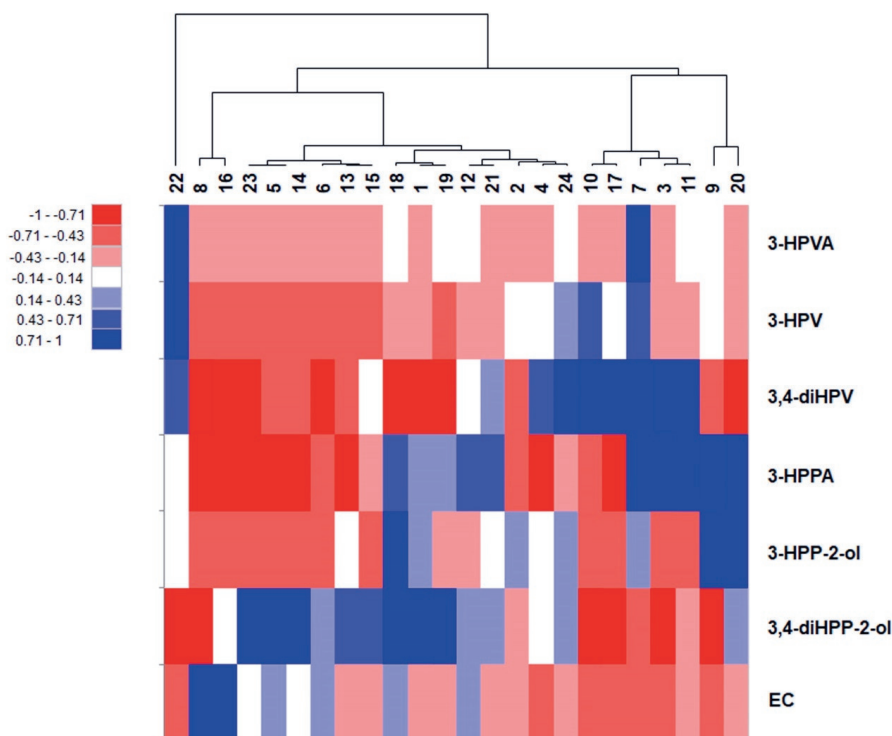
3.5 Quantitative microbial profile and correlation with metabolite formation

In **Figure 7**, the relative microbial profile at the *phylum* level of the 24 individual fecal samples is reported. The bacteria fall into nine different phyla, in particular *Firmicutes, Bacteroidetes, Actinobacteria, Proteobacteria, Verrucomicrobia, Tenericutes, Euryarchaeota, Fusobacterial* and *Fibrobacteres*. Interindividual differences in the microbial relative abundance were observed. However, bacteria belonging to *Firmicutes* and *Bacteroidetes* were consistently found to be the dominant phyla in all samples. Detailed information of the relative/absolute taxon abundances and diversity at the phylum/genus level were included in the Supporting Information File1.
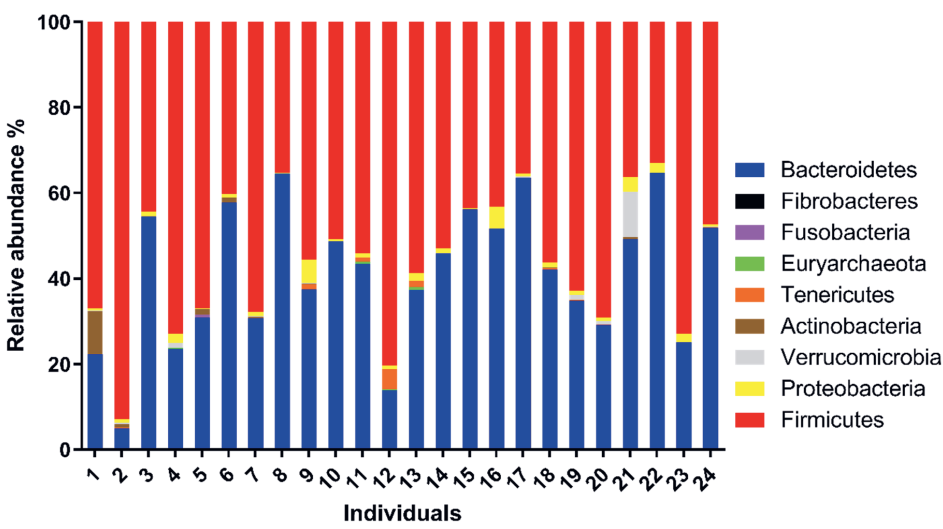
Figure 7. Relative microbial profile at the *phylum* level of the 24 human fecal samples

In order to reveal the interplay between the microbial taxonomic profile of the fecal samples of the 24 individuals and their intestinal microbial metabolite profiles, a Spearman correlation study was performed between the relative abundance of the bacterial phyla and the concentrations of the most relevant metabolites present after 2 hours of incubation in the fecal slurry incubations (correlations at bacterial genus level was presented in **Figure S6** in Supporting Information). **Figure 8** illustrates the Spearman correlation coefficients by a heatmap. The statistical correlation is significant ($p < 0.05$) with $\rho \leq -0.39$ or $\rho \geq 0.39$. The results thus obtain reveal several significant correlations for 3-HPP-2-ol, an early metabolite in the metabolic pattern of EC (**Figure 1**), showing a negative correlation with the amount of *Bacteroidetes* and positive correlations with the amount of *Firmicutes*, *Verrucomicrobia*, *Actinobacteria* and *Tenericutes*. A significant positive correlation was also found for 3,4-diHPP-2-ol with the amount of *Actinobacteria*.
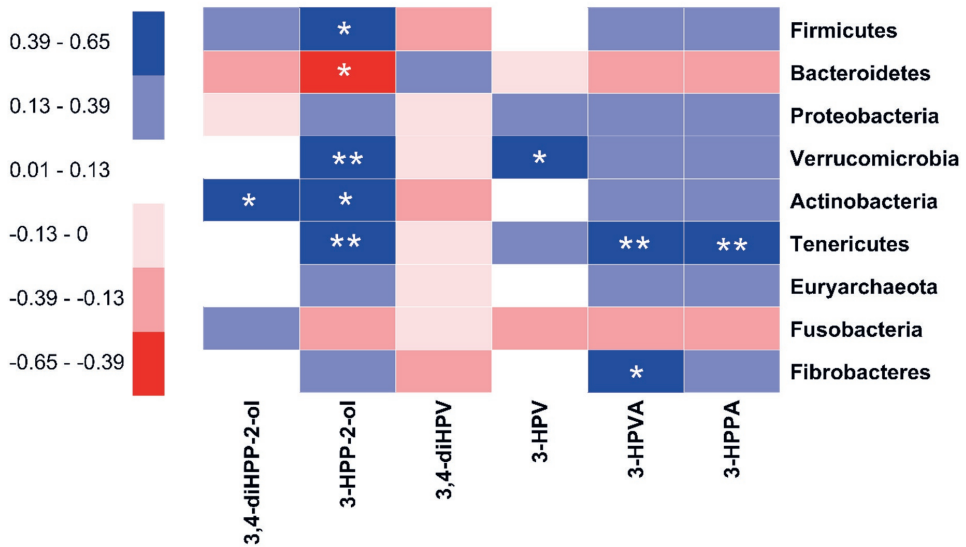
Figure 8. Spearman correlations between the taxon abundances of nine bacterial phyla and the concentration of six major EC microbial metabolites present in incubations with fecal slurries from 24 individuals at 2 h. The sign and strength of the Spearman correlation coefficients are represented as colors (blue: positive; red: negative). The significances of the correlations are indicated by asterisks: *****P < 0.05, ******P < 0.01.

4. Discussion

In the present study, it was shown that *in vitro* anaerobic fecal incubations can be used to characterize *in vivo* colonic metabolism and related human plasma metabolites of the model catechin EC. During pooled human fecal incubations, nine colonic metabolites of EC could be detected and quantified. Most of these intermediates are also reported in previous studies using human or animal *in vitro* fecal incubation models[21, 23-25] or in plasma, urine and feces in human or animal interventions.[8, 26-27] The relative abundance of these microbial metabolites varied between different studies. For instance, 3-HPPA was reported to be the predominant metabolite in two *in vitro* human fecal incubation studies[28-29] while it was detected in our *in vitro* model to only a limited extent. These different results could result from different materials used (e.g., different fecal sources) or different experimental conditions (e.g., different extraction methods) applied. The results obtained in our study showed that together with 3,4-diHPV, its precursor, 3,4-diHPP-2-ol were the two most dominant metabolites formed in the fecal incubations with pooled human fecal samples. The formation of 3,4-diHPV as a major EC colonic metabolite is

in line with previous studies.[30-32] The latter intermediate is often suggested to be a transient catabolite,[23, 25, 33] which was also confirmed in this study. Its formation is the result of the first step in EC colonic microbial metabolism, formed by the cleavage of the C ring of EC. This intermediate would be rapidly metabolized into 3,4-diHPV, which seemed to be more stable since this phenyl-γ-valerolactone was present at a high abundance at 3 h and beyond (around 45% - 50% of total mass balance). In the present study, we investigated the use of an *in vitro* anaerobic fecal incubation model to study the colonic metabolism of EC. This model does not account for the uptake of EC in the small intestine and its subsequent conjugation. However, under *in vivo* conditions, the percentage of EC ending up in the large intestine is known to be substantial (~ 70%), although it may vary with the individual.[20] This importance of colonic metabolism is corroborated by the fact that the absorption of EC in the small intestine was reported to be only up to ~ 20%.[11] The importance also follows from the fact that among all colonic metabolites, 3,4-diHPV derived metabolites were reported to account for 42 - 60% of the EC intake,[11, 34] which is in agreement with the results derived from the *in vitro* incubations in the present study. This emphasizes the importance of the intestinal microbiome in improving the bioavailability of catechins, or rather of their intestinal metabolites.

Furthermore, the results of the present study also revealed that 3-HPVA was the terminal metabolite upon 24 hours anaerobic incubations when EC was completely degraded. This metabolite may result from the further conversion of 3-HPV which is believed to be formed by reverse Claisen-driven degradation of the A-ring of EC.[35] 3-HPVA accounted for 86.1% of the total molar mass at 24 h (and even at 48 h (data not shown)) whereas at these time points the residual amounts of other phenolic metabolites were negligible, pointing at their further degradation by the colonic bacteria of these other phenolic metabolites, while the degradation of 3-HPVA is apparently limited. This result is in line with what was reported by Stoupi et al. (2010), demonstrating that 3-HPVA together with 3-HPPA and phenyl acetic acid were dominant metabolites after 24 h or longer incubations with human fecal samples.[28] However, this 3-HPVA metabolite may have very limited efficacy in the host because the phenylcarboxylic acids are hydrophilic with poor solubility within biological membranes, which restrict their bioavailability resulting in limited bioefficacies.[36] This is important when studying the physiological consequences of microbial metabolism of EC.

The *in vitro* time-dependent formation of the major metabolite 3,4-diHPV was compared with *in vivo* plasma and urinary data. The result indicates that the *in vitro* metabolite patterns matched the *in vivo* patterns quite well and that the fecal incubations may provide an adequate

mean to obtain insight into the intestinal microbial conversions. This conclusion is in line with that reported by Lagkouvardos et al. (2017), who performed a thorough review on the cultivation of bacteria from the intestine of mammals, concluding that up to 65% of molecular species detected by sequencing have corresponding strains in culture.[37] It is also in line with a study that compared microbial-related *in vivo* metabolic changes in gut tissue, cecum content and feces of rats treated with antibiotics concluding that 'as a non-invasive sampling method, feces provide a suitable matrix for studies on metabolism by the gut microbiota'.[38] Thus, using fecal incubations to describe intestinal microbial metabolism appears to provide a useful approach. In addition, it is noted that an *in vivo* study with the same donors as the ones used for donation of the fecal samples remains of interest for future studies to enable further evaluation of this *in vitro* incubation model. Also, comparison with more than the currently available *in vivo* studies, and/or similar studies with other substrates for colonic metabolism would be of use.

In the next step, the *in vitro* fecal incubation method was used to study interindividual differences in EC microbial metabolism. Substantial interindividual differences were observed in EC microbial metabolism both in terms of type and level of metabolites formed among 24 volunteers. To obtain insight in the potential underlying explanation, microbial taxonomy and relative abundance of the 24 fecal samples were characterized by 16S rRNA analysis. The results obtained indicate that, in line with the incubations with the pooled human fecal sample, 3,4-diHPP-2-ol and 3,4-diHPV were the two dominant colonic metabolites of EC. Interindividual differences in the rate of clearance of EC were observed, pointing at the existence of slow metabolizers of which 2 were identified among the 24 subjects. The difference in the rate of metabolism was also found previously for the conversion of 3-(4'-hydroxyphenyl)propionic acid to 3-phenylpropionic acid further indicating differences in the ability of the intestinal microbiota of individuals to metabolize phenolics.[29] Furthermore, differences in subsequent metabolic conversions resulted in different EC metabolite patterns among the individuals with 2 out 24 volunteers showing relatively high intermediate levels of accumulation of 3-HPP-2-ol and 3 individuals showing relatively high levels of the 3,4-diHPV, pointing at potentially slow metabolizers for respectively phenyl-γ-valerolactone formation or degradation. The high interindividual variations in metabolism (or formation) of EC and phenyl-γ-valerolactones was in agreement with reported *in vivo* human intervention studies.[32] For instance, Hollands and colleagues reported a 21-fold and 60-fold interindividual difference in urinary excretion of EC and phenyl-γ-valerolactones, respectively, after 28 days of daily

ingestion of high dose EC mixed with oligomeric procyanidins capsules.[39] Anesi and colleagues found a 7.5-fold variation in human urinary excretion of conjugated phenyl-γ-valerolactones after the consumption of apples.[2] These *in vivo* studies already pointed at interindividual differences in EC metabolism, based on two of its major urinary metabolites. The results of the present study reveal that interindividual differences in the microflora-derived production of EC metabolites may result in differences in colonic metabolites formed beyond differences in the formation of phenyl-γ-valerolactones. It is worth noting that some individuals might be able to form metabolites which were not included in the set of metabolites included in the present MS analytical methods, reflected by relatively lower mass recoveries, e.g., for individuals 8 and 6 a molar mass recovery of less than 60% was obtained (**Figure S7** in Supporting Information). We could hypothesize here that different individuals may have different metabolic pathways or different pathways could coexist at the same time, but the host may have its priorities from one another. However, for most individuals, the molecular mass balance of the metabolite patterns amounted to > 75% indicating the 11 metabolites now identified represent the majority of the patterns obtained.

There are a number of factors that can contribute to the interindividual metabotypes variations observed. Of all the factors, the host microbial profile is most obvious.[3, 40-41] There are 10^{11}-10^{12} bacteria/g in the colon content, the highest amount of all parts of the gastrointestinal tract of the host.[42] The individual microbiota composition patterns can be various because of different age, gender, ethnics, dietary and living habits, etc. Mena and colleagues were the first to describe three urinary metabotypes after daily ingestion of green tea extracts tablets for 8 weeks.[32, 40] The three putative metabotypes were characterized by different amounts of tri- and dihydroxyphenyl-γ-valerolactones and 3-(hydroxyphenyl)propionic acid produced among 11 volunteers. Given that in this study, green tea and not EC was dosed, the differences may in part also have been caused by differences in colonic metabolism of other green tea or dietary constituents, since in addition to EC also catechin, gallocatechins, procyanidins and prodelphinidins have been reported to be metabolized to phenyl-γ-valerolactones. Since the gut microbial compositions of these individuals were not studied, a link between the metabotypes and host microbial abundance was not established. In this sense, the microbial taxonomic abundance of 24 fecal samples was analyzed in the present study; correlations between microbial taxonomic abundance and metabolic abundance could be defined. The bacterial load results highlighted indeed rather a small variation where the loads of slow metabolizers (individuals 8 and 16) were not the lowest two among all individuals (**Figure S8** in Supporting

Information). The gene copy numbers per gram of fecal slurry were comparable to the ones of healthy human individuals reported in literature.[43] However, differences were observed both in the relative abundances and in the composition of the microbiota. To the best of our knowledge, *Eubacterium* SDG-2, *Lactobacillus plantarum*, *Eggerthella lenta* and *Adlercreutzia equolifaciens* are the only bacteria reported so far to be capable of producing the metabolite diphenylpropan-2-ol from epicatechin (or catechin), a reaction comparable to the formation of 3,4-diHPP-2-ol from EC detected in the present study. The first two belong to the phylum *Firmicutes* and the latter two to the phylum *Actinobacteria*.[44-46] Accordingly, in the present study, a statistically significant positive correlation was found between the abundance of *Actinobacteria* and the quantity of 3,4-diHPP-2-ol. In addition, we found statistically significant positive correlations between the relative abundance of *Lachnospiraceae NC2004 group* and the formation of 3,4-diHPP-2-ol, suggesting this bacterium to be able of cleaving the C-ring of EC, which was not reported before (**Figure S6** in Supporting Information). The levels of the dehydroxylated metabolite 3-HPP-2-ol were positively correlated with *Firmicutes*, *Verrucomicrobia*, *Actinobacteria* and *Tenericutes*, suggesting that the dehydroxylation reaction of phenolics is not a strain-specific microbial conversion. In the next metabolic step, diphenylpropan-2-ol is transformed into 3,4-diHPV and 4H-diHPVA, reported to be mediated by *Flavonifractor plautii*, which belongs to the family of *Ruminococcace*, phylum *Firmicutes*.[44] In the present study, we found that several bacteria from this family, *Ruminococcace*, were positively correlated with the formation of 3-HPP-2-ol, phenyl-γ-valerolactones and phenylvaleric acids (**Figure S6** in Supporting Information), indicating that these bacteria could be able to catalyze the conversion of diphenylpropan-2-ol to downstream metabolites and have the ability to perform a dehydroxylation reaction. Besides, *Phascolarctobacterium* was newly found to be significantly positively correlated with the concentration of 3,4-diHPV (**Figure S6** in Supporting Information). The relative abundance of *Prevotella 7* and *Bacteroides* were respectively positively and negatively associated with the production of 4H-diHPVA, phenyl-γ-valerolactones, phenylvaleric acids and 3-HPPA, which is in line with the conclusion derived from the human intervention study carried out by Trost and colleagues.[3] Additionally, several bacteria from other genera (e.g., *Barnesiella*, *Akkermansia*) also showed positive correlations with the formation of phenyl-γ-valerolactones, phenylvaleric acids and 3-HPPA, however, their relative abundances were generally lower than 1% in most individuals. Altogether, the correlations obtained support that in anaerobic fecal incubations provide a novel way to investigate the potential link between bacterial abundance and colonic metabolite patterns. Nevertheless, more work on screening and isolation of catechin-catalyzing bacteria is needed

in order to explain the observed different metabotypes after consumption of dietary flavan-3-ols.[47-48] Moreover, intestinal bacteria from different species also have the different metabolic ability in catechin biotransformation, which cannot be simply extrapolated from one species to another, further pointing at the relevance of developing and evaluating fecal incubations as an adequate model to obtain human data.[26]

It is interesting to note that the two major intermediates detected in our study, 3,4-diHPP-2-ol and 3,4-diHPV, both have a catechol moiety that possesses the potential to oxidize to quinones or semiquinones.[49] According to previous studies, catechins (or other flavonoids) were reported to activate the Keap1-Nrf2 pathway by means of their (semi)quinone formation.[50-51] The (semi)quinone-type metabolites were considered to play a role in the induction of detoxifying enzymes via activation of the Keap1-Nrf2 pathway.[51] Based on these considerations, we hypothesized that EC colonic metabolites (especially the catechol type phenolic EC metabolites), such as 3,4-diHPP-2-ol and 3,4-diHPV would be able to trigger the activation of the Keap1-Nrf2 pathway *in vivo* after EC-rich foods consumption, and may thus contribute to the observed health-promoting effects, as shown for other catechol containing phenolics.[52] The role of these EC colonic metabolites in inducing the beneficial effects of EC may also be relevant because these phenolic/catechol intestinal metabolites appear to be better bioavailable than the parent EC.[53] Although EC and its phenolic metabolites also have antioxidative properties, it should be noted that the capacity to activate the Keap1-Nrf2 pathway may prove more important for their beneficial health effects than their antioxidant activity since, given their low micromolar systemic concentrations[53-55] EC and its metabolites may *in vivo* not be able to effectively compete with the antioxidant activity of tocopherols and/or ascorbate, present in substantially higher concentrations. For instance, the *in vivo* concentrations of EC and its colonic metabolites were reported with a C_{max} of ~ 1.2 μM in plasma while α-tocopherol and ascorbic acid were reported to be around 24 μM and 70 μM, respectively, in the serum or plasma in Western populations.[11, 56]

In conclusion, microbial metabolism of EC is crucial in producing potential bioactive phenolics. Among all the colonic metabolites, 3,4-diHPV seems to be the most important metabolite considering its abundance, stability and catechol structural moiety. Striking inter-individual differences were found in the formation of EC intestinal microbial metabolites, including 3,4-diHPV, both in terms of type and level, which is likely due to the substantial variations of host microbiota composition. Altogether, our results suggest that substantial interindividual

differences in the gut microbial metabolism of EC may contribute to interindividual differences in the potential beneficial effects of EC-rich foods.

ABBREVIATIONS USED

LC-TQ-MS, liquid chromatograph triple quadrupole mass spectrometry; LC-TOF-MS, liquid chromatograph time-of-flight mass spectrometry; EC, (-)-epicatechin; ECG, (-)-epicatechin-3-*O*-galllate; EGC, (-)-epigallocatechin; EGCG, (-)-epigallocatechin-3-*O*-gallate; 3,4-diHPP-2-ol, 1-(3',4'-dihydroxyphenyl)-3-(2'',4'',6''-trihydroxyphenyl)-2-propanol; 3-HPP-2-ol, 1-(3'-hydroxyphenyl)-3-(2'',4'',6''-trihydroxyphenyl)-2-propanol; 4H-diHPVA, 4-hydroxy-5-(3',4'-dihydroxyphenyl)-valeric acid; 4H-HPVA, 4-hydroxy-5-(3'-hydroxyphenyl)-valeric acid; 3,4-diHPV, 5-(3',4'-dihydroxyphenyl)-γ-valerolactone; 3-HPV, 5-(3'-hydroxyphenyl)-γ-valerolactone; 3,4-diHPVA, 5-(3',4'-dihydroxyphenyl)valeric acid; 3-HPVA, 5-(3'-hydroxyphenyl)valeric acid; PVA, 5-phenylpentanoic acid; 3,4-diHPPA, 3-(3',4'-dihydroxyphenyl)propionic acid; 3-HPPA, 3-(3'-hydroxyphenyl)propionic acid; PPA, 3-phenylpropionic acid; 3,4-diHPAA, 3',4'-dihydroxyphenylacetic acid; 3-HPAA, 3'-hydroxyphenylacetic acid; 4-HPAA, 4'-hydroxyphenylacetic acid; PAA, phenylacetic acid; 3,4-diHPBA, 3',4'-dihydroxybenzoic acid; 4-HPBA, 4'-hydroxybenzoic acid; BA, hydroxybenzoic acid.

Notes

The authors declare no competing financial interest.

5. References

1.   Rodriguez-Mateos, A.; Cifuentes-Gomez, T.; Gonzalez-Salvador, I.; Ottaviani, J. I.; Schroeter, H.; Kelm, M.; Heiss, C.; Spencer, J. P., Influence of age on the absorption, metabolism, and excretion of cocoa flavanols in healthy subjects. *Mol. Nutr. Food Res.* **2015,** *59*, 1504-1512.

2.   Anesi, A.; Mena, P.; Bub, A.; Ulaszewska, M.; Del Rio, D.; Kulling, S. E.; Mattivi, F., Quantification of urinary phenyl-γ-valerolactones and related valeric acids in human urine on consumption of apples. *Metabolites* **2019,** *9*, 254.

3.   Trošt, K.; Ulaszewska, M. M.; Stanstrup, J.; Albanese, D.; De Filippo, C.; Tuohy, K. M.; Natella, F.; Scaccini, C.; Mattivi, F., Host: Microbiome co-metabolic processing of dietary polyphenols–An acute, single blinded, cross-over study with different doses of apple polyphenols in healthy subjects. *Food Res. Int.* **2018,** *112*, 108-128.

4.   Ruijters, E. J.; Weseler, A. R.; Kicken, C.; Haenen, G. R.; Bast, A., The flavanol (-)-epicatechin and its metabolites protect against oxidative stress in primary endothelial cells via a direct antioxidant effect. *Eur. J. Pharmacol.* **2013,** *715*, 147-153.

5.   Morrison, M.; van der Heijden, R.; Heeringa, P.; Kaijzel, E.; Verschuren, L.; Blomhoff, R.; Kooistra, T.; Kleemann, R., Epicatechin attenuates atherosclerosis and exerts anti-inflammatory effects on diet-induced human-CRP and NFκB in vivo. *Atherosclerosis* **2014,** *233*, 149-156.

6.   Claude, S.; Boby, C.; Rodriguez-Mateos, A.; Spencer, J. P.; Gérard, N.; Morand, C.; Milenkovic, D., Flavanol metabolites reduce monocyte adhesion to endothelial cells through modulation of expression of genes via p38-MAPK and p65-Nf-kB pathways. *Mol. Nutr. Food Res.* **2014,** *58*, 1016-1027.

7.   Saha, A.; Kuzuhara, T.; Echigo, N.; Suganuma, M.; Fujiki, H., New role of (−)-epicatechin in enhancing the induction of growth inhibition and apoptosis in human lung cancer cells by curcumin. *Cancer Prev. Res.* **2010,** *3*, 953-962.

8.   Wiese, S.; Esatbeyoglu, T.; Winterhalter, P.; Kruse, H. P.; Winkler, S.; Bub, A.; Kulling, S. E., Comparative biokinetics and metabolism of pure monomeric, dimeric, and polymeric flavan-3-ols: A randomized cross-over study in humans. *Mol. Nutr. Food Res.* **2015,** *59*, 610-621.

9.   Monagas, M.; Urpi-Sarda, M.; Sánchez-Patán, F.; Llorach, R.; Garrido, I.; Gómez-Cordovés, C.; Andres-Lacueva, C.; Bartolomé, B., Insights into the metabolism and microbial biotransformation of dietary flavan-3-ols and the bioactivity of their metabolites. *Food Funct.* **2010,** *1*, 233-253.

10.   Fraga, C. G.; Oteiza, P. I.; Galleano, M., Plant bioactives and redox signaling:(−)-Epicatechin as a paradigm. *Mol. Aspects Med.* **2018,** *61*, 31-40.

11.   Ottaviani, J. I.; Borges, G.; Momma, T. Y.; Spencer, J. P.; Keen, C. L.; Crozier, A.; Schroeter, H., The metabolome of [2-14 C](−)-epicatechin in humans: Implications for the assessment of efficacy, safety, and mechanisms of action of polyphenolic bioactives. *Sci. Rep.* **2016,** *6*, 29034.

12.   Stalmach, A.; Troufflard, S.; Serafini, M.; Crozier, A., Absorption, metabolism and excretion of Choladi green tea flavan-3-ols by humans. *Mol. Nutr. Food Res.* **2009,** *53*, S44-S53.

13.   Del Rio, D.; Calani, L.; Cordero, C.; Salvatore, S.; Pellegrini, N.; Brighenti, F., Bioavailability and catabolism of green tea flavan-3-ols in humans. *Nutrition* **2010,** *26*, 1110-1116.

14.   Guarner, F.; Malagelada, J.-R., Gut flora in health and disease. *Lancet* **2003,** *361*, 512-519.

15.   Eckburg, P. B.; Bik, E. M.; Bernstein, C. N.; Purdom, E.; Dethlefsen, L.; Sargent, M.; Gill, S. R.; Nelson, K. E.; Relman, D. A., Diversity of the human intestinal microbial flora. *Science* **2005,** *308*, 1635-1638.

16.   Koppel, N.; Rekdal, V. M.; Balskus, E. P., Chemical transformation of xenobiotics by the human gut microbiota. *Science* **2017,** *356*, eaag2770.

17.   Ozdal, T.; Sela, D. A.; Xiao, J.; Boyacioglu, D.; Chen, F.; Capanoglu, E., The reciprocal interactions between polyphenols and gut microbiota and effects on bioaccessibility. *Nutrients* **2016,** *8*, 78.

18.   Williamson, G.; Clifford, M. N., Role of the small intestine, colon and microbiota in determining the metabolic fate of polyphenols. *Biochem. Pharmacol.* **2017**, *139*, 24-39.

19.   Puupponen-Pimiä, R.; Nohynek, L.; Meier, C.; Kähkönen, M.; Heinonen, M.; Hopia, A.; Oksman-Caldentey, K. M., Antimicrobial properties of phenolic compounds from berries. *J. Appl. Microbiol.* **2001,** *90*, 494-507.

20.   Borges, G.; Ottaviani, J. I.; van der Hooft, J. J.; Schroeter, H.; Crozier, A., Absorption, metabolism, distribution and excretion of (−)-epicatechin: A review of recent findings. *Mol. Aspects Med.* **2018,** *61*, 18-30.

21.   Roowi, S.; Stalmach, A.; Mullen, W.; Lean, M. E.; Edwards, C. A.; Crozier, A., Green tea flavan-3-ols: colonic degradation and urinary excretion of catabolites by humans. *J. Agric. Food. Chem.* **2010,** *58*, 1296-1304.

22.   Chen, H.; Sang, S., Biotransformation of tea polyphenols by gut microbiota. *J. Funct. Foods* **2014,** *7*, 26-42.

23.   Takagaki, A.; Nanjo, F., Catabolism of (+)-catechin and (−)-epicatechin by rat intestinal microbiota. *J. Agric. Food. Chem.* **2013,** *61*, 4927-4935.

24.   Schantz, M.; Erk, T.; Richling, E., Metabolism of green tea catechins by the human small intestine. *Biotechnol. J.* **2010,** *5*, 1050-1059.

25.   Meselhy, M. R.; Nakamura, N.; Hattori, M., Biotransformation of (-)-epicatechin 3-O-gallate by human intestinal bacteria. *Chem. Pharm. Bull* **1997,** *45*, 888-893.

26.   Meng, X.; Sang, S.; Zhu, N.; Lu, H.; Sheng, S.; Lee, M.-J.; Ho, C.-T.; Yang, C. S., Identification and characterization of methylated and ring-fission metabolites of tea catechins formed in humans, mice, and rats. *Chem. Res. Toxicol.* **2002,** *15*, 1042-1050.

27.   Stalmach, A.; Mullen, W.; Steiling, H.; Williamson, G.; Lean, M. E.; Crozier, A., Absorption, metabolism, and excretion of green tea flavan-3-ols in humans with an ileostomy. *Mol. Nutr. Food Res.* **2010,** *54*, 323-334.

28.   Stoupi, S.; Williamson, G.; Drynan, J. W.; Barron, D.; Clifford, M. N., A comparison of the in vitro biotransformation of (−)-epicatechin and procyanidin B2 by human faecal microbiota. *Mol. Nutr. Food Res.* **2010,** *54*, 747-759.

29.   Gross, G.; Jacobs, D. M.; Peters, S.; Possemiers, S.; van Duynhoven, J.; Vaughan, E. E.; Van de Wiele, T., In vitro bioconversion of polyphenols from black tea and red wine/grape juice by human intestinal microbiota displays strong interindividual variability. *J. Agric. Food. Chem.* **2010,** *58*, 10236-10246.

30.   Appeldoorn, M. M.; Vincken, J.-P.; Aura, A.-M.; Hollman, P. C.; Gruppen, H., Procyanidin dimers are metabolized by human microbiota with 2-(3, 4-dihydroxyphenyl) acetic acid and 5-(3, 4-dihydroxyphenyl)-γ-valerolactone as the major metabolites. *J. Agric. Food. Chem.* **2009,** *57*, 1084-1092.

31.   Das, N., Studies on flavonoid metabolism: Absorption and metabolism of (+)-catechin in man. *Biochem. Pharmacol.* **1971,** *20*, 3435-3445.

32.   Mena, P.; Bresciani, L.; Brindani, N.; Ludwig, I. A.; Pereira-Caro, G.; Angelino, D.; Llorach, R.; Calani, L.; Brighenti, F.; Clifford, M. N., Phenyl-γ-valerolactones and phenylvaleric acids, the main colonic metabolites of flavan-3-ols: Synthesis, analysis, bioavailability, and bioactivity. *Nat. Prod. Rep.* **2019,** *36*, 714-752.

33.   Groenewoud, G.; Hundt, H., The microbial metabolism of (+)-catechin to two novel diarylpropan-2-ol metabolites in vitro. *Xenobiotica* **1984,** *14*, 711-717.

34.   Ottaviani, J. I.; Fong, R.; Kimball, J.; Ensunsa, J. L.; Britten, A.; Lucarelli, D.; Luben, R.; Grace, P. B.; Mawson, D. H.; Tym, A., Evaluation at scale of microbiome-derived metabolites as biomarker of flavan-3-ol intake in epidemiological studies. *Sci. Rep.* **2018,** *8*, 1-11.

35.   Stevens, J. F.; Maier, C. S., The chemistry of gut microbial metabolism of polyphenols. *Phytochem. Rev.* **2016,** *15*, 425-444.

36.   Semalty, A.; Semalty, M.; Singh, D.; Rawat, M., Phyto-phospholipid complex of catechin in value added herbal drug delivery. *J. Inclusion Phenom. Macrocyclic Chem.* **2012,** *73*, 377-386.

37.   Lagkouvardos, I.; Overmann, J.; Clavel, T., Cultured microbes represent a substantial fraction of the human and mouse gut microbiota. *Gut microbes* **2017,** *8*, 493-503.

38.   Behr, C.; Sperber, S.; Jiang, X.; Strauss, V.; Kamp, H.; Walk, T.; Herold, M.; Beekmann, K.; Rietjens, I.; Van Ravenzwaay, B., Microbiome-related metabolite changes in gut tissue, cecum content and feces of rats treated with antibiotics. *Toxicol. Appl. Pharmacol.* **2018,** *355*, 198-210.

39.   Hollands, W. J.; Philo, M.; Perez-Moral, N.; Needs, P. W.; Savva, G. M.; Kroon, P. A., Monomeric Flavanols Are More Efficient Substrates for Gut Microbiota Conversion to Hydroxyphenyl-γ-Valerolactone Metabolites Than Oligomeric Procyanidins: A Randomized, Placebo-Controlled Human Intervention Trial. *Mol. Nutr. Food Res.* **2020,** *64*, 1901135.

40.   Mena, P.; Ludwig, I. A.; Tomatis, V. B.; Acharjee, A.; Calani, L.; Rosi, A.; Brighenti, F.; Ray, S.; Griffin, J. L.; Bluck, L. J., Inter-individual variability in the production of flavan-3-ol colonic metabolites: Preliminary elucidation of urinary metabotypes. *European journal of nutrition* **2019,** *58* (4), 1529-1543.

41.   Eker, M. E.; Aaby, K.; Budic-Leto, I.; Rimac Brnčić, S.; El, S. N.; Karakaya, S.; Simsek, S.; Manach, C.; Wiczkowski, W.; de Pascual-Teresa, S., A review of factors affecting anthocyanin bioavailability: Possible implications for the inter-individual variability. *Foods* **2020,** *9*, 2.

42.   Possemiers, S.; Grootaert, C.; Vermeiren, J.; Gross, G.; Marzorati, M.; Verstraete, W.; de Wiele, T. V., The intestinal environment in health and disease-recent insights on the potential of intestinal bacteria to influence human health. *Curr. Pharm. Des.* **2009,** *15*, 2051-2065.

43.   Brukner, I.; Longtin, Y.; Oughton, M.; Forgetta, V.; Dascal, A., Assay for estimating total bacterial load: relative qPCR normalisation of bacterial load with associated clinical implications. *Diagn. Microbiol. Infect. Dis.* **2015,** *83*, 1-6.

44.   Kutschera, M.; Engst, W.; Blaut, M.; Braune, A., Isolation of catechin-converting human intestinal bacteria. *J. Appl. Microbiol.* **2011,** *111*, 165-175.

45.   Takagaki, A.; Nanjo, F., Bioconversion of (−)-epicatechin,(+)-epicatechin,(−)-catechin, and (+)-catechin by (−)-epigallocatechin-metabolizing bacteria. *Biol. Pharm. Bull.* **2015,** *38*, 789-794.

46.   Sánchez-Patán, F.; Tabasco, R.; Monagas, M.; Requena, T.; Peláez, C.; Moreno-Arribas, M. V.; Bartolomé, B. a., Capability of Lactobacillus plantarum IFPL935 to catabolize flavan-3-ol compounds and complex phenolic extracts. *J. Agric. Food. Chem.* **2012,** *60*, 7142-7151.

47.   Cortés-Martín, A.; Selma, M. V.; Tomás-Barberán, F. A.; González-Sarrías, A.; Espín, J. C., Where to look into the puzzle of polyphenols and health? The postbiotics and gut microbiota associated with human metabotypes. *Mol. Nutr. Food Res.* **2020,** *64*, 1900952.

48.   Espín, J. C.; González-Sarrías, A.; Tomás-Barberán, F. A., The gut microbiota: A key factor in the therapeutic effects of (poly) phenols. *Biochem. Pharmacol.* **2017,** *139*, 82-93.

49.   Awad, H. M.; Boersma, M. G.; Boeren, S.; van Bladeren, P. J.; Vervoort, J.; Rietjens, I. M., Structure−activity study on the quinone/quinone methide chemistry of flavonoids. *Chem. Res. Toxicol.* **2001,** *14*, 398-408.

50.   Lee-Hilz, Y. Y.; Boerboom, A.-M. J.; Westphal, A. H.; van Berkel, W. J.; Aarts, J. M.; Rietjens, I. M., Pro-oxidant activity of flavonoids induces EpRE-mediated gene expression. *Chem. Res. Toxicol.* **2006,** *19*, 1499-1505.

51.   Muzolf-Panek, M.; Gliszczyńska-Świgło, A.; de Haan, L.; Aarts, J. M.; Szymusiak, H.; Vervoort, J. M.; Tyrakowska, B.; Rietjens, I. M., Role of catechin quinones in the induction of EpRE-mediated gene expression. *Chem. Res. Toxicol.* **2008,** *21*, 2352-2360.

52.   Bolton, J. L.; Dunlap, T. L.; Dietz, B. M., Formation and biological targets of botanical o-quinones. *Food. Chem. Toxicol.* **2018,** *120*, 700-707.

53.   Clifford, M. N.; van der Hooft, J. J.; Crozier, A., Human studies on the absorption, distribution, metabolism, and excretion of tea polyphenols. *Am. J. Clin. Nutr.* **2013,** *98*, 1619S-1630S.

Chapter 2

54.   van Duynhoven, J.; van der Hooft, J. J.; van Dorsten, F. A.; Peters, S.; Foltz, M.; Gomez-Roldan, V.; Vervoort, J.; de Vos, R. C.; Jacobs, D. M., Rapid and sustained systemic circulation of conjugated gut microbial catabolites after single-dose black tea extract consumption. *J. Proteome Res.* **2014,** *13*, 2668-2678.

55.   Manach, C.; Williamson, G.; Morand, C.; Scalbert, A.; Rémésy, C., Bioavailability and bioefficacy of polyphenols in humans. I. Review of 97 bioavailability studies. *Am. J. Clin. Nutr.* **2005,** *81*, 230S-242S.

56.   Schwedhelm, E.; Maas, R.; Troost, R.; Böger, R. H., Clinical pharmacokinetics of antioxidants and their impact on systemic oxidative stress. *Clin. Pharmacokinet.* **2003,** *42*, 437-459.

Supporting Information

LOD and LOQ of EC and its major metabolites (Table S1); fresh and frozen faecal incubations (Figure S1); negative controls of pooled faecal incubations (Figure S2); negative controls of individual faecal incubations (Figure S3); EC contents of blank control (Figure S4); PCA of EC and its 11 metabolites (Figure S5); Spearman correlations between the taxon abundances of bacterial genera and the concentration of residual EC and eight EC microbial metabolites (Figure S6); total mass recoveries of 24 individuals (Figure S7); bacterial load of 24 individuals (Figure S8); absolute and relative bacteria in phylum and genus level (Supporting Information File1) (excel, can be found in the journal website).

Table S1. The limit of detection (LOD) and the limit of quantification (LOQ) of EC and its major colonic metabolites in LC-TQ-MS.

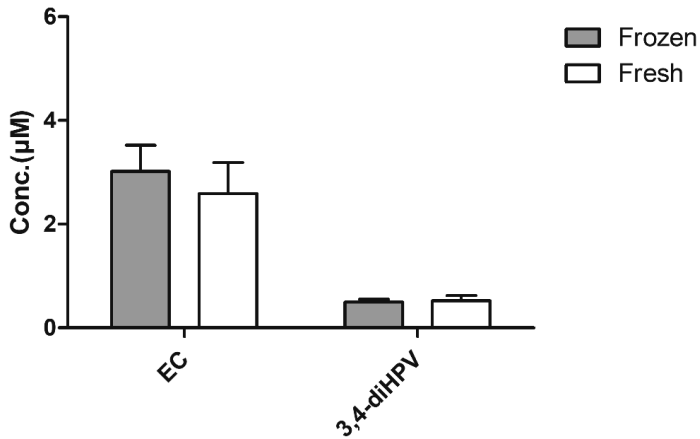| Compound	EC	3,4-diHPV	3-HPV	3,4-diHPVA	3-HPVA	3,4-diHPPA	3-HPPA	3-HPAA	4-HPAA	Catechol
LOD (nM)	88.05	27.83	50.89	25.07	31.60	443.15	468.66	67.20	25.83	74.56
LOQ (nM)	266.83	84.32	154.20	75.98	95.76	1342.87	1420.18	203.64	78.28	225.93

Figure S1. Residual EC and 3,4-diHPV formed in incubations with the fresh faecal slurry and the same faecal slurry but frozen for 1 week prior to incubation.
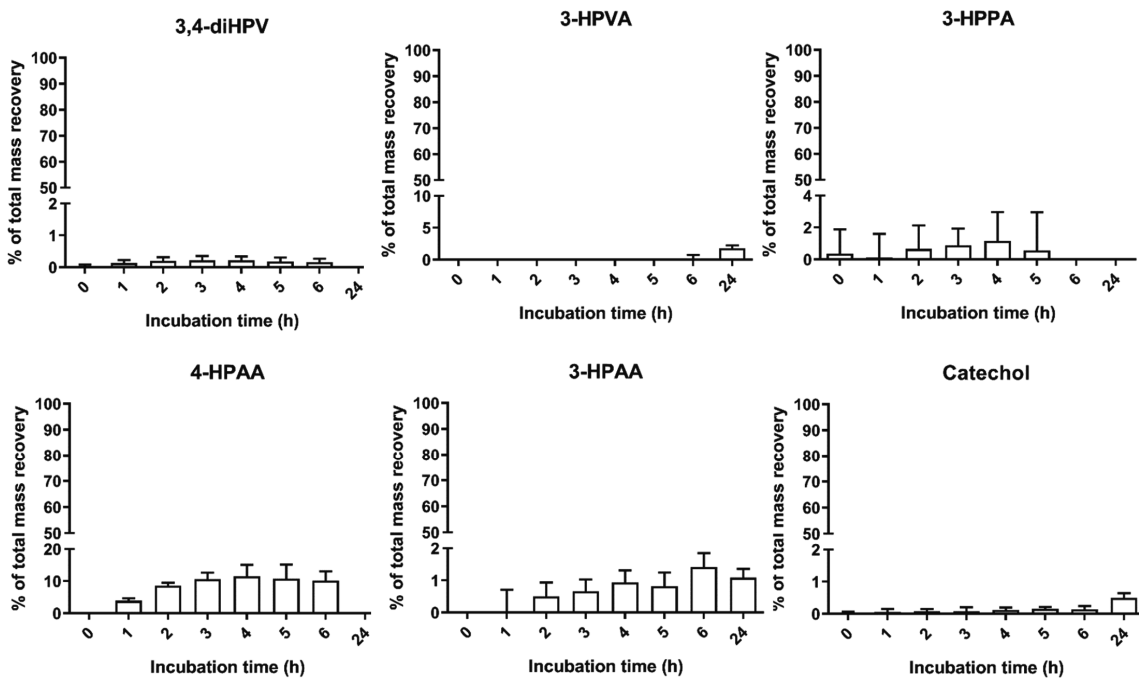

Figure S2. Phenolic compounds quantified in the negative control samples (without adding EC in pooled faecal incubations) at different incubation timepoints. Results are shown as mean ± SD from 3 independent incubations.
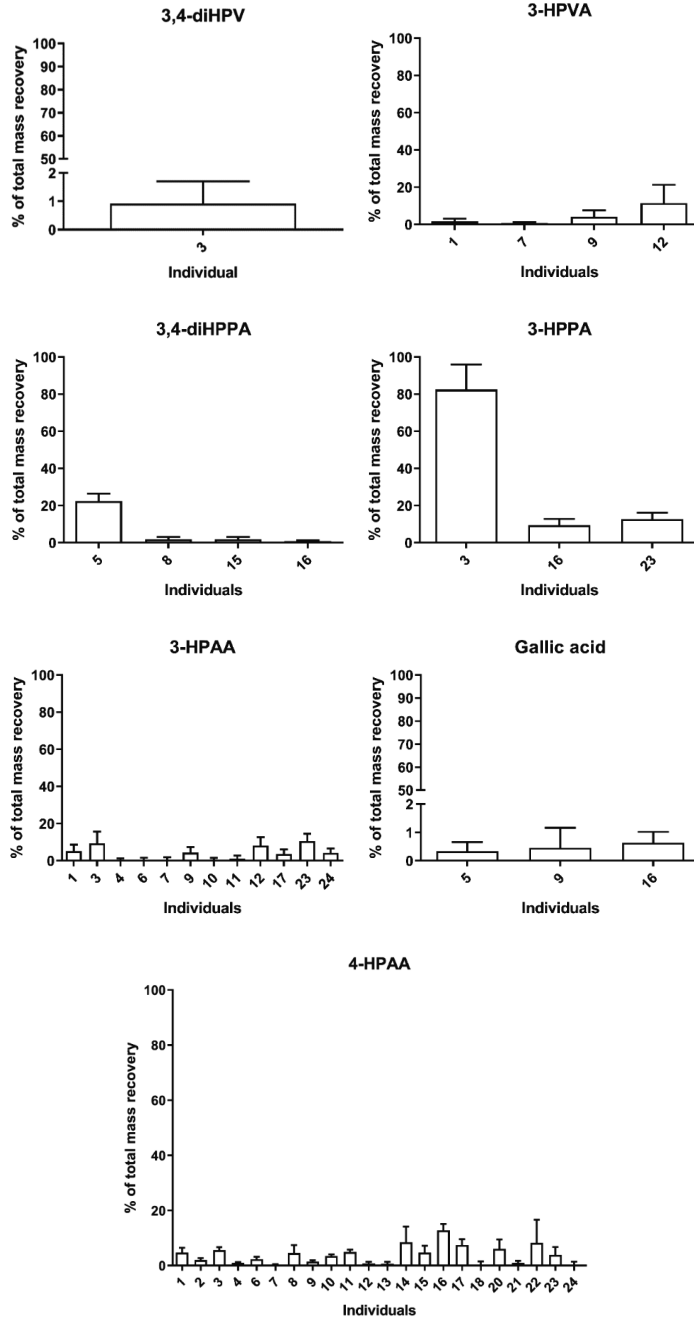
Figure S3. Phenolic compounds quantified in different individuals in the negative control (without adding EC in individual faecal incubations) at 2 h of incubations. Results are shown as mean ± SD from 3 independent incubations. Values below the LOD are not presented.
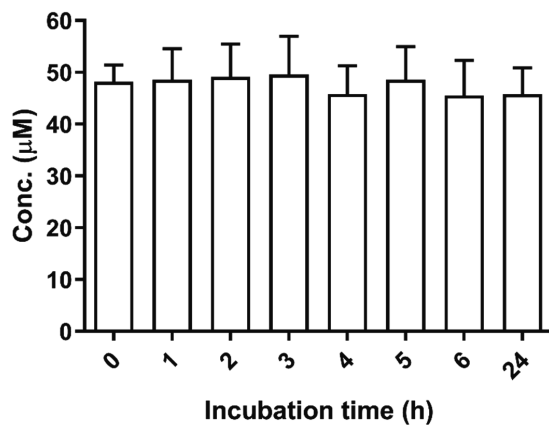
Figure S4. EC contents of blank control (incubated without faecal slurry) at different incubation timepoints. Results are shown as mean ± SD from three independent incubations.
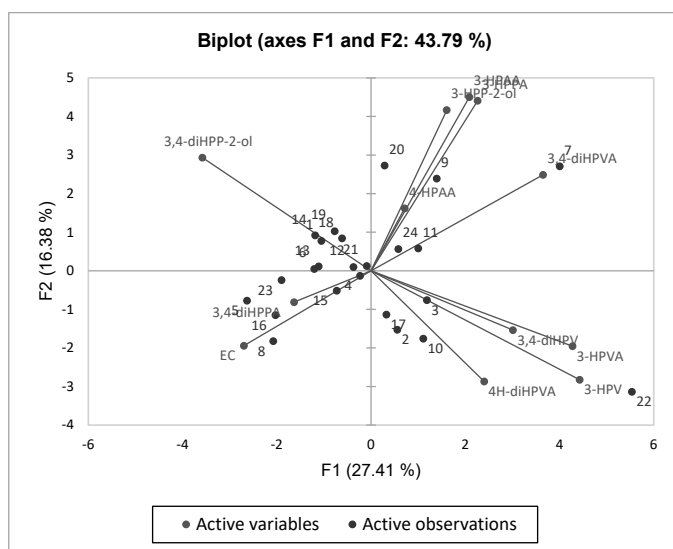

Figure S5. PCA based on the concentration of residual EC and the 11 EC microbial metabolites present in incubations with faecal slurries from 24 individuals at 2 h.
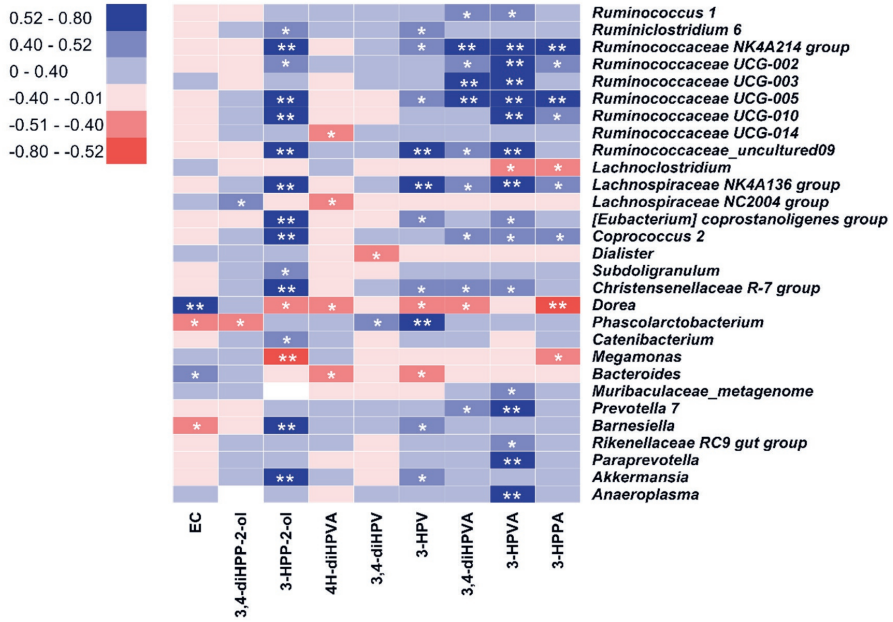
Figure S6. Spearman correlations between the taxon abundances of bacterial genera and the concentration of residual EC and 8 EC microbial metabolites present in incubations with faecal slurries from 24 individuals at 2 h. The sign and strength of the Spearman correlation coefficients are represented as colours (blue: positive; red: negative). The significances of the correlations are indicated by asterisks: *$P < 0.05$, **$P < 0.01$.
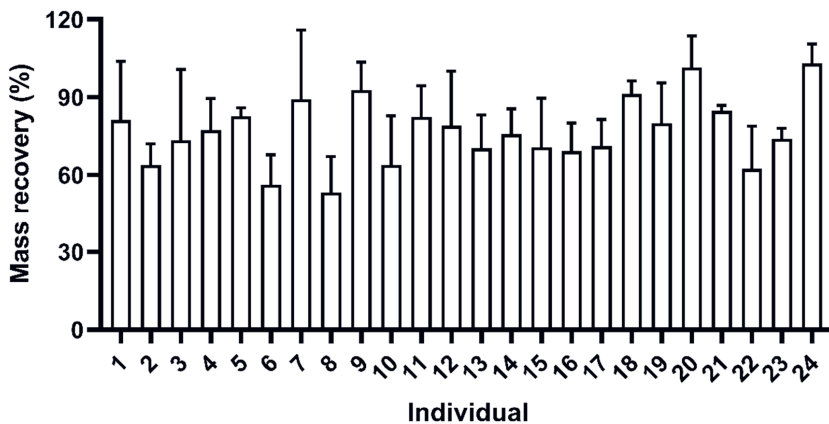

Figure S7. Total mass recoveries of 24 individuals for their EC faecal incubations at t = 2 h. Results are shown as mean ± SD from three independent incubations.
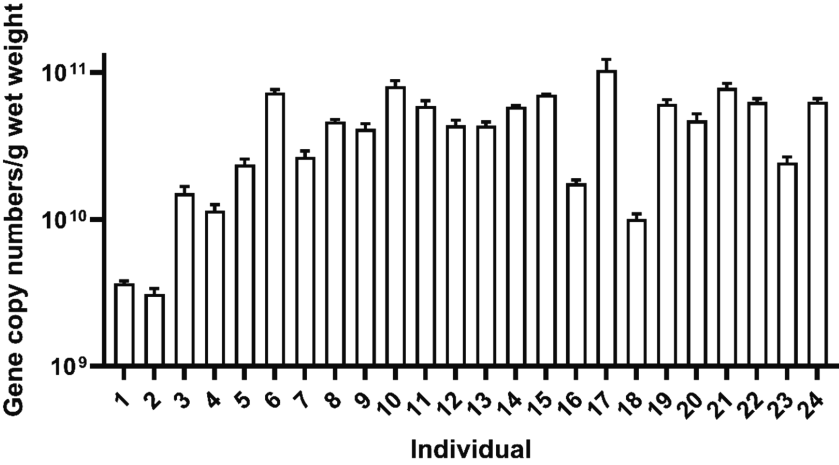
Figure S8. Bacterial load of 24 individuals, expressed as gene copy numbers per gram of wet weight of faecal slurry (mean value ± SD, n = 3)

3

Chapter 3

Interindividual differences in human *in vitro* intestinal microbial conversion of green tea (-)-epigallocatechin-3-*O*-gallate and consequences for activation of Nrf2 mediated gene expression

Chen Liu, Jacques Vervoort, Joris van den Elzen, Karsten Beekmann, Marta Baccaro, Laura de Haan, Ivonne M.C.M. Rietjens

Abstract

Scope. An *in vitro* faecal incubation model combined with reporter gene assay based testing strategy is developed to characterise interindividual differences in the gut microbial conversion of (-)-epigallocatechin-3-*O*-gallate (EGCG) and its consequences for potential activation of Nrf2-mediated gene expression.

Method & Results. Anaerobic human faecal incubations were performed to characterise the microbial metabolism of EGCG including interindividual variability. EGCG derived intestinal microbial metabolite patterns showed substantial interindividual differences that were correlated to relative microbial abundances determined by 16S rRNA sequencing. Results obtained showed the time-dependent formation of gallic acid, pyrogallol, phenylpropane-2-ols, phenyl-γ-valerolactones and 5-(3',5'-dihydroxyphenyl)valeric acid (3,5-diHPVA) as the major metabolites, with substantial interindividual differences. The activity of the formed metabolites in the activation of EpRE-mediated gene expression was tested by EpRE-LUX reporter gene assay. In contrast to EGCG, at low micromolar concentrations, especially gallic acid, pyrogallol and catechol induced significant activity in the EpRE-LUX assay.

Conclusions. Given these results and taking the level of formation into account, it is concluded that especially gallic acid and pyrogallol contribute to the EpRE-mediated beneficial effects of EGCG. The interindividual differences in their formation may result in interindividual differences in the beneficial effects of EGCG and green tea consumption.

Keywords: EGCG, microbial metabolism, gallic acid, pyrogallol, Nrf2 activation

1. Introduction

Green tea is rich in some natural polyphenolic compounds, especially catechins including (-)-epicatechin (EC), (-)-epigallocatechin (EGC), (-)-epicatechin-3-*O*-gallate (ECG) and (-)-epigallocatechin-3-*O*-gallate (EGCG), which comprise 30 - 42% (w/w) of the solids in green tea infusion.[1] Among these components, EGCG is the most abundant polyphenol, making up more than 50% of the total catechin constituents.[2] Regular consumption of green tea is often considered to have protective effects against cardiovascular diseases and certain forms of cancer.[3] The mode of action underlying these potential beneficial health effects may in part be related to activation of the Keap1/Nrf2 (Kelch ECH associating protein 1/nuclear factor erythroid 2-related factor 2) system, a thiol-based sensor-effector apparatus that is involved in redox homeostasis.[4] Once Nrf2 is released from its complex with Keap1, it will translocate from cytoplasm to nucleus where its binding to the electrophile-responsive element (EpRE) with small Maf proteins, results in the up-regulation of EpRE-mediated gene expression.[4] This EpRE-mediated gene expression is considered to play an essential role in the prevention of various adverse health effects.[5-6] EGCG was reported to be able to increase both mRNA and protein levels of Nrf2 in mice. The upregulation and nuclear translocation of Nrf2 induces the expression of EpRE-regulated conjugation enzymes including for example UDP-glucuronosyltransferases (UGTs). The increased UGT activity facilitates conjugation, detoxification and excretion of toxic electrophiles able to generate protein and DNA damage, thereby contributing to prevention of a range of adverse health effects including carcinogenicity. It was reported, for example, that EGCG could inhibit the growth and metastasis of orthotopic colon cancer implants in nude mice in a dose-dependent manner.[3, 7]

Several green tea catechins have been reported to activate Keap1/Nrf2 in *in vitro* models at high μM concentrations.[8-9] However, *in vivo* the bioavailability and plasma concentrations of catechins are usually quite low.[10] After intake of green tea infusion, only a small proportion of the ingested catechins is absorbed by the small intestine, while a large fraction reaches the large intestine where the catechins are metabolised by colonic microbiota. It has been estimated that only 5% - 10% of ingested dietary polyphenols are absorbed in the small intestine, while substantial amounts reach the colon where they are intensively degraded by microbiota into a diversity of bioactive phenols, phenyl-γ-valerolactones and phenolic acids that are subsequently absorbed.[11-13] To characterise the colonic microbial metabolite pattern of EGCG, in the present study an *in vitro* anaerobic incubation model was applied. **Figure 1** provides an overview of the tentative metabolic pathways for EGCG as derived from literature data,[3, 13] and results we

obtained on intestinal microbial metabolism from the present study. Given the low systemic concentrations of EGCG (and/or EGCG conjugates) and the (in some cases) even higher systemic concentrations of microbial metabolites, it can be hypothesized that their microbial metabolites may contribute to (some of) their health-promoting effects. For example, one of the important microflora-derived catechin metabolites, 5-(3',4'-dihydroxyphenyl)-γ-valerolactone (3,4-diHPV), was reported to be able to inhibit NO production and iNOS expression in RAW 264.7 cells, suggesting potential anti-inflammatory activity.[14]

There are trillions of microbes inhabiting the human intestine and the host intestinal microbiome can be remarkably variable across individuals due to the differences in age, gender, dietary and lifestyle, etc.[15] Thus, the microbial metabolism of EGCG could also vary between individuals. As a result, interindividual differences in the levels of potential health promoting metabolites resulting from EGCG or green tea consumption may also exist.

The aim of the present study was to characterise the human intestinal microbiota-mediated conversion of EGCG, including the interindividual variability, using an *in vitro* testing strategy, and to identify the activity of the formed metabolites in the activation of EpRE-mediated gene expression. To this end, the time-dependent metabolite pattern of EGCG was quantified in *in vitro* human faecal incubations. Faecal microbial taxonomy profiles were characterised by 16S rRNA analysis and bacterial loads quantified by quantitative PCR (qPCR), which allowed the identification of correlations between taxon abundances and formation of colonic metabolites. Furthermore, EpRE-mediated Nrf2 activation by the formed metabolites was characterised using an EpRE-LUX reporter cell line previously developed in our lab.[16]
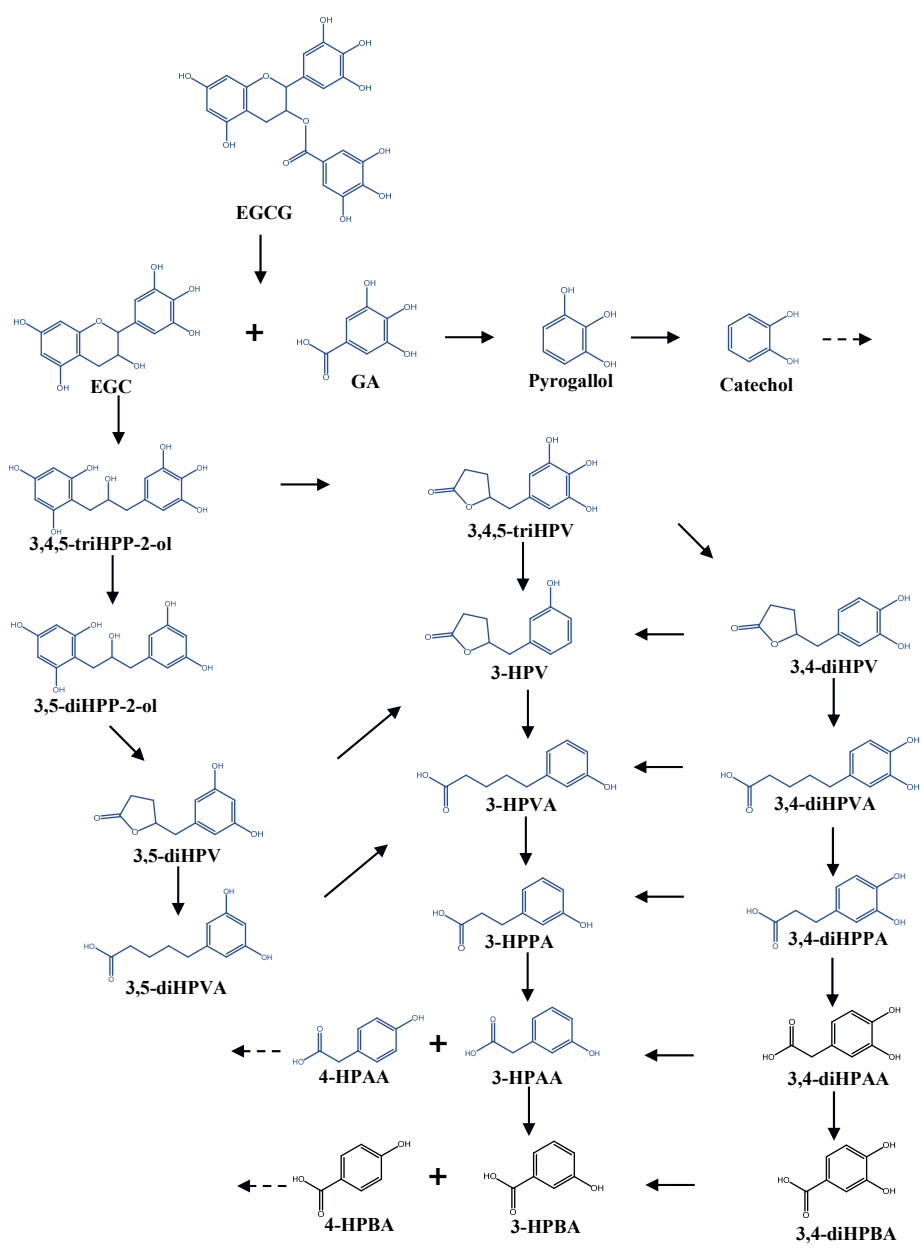
Figure 1. Tentative pathways in the human intestinal microbial metabolism of EGCG. Structures in blue colour were observed in the present study.

2. Experimental Section

2.1 Chemicals and instruments

The test compounds were ordered either from Sigma-Aldrich (Zwijndrecht, The Netherlands) or Enamine (Kyiv, Ukraine). WST-1 reagent was purchased from Roche (Mannheim, Germany). Alpha-Modified Eagle's Medium (α-MEM), Dulbecco's Modified Eagle Medium with 1:1 Ham's Nutrient Mixture F-12 (DMEM/F12), penicillin/streptomycin and phosphate buffered saline (PBS) were purchased from Gibco (Paisley, UK). Nonessential amino acids (NEAA), trypsin and geneticin (G418) were supplied by Invitrogen Corporation (Breda, The Netherlands). Foetal calf serum (FCS) was obtained from Bodinco (Alkmaar, The Netherlands). Methanol and acetonitrile (ACN) were obtained from Biosolve BV (Valkenswaard, The Netherlands). Acetic acid was ordered from Merck KGaA (Darmstadt, Germany) and formic acid was purchased from VWR CHEMICA (Amsterdam, The Netherlands). The anaerobic chamber used was a BACTRON300 produced by Sheldon manufacturing INC (Cornelius, USA). Para-Pak SpinCon tubes were purchased from Fisher Scientific (New Hampshire, USA).

2.2 Cell lines

The EpRE-LUX cells are Hepa-1c1c7 mouse hepatoma cells, stably transfected with a reporter construct carrying a luciferase reporter gene under transcriptional control of an EpRE from the human NAD(P)H: quinone oxidoreductase 1 (NQO1) gene in conjunction with a minimal promoter and an initiator.[16] The cells were cultured in α-MEM supplemented with 10% FCS and penicillin/streptomycin (final concentrations 10 U/ml and 10 µg/ml, respectively) (designated as growth medium).

The Cytotox CALUX cells are human osteosarcoma U2OS cells stably transfected with a reporter construct carrying a luciferase reporter gene under transcriptional control of a constitutive promoter. The reporter construct was generated by inserting the luciferase gene into the multiple cloning site of the pSG5-neo vector.[17] These cells have an invariant luciferase expression and were originally designed to discover cytotoxicity.[18] The Cytotox CALUX cells were cultured in DMEM/F12 supplemented with 7.5% FCS, %1 NEAA, and penicillin/streptomycin (final concentrations 10 U/ml and 10 µg/ml, respectively). Both cell lines were maintained at 37°C in a humidified atmosphere with 5% CO_2 and 200 µg/ml G418 was added to the culture medium once a week in order to maintain the selection pressure.

2.3 Faecal sample preparation

Faeces were collected from 14 healthy individuals without dietary restriction. They were of different gender, age, and ethnicity. All of them had not taken antibiotics for at least 3 months prior to the study. The donors consisted of 5 males and 9 females and their age ranged between 19 to 65. After donations, faecal samples were collected and weighed, and then immediately transferred to the anaerobic operating chamber. The whole process was finished within 5 minutes to ensure the quality of faecal samples. Subsequently, these faecal samples were diluted with an anaerobic solution of 10% (v/v) glycerol in PBS to get a final faecal concentration of 20% (w/v). After that, samples were filtered using a Para-Pak SpinCon tube and centrifuged at $21,500 \times g$ for 5 minutes at 4 °C to remove larger particles. The resulting faecal suspension was collected and aliquoted. All the steps mentioned above were carried out under anaerobic conditions. Aliquots of faecal suspension were stored at -80 °C until use. The effect of freezing, storing and thawing on the microbial metabolism of EGCG by the faecal samples was tested and it was shown not to affect the activity (Supporting Information **Figure S1**). The experimental protocol was evaluated and approved to not require further evaluation by the Medical Ethical Reviewing Committee of Wageningen University (METC-WU) based on the Dutch Medical Research Involving Human Subjects Act. All participants gave their written consent.

2.4 Faecal batch-culture incubation

Faecal incubations were performed in 1.5 mL Eppendorf tubes containing 79% anaerobic PBS, 20% of the above-mentioned faecal slurries (final faecal concentration: 40 mg/ml) and 1% (v/v) of 10 mM EGCG (in methanol) or methanol as control (referred to as "negative control"). The resulting final concentration of EGCG in the solution was 100 µM, which has been shown not to affect the microbiota,[19] while permitting detection of substrate and metabolites. Incubations of EGCG without faecal slurries were included as blank control. All faecal incubations were carried out in the BACTRON300 anaerobic chamber with an atmosphere of 85% N_2, 10% CO_2, and 5% H_2 at 37 °C. Aliquots of incubated faecal samples (50 µL) were collected after 0, 1, 2, 3, 4, 5, 6, and 24 h of incubation for pooled faecal slurries and mixed with 1 volume of ice-cold methanol to terminate the reactions. For studies on interindividual differences, a timepoint of 2 h was selected and incubations were carried out with faecal slurries from each individual. Subsequently, samples were put on ice for at least 15 minutes, followed by centrifuging at $21,500 \times g$ for 15 minutes at 4 °C to precipitate proteins, microorganisms, etc. The supernatant of each sample was collected and stored immediately at -80 °C until liquid chromatograph triple quadrupole mass spectrometry (LC-TQ-MS) and liquid chromatograph time-of-flight mass

spectrometry (LC-TOF-MS) analysis for metabolite levels. All the incubations were performed in at least triplicate.

2.5 LC-TQ-MS analysis

A Shimadzu LC-TQ-MS 8045 was used to quantify the concentration of EGCG and its metabolites. This equipment consisted of an ultra high-performance liquid chromatography (UHPLC) system coupled to a tandem triple quadrupole mass spectrometer, fitted with an ESI source (Shimadzu, Benelux, B.V. The Netherlands). The ESI source was operated in negative ion mode, and fragment ions *m/z* were obtained. Chromatographic separation was performed on a Waters Acquity UPLC® BEH C18 column (2.1 × 50 mm; 1.7 µm) at 40 °C. Solvent A was composed of water : acetic acid (999 : 1, v/v), and solvent B was methanol absolute. The eluents was delivered at a flow rate of 0.4 mL/min and the following gradient was used: 0 - 0.5 min: 5% B, 0.5 - 5 min: 5 - 25% B, 5 - 6 min: 25 - 100% B, 6 - 7 min: 100% B, 7 - 8 min: 100 - 5% B, 8 - 13 min: 5% B.

Chromatographic peaks were identified by comparison of the retention time and ion values with those of commercially available authentic standards. The identification information for EGCG and its potential colonic metabolites is summarised in Table S1 in Supporting Information. To quantify the metabolites formed during *in vitro* incubations, a set of mixed authentic standard calibrators was used to build calibration curves using fourteen concentrations between 0.01 µM and 50 µM, and plotting the peak area against the concentration to define the linear regression equation used for quantification. Concentrations of metabolites formed were calculated, including a correction for the amounts detected in corresponding negative controls incubated without adding EGCG. Each experimental replicate was corrected with the mean value of the 3 negative controls.

2.6 LC-TOF-MS analysis

An Agilent 1200 series high performance liquid chromatography (HPLC) system coupled with a Bruker micrOTOF (time-of-flight mass analyser) was used to qualitatively and quantitively detect pyrogallol and other metabolites whose standard references were not available. Chromatographic separation was performed on the same column as used in the LC-TQ-MS analysis. Solvent A was composed of water : formic acid (999 : 1, v/v) and solvent B was ACN : water (999 : 1, v/v). The eluents were delivered at a flow rate of 0.2 mL/min and the following gradient was used: 0 - 2.5 min: 100% A, 2.5 - 40 min: 0 - 40% B, 40 - 45 min: 40 - 100% B, 45 - 50 min: 100% B, 50 - 55 min: 100 - 0% B, 55 - 90 min: 100% A. Relative retention time and

M-H value were used to identify the aforementioned EGCG colonic metabolites. Specifically, molecules such as 3,4,5-triHPP-2-ol, 3-HPP-2-ol and 3,4,5-triHPV have high M-H values (i.e., 307.08, 275.09, 223.06) which are unique in EGCG microbial conversion pathway. Moreover, chemical standards mentioned in LC-TQ-MS were also analysed in LC-TOF-MS, which helped to annotate compounds sharing the same M-H values. For example, although 3,5-diHPV and 3,4-diHPV have the same M-H values, i.e., 207.07, the measurement of the 3,4-diHPV standard in LC-TOF-MS ensured the distinguishing of these two chemicals. Furthermore, previous data from EC microbial conversion samples (unpublished data) and time-dependent formation in the pathway were also taken into consideration. For instance, 3,4-diHPP-2-ol was the unique metabolite in EC microbial conversion pathway with a retention time of 19.6 min, which was used to differentiate it from its isomer 3,5-diHPP-2-ol that has a retention time of 18.5 min. Altogether, these ensured the unequivocal identifications of those metabolites for which no standards were available. With the exception of pyrogallol, all the other metabolites were quantified using calibration curves of EC because of the absence of commercial standards. Detailed identification information is summarised in Table S1 in Supporting Information.

2.7 Microbial taxonomic profiling and total bacterial load

Aliquots of all 14 faecal samples were sent to an accredited commercial laboratory (IMGM Laboratories GmbH, Martinsried, Germany) for DNA extraction, PCR, library preparation, and sequencing. Additionally, quantification of the bacterial load was carried out by real-time qPCR. PCR products were generated by amplification using 16S V3-V4 primers (F-NXT-Bakt-341F: 5'-CCTACGGGNGGCWGCAG-3' and R-NXT-Bakt-805R: 5'-GACTACHVGGGTATCTAATCC-3'). During an index PCR, barcodes for multiplexed sequencing were introduced using overhang tags. A sequencing library was prepared from barcoded PCR products and sequenced on the Illumina® MiSeq next generation sequencing system (Illumina® Inc.). Signals were processed to *.fastq-files and the resulting 2×250 bp reads were demultiplexed. Microbiota identification was carried out by clustering the sequences at a 97% identity threshold defining operational taxonomic units (OTU), according to the taxonomy of the SILVA 132 16S rRNA sequence database.

2.8 EpRE-LUX assay

The EpRE-mediated induction of gene expression by EGCG and its major intestinal microbial metabolites was tested by measuring the induction of luciferase activity in the EpRE-LUX cells. The assay was performed as described before.[9, 16] In brief, EpRE-LUX cells were seeded in the

inner 60 wells of a white 96-well microplate with a clear bottom (PerkinElmer) at a density of 2×10^4 cells per well in 100 µl growth medium. The microplates were incubated at 37 °C in a humidified atmosphere with 5% CO_2 for 24 h to allow the cells to form a confluent monolayer. Subsequently, the growth medium was replaced by assay medium (α-MEM without FCS and antibiotics) containing different concentrations of the phenolic test compounds for a continuous 24 h exposure. A total of eight to twelve different concentrations of each compound were tested, ranging from 2 µM to 125 µM. t-BHQ at 30 µM was used as the positive control in each plate. All test compounds, including t-BHQ, were dissolved in DMSO and added to the cells from 200 times concentrated stock solutions in DMSO. The final concentration of DMSO in the exposure medium was 0.5%. After the 24 h exposure, the assay medium was discarded and the cells were carefully washed and lysed. Subsequently, the microplates were first put on ice for 15 min and then frozen in -80 ℃ for at least 1 h. Before measuring the luciferase activities of each well using a luminometer (GloMax-Multi Detection System-Promega), the microplates were thawed and raised to room temperature. Relative light units (RLU) were measured after the addition of 100 µl flash mix (20 mM Tricine, 1.07 mM $(MgCO_3)_4Mg(OH)_2 \cdot 5H_2O$, 2.67 mM $MgSO_4$, 0.1 mM EDTA, 2.0 mM DTT, 470 µM D-luciferine, 5.0 mM ATP; pH 7.8) into each well. The results are presented as the induction factor (IF) compared to the solvent control. At least three independent biological replicates were performed for all the compounds tested.

2.9 Cytotox CALUX assay

To investigate whether stabilisation of the luciferase enzyme (false positive) is occurring during the exposure to tested compounds, a parallel Cytotox CALUX assay was performed using U2OS Cytotox CALUX cells that express a constant amount of luciferase.[20] This assay was performed in the same way as described above for the EpRE-LUX assay except for the fact that 1×10^4 cells per well were seeded in a 96-well microplate and DMEM/F12 was used instead of α-MEM.[20]

2.10 Cell viability assay

To avoid false negative results, EpRE-LUX cell viability was assessed using the WST-1 assay. Briefly, after the same seeding and exposure steps as EpRE-LUX assay, 6 µl of WST-1 solution was added to each well of the inner 60 wells of the 96-well microplates. Subsequently, microplates were placed in the incubator at 37 °C in a humidified atmosphere with 5% CO_2 for 1 h, followed by measurements of absorbance at 440 nm and 620 nm by a microplate spectrophotometer. The amount of formazan dye produced by cells was calculated using the

values at 440 nm subtracted from the values at 620 nm. The results are presented as viability (%) compared to the solvent control set at 100%.

2.11 Dosage information

The concentration of EGCG used in the faecal incubations was 100 µM. This concentration will result from an oral dose of about 33 mg/person assuming 52% of the dose would reach the large intestine,[21-22] and a large intestinal volume of 371 ml for a 70 kg person.[23] This dose level would be achieved by drinking 1/3 of a cup of green tea containing 110 mg of EGCG.[21-22] The concentrations of catechol, pyrogallol and gallic acid used in EpRE-LUX reporter gene assay ranged between 2 to 125 µM. Based on the assumptions presented above drinking a cup of green tea containing 110 mg EGCG would result in a concentration of EGCG in the large intestine of 337 µM. The concentrations of gallic acid and pyrogallol formed in the anaerobic faecal incubations of the present study amounted respectively up to 34% and 32% of the original concentration of EGCG. A similar conversion of 337 µM EGCG in the large intestine will result in concentrations up to 115 µM and 108 µM, which are in line with the concentration range tested in the EpRE-LUX reporter gene assay.

2.12 Data analysis

LC-TQ-MS data were obtained and processed by Shimadzu Labsolutions software. LC-TOF-MS data were obtained and processed by HyStar software. ChemDraw 18.0 (PerkinElmer, Waltham, USA) was used to draw chemical structures. Graphpad Prism 8.2 (San Diego, USA) was used to plot graphics. Spearman's rank correlation coefficients ρ ($-1 \leq \rho \leq 1$) were calculated between the concentrations of the 8 most relevant metabolites present after 2 hours of incubation and the relative abundances of the bacterial genera (range between 0 - 100%). To display the correlations, a heatmap was constructed. The benchmark dose (BMD) approach was applied on the *in vitro* concentration response curves obtained from the EpRE-LUX assay. The European Food Safety Authority BMD modelling web tool was used to calculate benchmark concentration (BMC) according to its manual.[24]

3. Results

### 3.1 LC-TQ-MS and LC-TOF-MS based identification of colonic metabolites of EGCG

Figure 2 presents the time-dependent formation of EGCG metabolites formed in anaerobic incubations with a pooled human faecal sample. Concentrations of metabolites formed were corrected for the amounts detected in corresponding negative controls incubated without adding

EGCG. Six polyphenols were detected in the negative controls but in limited amounts (< 11.5% of the total mass recovery, Supporting Information **Figure S2**). The chemical structures of the metabolites detected by LC-TQ-MS and LC-TOF-MS are highlighted in blue colour in **Figure 1**.

The metabolic profiles observed corroborate that the first step of EGCG bioconversion consists of its hydrolysis to produce gallic acid and EGC. During the first 2 h incubation, gallic acid formation reached a plateau at 17.0 μM, accounting for 33.9% (mol/mol) of the EGCG added to the incubation. Upon further incubation, gallic acid levels gradually decreased with only 0.3 μM detected at 6 h, representing 0.6% of the original EGCG equivalents. Further metabolism of gallic acid proceeds by its decarboxylation to generate pyrogallol. Pyrogallol peaked at 4 h incubation with 15.9 μM, amounting to 31.7% of the original EGCG equivalents. Additionally, a limited amount of catechol was detected resulting from the further conversion of pyrogallol, pointing at swift further degradation of catechol preventing its accumulation.

The second metabolite resulting from the initial EGCG hydrolysis, EGC, was detected at concentrations that were at most 8.2 μM at 1 h, accounting for 16.4% of the original EGCG equivalents. After 3 h incubation, EGC was almost fully degraded with only 0.8 μM (1.6% EGCG equivalents) remaining at 3 h. EGC underwent reductive cleavage in the C-ring producing 3,4,5-triHPP-2-ol. This intermediate maximized at 2 h incubation, amounting to 11.0 μM, (22.1% of the original EGCG equivalents). Subsequently, 3,4,5-triHPP-2-ol can be degraded through two major pathways, dehydroxylation to generate 3,5-diHPP-2-ol or A-ring
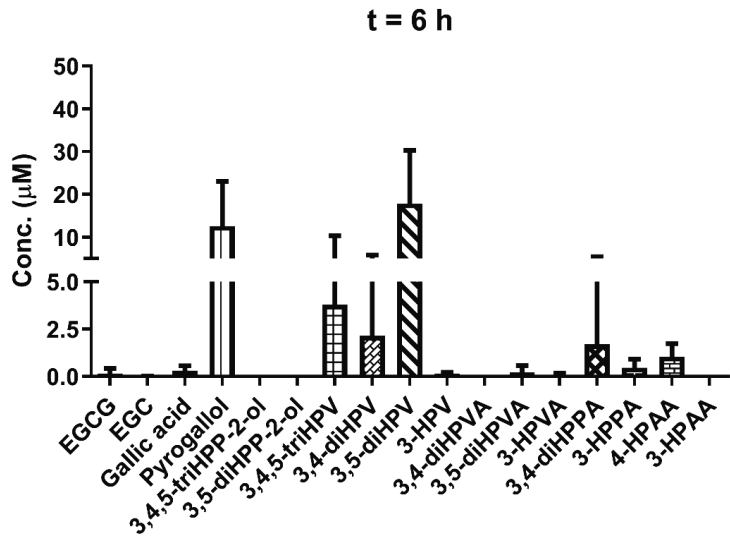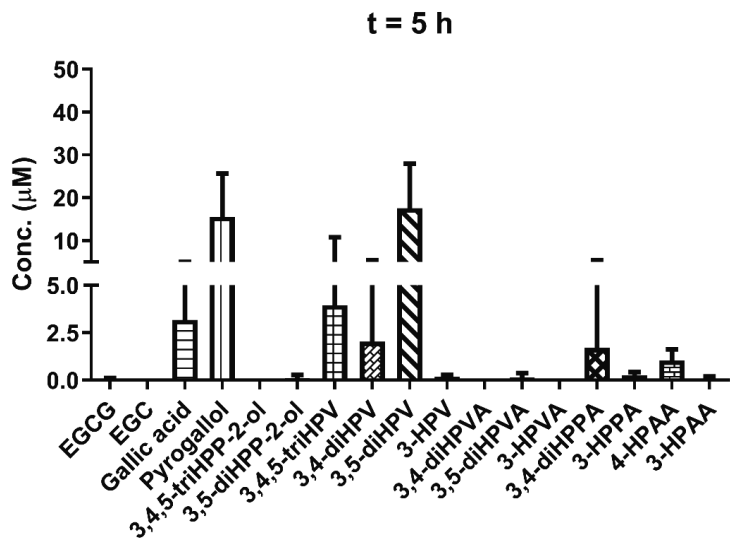
t = 1 h

t = 2 h

t = 3 h
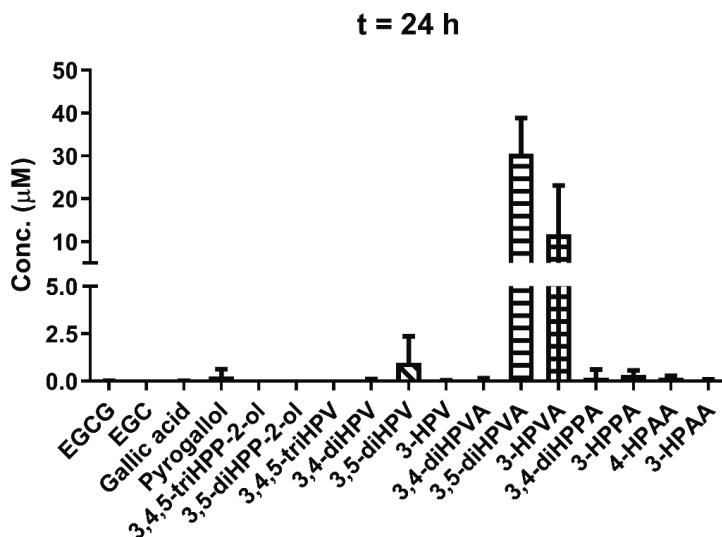
t = 4 h

t = 5 h

t = 6 h
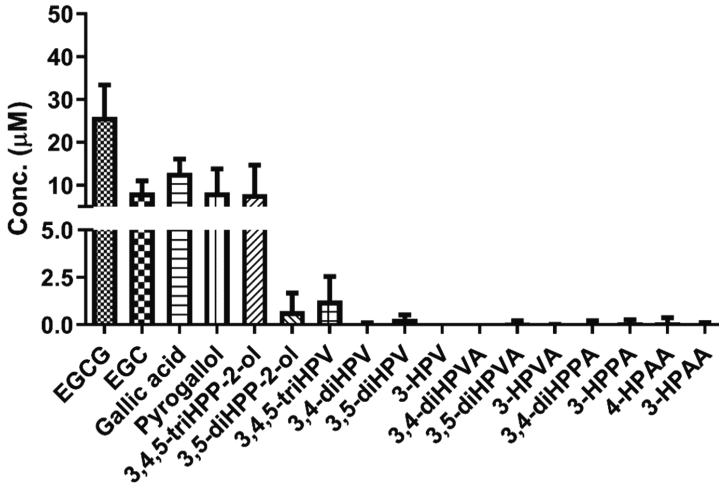
t = 24 h
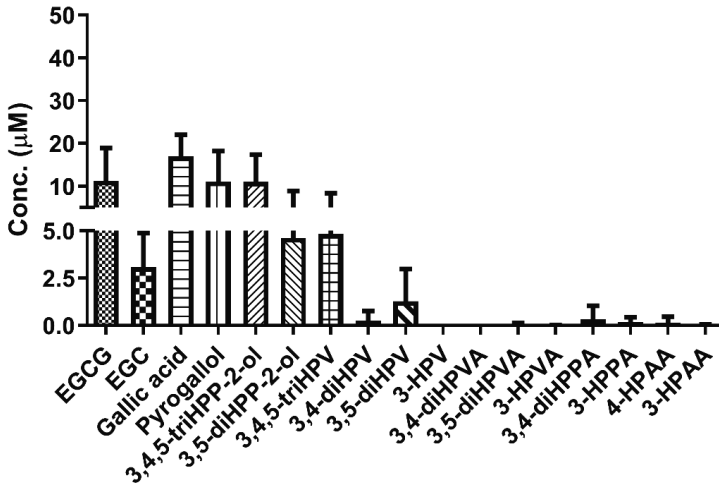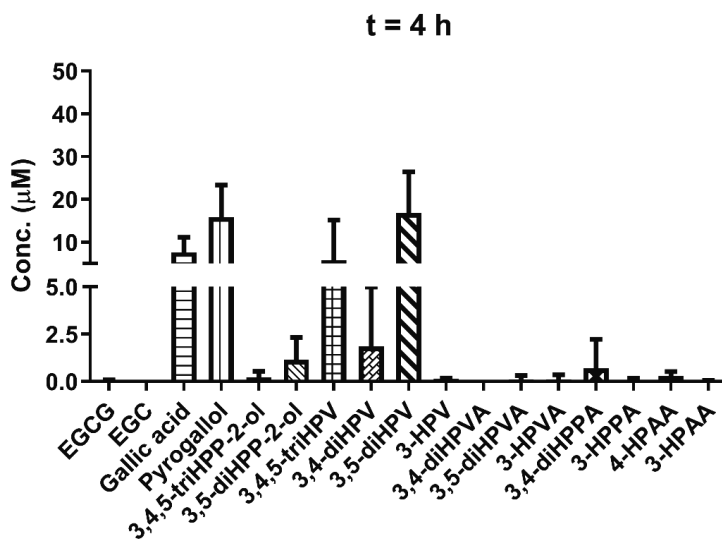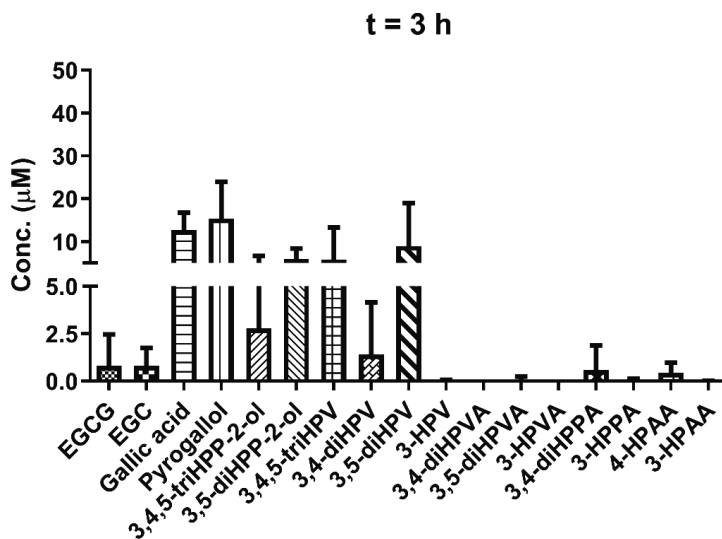
Figure 2. Quantitative time-dependent intestinal microbial metabolite patterns of EGCG formed during 24 hours of *in vitro* anaerobic incubations with a pooled human faecal sample. The value above each graph indicates the time of incubation in hours. Results are shown as mean ± standard deviation (SD) from three independent incubations. The same data are presented as time-dependent concentrations for each metabolite in **Figure S9** in the Supporting Information.

fission to form 4-H-triHPVA, which was a transient metabolite that appeared to isomerize to 3,4,5-triHPV. The first compound, 3,5-diHPP-2-ol, further converted into 3,5-diHPV which was one of the main intermediates, detected at 1 h in still small amounts (0.3 µM, 0.6% EGCG equivalents) but increasing until it peaked at 6 h at 17.9 µM, (35.7% EGCG equivalents). After 24 h incubation, the two phenyl-γ-valerolactones were almost fully converted into 3,5-diHPVA and 3-HPVA, respectively, that accounted for 61.0% (30.5 µM) and 23.4% (11.7 µM) of the originally added amount of EGCG. In addition to these major metabolites, small amounts of some phenol propionic acids and phenol acetic acids were also quantitively detected in the incubations (**Figure 2**). **Figure 3A** and **Figure 3B** show the total molar mass recovery at different incubation timepoints for the gallic acid and EGC degradation routes, respectively. For the gallic acid degradation route, the total mass recovery started to decrease from 1 h onwards, dropping from 99.8% at 1 h to 25.7% at 6 h and being almost undetectable at 24 h. This indicates that eventually pyrogallol is further degraded into metabolites that were not included in the present MS measurement. For the EGC degradation route, the total mass

recovery also started to decrease from 1 h (94.5%) onwards but remained relatively high during the further incubation (≥ 57.5%).
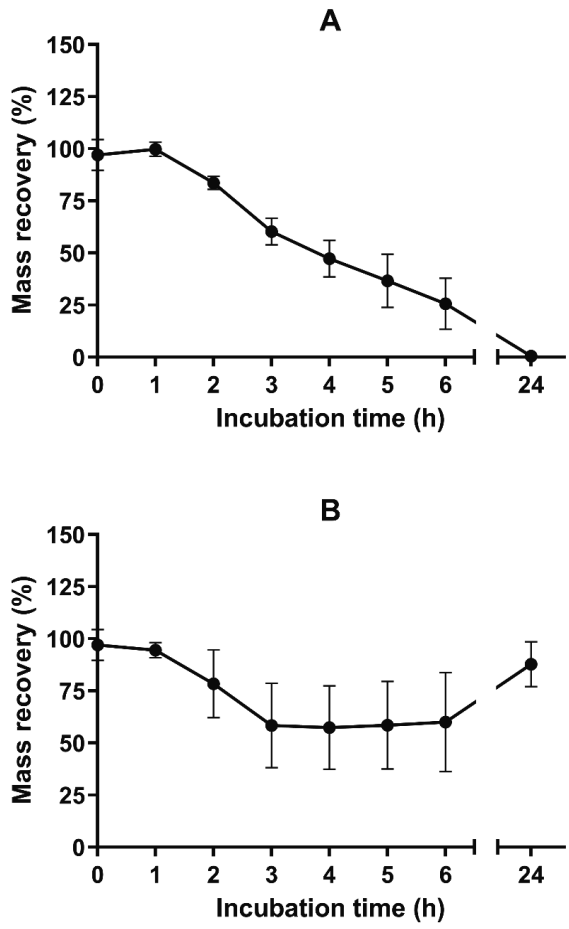
Figure 3. Total mass recovery at different incubation timepoints for gallic acid degradation route (A) and EGC degradation route (B). Results are shown as mean ± standard error of mean (SEM) from three independent incubations.

3.2 Interindividual differences of EGCG bioconversion by human colonic microbiota

Based on the results obtained for the time-dependent *in vitro* microbial EGCG conversion in incubations with a pooled faecal sample, a period of 2 hours was selected to quantify potential human interindividual differences in EGCG intestinal microbial metabolism. This time point

was selected as still residual EGCG was present while at the same time substantial metabolite formation was observed. **Figure 4** shows the amount of residual EGCG and of 7 main metabolites formed after incubating EGCG for 2 h with faecal suspensions from 14 human volunteers. Phenolic compounds quantified in different individuals in the negative control are presented in Supporting Information **Figure S3**. All phenolics were present in the negative controls at levels < 12.8% of total mass recovery with the exception of 3-HPPA (82.5% of total mass recovery) in individual 3 and 3,4-diHPPA (22.5% of total mass recovery) in individual 5. Meanwhile, substantial differences were observed both in terms of types and amounts of metabolites produced as well as in the level of EGCG depletion as shown in **Figure 4**. For example, upon 2 h incubation, less than 1 μM (<1.3% of the initial concentration) of EGCG was detected in the incubations with faecal slurries from individuals 9 and 10, while 26.5 μM (52.9% of the original amount) of EGCG was detected in the incubation with faecal slurry from individual 8. Likewise, substantial differences were also observed for the formation of major metabolites EGC, gallic acid, pyrogallol, 3,4,5-triHPP-2-ol, 3,5-diHPP-2-ol, 3,4,5-triHPV and 3,5-diHPV. For instance, 23.2 μM (46.3% of original EGCG equivalents) of pyrogallol was quantified after 2 h incubation with faecal slurry from individual 14, while only 2.8 μM (5.7% of original EGCG equivalents) of pyrogallol was detected in the incubation with faecal slurry from individual 12. Besides the variable amounts of metabolites formed, there were also differences in the type of metabolites formed among individuals. For example, 3,5-diHPV was not observed in some individuals' incubations (i.e. individuals 1, 5, 6, 8, and 14.) which is likely due to a relatively low EGCG clearance rate (i.e. individual 8) or because of the accumulation of the upstream precursors EGC and 3,4,5-triHPP-2-ol (i.e. individual 14). For individuals 1, 5 and 6, the non-detectable level of 3,5-diHPV can be either due to a swift further degradation or simply because of the incompetence of the faecal microbiota derived from these individuals in forming the compound.
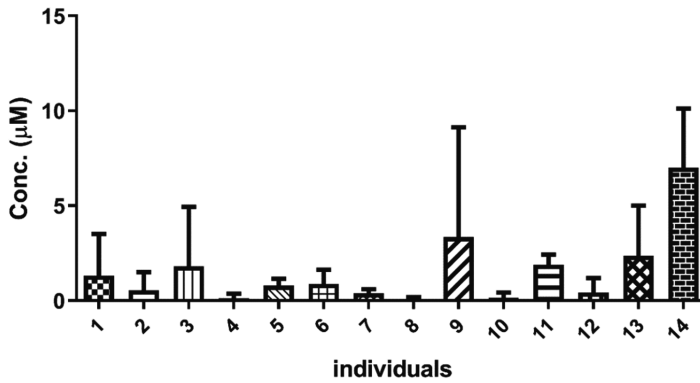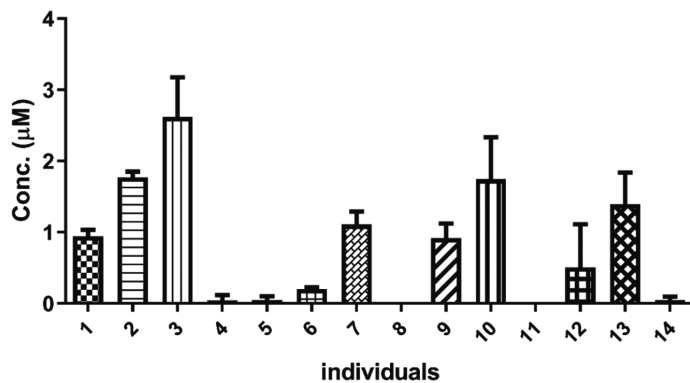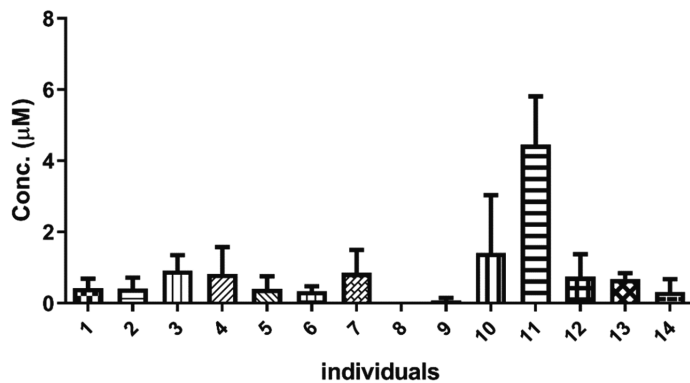
EGCG

EGC
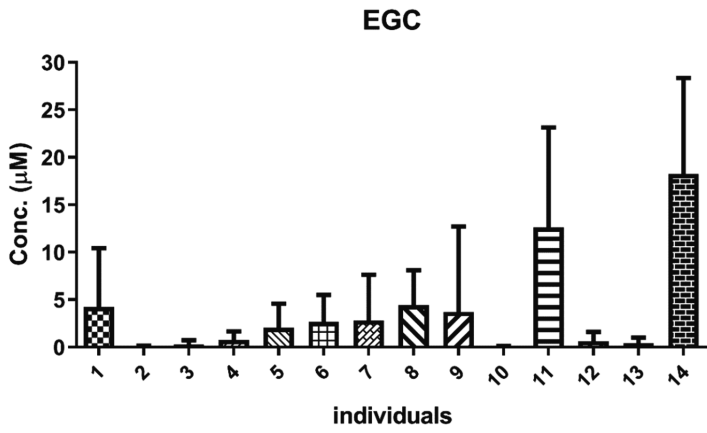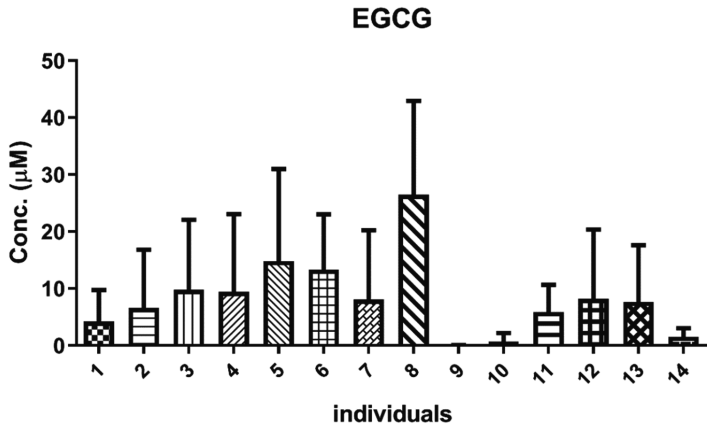
Gallic acid
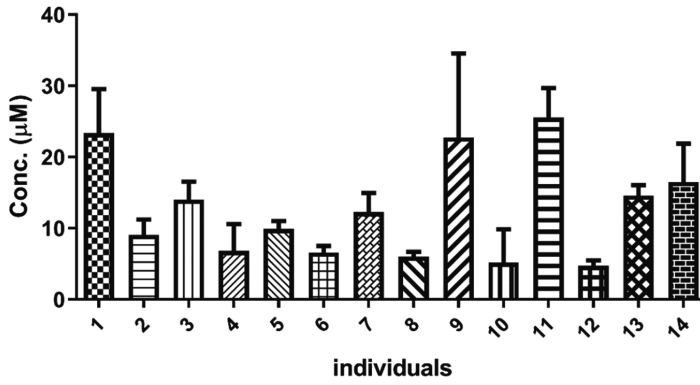
Pyrogallol
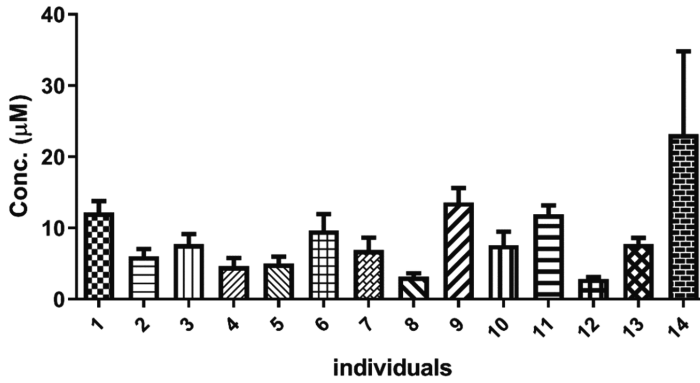
3,4,5-triHPP-2-ol

3,5-diHPP-2-ol
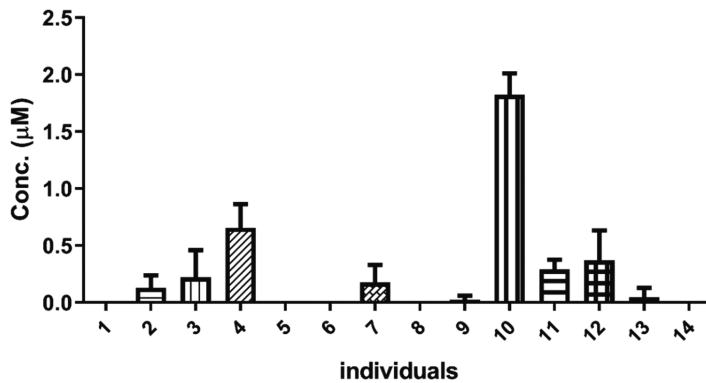
3,4,5-triHPV

3,5-diHPV

Figure 4. EGCG metabolite patterns formed in incubations with faecal slurries from 14 individuals at 2 h. Results are shown as mean ± SD from three independent incubations.

3.3 Quantitative microbial profile and correlation with metabolite formation.

Figure 5A presents the relative microbial profile at the genus level in the faecal slurries from the 14 individuals (a cut-off of more than 1% of the total bacterial amount in at least one individual was applied). The bacteria fall into 47 genera. Shannon diversity indices of microbial profiles among the 14 individuals ranged between 2.15 to 3.72, indicating that interindividual differences in the microbial relative abundance existed (Supporting Information **Figure S4**). Nevertheless, *Firmicutes* and *Bacteroidetes* were consistently found to be the dominant phyla in all samples (Supporting Information **Figure S5**). More specifically, except for individual 8, *Faecalibacterium* was found in all individuals in relatively large amounts (15.9% to 40.3% of the total bacteria). In individual 8, *Faecalibacterium* amounted to only 4.9% of the total bacteria. *Bacteroides* was also detected in all individuals, but its level varied strongly between different individuals. For example, the amount was only 2.9% of total bacteria for individual 2 but 66.4% for individual 8. *Prevotella 9* made up 23.1% to 53.4% of total bacteria in individuals 3, 6, and 9, but did not have a noteworthy contribution in other individuals (**Figure 5A**). In contrast, the total bacterial load of the 14 individuals showed only small variations (Supporting Information **Figure S6**).

To reveal the interplay between the microbial taxonomic profile of the faecal samples of the 14 individuals and their intestinal microbial metabolite profiles, Spearman correlation was performed between the relative abundance of the bacteria (as described above) and the concentrations of residual EGCG plus the concentrations of its 7 major metabolites present in the faecal slurry after 2 hours of incubation. Statistically significant correlations were found between compound concentrations and bacterial abundance at genus level but not at the phylum level. **Figure 5B** illustrates the Spearman correlation coefficients at the genus level by a heatmap. The statistical correlation is significant ($P < 0.05$) with $\rho < -0.53$ or $\rho > 0.53$. In total, bacteria from 20 different genera were found to be significantly correlated with at least one of the 8 compounds mentioned above. The concentration of residual EGCG showed an inverse correlation with several genera of the family of *Ruminococcace,* i.e.*, Ruminococcus 1*, *Ruminococcaceae UCG-005*, *Ruminococcace_uncultured-09* and *Ruminiclostridium 9*, of which the inverse correlation with *Ruminococcaceae UCG-005* was statistically significant ($P < 0.01$). In addition, also *Bilophila* showed an inverse correlation with residual EGCG ($P <$

0.05). *Ruminococcaceae UCG-005* was further positively correlated with the concentrations of all 7 major metabolites, among which, the correlation with the concentration of gallic acid was statistically significant (P < 0.05). *Lachnospiraceae NK4A136* group and *Lachnospiraceae UCG-001*, which are from the same family of *Lachnospiraceae*, showed similar correlations with 7 of the 8 compounds. Specifically, both *Lachnospiraceae NK4A136 group* and *Lachnospiraceae UCG-001* showed statistically positive correlation with the concentration of 3,4,5-triHPV (P < 0.05). In addition, *Lachnospiraceae NK4A136* positively correlated with the concentration of 3,5-diHPV (P < 0.01).
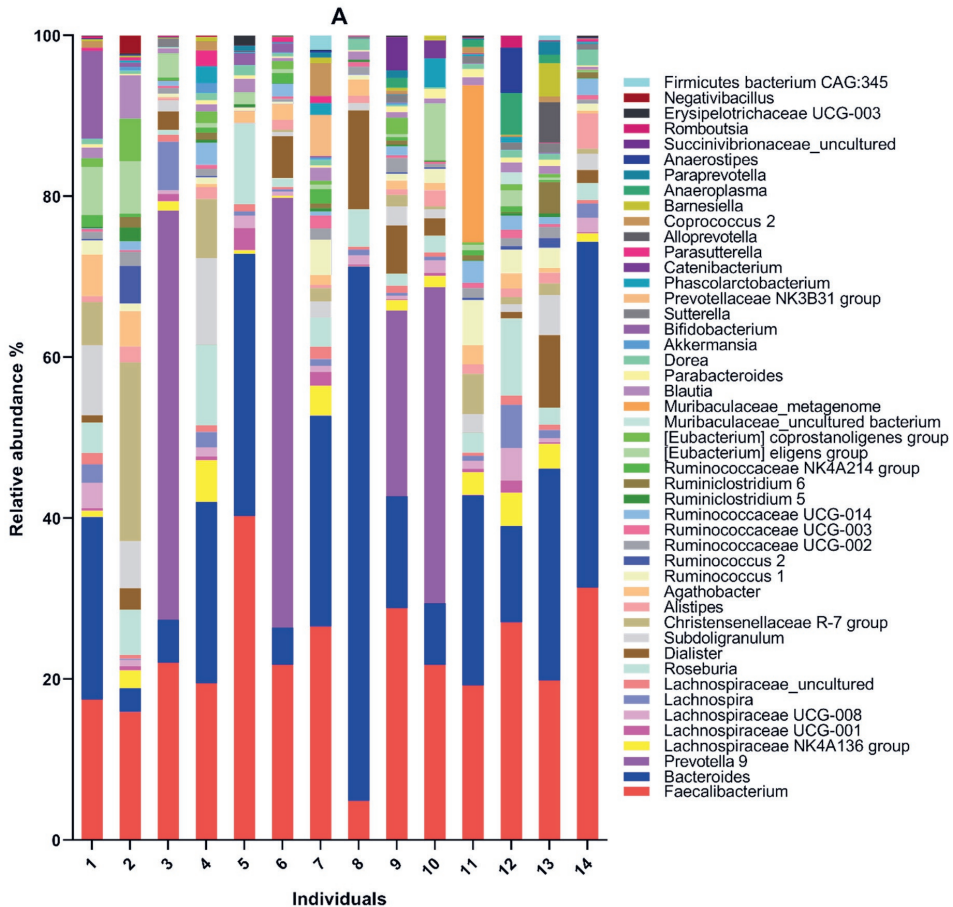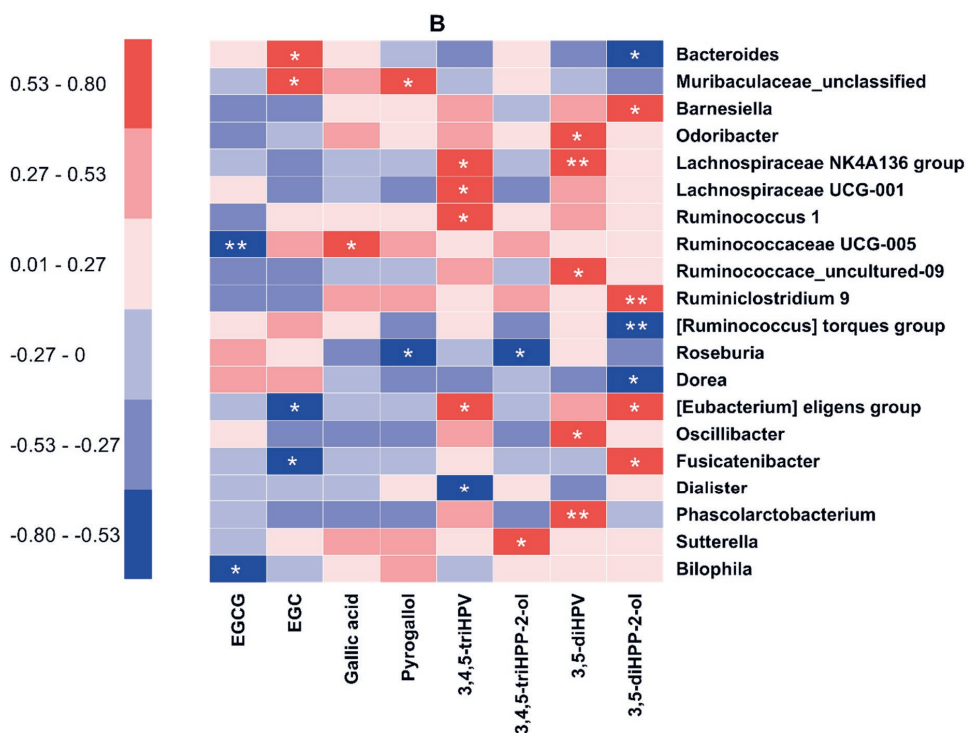
Figure 5. (A) Relative microbial abundance at the genus level of the 14 human faecal samples. (B) Spearman correlations between the taxon abundances of 20 bacterial genera and the concentration of EGCG and its 7 major microbial metabolites present in faecal slurries of 14 individuals after 2 h incubation. The sign and strength of the Spearman correlation coefficients are represented as colours (blue: negative; red: positive). The significances of the correlations are indicated by asterisks: *P < 0.05, **P < 0.01.

3.4 Activation of EpRE-mediated luciferase expression by EGCG and its microbial metabolites

Figure 6A shows the luciferase induction by EGCG and its 17 microbial metabolites at 30 μM in the EpRE-LUX assay and the Cytotox CALUX assay. The induction factors obtained in the EpRE-LUX assay were corrected using the respective results from the WST-1 cell viability assay (Supporting Information **Figure S7**). Results of the Cytotox CALUX assay show no increase in luciferase activity, ensuring that there was no false positive result in the EpRE-LUX assay due to stabilisation of the luciferase reporter protein. The positive control, i.e., 30 μM t-BHQ exhibited, a 7.8-fold induction, corroborating the sensitivity of the reporter gene assay.

The results reveal that at 30 μM concentration only gallic acid, pyrogallol and catechol were able to induce EpRE-mediated gene expression by more than 2 fold compared to the solvent control. Among these 3 metabolites, gallic acid exhibited the highest efficacy in activating the EpRE-mediated gene expression, with an induction factor of 6.1. The results obtained reveal that these 3 microbial metabolites are more potent than the parent compound EGCG. **Figure 6B-D** present full concentration-response curves for gallic acid, pyrogallol and catechol, respectively, enabling definition of the $BMCL_5$ and $BMCU_5$, i.e., the lower and upper 95% confidence limit of the concentration inducing 5% response. These two values amounted 6.7 μM and 25.2 μM for gallic acid; 8.0 μM and 25.3 μM for pyrogallol; 0.1 μM and 2.9 μM for catechol (Supporting Information **Figure S8**). **Figure 6B-D** also present the concentration-dependent luciferase activity detected in the Cytotox CALUX reporter cells. No increased luciferase activity was observed in the Cytotox CALUX assay upon exposure to increasing concentrations of gallic acid, pyrogallol and catechol, again, indicating the absence of luciferase stabilisation.
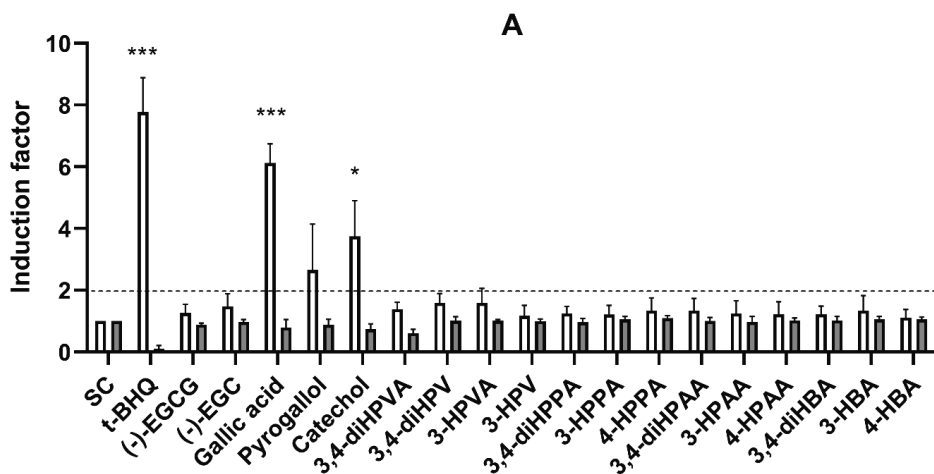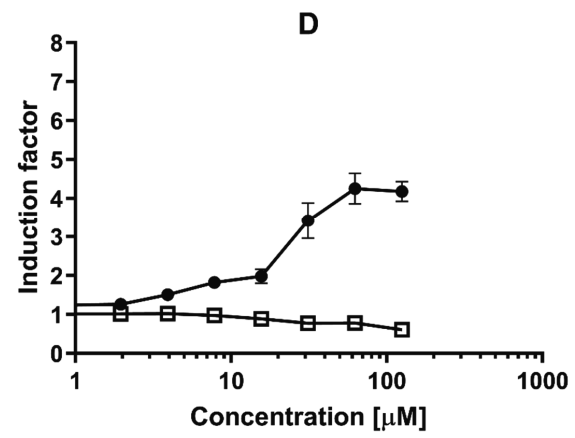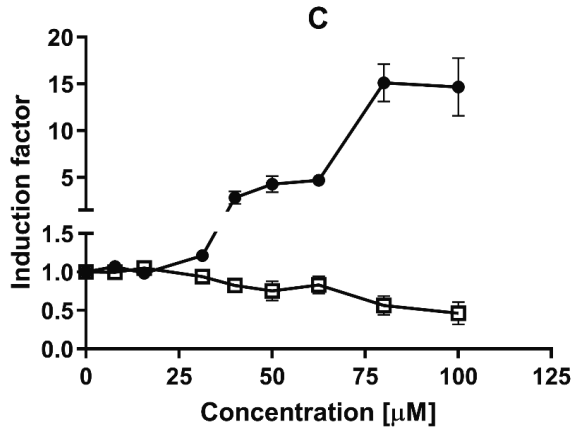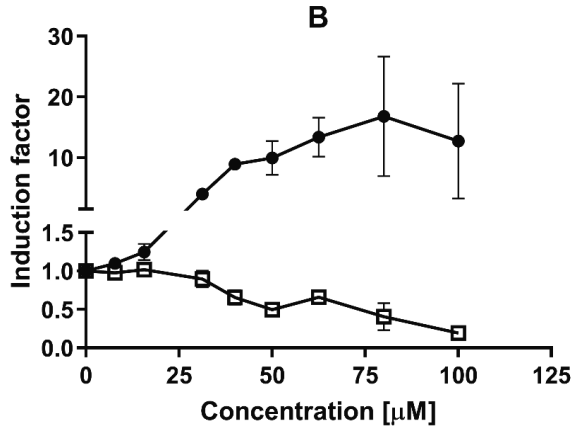
Figure 6. (A) Induction of luciferase activity in EpRE-LUX (white bars) and Cytotox CALUX (grey bar) reporter cells after 24 h exposure to EGCG and 17 EGCG microbial metabolites at 30 μM. The results are presented as mean ± SD of 3 replicates and the significance of the induction as compared to the solvent control is indicated by asterisks: *$P < 0.05$, **$P < 0.01$, ***$P < 0.001$. (B, C, D) Induction of luciferase activity in EpRE-LUX reporter cells (closed symbols) and in Cytotox CALUX cells (open symbols) after 24 h exposure to gallic acid (B), pyrogallol (C) and catechol (D) at increasing concentrations. Luciferase activity is expressed as induction factor (IF) compared to solvent control and data are presented as mean ± SEM of at least 4 independent replicates. All IFs were corrected for the viability measured by WST-1 assay showing by **Figure S7** in Supporting Information.

4. Discussion

The present paper quantified the time-dependent conversion of EGCG in *in vitro* faecal incubations with pooled and individual human samples in order to characterise the human intestinal microbiota-mediated conversion of EGCG, including the interindividual variability. In addition, EGCG and its microbial metabolites were tested in the EpRE-LUX assay to quantify their potential to induce beneficial EpRE-mediated gene expression.

Using *in vitro* faecal incubations, combined with LC-TQ-MS and LC-TOF-MS analysis, we successfully characterised the time-dependent metabolite profiles of EGCG, identifying seventeen EGCG colonic microbial metabolites and quantifying sixteen of them. The results revealed that gallic acid, pyrogallol, phenylpropane-2-ols, phenyl-γ-valerolactones and 3,5-diHPVA were the major intermediate metabolites formed during the time-dependent human faecal incubations of EGCG. Meanwhile, in the incubations with faecal samples from different individuals, substantial differences in the time-dependent EGCG microbial degradation and the accompanying metabolite patterns were observed among the individuals. Based on the observed differences in the rate of clearance of EGCG, individual 8 was identified as a slow metaboliser. This individual was previously also classified as a slow metaboliser of the related catechin EC using the *in vitro* faecal incubation model.[25] Gallic acid and pyrogallol, which were proven to be potent activators for EpRE-mediated genes expression also showed substantial interindividual differences in the amounts produced, amounting to levels between 9.4% to 51.0% and 5.7% to 46.3% of the EGCG equivalents, respectively.

Gallic acid and EGC are the primary metabolites resulting from degalloylation of the D-ring at the 3'' position of EGCG. This reaction was reported before to be catalysed by microbial galloyl

esterases present in microbiota, such as *Lactobacillus plantarum* IFPL935, *Enterobacter aerogenes*, *Raoultella planticola*, *Klebsiella pneumoniae* susp. *pneumoniae*, and *Bifidobacterium longum* subsp. *Infantis*.[26-27] Based on the analysis of the microbial taxonomic abundance of the individual faecal samples, correlations between microbial taxonomic abundance and metabolic abundance were defined in the present study. The results obtained showed statistically significant negative correlations between the quantity of residual EGCG and the relative abundance of *Ruminococcaceae UCG-005* and *Bilophila* which belong to the phyla *Firmicutes* and *Proteobacteria*. The finding of the latter correlation may point at another phylum that involves in the degalloylation of EGCG besides the ones identified previously. So far, there is no information regarding the enzymes or metabolic pathways responsible for EGCG metabolism in this genus. Perhaps, EGCG or (one of) its metabolites could serve as carbon or energy source or act as a terminal electron acceptor in anaerobic respiration.[28]

In line with above observation, *Ruminococcaceae UCG-005* showed a significant positive correlation with the amount of gallic acid formed. Gallic acid is subsequently decarboxylated by gallate decarboxylase to yield pyrogallol, which can be further metabolised by benzyl alcohol dehydrogenases, leading to the formation of catechol.[29] The concentration of gallic acid is inversely correlated with the amounts of *Lachnospiraceae* (although is not statistically significant), suggesting *Lachnospiraceae* is capable of the decarboxylation reaction, which is in agreement with the review written by Cortés-Martín and colleagues.[30] Catechol appeared to accumulate only to a limited extent, which hampered its quantification, probably because of its swift further conversion by catechol 1,2-dioxygenases.[31] In contrast, relatively large amounts of gallic acid and pyrogallol were detected at multiple timepoints of the incubation with pooled faecal samples.

Furthermore, the reductive cleavage of the heterocyclic C-ring of EGC resulted in time-dependent increases in the concentration of 3,4,5-triHPP-2-ol. *Eubacterium* SDG-2, *Lactobacillus plantarum*, *Eggerthella lenta* rK3 and *Adlercreutzia equolifaciens* were reported to be able to produce the metabolite phenylpropan-2-ol from catechins.[27, 32-33] In this study, we found a significant positive correlation between the relative abundance of *[Eubacterium] eligens group* and the formation of 3,5-diHPP-2-ol. It was reported that *Flavonifractor plautii*, which belongs to the class of *Clostridia*, was capable of the further metabolism of phenylpropan-2-ol into phenyl-γ-valerolactones.[27, 32] In our study, several genera of *Clostridia* were significantly positively correlated with the formation of 3,4,5-triHPV or 3,5-diHPV, i.e., *Lachnospiraceae NK4A136 group*, *Lachnospiraceae UCG-001*, *Ruminococcus 1*,

Ruminococcace_uncultured-09, *[Eubacterium] eligens group,* and *Oscillibacter*. It is of note that studies reported so far in this field focused on the identification of the potential involvement of specific genera in EGCG metabolism by elucidating correlations between bacterial genera and metabolites formed.[34-35] However, detailed information on actual enzymes and pathways in the respective intestinal microbiota responsible for the EGCG conversion have not yet been elucidated and provide an interesting topic for future research.

Both 3,5-diHPV and its precursor 3,5-diHPP-2-ol were quantified at higher levels than their isomers 3,4-diHPP-2-ol and 3,4-diHPV (the latter was identified and quantified with reference standard), respectively, indicating a preference of the intestinal microbiota for performing 4'-dehydroxylation over 5'-dehydroxylation in the B-ring of the molecular skeleton. In the study of van Duynhoven et al. (2014), 3,5-diHPV and 3,4-diHPV were both purified and subsequently identified using Orbitrap MS and 1H NMR, so both isomers can be expected to be present in the microbial conversion of EGCG.[36] The latter molecule, 3,4-diHPV, was proposed by van Duynhoven et al. (2014) to be formed primarily from microbial conversion of EC.[36] This high level of formation of 3,5-diHPV in EGCG conversion is in line with an *in vivo* study that reported high human urinary levels (8.3 µM) of 3,5-diHPV at 9 - 12 hours following an oral dose of 200 mg pure EGCG, suggesting a considerable amount of this compound entered the systemic circulation of human subjects.[37]

Also, other characteristics of the *in vitro* faecal metabolite patterns were consistent with *in vivo* data. For example, phenyl-γ-valerolactones were proven to be among the most abundant metabolites detected in plasma and urine in several *in vivo* studies in which human volunteers were exposed to green tea or catechin standards.[10-11, 38-39] Moreover, the major metabolite pyrogallol detected in high abundance in the *in vitro* incubation was also reported to be one of the main metabolites in urinary excretion after green tea consumption by human volunteers.[39] It is worth noting that consumption of black tea could also result in relatively high amounts of gallic acid and pyrogallol detected *in vivo*.[40-41] For instance, Duynhoven et al. (2014) quantified eleven polyphenols and microflora-derived metabolites in plasma after a single-dose black tea extract consumption by human subjects. Among all, pyrogallol-2-*O*-sulfate was found to be the most abundant conjugated metabolite with a C_{max} of 2.6 µM and t_{max} of 8 h.[36]

There are 10^{11}-10^{12} bacteria/g in the colon content, the highest amount of all parts of the gastrointestinal tract of the host.[42] By combining innovative cultivation techniques with high-throughput sequencing techniques, it was shown that up to 95% of molecular species detected in the cecum have corresponding strains in faecal cultures of mammalian gut microbes.[43-44]

Moreover, use of anaerobic faecal *in vitro* incubations to study colonic metabolism was previously evaluated in a study in which microbial-related *in vivo* metabolic changes in gut tissue, cecum content and feces of rats treated with antibiotics were compared [45]. Based on the results obtained it was concluded that 'as a non-invasive sampling method, feces provide a suitable matrix for studies on metabolism by the gut microbiota'.[45]

The beneficial health effects associated with green tea consumption are often ascribed to the tea catechins including EC, ECG, EGC and EGCG, of which EGCG is the most abundant.[2] However, EGCG has been reported to show the lowest absorption of all tea catechins because of its 3-*O*-galloyl moiety, with a C_{max} of 0.12 µM in human plasma upon a single 50-mg dose.[46] This concentration of ECGC appears to be unable to activate EpRE-mediated gene expression (**Figure 6**).[9, 47] For this reason, in the present study we, investigated whether the microflora-derived EGCG metabolites possess the potential to activate EpRE-mediated gene expression. From the results obtained in the EpRE-LUX reporter gene assay, especially the EGCG metabolites gallic acid, pyrogallol and catechol showed a high capacity for inducing Nrf2 activation. These three compounds have at least two adjacent hydroxyl moieties on their benzene rings, facilitating their (auto)oxidation to (semi)quinones, required to enable activation of EpRE-mediated gene expression.[48] In the present study, gallic acid, pyrogallol and catechol were shown to be able to activate EpRE-mediated gene expression in a concentration-dependent manner with a $BMCL_5$ of 6.7 µM, 8.0 µM and 0.1 µM, respectively, i.e., at concentrations that are reported to be physiologically achievable in *in vivo* studies.[49-50] The maximum EpRE-mediated induction of luciferase activity by gallic acid and pyrogallol were comparable, with an IF of 16.8 and 15.1, respectively, being substantially higher than that of catechol (IF = 5.0). This might be related to the fact that anti-radical and antioxidant activity, and thus electron donating capacity and potential to generate (semi)quinones were reported to be positively correlated with the number of hydroxyl moieties on the aromatic ring.[51] This also explains the absence of EpRE-mediated luciferase induction for monohydroxylated phenolics. Additionally, the high Nrf2-activation induction by gallic acid and pyrogallol also corroborates the importance of the galloyl moiety in their chemoprotective properties.[47]

Interestingly, EGCG was reported to be the most potent inducer of EpRE-mediated gene expression compared with other major tea catechins.[9, 47] We now report that its microbial intestinal metabolites gallic acid, pyrogallol and catechol are substantially more potent than the parent catechin EGCG and more likely to activate EpRE-mediated luciferase gene expression at physiologically relevant low and even subµM concentrations. A possible reason for the

relatively lower EpRE-mediated activity of EGCG as compared to its degradation products could be that in contrast to gallic acid, pyrogallol and catechol, EGCG has a bulky three-dimensional structure which may hamper interaction of its quinone type metabolites with the respective cysteine residues in Keap1 and/or its cellular uptake as compared to that of the lower molecular weight phenolics. Given these differences between EGCG and its low molecular weight metabolites it is also of interest to note that after a similar dose of EGCG and gallic acid, the plasma C_{max} of gallic acid is 33.3 times the C_{max} of EGCG.[46] Additionally, gallic acid, pyrogallol and catechol obtain a planar molecular structure while EGCG is a non-planar chemical. Boerboom, *et al*. (2006) emphasized the necessity of the planar structure of phenolics in inducing EpRE-mediated gene expression in the EpRE reporter gene assay. They compared EpRE-mediated transcription activation of five planar flavonoids and one non-planar flavonoid, and reported that the lack of the C2-C3 double bond causing a non-planar aliphatic C-ring in taxifolin could be a possible reason for the distinctive unresponsiveness of this non-planar flavonoid in the EpRE-LUX reporter gene assay.[16] Moreover, various phenylcarboxylic acid metabolites were found in the present study to be less potent or even inactive in inducing EpRE-mediated gene expression in spite of the presence of a catechol moiety in their chemical structure (e.g., 3,4-diHPVA, 3-HPVA, etc.). This is likely due to the fact that at the neutral pH in the EpRE-LUX assay medium, their carboxyl moiety will be largely deprotonated, hampering their diffusion over the cellular membranes. As a result, their low intracellular concentrations may explain their low activity in the bioassay.[52-53]

In conclusion, this study introduced an *in vitro* anaerobic incubation model to study microbial metabolism of EGCG. The microflora-derived metabolites were qualitatively and quantitatively detected with the LC-TQ-MS and LC-TOF-MS. Substantial interindividual differences were found in the formation of EGCG gut microbial metabolites both in terms of type and level, which is likely due to the differences in host microbiota composition. EGCG and its major microbial metabolites were subsequently tested in the EpRE-LUX reporter gene assay to compare their potency for Nrf2-activation. Two major metabolites, i.e., gallic acid and pyrogallol, together with a minor metabolite catechol, were shown to be potent inducers of EpRE-mediated gene expression. Because these two major metabolites, at physiologically relevant concentrations, showed higher potential for EpRE-mediated gene expression than EGCG, it is concluded that these microbial metabolites may contribute to the potential beneficial effects of EGCG. The interindividual differences in the level of their formation and

bioaccumulation may result in interindividual differences in the beneficial effects of EGCG and the potential health-promoting effects of green tea consumption.

Abbreviations: EC, (-)-epicatechin; ECG, (-)-epicatechin-3-*O*-galllate; EGC, (-)-epigallocatechin; EGCG, (-)-epigallocatechin-3-*O*-gallate; LC-TOF-MS, liquid chromatograph time-of-flight mass spectrometry; LC-TQ-MS, liquid chromatograph triple quadrupole mass spectrometry; 3,4-diHPP-2-ol, 1-(3',4'-dihydroxyphenyl)-3-(2'',4'',6''-trihydroxyphenyl)-2-propanol; 3,5-diHPP-2-ol, 1-(3',5'-dihydroxyphenyl)-3-(2'',4'',6''-trihydroxyphenyl)-2-propanol; 3,4,5-triHPP-2-ol, 1-(3',4',5'-trihydroxyphenyl)-3-(2'',4'',6''-trihydroxyphenyl)-2-propanol; 3-HPP-2-ol, 1-(3'-hydroxyphenyl)-3-(2'',4'',6''-trihydroxyphenyl)-2-propanol; 4H-HPVA, 4-hydroxy-5-(3'-hydroxyphenyl)-valeric acid; 3,4-diHPV, 5-(3',4'-dihydroxyphenyl)-γ-valerolactone; 3,5-diHPV, 5-(3',5'-dihydroxyphenyl)-γ-valerolactone; 3-HPV, 5-(3'-hydroxyphenyl)-γ-valerolactone; 3,4-diHPVA, 5-(3',4'-dihydroxyphenyl)valeric acid; 3,5-diHPVA, 5-(3',5'-dihydroxyphenyl)valeric acid; 3-HPVA, 5-(3'-hydroxyphenyl)valeric acid; 3,4-diHPPA, 3-(3',4'-dihydroxyphenyl)propionic acid; 3-HPPA, 3-(3'-hydroxyphenyl)propionic acid; 3,4-diHPAA, 3',4'-dihydroxyphenylacetic acid; 3-HPAA, 3'-hydroxyphenylacetic acid; 4-HPAA, 4'-hydroxyphenylacetic acid; 3,4-diHPBA, 3',4'-dihydroxybenzoic acid; 4-HPBA, 4'-hydroxybenzoic acid.

Acknowledgement

Author Contributions

C.L. and E.J. performed experiments. J.V. and L.H. provided technical support. C.L. and M.B. interpreted data. C.L. wrote the manuscript. I.M.C.M.R. and K.B. designed the scope of the manuscript and revised the manuscript. All authors read and approved the final manuscript.

Conflict of interest

The authors declare that there is no conflict of interest.

5. References

1.   Sang, S.; Lambert, J. D.; Ho, C.-T.; Yang, C. S., The chemistry and biotransformation of tea constituents. *Pharmacol. Res.* **2011,** *64*, 87-99.

2.   Liu, Z.; Bruins, M. E.; Ni, L.; Vincken, J.-P., Green and black tea phenolics: Bioavailability, transformation by colonic microbiota, and modulation of colonic microbiota. *J. Agric. Food Chem.* **2018,** *66*, 8469-8477.

3.   Gan, R.-Y.; Li, H.-B.; Sui, Z.-Q.; Corke, H., Absorption, metabolism, anti-cancer effect and molecular targets of epigallocatechin gallate (EGCG): An updated review. *Crit. Rev. Food Sci. Nutr.* **2018,** *58*, 924-941.

4.   Yamamoto, M.; Kensler, T. W.; Motohashi, H., The KEAP1-NRF2 system: a thiol-based sensor-effector apparatus for maintaining redox homeostasis. *Physiol. Rev.* **2018,** *98*, 1169-1203.

5.   Krajka-Kuźniak, V.; Paluszczak, J.; Baer-Dubowska, W., The Nrf2-ARE signaling pathway: an update on its regulation and possible role in cancer prevention and treatment. *Pharmacol. Rep.* **2017,** *69*, 393-402.

6.   Sun, W.; Liu, X.; Zhang, H.; Song, Y.; Li, T.; Liu, X.; Liu, Y.; Guo, L.; Wang, F.; Yang, T., Epigallocatechin gallate upregulates NRF2 to prevent diabetic nephropathy via disabling KEAP1. *Free Radical Biol. Med.* **2017,** *108*, 840-857.

7.   Yuan, J.-H.; Li, Y.-Q.; Yang, X.-Y., Inhibition of epigallocatechin gallate on orthotopic colon cancer by upregulating the Nrf2-UGT1A signal pathway in nude mice. *Pharmacology* **2007,** *80*, 269-278.

8.   Lee-Hilz, Y. Y.; Boerboom, A.-M. J.; Westphal, A. H.; van Berkel, W. J.; Aarts, J. M.; Rietjens, I. M., Pro-oxidant activity of flavonoids induces EpRE-mediated gene expression. *Chem. Res. Toxicol.* **2006,** *19*, 1499-1505.

9.   Muzolf-Panek, M.; Gliszczyńska-Świgło, A.; de Haan, L.; Aarts, J. M.; Szymusiak, H.; Vervoort, J. M.; Tyrakowska, B.; Rietjens, I. M., Role of catechin quinones in the induction of EpRE-mediated gene expression. *Chem. Res. Toxicol.* **2008,** *21*, 2352-2360.

10.   Del Rio, D.; Calani, L.; Cordero, C.; Salvatore, S.; Pellegrini, N.; Brighenti, F., Bioavailability and catabolism of green tea flavan-3-ols in humans. *Nutrition* **2010,** *26*, 1110-1116.

11.   Ottaviani, J. I.; Fong, R.; Kimball, J.; Ensunsa, J. L.; Britten, A.; Lucarelli, D.; Luben, R.; Grace, P. B.; Mawson, D. H.; Tym, A., Evaluation at scale of microbiome-derived metabolites as biomarker of flavan-3-ol intake in epidemiological studies. *Sci. Rep.* **2018,** *8*, 1-11.

12.   Monagas, M.; Urpi-Sarda, M.; Sánchez-Patán, F.; Llorach, R.; Garrido, I.; Gómez-Cordovés, C.; Andres-Lacueva, C.; Bartolomé, B., Insights into the metabolism and microbial biotransformation of dietary flavan-3-ols and the bioactivity of their metabolites. *Food & function* **2010,** *1* (3), 233-253.

13.   Márquez Campos, E.; Stehle, P.; Simon, M.-C., Microbial metabolites of flavan-3-ols and their biological activity. *Nutrients* **2019,** *11*, 2260.

14.   Uhlenhut, K.; Högger, P., Facilitated cellular uptake and suppression of inducible nitric oxide synthase by a metabolite of maritime pine bark extract (Pycnogenol). *Free Radical Biol. Med.* **2012,** *53*, 305-313.

15.   Lozupone, C. A.; Stombaugh, J. I.; Gordon, J. I.; Jansson, J. K.; Knight, R., Diversity, stability and resilience of the human gut microbiota. *Nature* **2012,** *489*, 220-230.

16.   Boerboom, A.-M. J.; Vermeulen, M.; van der Woude, H.; Bremer, B. I.; Lee-Hilz, Y. Y.; Kampman, E.; Van Bladeren, P. J.; Rietjens, I. M.; Aarts, J. M., Newly constructed stable reporter cell lines for mechanistic studies on electrophile-responsive element-mediated gene expression reveal a role for flavonoid planarity. *Biochem. Pharmacol.* **2006,** *72*, 217-226.

17.   Sonneveld, E.; Van den Brink, C. E.; Van der Leede, B.; Schulkes, R.-K. A.; Petkovich, M.; Van der Burg, B.; Van der Saag, P., Human retinoic acid (RA) 4-hydroxylase (CYP26) is highly specific for all-trans-RA and can be induced through RA receptors in human breast and colon carcinoma cells. *Cell Growth Differ.* **1998,** *9*, 629-638.

18.   van der Linden, S. C.; von Bergh, A. R.; van Vught-Lussenburg, B. M.; Jonker, L. R.; Teunis, M.; Krul, C. A.; van der Burg, B., Development of a panel of high-throughput reporter-gene assays to detect genotoxicity and oxidative stress. *Mutat. Res. Genet. Toxicol. Environ. Mutagen.* **2014,** *760*, 23-32.

19.   Puupponen-Pimia, R.; Nohynek, L.; Meier, C.; Kahkonen, M.; Heinonen, M.; Hopia, A.; Oksman-Caldentey, K. M., Antimicrobial properties of phenolic compounds from berries. *J. Appl. Microbiol.* **2001,** *90* (4), 494-507.

20.   Gijsbers, L.; van Eekelen, H. D.; Nguyen, T. H.; De Haan, L. H.; van der Burg, B.; Aarts, J. M.; Rietjens, I. M.; Bovy, A. G., Induction of electrophile-responsive element (EpRE)-mediated gene expression by tomato extracts in vitro. *Food Chem.* **2012,** *135*, 1166-1172.

21.   Stalmach, A.; Mullen, W.; Steiling, H.; Williamson, G.; Lean, M. E.; Crozier, A., Absorption, metabolism, and excretion of green tea flavan-3-ols in humans with an ileostomy. *Mol. Nutr. Food Res.* **2010,** *54*, 323-334.

22.   Roowi, S.; Stalmach, A.; Mullen, W.; Lean, M. E.; Edwards, C. A.; Crozier, A., Green tea flavan-3-ols: colonic degradation and urinary excretion of catabolites by humans. *J. Agric. Food Chem.* **2010,** *58*, 1296-1304.

23.   Brown, R. P.; Delp, M. D.; Lindstedt, S. L.; Rhomberg, L. R.; Beliles, R. P., Physiological parameter values for physiologically based pharmacokinetic models. *Toxicol. Ind. Health* **1997,** *13*, 407-484.

24.   EFSA; RIVM EFSA Statistical Models (https://shiny-efsa.openanalytics.eu/app/bmd). https://shiny-efsa.openanalytics.eu/app/bmd (accessed August 26).

25.   Liu, C.; Vervoort, J.; Beekmann, K.; Baccaro, M.; Kamelia, L.; Wesseling, S.; Rietjens, I. M., Interindividual differences in human intestinal microbial conversion of (−)-epicatechin to bioactive phenolic compounds. *Journal of agricultural and food chemistry* **2020,** *68* (48), 14168-14181.

26.   Takagaki, A.; Nanjo, F., Metabolism of (−)-epigallocatechin gallate by rat intestinal flora. *J. Agric. Food Chem.* **2010,** *58*, 1313-1321.

27.   Sánchez-Patán, F.; Tabasco, R.; Monagas, M.; Requena, T.; Peláez, C.; Moreno-Arribas, M. V.; Bartolomé, B. a., Capability of Lactobacillus plantarum IFPL935 to catabolize flavan-3-ol compounds and complex phenolic extracts. *J. Agric. Food Chem.* **2012,** *60*, 7142-7151.

28.   Da Silva, S. M.; Venceslau, S. S.; Fernandes, C. L.; Valente, F. M.; Pereira, I. A., Hydrogen as an energy source for the human pathogen Bilophila wadsworthia. *Antonie Van Leeuwenhoek* **2008,** *93*, 381-390.

29.   Rodríguez, H.; Curiel, J. A.; Landete, J. M.; de las Rivas, B.; de Felipe, F. L.; Gómez-Cordovés, C.; Mancheño, J. M.; Muñoz, R., Food phenolics and lactic acid bacteria. *Int. J. Food Microbiol.* **2009,** *132*, 79-90.

30.   Cortés-Martín, A.; Selma, M. V.; Tomás-Barberán, F. A.; González-Sarrías, A.; Espín, J. C., Where to look into the puzzle of polyphenols and health? The postbiotics and gut microbiota associated with human metabotypes. *Mol. Nutr. Food Res.* **2020,** *64*, 1900952.

31.   Broderick, J. B., Catechol dioxygenases. *Essays Biochem.* **1999,** *34*, 173-189.

32.   Kutschera, M.; Engst, W.; Blaut, M.; Braune, A., Isolation of catechin-converting human intestinal bacteria. *J. Appl. Microbiol.* **2011,** *111*, 165-175.

33.   Takagaki, A.; Nanjo, F., Bioconversion of (−)-epicatechin,(+)-epicatechin,(−)-catechin, and (+)-catechin by (−)-epigallocatechin-metabolizing bacteria. *Biol. Pharm. Bull.* **2015,** *38*, 789-794.

34.   Liu, Z.; de Bruijn, W. J.; Bruins, M. E.; Vincken, J.-P., Reciprocal Interactions between Epigallocatechin-3-gallate (EGCG) and Human Gut Microbiota In Vitro. *J. Agric. Food Chem.* **2020,** *68*, 9804-9815.

35.   Trošt, K.; Ulaszewska, M. M.; Stanstrup, J.; Albanese, D.; De Filippo, C.; Tuohy, K. M.; Natella, F.; Scaccini, C.; Mattivi, F., Host: Microbiome co-metabolic processing of dietary polyphenols–An acute, single blinded, cross-over study with different doses of apple polyphenols in healthy subjects. *Food Res. Int.* **2018,** *112*, 108-128.

36.   van Duynhoven, J.; van der Hooft, J. J.; van Dorsten, F. A.; Peters, S.; Foltz, M.; Gomez-Roldan, V.; Vervoort, J.; de Vos, R. C.; Jacobs, D. M., Rapid and sustained systemic circulation of conjugated gut microbial catabolites after single-dose black tea extract consumption. *J. Proteome Res.* **2014**, *13*, 2668-2678.

37.   Meng, X.; Sang, S.; Zhu, N.; Lu, H.; Sheng, S.; Lee, M.-J.; Ho, C.-T.; Yang, C. S., Identification and characterization of methylated and ring-fission metabolites of tea catechins formed in humans, mice, and rats. *Chem. Res. Toxicol.* **2002**, *15*, 1042-1050.

38.   Ottaviani, J. I.; Borges, G.; Momma, T. Y.; Spencer, J. P.; Keen, C. L.; Crozier, A.; Schroeter, H., The metabolome of [2-14 C](−)-epicatechin in humans: Implications for the assessment of efficacy, safety, and mechanisms of action of polyphenolic bioactives. *Sci. Rep.* **2016,** *6*, 29034.

39.   van der Hooft, J. J.; de Vos, R. C.; Mihaleva, V.; Bino, R. J.; Ridder, L.; de Roo, N.; Jacobs, D. M.; van Duynhoven, J. P.; Vervoort, J., Structural elucidation and quantification of phenolic conjugates present in human urine after tea intake. *Anal. Chem.* **2012,** *84*, 7263-7271.

40.   Hodgson, J. M.; Morton, L. W.; Puddey, I. B.; Beilin, L. J.; Croft, K. D., Gallic acid metabolites are markers of black tea intake in humans. *J. Agric. Food Chem.* **2000**, *48*, 2276-2280.

41.   Pereira-Caro, G.; Moreno-Rojas, J. M.; Brindani, N.; Del Rio, D.; Lean, M. E.; Hara, Y.; Crozier, A., Bioavailability of black tea theaflavins: absorption, metabolism, and colonic catabolism. *J. Agric. Food Chem.* **2017,** *65*, 5365-5374.

42.   Possemiers, S.; Grootaert, C.; Vermeiren, J.; Gross, G.; Marzorati, M.; Verstraete, W.; de Wiele, T. V., The intestinal environment in health and disease-recent insights on the potential of intestinal bacteria to influence human health. *Curr. Pharm. Des.* **2009**, *15*, 2051-2065.

43.   Lagkouvardos, I.; Overmann, J.; Clavel, T., Cultured microbes represent a substantial fraction of the human and mouse gut microbiota. *Gut microbes* **2017,** *8*, 493-503.

44.   Lau, J. T.; Whelan, F. J.; Herath, I.; Lee, C. H.; Collins, S. M.; Bercik, P.; Surette, M. G., Capturing the diversity of the human gut microbiota through culture-enriched molecular profiling. *Genome Med.* **2016,** *8*, 1-10.

45.   Behr, C.; Sperber, S.; Jiang, X.; Strauss, V.; Kamp, H.; Walk, T.; Herold, M.; Beekmann, K.; Rietjens, I.; Van Ravenzwaay, B., Microbiome-related metabolite changes in gut tissue, cecum content and feces of rats treated with antibiotics. *Toxicol. Appl. Pharmacol.* **2018,** *355*, 198-210.

46.   Manach, C.; Williamson, G.; Morand, C.; Scalbert, A.; Rémésy, C., Bioavailability and bioefficacy of polyphenols in humans. I. Review of 97 bioavailability studies. *Am. J. Clin. Nutr.* **2005,** *81*, 230S-242S.

47.   Chen, C.; Yu, R.; Owuor, E. D.; Kong, A.-N. T., Activation of antioxidant-response element (ARE), mitogen-activated protein kinases (MAPKs) and caspases by major green tea polyphenol components during cell survival and death. *Arch. Pharmacal Res.* **2000,** *23*, 605.

48.   Awad, H. M.; Boersma, M. G.; Boeren, S.; van Bladeren, P. J.; Vervoort, J.; Rietjens, I. M., Structure−activity study on the quinone/quinone methide chemistry of flavonoids. *Chem. Res. Toxicol.* **2001,** *14*, 398-408.

49.   van der Pijl, P. C.; Foltz, M.; Glube, N. D.; Peters, S.; Duchateau, G. S., Pharmacokinetics of black tea-derived phenolic acids in plasma. *J. Funct. Foods* **2015**, *17*, 667-675.

50.   Sun, Z.; Zhao, L.; Zuo, L.; Qi, C.; Zhao, P.; Hou, X., A UHPLC–MS/MS method for simultaneous determination of six flavonoids, gallic acid and 5, 8-dihydroxy-1, 4-naphthoquinone in rat plasma and its application to a pharmacokinetic study of Cortex Juglandis Mandshuricae extract. *J. Chromatogr. B: Anal. Technol. Biomed. Life Sci.* **2014,** *958*, 55-62.

51.   Sroka, Z.; Cisowski, W., Hydrogen peroxide scavenging, antioxidant and anti-radical activity of some phenolic acids. *Food Chem. Toxicol.* **2003,** *41*, 753-758.

52.   de Pinedo, A. T.; Peñalver, P.; Pérez-Victoria, I.; Rondón, D.; Morales, J. C., Synthesis of new phenolic fatty acid esters and their evaluation as lipophilic antioxidants in an oil matrix. *Food Chem.* **2007,** *105*, 657-665.

53.   Lue, B.-M.; Nielsen, N. S.; Jacobsen, C.; Hellgren, L.; Guo, Z.; Xu, X., Antioxidant properties of modified rutin esters by DPPH, reducing power, iron chelation and human low density lipoprotein assays. *Food Chem.* **2010,** *123*, 221-230.

Supporting Information

Table S1. LC-TQ-MS and LC-TOF-MS identification of green tea catechins (in negative mode) and their potential colonic metabolites, based on relative retention time and MS (or MS fragmentation) values.

Analytical platform	Chemical	Parent ion (m/z)	Product ion (m/z)	Collision energy (V)	Retention time
LC-TQ-MS	EGCG	457.1	169.05, 125.05, 305.15	18, 38, 17	5.33
	ECG	441.1	168.95, 289.05, 125.05	21, 17, 39	7.15
	EGC	305.1	125.10, 219.00, 137.10	22, 18, 22	3.80
	EC	289.1	245.10, 109.10, 203.00	14, 25, 18	5.72
	3,4-diHPVA	209.0	135.10, 191.05, 122.10	18, 15, 21	7.60
	3,4-diHPV	207.1	163.05, 122.15, 161.10	16, 21, 21	5.00
	3-HPVA	193.1	106.15, 149.05, 175.05	23, 17, 15	7.88
	3-HPV	191.1	147.05, 102.90, 135.00	8, 15, 15	6.93
	3,4-diHPPA	181.1	137.10, 59.00, 109.00	14, 17, 15	3.95
	gallic acid	169.1	125.10, 79.00, 81.10	15, 24, 18	0.75
	3-HPPA	165.1	121.20, 106.10, 119.15	13, 22, 16	6.33
	3-HPAA	151.0	107.10, 65.00	12, 25	4.30
	4-HPAA	151.0	107.10, 79.15, 93.20	10, 20, 22	3.82
	catechol	109.2	90.95, 81.10, 53.15	22, 21, 20	1.85
LC-TOF-MS	3,4,5-triHPP-2-ol	307.08	\	\	16.4
	3,4-diHPP-2-ol	291.09	\	\	19.6
	3,5-diHPP-2-ol	291.09	\	\	18.5
	3-HPP-2-ol	275.09	\	\	23.1
	3,4,5-triHPV	223.06	\	\	14.4
	3,5-diHPVA	209.08	\	\	22.4
	3,5-diHPV	207.07	\	\	17.4
	4H-HPVA	209.08	\	\	15.2
	pyrogallol	125.02	\	\	2.6
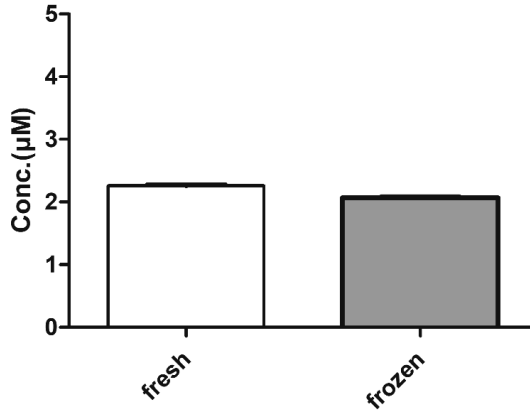
Figure S1. Gallic acid formation after 1.5 h anaerobic incubation with the fresh faecal slurry and the same faecal slurry but frozen for 1 week prior to incubation.
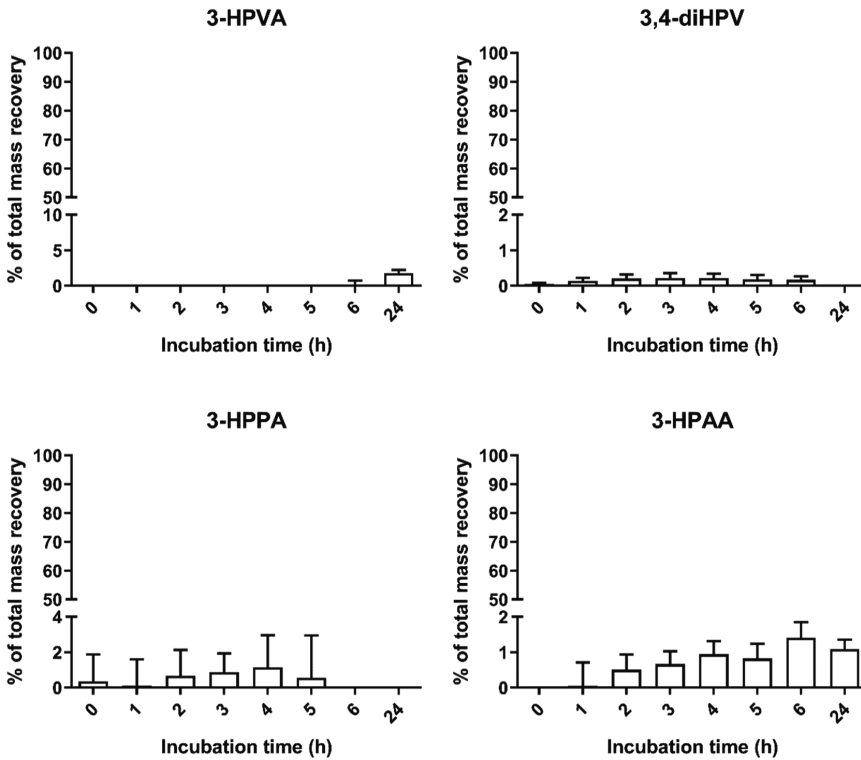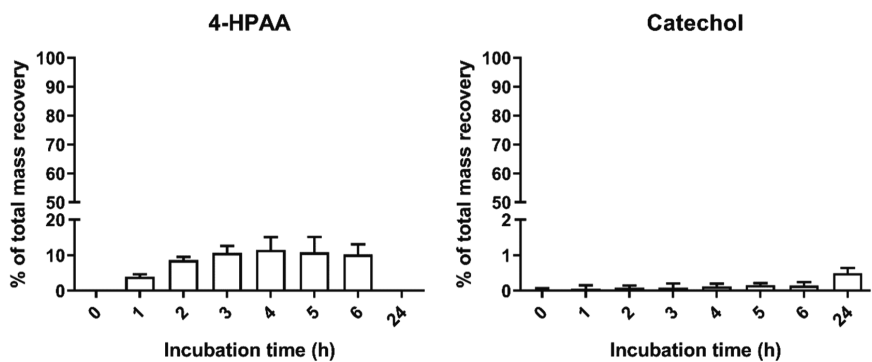
Figure S2. Phenolic compounds quantified in the negative control (without adding EGCG in pooled faecal incubations) at different incubation timepoints. Results are shown as mean ± SD from 3 independent incubations.
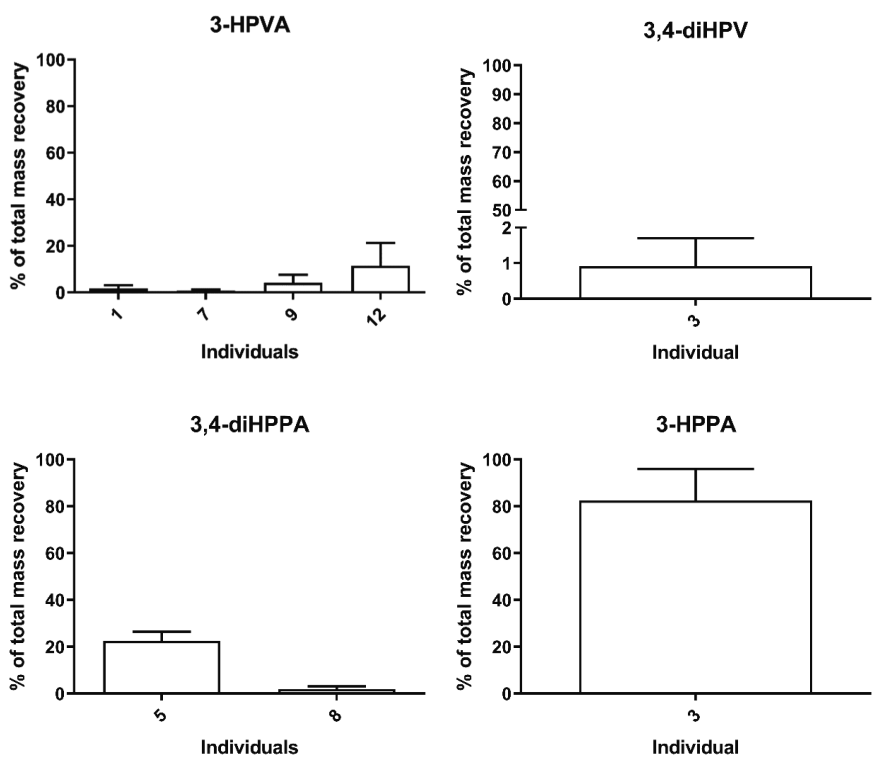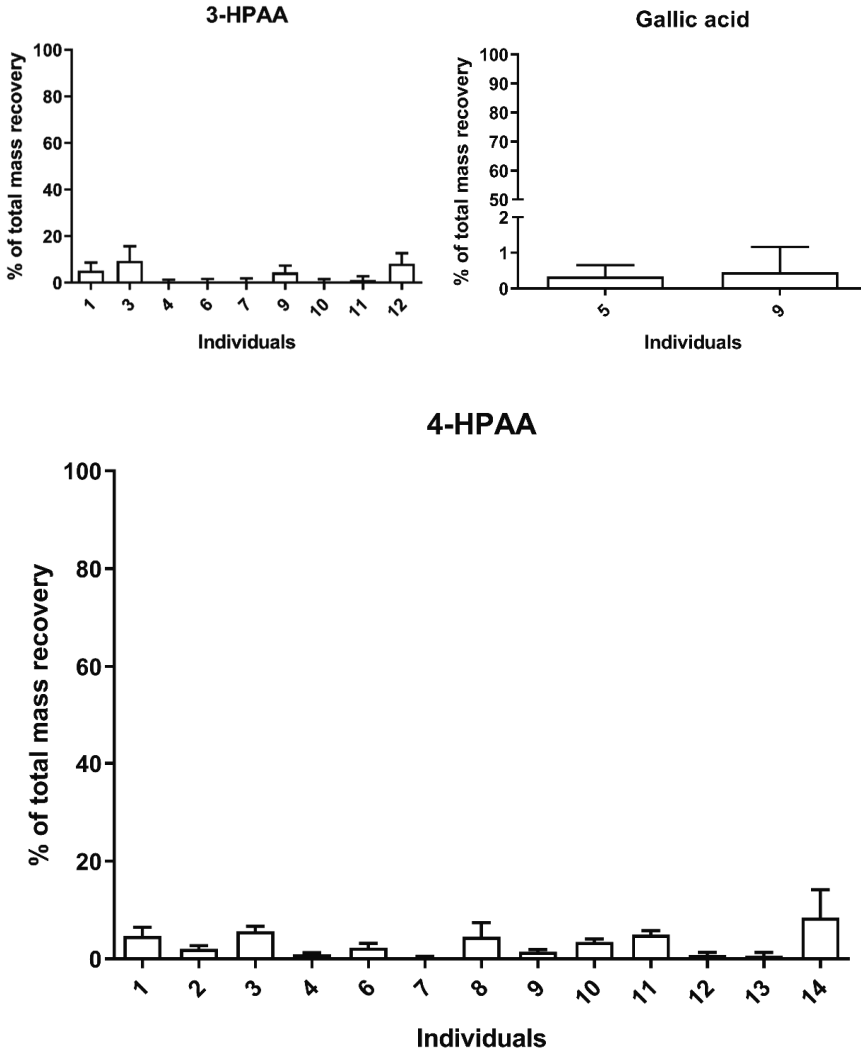
Figure S3. Phenolic compounds quantified in different individuals in the negative control (without adding EGCG in individual faecal incubations) at 2 h of incubations. Results are shown as mean ± SD from 3 independent incubations.
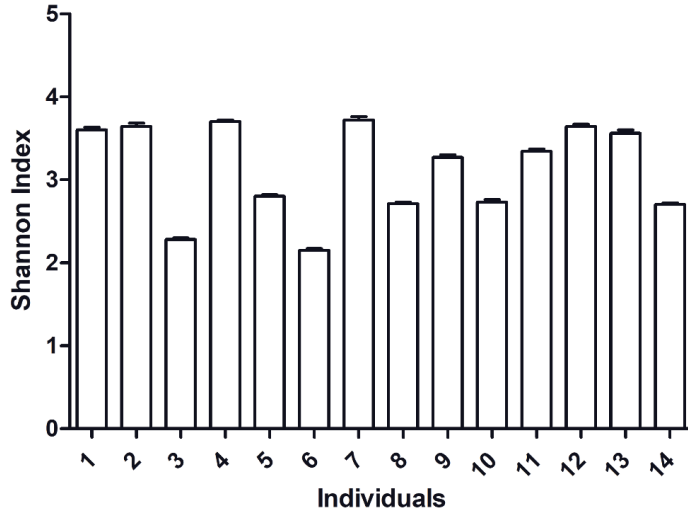
Figure S4. Shannon diversity indices of microbial compositions of the 14 human faecal samples.
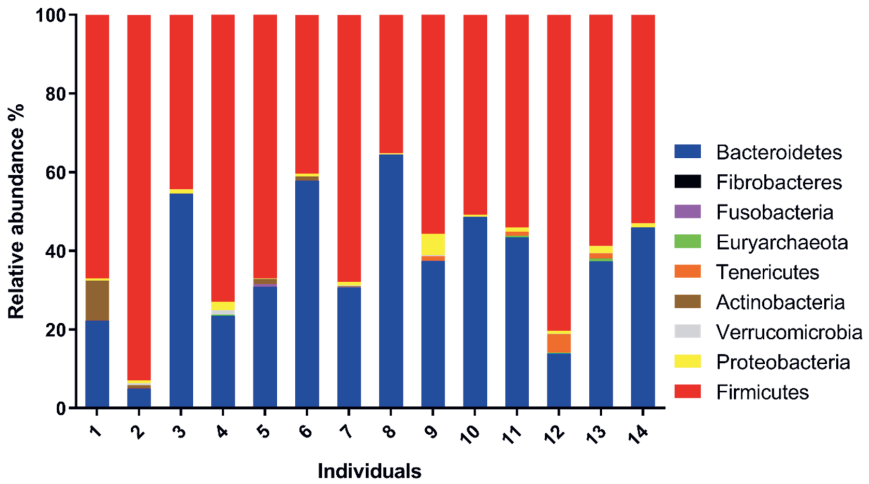
Figure S5. Relative microbial abundances at the *phylum* level of the 14 human faecal samples.
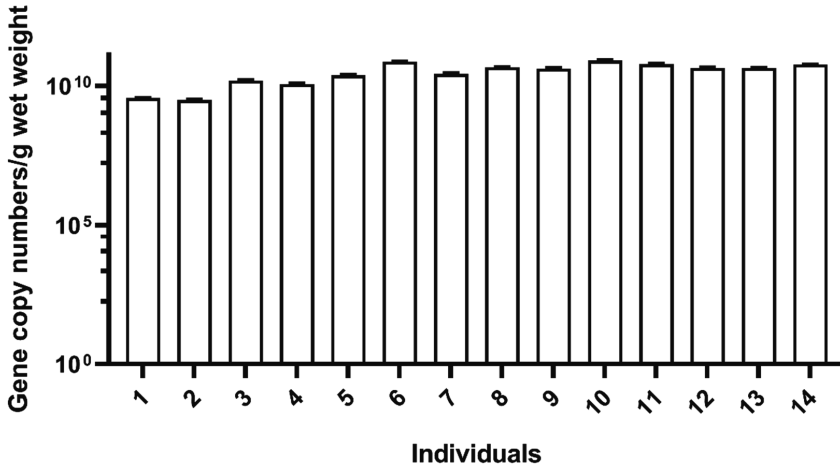
Figure S6. Bacterial load of faecal samples from 14 individuals, expressed as gene copy numbers per gram of wet weight of faecal slurry (mean value ± SD, n = 3)
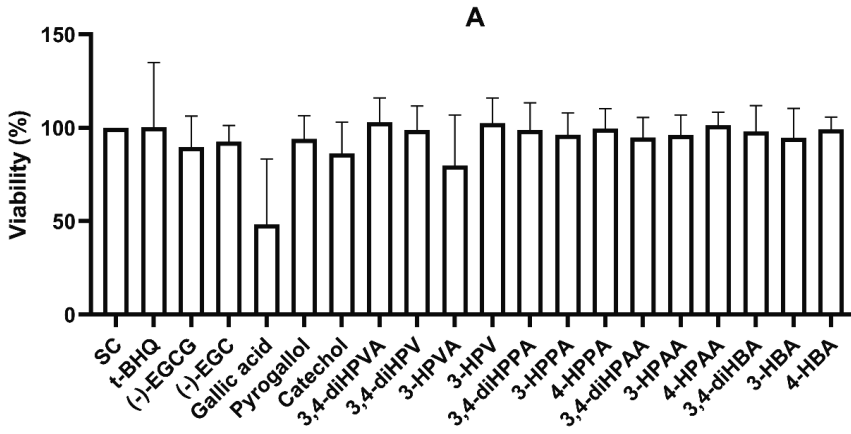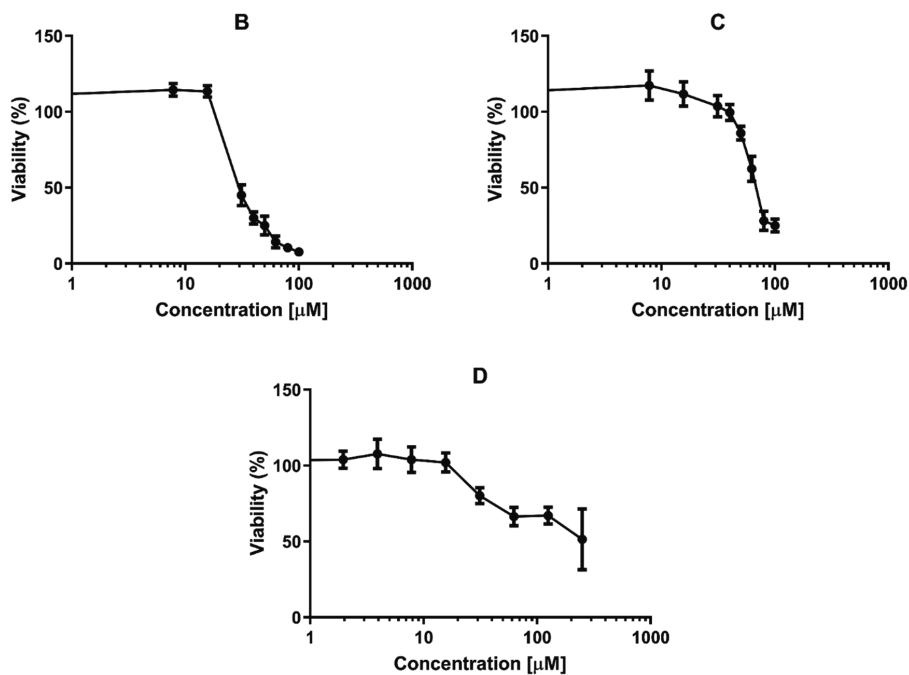
Figure S7. Cell viability (% control) of EpRE-LUX reporter cells determined by WST-1 assay. A: cells were exposed to EGCG and its 17 phenolic metabolites for 24 h (all compounds were at 30 μM including t-BHQ, mean value ± SD, n = 4). B, C, D: cells were exposed for 24 h at increasing concentrations of gallic acid, pyrogallol and catechol, respectively. Data are presented as mean ± SEM of at least 4 independent replicates.

A

**bootstrap curves
based on model averaging**
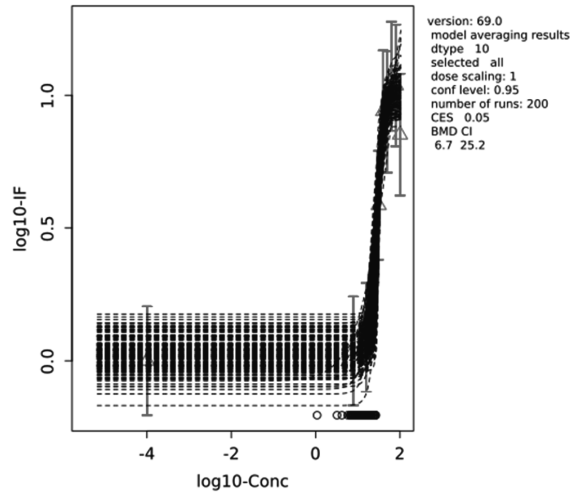
version: 69.0
model averaging results
dtype   10
selected   all
dose scaling: 1
conf level: 0.95
number of runs: 200
CES   0.05
BMD CI
 6.7 25.2

B

**bootstrap curves
based on model averaging**

version: 69.0
model averaging results
dtype   10
selected   all
dose scaling: 1
conf level: 0.95
number of runs: 200
CES   0.05
BMD CI
 8 25.3
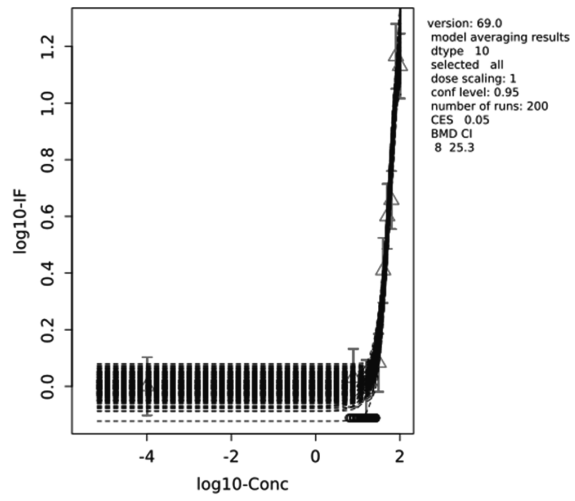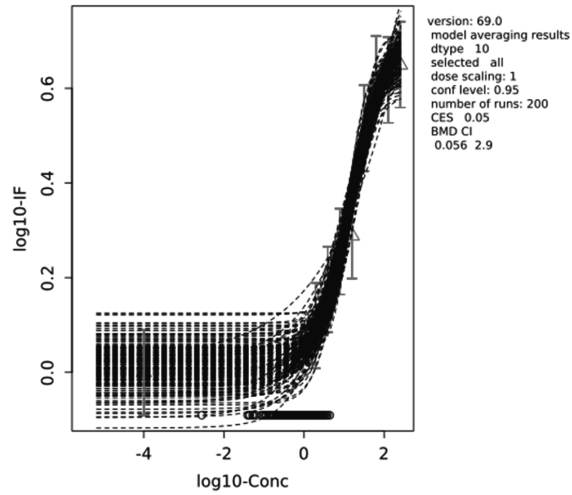
Figure S8. Fitted concentration-response-curves from the benchmark dose modelling (BMD) analysis of the data on the EpRE-LUX reporter gene assay for gallic acid (A), pyrogallol (B) and catechol (D).
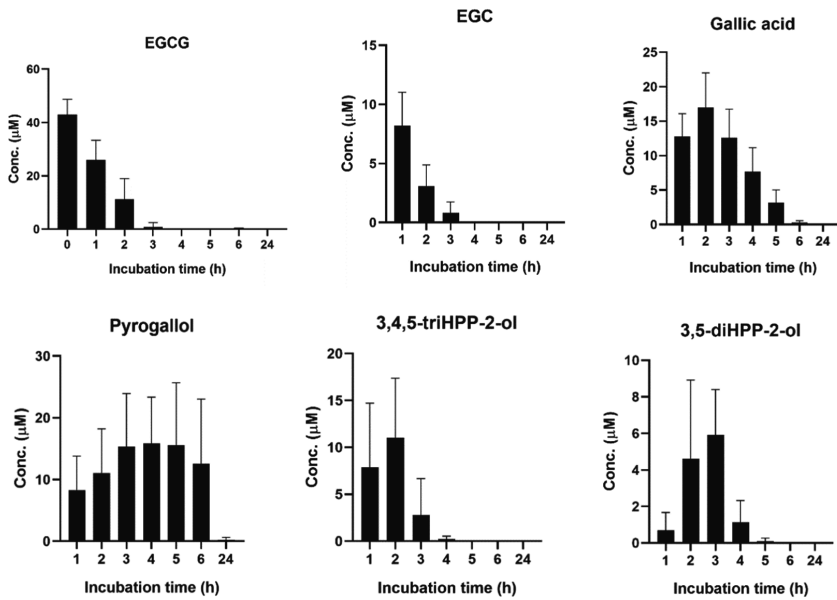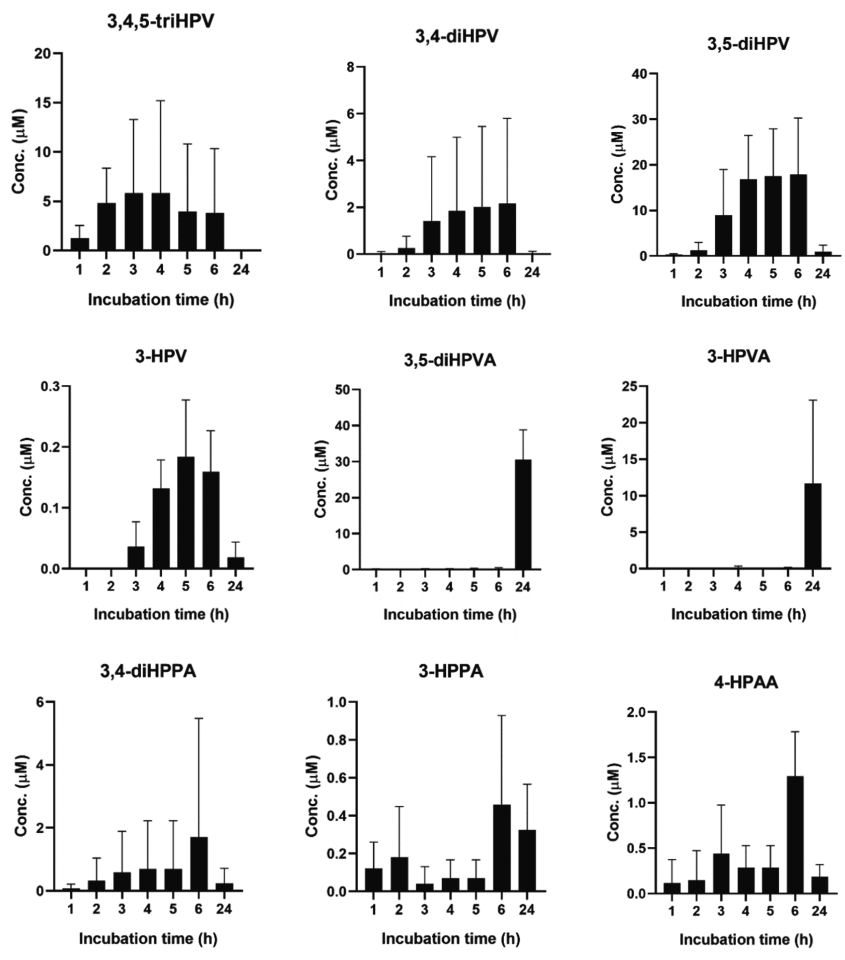
Figure S9. Changes in the concentrations of EGCG and its metabolites formed during 24 hours of *in vitro* anaerobic incubations with a pooled human faecal sample. Results are shown as mean ± standard deviation (SD) from three independent incubations.

4

Chapter 4

Intra- and inter-individual differences in the human intestinal microbial conversion of (-)-epicatechin and bioactivity of its major colonic metabolite 5-(3',4'-dihydroxyphenyl)-γ-valerolactone in regulating Nrf2-mediated gene expression

Chen Liu, Sjef Boeren, Ivonne M.C.M. Rietjens

Abstract

(-)-Epicatechin (EC) is one of the most popular polyphenols present in various food products in daily life. Upon intake, it is intensively metabolised by microbiota in the large intestine. In the present study, intra- and inter-individual variations in this gut microbial conversion of EC and the concomitant formation of its major metabolites, including 5-(3',4'-dihydroxyphenyl)-γ-valerolactone (3,4-diHPV), were identified and quantified via liquid chromatography triple quadrupole mass spectrometry (LC-TQ-MS) in anaerobic fecal incubations. In addition, the bioactivity of EC and 3,4-diHPV in activating Nrf2-mediated gene expression was tested quantifying their effects in the U2OS Nrf2 CALUX assay, and on the expression levels of Nrf2-related proteins in Hepa1c1c7 and Caco-2 cells via nanoLC-MSMS. RT-qPCR was carried out to confirm selected Nrf2-regulated gene expressions at the mRNA level. Results obtained show that both intra- and inter-individual differences exist in human gut microbial EC degradation and 3,4-diHPV formation, with inter-individual differences being more distinct than intra-individual differences. The metabolite, 3,4-diHPV, showed higher potency in the U2OS Nrf2 CALUX assay than EC itself. Among the obviously altered Nrf2-related proteins, 14 and 10 Nrf2-associated proteins were upregulated to a higher extent upon 3,4-diHPV treatment than in the EC treated group for Hepa1c1c7 and Caco-2 cells, respectively. While only three and four of these Nrf2-associated proteins were induced at a higher level upon EC than upon 3,4-diHPV treatment for Hepa1c1c7 and Caco-2 cells, respectively. RT-qPCR results showed that indeed Nrf2-mediated genes (e.g., Nqo1 and Ugt1a) were only induced significantly in 3,4-diHPV treated and not in EC treated Hepa1c1c7 cells. Taken together, the results suggest that the major colonic EC metabolite, 3,4-diHPV, was more capable of inducing Nrf2-mediated gene expression than its parent compound EC. This implies that the evident inter- and intra-individual differences in the microbial conversion of EC to this major metabolite 3,4-diHPV may affect the overall health-promoting effects of EC consumption related to the Nrf2 pathway activation.

Keywords: 5-(3',4'-dihydroxyphenyl)-γ-valerolactone, (-)-epicatechin, inter-individual difference, intra-individual difference, microbial conversion, Nrf2

1. Introduction

(-)-Epicatechin (EC) is one of the most common dietary catechins known to occur widely in various food sources, e.g., cocoa, green tea, wine and apple, etc.[1-2] EC consumption has been linked to a series of beneficial health effects such as anti-oxidant, anti-inflammatory, anti-cancer and anti-cardiovascular disease activities.[3-6] These pharmacological effects of EC have been ascribed to the direct anti-oxidative property of its phenolic hydroxyl groups but, more recently, also to its "indirect" cytoprotective properties via activation of the cascade signalling, Kelch-like ECH-associated protein 1-NF-E2-related factor 2 (Keap1-Nrf2) signalling pathway, which is crucial in maintaining cellular redox homeostasis.[7] Keap1-Nrf2 is considered to represent an important human health hub given its vital regulatory role in many physiological activities.[2, 8] Certain polyphenols are able to react with the thiol groups of Keap1, resulting in the dissociation of Nrf2 thereby preventing Nrf2 from rapid degradation through the proteasome system, and facilitating the nuclear translocation of nascent Nrf2. Ultimately, a diverse array of Nrf2 regulated cytoprotective genes are transcribed, including for example UDP-glucuronosyltransferases (UGTs), NAD(P)H quinone dehydrogenase 1 (NQO1), and many others.[8-9]

Despite the fact that the daily intake of polyphenols is ten times that of vitamin C,[2] the overall bioavailability of polyphenols is considered to be lower than 10% resulting in plasma concentration of catechins to be more than 50 times lower than those of vitamin C.[10-12] EC is recognized as a well-absorbed catechin but still only about 20% of the intake is absorbed directly in the small gastrointestinal tract and subsequently passed into systemic circulations.[12] Over 70% of total EC intake reaches the large intestine where it is subject to extensively degradation by intestinal microbiota.[12-13] Among all the colonic metabolites, 5-(3',4'-dihydroxyphenyl)-γ-valerolactone (3,4-diHPV) and its downstream metabolites have been reported to account for 42 to 60% of total EC intake.[12, 14] This 3,4-diHPV metabolite results from the A-ring cleavage of the EC C-ring fission intermediate, 1-(3',4'-dihydroxyphenyl)-3-(2'',4'',6''-trihydroxyphenyl)-2-propanol (3,4-diHPP-2-ol).[15] Compared with this transient precursor, 3,4-diHPV appeared to accumulate to a substantial level in both *in vitro* and *in vivo* investigations. For instance, valerolactones were reported to persist for a long time in the human or rat body following tea catechin intake. It has also been demonstrated that valerolactones were maximally detected in plasma or urine at 6 to 24 hours (or even longer) following oral intake (or intravenous administration) of different catechins.[12, 16-19] The C_{max} of structurally-related EC metabolites in human plasma appeared to occur much earlier namely shortly after one hour

following intervention.[12] During *in vitro* anaerobic fecal incubations of EC, the metabolite 3,4-diHPV also appeared to be the dominate metabolite formed, with maximum levels observed from 3 to 6 hours amounting to 45 to 49% of the originally incubated concentration of EC, while EC was rapidly degraded already within the first 2 hours.[20] However, studies on bioactivities of 3,4-diHPV, especially its ability in activating Keap1-Nrf2 pathway, are still absent.

As is well-known, colonic microbiota play a critical role in degradation of EC and formation of 3,4-diHPV. It has been widely accepted that due to different age, gender, ethnic factors and diverse lifestyle, the inter-individual microbial compositions could vary substantially,[21] hence affecting the metabolic profiles.[20, 22] On the other hand, the microbiota composition is considered to be relatively stable within healthy individuals.[23] However, to what extent the inter- and intra-individual differences of microbiota composition can cause differences in the metabolic pattern of conversion of EC still needs to be unveiled.

The aim of the present study was to compare the inter- and intra-individual differences in the metabolic pattern of EC microbial conversion, focussing on the depletion of EC and the formation of 3,4-diHPV, and to better quantify the potential role of this major EC microbial metabolite in inducing Nrf2-mediated gene expression. This will provide novel insights in the health-promoting mechanisms related to dietary EC consumption.

2. Materials and Methods

2.1 Chemicals and reagents.

EC and L-ascorbic acid were ordered from Sigma-Aldrich (Zwijndrecht, The Netherlands). 3,4-diHPV was purchased from BOC sciences (Shirley, USA). Minimum Essential Medium (MEM), MEM-Alpha, Dulbecco's Modified Eagle Medium with 1:1 F-12 Nutrient Mixture (DMEM/F-12), Penicillin Streptomycin (PS), Penicillin Streptomycin Glutamine (PSG), pyruvate, dextran-coated charcoal-treated fetal calf serum (DCC-FCS) and phosphate buffered saline (PBS) were obtained from Gibco (Paisley, UK). Foetal calf serum (FCS) was ordered from Bodinco (Alkmaar, The Netherlands). Geneticin (G418), trypsin and Nonessential amino acids (NEAA) were supplied by Invitrogen Corporation (Breda, The Netherlands).

2.2 Cell lines

The U2OS Cytotox CALUX cells and the U2OS Nrf2 CALUX cells were both obtained from Biodetection Systems, (Amsterdam, The Netherlands). Both cell lines are derived from human

osteoblastic cells, transfected with a reporter construct carrying a luciferase reporter gene under transcriptional control of a constitutive promoter or four EpRE sequences, respectively.[24] Thus, the luciferase expression of U2OS Cytotox cells is invariant, and can be used to check the cytotoxicity and luciferase stabilisation after exposure to chemicals, enabling identification of false negatives and false positives, respectively. Meanwhile, the U2OS Nrf2 CALUX cells can be used to measure the luciferase induction after exposure to a potential Nrf2-activator. The cells of both cell lines were cultured in DMEM/F-12 culture medium, supplemented with 10% (v/v) FCS, 1% (v/v) NEAA and 1% (v/v) PS. The Hepa1c1c7 cells are murine hepatoma cells and were cultured in MEM-Alpha supplemented with 10% (v/v) FCS and 1% (v/v) P/S. In order to maintain the selection pressure for all three afore-mentioned cells lines, 200 µg/mL G418 was added to the culture medium during every other subculturing. The Caco-2 cells were obtained from ATCC (Gaithersburg, Maryland, USA) and are derived from a human colorectal adenocarcinoma. They were cultured in MEM culturing medium, supplemented with 20% (v/v) FCS, 1% (v/v) pyruvate and 1% (v/v) PSG. All cell lines mentioned were cultured in an incubator, at 37°C in a humidified atmosphere with 5% CO_2.

2.3 Fecal anaerobic incubation of EC

Fecal samples were donated by six healthy volunteers with from each individual three different samples collected with two-week intervals. These volunteers consisted of two males and four females and aged from 25 to 60 years old. No antibiotics have been taken by the volunteers at least three months before sampling. The collecting and processing of fecal samples and subsequent fecal anaerobic incubations were carried out according to the methodology described previously.[20] This methodology was approved by the Medical Ethical Reviewing Committee of Wageningen University (METC-WU) not to require further evaluations based on the Dutch Medical Research Involving Human Subjects Act. In brief, the experimental fecal incubations consisted of 79% (v/v) anaerobic PBS, 20% of the fecal slurries (from different individuals at different visits, final fecal concentration: 40 mg/mL) and 1% (v/v) 10 mM EC (in methanol, final concentration being 100 µM). For the negative control, instead of adding EC, 1% (v/v) methanol was added. And the blank control comprised 99% (v/v) PBS and 1% (v/v) 10 mM EC. After 0, 2, 4, 6 and 24 h of anaerobic incubation in the atmosphere of 85% N_2, 10% CO_2, and 5% H_2 at 37 °C in a BACTRON300 anaerobic chamber, reactions were terminated by adding one volume of ice-cold methanol followed by putting the sample on ice for 15 minutes and centrifugation at 21500 × g (VWR, Hitachi Koki Co., Ltd.). In the end, supernatants were collected and stored immediately at -80 °C until analysis via liquid

chromatograph triple quadrupole mass spectrometry (LC-TQ-MS). At least three independent incubations were performed for all the different fecal samples.

2.4 LC-TQ-MS analysis

EC and 3,4-diHPV contents were measured using a Shimadzu LC-TQ-MS 8045 (Shimadzu, Benelux, B.V. The Netherlands). A previously optimized method was used to qualitatively and quantitatively identify the two compounds.[20] Briefly, mobile phase A was composed of water : acetic acid (999 : 1, v/v), and mobile phase B was methanol. The flow rate was 0.4 mL/min with the following gradient: 0 - 0.5 min: 5% B, 0.5 - 5 min: 5 - 25% B, 5 - 6 min: 25 - 100% B, 6 - 7 min: 100% B, 7 - 8 min: 100 - 5% B, 8 - 13 min: 5% B. Authentic chemical standards of EC and 3,4-diHPV were used for identification and defining calibration curves for quantifications. Since there was no degradation of EC detected in blank control samples (data not shown), concentrations of compounds in the incubated samples were calculated by subtracting the concentrations quantified in corresponding negative controls incubated without adding EC.

2.5 Reporter gene assay

The activity of EC and 3,4-diHPV in inducing Nrf2 gene transcription was determined using the U2OS Nrf2 CALUX reporter gene assay. The method was performed essentially as previously described.[22] Briefly, U2OS Nrf2 CALUX cells were cultured in a black 96-well microplate with a clear bottom (greiner bio-one) at a density of 2×10^5 cells/mL (2×10^4 cells in 100 µL culture medium per well) for 24 hours to let the cells attach to the bottom. The culture medium was then replaced with exposure medium containing model compounds at different concentrations to expose the cells for another 24 hours. In total, eight exposure concentrations were applied for both EC and 3,4-diHPV, ranging from 15 µM to 150 µM, added from 200 times concentrated stock solutions in DMSO. After exposure, the luminometer (GloMax-Multi Detection System-Promega) was used to measure the luciferase activity of each well. The relative light units (RLUs) of all the wells were measured after the automatic injection of 100 µl flash mix (2.67 mM $MgSO_4$, 1.07 mM $(MgCO_3)_4Mg(OH)_2 \cdot 5H_2O$, 20 mM Tricine, 0.1 mM EDTA, 5.0 mM ATP; 2.0 mM DTT, 470 µM D-luciferine, pH 7.8).

In addition, a paralleled U2OS Cytotox CALUX assay was performed to investigate the potential cytotoxicity and whether luciferase stabilisation occurred during the exposure to EC or 3,4-diHPV. This assay was performed using the same conditions as described above for the

U2OS Nrf2 CALUX assay. Results are shown as the induction factor (IF) compared to the solvent control. At least three independent assays were carried out for both test compounds.

2.6 Sample preparation and protein identification

A label-free relative protein quantitation was performed to characterize the protein level change in EC or 3,4-diHPV treated cells. The identification and relative quantification was conducted via a Thermo EASY nanoLC 1000 (Thermo, Waltham, MA, USA) coupled with an Orbitrap Exploris 480 (Thermo electron, San Jose, CA, USA). Both Hepa1c1c7 cells and Caco-2 cells were seeded in T25 flasks at a density of 6.25×10^4 cells/cm^2 for 24 h. Subsequently, the culture medium was replaced with exposure medium containing 30 µM EC or 3,4-diHPV in the presence of 0.5 mM L-ascorbic acid for a continuous 24 h exposure. The selection of the test compound concentration took into account the results of both a WST-1 assay (Figure S1 in Support Information1) and the U2OS Cytotox CALUX reporter gene assay, to make sure non-cytotoxic concentrations were tested. After exposure, the cells were washed twice with PBS and 1.5 mL 100 mM Tris-HCl, pH 8 was added. Afterwards, the cells were scraped off and transferred to 2 mL Eppendorf low binding tubes for centrifuging at 1×10^4 rpm (9391 $\times$ g) for three minutes. Finally, the cell pellets were dissolved in 100 µL 100 mM Tris-HCl, pH 8 and sonicated. Protein concentrations were determined by the Bicinchoninic Acid (BCA) method.[25] The protein aggregation capture (PAC) method was applied to obtain peptide samples from protein samples for Thermo EASY nanoLC analysis.[26] Peptides of all samples were stored immediately at -20 °C until further analysis. Four independent biological replicates were collected for all treatments.

The LC-MS/MS parameters were adapted from a previous chromatographic method.[27] In brief, 4 µL (Caco-2 cell samples) or 5 µL (Hepa1c1c7 cell samples) peptide samples were loaded onto an in-house prepared 0.10 $\times$ 250 mm ReproSil-Pur 120 C18-AQ 1.9 µm beads analytical column at a constant pressure of 825 bar. The mobile phase A was 0.1% formic acid in water (v/v), and mobile phase B was 0.1% formic acid in acetonitrile (v/v). The flow rate was 0.5 µL/min with a 50 min linear gradient from 9% to 34% mobile phase B. An electrospray potential of 3.5 kV was applied directly to the eluent via a stainless steel needle fitted into the waste line of a micro cross that was connected between the nLC and the analytical column. MS and MSMS AGC targets were set to 300%, 100% respectively or maximum ion injection times of 50 ms (MS) and 30 ms (MSMS) were used. HCD fragmented (isolation width 1.2 m/z, 28% normalized collision energy) MSMS scans in a cycle time of 1.1 s/of the most abundant 2 - 5+

charged peaks in the MS scan were recorded in data dependent mode (resolution 15000, threshold 2e4, 15 s exclusion duration for the selected m/z ± 10 ppm).

The MaxQuant software package (1.6.3.4) was used to identify and relative quantify the peptides.[28] Human (UP000005640) and Mouse (UP000000589) databases were downloaded from Uniprot which was used together with a contaminants database that contains sequences of common contaminants like Trypsins (P00760, bovin and P00761, porcin) and human keratins (Keratin K22E (P35908), Keratin K1C9 (P35527), Keratin K2C1 (P04264) and Keratin K1CI (P35527)). The "label-free quantification" as well as the "match between runs" options were enabled. Deamidated peptides were allowed to be used for protein quantification and all other quantification settings were kept default. Data were filtered to show only proteins reliably identified by minimally 2 peptides of which at least one is unique and one is unmodified using a false discovery rate (FDR) of less than 1% on both protein and peptide level. After grouping sample replicate injections, an extra filtering step leaving only protein groups consisting of minimally two label-free quantitation (LFQ) intensities in at least one group, was performed. Normal log was applied to all LFQ intensities. All remaining not existing LFQ intensities were replaced by a value slightly lower than the lowest measured value. For the Hepa1c1c7 cells this was done by replacing the values from a normal distribution with default settings (width = 0.3, down shift = 1.8) and for the Caco-2 cells samples a constant value of 6.6 was used.

2.7 Data analysis and bioinformatics

From the derived protein expression profiles, Nrf2-asscociated proteins were selected manually based on literature information.[8-9, 29-31] The protein expression fold changes (FCs) were calculated as the ratio of normalized label-free quantitation (LFQ) intensity of a specific treatment and that of the solvent control. Besides this dedicated protein dataset analysis, a general proteomics bioinformatical analysis was also performed. The statistical program Perseus (Max Planck Institute, Germany) was used for filtering and a Student's t-test for statistical analysis of the changes in the derived protein expression profiles. The differentially expressed proteins (DEPs) were characterized based on meeting two criteria which are FC less than 0.8 or greater than 1.2 and the P-value less than 0.05. Subsequently, the DEPs in EC or 3,4-diHPV treatment were used as input for gene ontology functional classifications and Kyoto Encyclopedia of Genes and Genomes (KEGG) pathway annotation by the DAVID Bioinformatics Resources 6.8 (https://david.ncifcrf.gov/tools.jsp). Furthermore, DEPs were used for protein-protein interaction (PPI) network analysis which was explored in the STRING database (https://string-db.org/) and results were further visualized with Cytoscape 3.8.2

(Seattle, USA). Hub protein networks were produced by the Cytoscape 3.8.2 plugin programme MCODE.

2.8 RT-qPCR

To study the Nrf2 mediated gene expression after exposure to EC or 3,4-diHPV, an RT-qPCR was performed. To this end, both Hepa1c1c7 cells and Caco-2 cells were seeded in a 6-well plate at a density of 6.25×10^4 cells/cm^2 for 24 h followed by a continuous 24 h exposure to EC or 3,4-diHPV at 30 µM in the presence of 0.5 mM L-ascorbic acid. Subsequent RNA extraction and purification were carried with the help of QIAshredder and RNeasy kits (Qiagen, Venlo, The Netherlands). The Nanodrop One (Thermoscientific, Delaware, USA) was used to measure the A260/230, A260/A280 and RNA concentrations. RNA reverse-transcription was performed using the QuantiTect Reverse Transcription Kit (Qiagen, Venlo, The Netherlands) to get cDNA. Gapdh and Actin-beta were chosen as the reference genes for Hepa1c1c7 samples and Caco-2 samples, respectively. The relative transcription levels of Nqo1, Gclc and Ugt1a6 were determined in Hepa1c1c7 cells and the relative transcription levels of TP53I3, MGST3 and HMOX1 were checked in Caco-2 cells using SYBR Green-based (Qiagen, Venlo, The Netherlands) RT-qPCR. These genes were chosen because they were highly induced in the respective proteomics datasets and/or because they are typical Nrf2-mediated genes. Ct (cycle threshold) values were recorded using a Rotor-Gene 6000 cycler (Qiagen, Venlo, The Netherlands), and used to calculate relative RNA levels by the $2^{-\Delta\Delta Ct}$ method. Primers were from QuantiTect Pimer Assays (Qiagen, Venlo, The Netherlands), namely Mm_Gapdh_3_SG, Mm_Nqo1_1_SG, Mm_Gclc_1_SG, Mm_Ugt1a6_1_SG, Hs_ACTB_1_SG, Hs_TP53I3_va.1_SG, Hs_MGST3_1_SG, and Hs_HMOX1_1_SG.

2.9 Data analysis

Data are presented as mean ± SEM, unless stated otherwise. All experiments were conducted in at least three independent biological replications. Student's t-test was applied to analyse the statistical significances between treatments and the control group. Statistical significance was determined at P-values < 0.05.

3. Results

3.1 Inter- and intra-individual differences in EC depletion and 3,4-diHPV formation

The time-dependent microbial depletion of EC and formation of 3,4-diHPV in anaerobic incubations with fecal samples from six individuals from three independent visits are presented

in Figure 1. EC was swiftly degraded after 2 h of incubation except for incubations with the fecal samples from individual 2 (Figure 1B), in which still $86.9 \pm 4.1\%$ of the initial concentration was present. For the incubations with the fecal samples of the other five individuals (Figure 1A, C, D, E, F), the average residual EC concentration at 2 h was $18.8 \pm 3.5\%$ of the initial concentration, while the initial 50 µM was almost completely degraded at 4 or 6 h. Figure 1G – L show the time-dependent formation of 3,4-diHPV in these fecal incubations. For most incubations, the 3,4-diHPV formation reached a plateau at 4 – 6 h and decreased after that to show lower levels at 24 h. Also, for 3,4-diHPV the results for individual 2 deviated from the others showing a peak of 3,4-diHPV at 24 h (Figure 1H), in line with this volunteer's relatively slow metabolism of EC (Figure 1B). Besides the differences found between individuals, also intra-individual differences were observed when comparing the results within the individuals for the three fecal samples obtained at different points in time. For instance, only 3.6 µM (7.4% of total mass recovery) 3,4-diHPV was detected in the anaerobic fecal incubation for individual 1 at 6 h for the second sample, while for the third sample, obtained 2 weeks later, this value amounted to 41.8 µM (83.9% of total mass recovery) (Figure 1G).

To better characterize the inter- and intra-individual differences in the microbial depletion of EC and formation of 3,4-diHPV, the standard deviations (SDs) for the amounts of EC and 3,4-diHPV quantified were calculated within individuals (representing intra-individual differences) and between individuals (representing inter-individual differences), and the results thus obtained are presented in Figure 2. Based on the SDs the inter-individual differences appeared to be larger than the intra-individual differences at all incubation time points for both the EC and the 3,4-diHPV levels. The highest SD of intra-individual variations for EC and 3,4-diHPV were 4.4 µM (8.8 % of the initial mass) (t = 2 h) and 9.1 µM (18.2 %) (t = 6 h). While the highest SD of inter-individual variations for EC and 3,4-diHPV were 12.5 µM (25.0%) (t = 2 h) and 14.5 µM (29.0%) (t = 6 h).
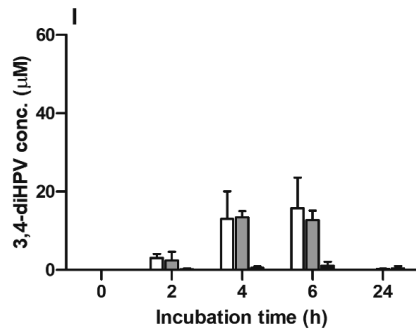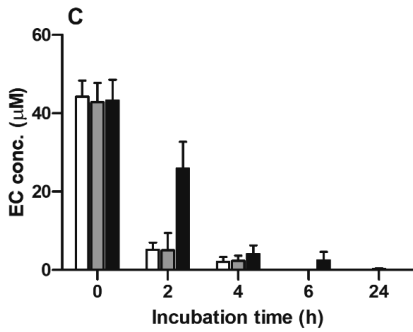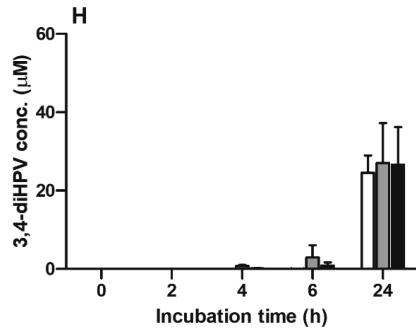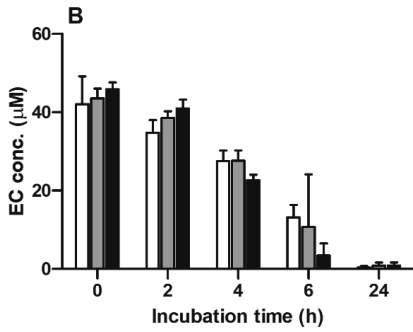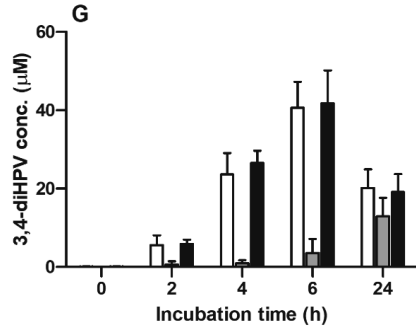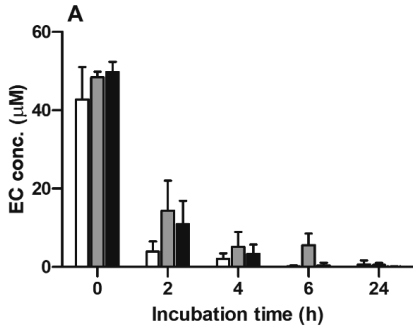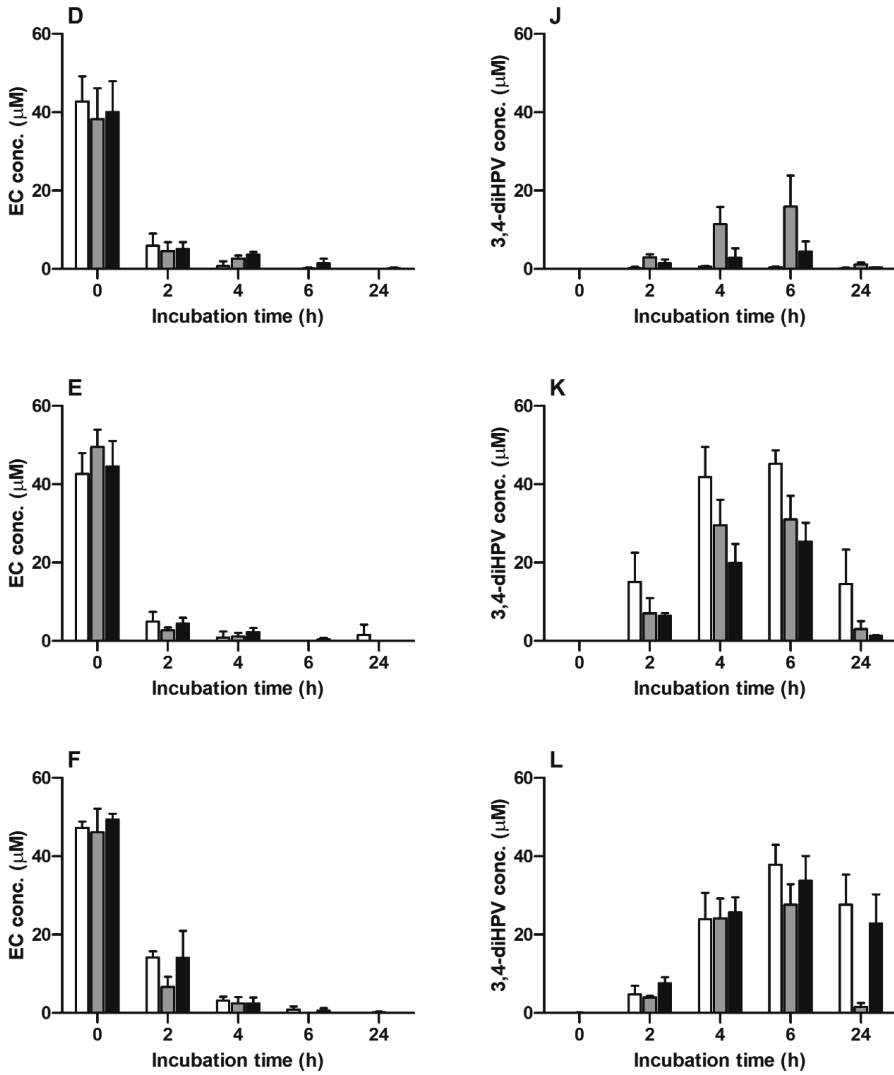
Figure 1. Time-dependent microbial depletion of EC and formation of 3,4-diHPV in anaerobic incubations with fecal samples from six individuals obtained in three collecting weeks. A - F: EC depletion in individual 1 to 6; G – L: 3,4-diHPV formation in individual 1 to 6. White column: collection 1; grey column: collection 2; black column: collection 3.
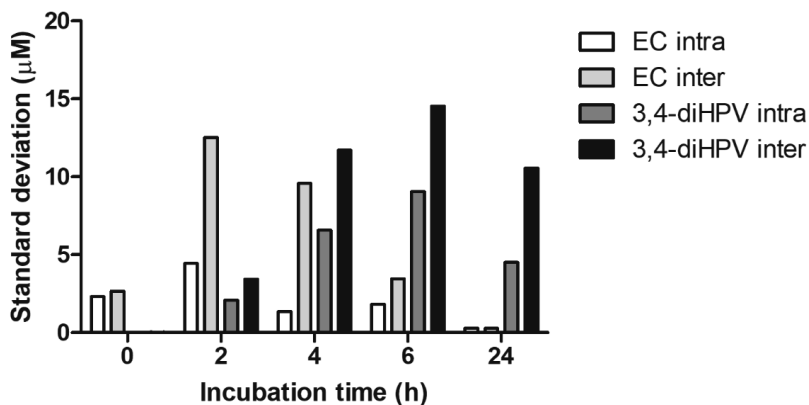
Figure 2. Standard deviations (SDs) that represent intra- and inter-individual differences in EC depletion and 3,4-diHPV formation among six individuals over three collecting weeks.

3.2 Activation of Nrf2-mediated luciferase expression by EC and 3,4-diHPV

Figure 3A and Figure 3B show the concentration-dependent induction of luciferase expression after 24 h exposure of U2OS Nrf2 cells to EC and 3,4-diHPV, respectively. EC barely showed any activation at all exposure concentrations both in the absence or presence of 0.5 mM L-ascorbic acid (Figure 3A). In contrast, 3,4-diHPV induced significant substantial luciferase induction, with a maximum IF of 2.1 or 3.7 at 150 μM with or without the presence of L-ascorbic acid, respectively (Figure 3B). Besides, the results also show that the presence of 0.5 mM L-ascorbic acid in the exposure medium reduced the luciferase expression triggered by 3,4-diHPV (Figure 3B). Results of the U2OS Cytotox CALUX assay confirm that the luciferase induction by 3,4-diHPV is not due to stabilisation of the luciferase reporter protein (Figure S2). Moreover, no cytotoxicity was found even at the highest concentration (150 μM) tested for both EC and 3,4-diHPV (Figure S2).
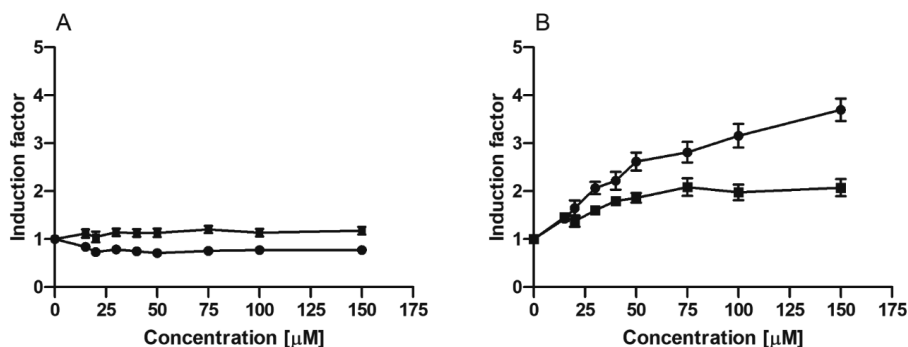
Figure 3. Induction of luciferase expression in U2OS Nrf2 CALUX reporter cells after 24 h exposure to EC (A) and 3,4-diHPV (B). Line curves with square symbols represent co-exposure with 0.5 mM L-ascorbic acid (final concentration). While line curves with circular symbols represent exposure with only selected model compounds. Results are presented as mean ± SEM compared with the solvent control, derived from at least three independent experiments.

3.3 Qualitative and quantitative Nrf2-associated protein identification

Before initiating the proteomics analysis, the viability of Hepa1c1c7 cells and Caco-2 cells after exposure to EC and 3,4-diHPV for 24 h was analysed via the WST-1 assay. The results show that no significant changes in cell viability were observed at test concentrations up to at least 40 μM (Figure S1 in Support Information1). Label-free proteomics subsequently qualitatively and quantitatively identified in total 3991 proteins in Hepa1c1c7 cells and 3929 proteins and Caco-2 cells, respectively (Table S1 and Table S2 in Support Information2). When selecting from Nrf2-related proteins (Table S3 and Table S4 in Support Information2) and applying a selection criterium of a fold change (FC) of >1.2 upon EC or 3,4-diHPV treatment compared to control 17 and 14 proteins were derived from the dataset of the Hepa1c1c7 cells and Caco-2 cells, respectively (Table 1A, B). 3,4-diHPV induced higher fold changes for inducing Nrf2-related protein expression than EC both in Hepa1c1c7 cells and Caco-2 cells (Table 1A, B). Among the 17 Nrf2-related proteins induced in Hepa1c1c7 cells, 14 were induced with a higher FC in the 3,4-diHPV treated cells as compared to the EC treated cells, while only three proteins showed a higher FC upon EC treatment than upon 3,4-diHPV exposure of the cells (Table 1A). For instance, both Nqo1 and Nqo2 proteins were upregulated with a 3.6 and 1.3 higher FC upon 3,4-diHPV as compared to EC exposure, respectively. Similarly, for the Nrf2-related proteins in the Caco-2 dataset, 3,4-diHPV was also more inducive than EC, with 10 proteins showing

higher FCs in 3,4-diHPV exposed cells than in the EC group while again only four proteins showed higher FCs in the EC group than in the 3,4-diHPV group (Table 1B).

Table 1. A comparison of fold change (FC) of Nrf2-associated proteins after exposure to EC and 3,4-diHPV for 24 h at 30 μM. A selection criterion of FC > 1.2 in either EC or 3,4-diHPV treatment compared with control was applied. Table 1A and Table 1B were derived from Hepa1c1c7 cells and Caco-2 cells, respectively (numbers in parentheses are p values)

Table 1A: Hepa1c1c7 cell samples.

Protein IDs	Protein names	Gene names	EC	3,4-diHPV
Q64669	NAD(P)H dehydrogenase [quinone] 1	Nqo1	1.15 (0.901)	3.60 (0.138)
Q9JI75	Ribosyldihydronicotinamide dehydrogenase [quinone]	Nqo2	1.08 (0.294)	1.31 (0.041)
Q8CHT0	Aldehyde dehydrogenase family 4 memberA1	Aldh4a1	1.21 (0.317)	1.46 (0.045)
D3Z0B9	Aldehyde dehydrogenase family 16 member A1	Aldh16a1	1.03 (0.976)	1.73 (0.384)
P19157	Glutathione S-transferase P 1	Gstp1	1.26 (0.018)	1.57 (0.001)
P97494	Glutamate--cysteine ligase catalytic	Gclc	1.13 (0.374)	1.36 (0.026)
P09671	Superoxide dismutase (10), mitochondrial	Sod2	1.06 (0.733)	1.28 (0.252)
P10639	Thioredoxin	Txn	1.10 (0.166)	1.36 (0.015)
Q9JMH6	Thioredoxin reductase 1, cytoplasmic	Txnrd1	1.20 (0.419)	1.52 (0.179)
J3QMN4	Thioredoxin reductase 2, mitochondrial	Txnrd2	1.17 (0.350)	1.46 (0.066)
A0A1L1STE6	Isocitrate dehydrogenase (56) subunit, mitochondrial	Idh3a	1.19 (0.388)	1.28 (0.210)
P70404	Isocitrate dehydrogenase (56) subunit gamma 1, mitochondrial	Idh3g	1.24 (0.265)	1.20 (0.330)
P61222	ABCE1	Abce1	1.01 (0.916)	1.26 (0.074)
Q61753	D-3-phosphoglycerate dehydrogenase	Phgdh	1.05 (0.608)	1.20 (0.089)
P39689	Cyclin-dependent kinase inhibitor 1	Cdkn1a	2.32 (0.513)	6.16 (0.093)
P28033	CCAAT/enhancer-binding protein beta	Cebpb	1.20 (0.427)	1.04 (0.868)
O54790	Transcription factor MafG	Mafg	1.23 (0.249)	1.06 (0.718)

Table 1B: Caco-2 cell samples.

Protein IDs	Protein names	Gene names	EC	3,4-diHPV
Q53FA7	Quinone oxidoreductase PIG3	TP53I3	1.74 (0.577)	3.53 (0.130)
Q9Y6N5	Sulfide:quinone oxidoreductase	SQRDL	2.93 (0.237)	2.05 (0.416)
Q04828	Aldo-keto reductase family 1 member C1	AKR1C1	2.10 (0.456)	2.94 (0.291)

Q14914	Prostaglandin reductase 1	PTGR1	2.04 (0.420)	2.43 (0.320)
O75223	Gamma-glutamylcyclotransferase	GGCT	2.21 (0.455)	2.72 (0.344)
Q8TED1	Probable glutathione peroxidase 8	GPX8	2.11 (0.376)	0.97 (0.979)
Q13162	Peroxiredoxin-4	PRDX4	1.57 (0.034)	1.24 (0.410)
P19224	UDP-glucuronosyltransferase	UGT1A6	1.10 (0.749)	1.31 (0.344)
P34913	Bifunctional epoxide hydrolase 2	EPHX2	1.14 (0.440)	1.40 (0.043)
Q13501	Sequestosome-1	SQSTM1	1.05 (0.969)	1.21 (0.874)
O75027	ABCB7	ABCB7	0.49 (0.526)	2.31 (0.297)
Q9NRK6	ABCB10	ABCB10	1.07 (0.763)	1.30 (0.249)
Q9NP58	ABCB6	ABCB6	1.31 (0.027)	1.28 (0.007)
O15439	ABCC4	ABCC4	1.16 (0.643)	1.41 (0.282)

3.4 Identification of statistically significant differentially expressed proteins (DEPs) and functional annotations

To further obtain more insights in changes of protein profiles upon exposure of Hepa1c1c7 cells or Caco-2 cells to either EC or 3,4-diHPV, statistically significant differentially expressed proteins (DEPs) were derived from both EC and 3,4-diHPV treated Caco-2 cells and Hep1c1c7 cells using two criteria which were FC less than 0.8 or greater than 1.2 and the P-value less than 0.05 (Figure 4). The protein dataset of Hepa1c1c7 cells revealed 108 and 601 DEPs characterized upon EC and 3,4-diHPV treatments, respectively, with 64 of these DEPs being shared for both treatments (Figure 4A). Meanwhile, the Caco-2 protein dataset, revealed 63 and 60 DEPs, upon exposure to EC and 3,4-diHPV, respectively, with nine DEPs in common between both treatments (Figure 4B).

Subsequently, DEPs were used to do a gene ontology (GO) enrichment to determine their role in the categories biological processes (BP), cellular component (CC) and molecular function (MF). Full GO enrichment analysis results can be found in Support Information2. Figure 4C – F depict the top five most significant enriched terms in the three different categories after exposure of Hepa1c1c7 cells and Caco-2 cells to EC and 3,4-diHPV. The x-axis presents different terms enriched and the y-axis indicates the number of proteins that fell into the enriched terms. Several mutual terms were obtained for EC and 3,4-diHPV treated Hep1c1c7 cells (Figure 4C, D). For example, translation and rRNA processing of the category BP were enriched after both treatments. In the category CC, the DEPs were enriched in intracellular

ribonucleoprotein complex, ribosome and nucleolus for both treatments. MF comprised poly(A) RNA binding, RNA binding and structural constituent of ribosome in both treatments (Figure C, D). This result suggests that EC and 3,4-diHPV stimulated some comparable cellular responses in Hepa1c1c7 cells and translation-related activities were likely to be affected most in both EC and 3,4-diHPV groups. Moreover, EC exposure resulted in most protein changes in mitochondria while 3,4-diHPV exposure caused the most protein changes in the nucleus, suggesting also differences in the target sites of the two compounds. Additionally, in line with the fact that more DEPs were characterized in the 3,4-diHPV group, the protein counts in its enriched terms for the BP, CC and MF categories were also higher than those for the EC treatment (Figure C, D). In contrast, in Caco-2-cells not many terms were enriched upon either EC or 3,4-diHPV exposure. The data showing that only nucleus in the terms of CC and poly(A) RNA binding in the category of MF were mutually enriched after both EC and 3,4-diHPV treatments (Figure E, F).

Furthermore, to better understand to which signaling pathways and metabolic activities the DEPs contribute, a KEGG pathway enrichment analysis was conducted for the Hepa1c1c7 and Caco-2 datasets. Figure 4G describes the enriched pathways in Hepa1c1c7 cells. Ribosome and Spliceosome were significantly enriched both upon EC and 3,4-diHPV treatments. Folate biosynthesis was also found to be enriched in the two groups albeit not to a statistically significant extent (Figure 4G). On the other hand, the pathways enriched in Caco-2 cells were very limited. Only two pathways were obtained for each treatment while regulation of actin cytoskeleton appeared to represent the only statistically significant enriched pathway (Figure 4H). From these results, it thus also follows that Hepa1c1c7 cells were more responsive to EC and 3,4-diHPV than the Caco-2 cells, and that 3,4-diHPV was more potent in triggering a cellular response. Additionally, to further explore the possible interactions of the DEPs, a protein-protein interaction (PPI) network analysis was conducted, including a hub PPI network analysis if applicable. Figure S3A – D in Support Information1 show results of this PPI network analysis also presenting the hub proteins for Hepa1c1c7 DEPs. The derived hub PPI networks (Figure S3B, D in Support Information1) for both treatments indicate that ribosome proteins played important roles among these DEPs, which is in line with the GO enrichment analysis. Figure S3E, F in Support Information1 present results of a PPI network analysis for Caco-2 DEPs following treatment with EC and 3,4-diHPV, respectively. Much less protein-protein interactions were derived compared to the results obtained for the Hepa1c1c7 cells, while there were no relevant hub proteins found for these two treatments of Caco-2 cells.

F

G
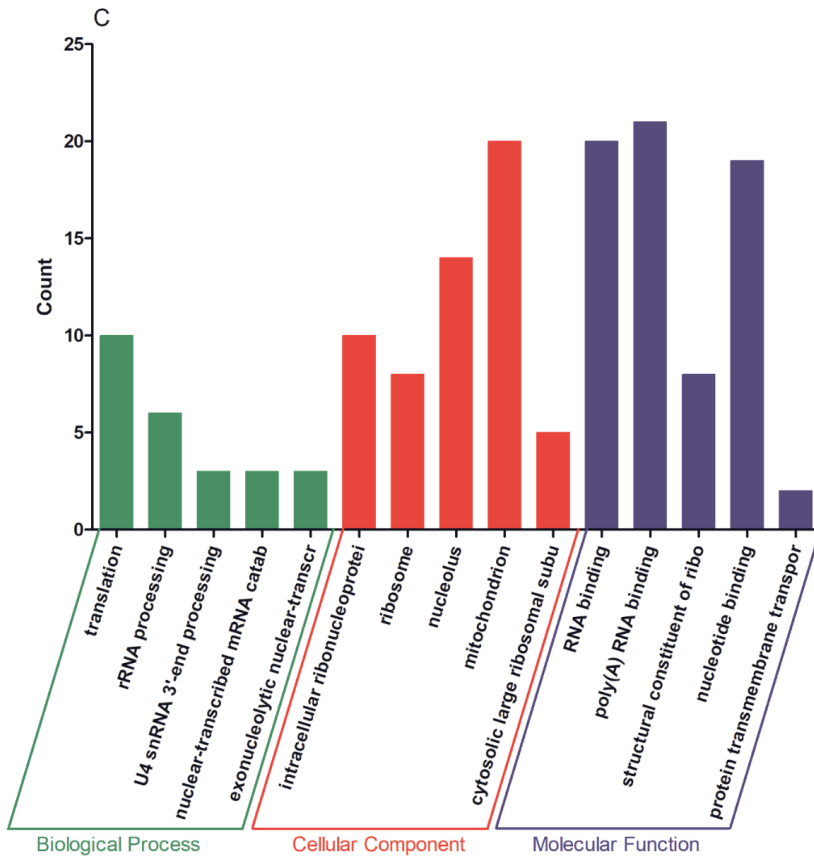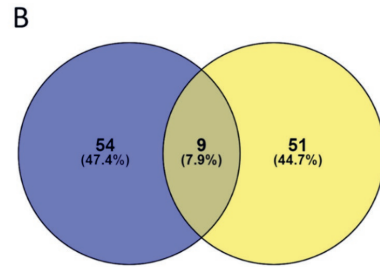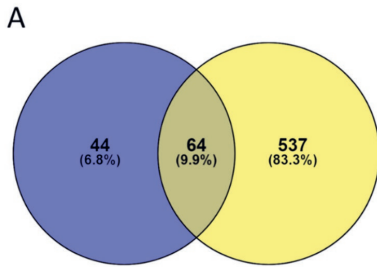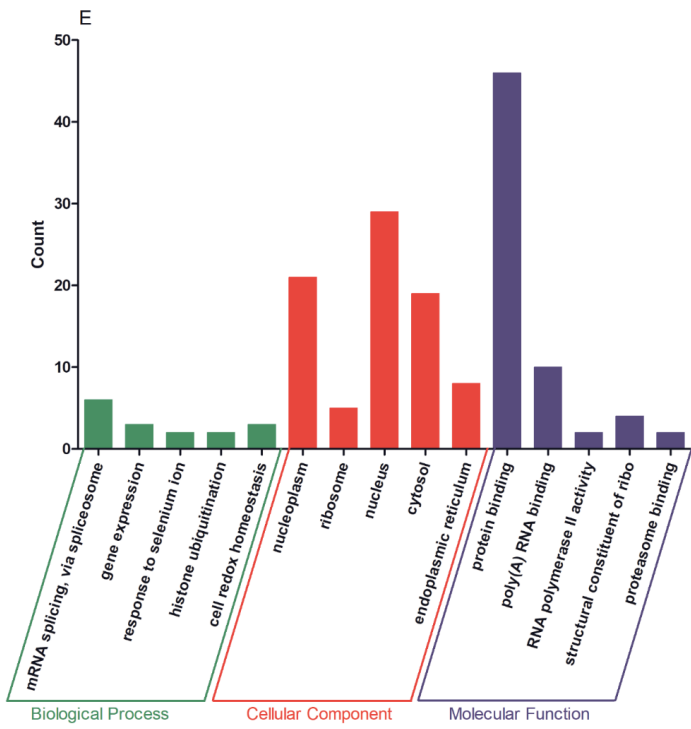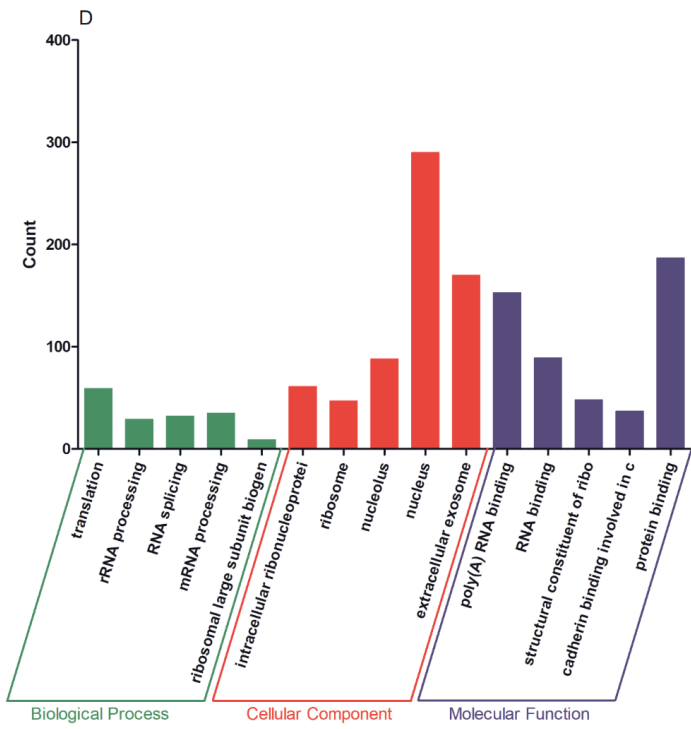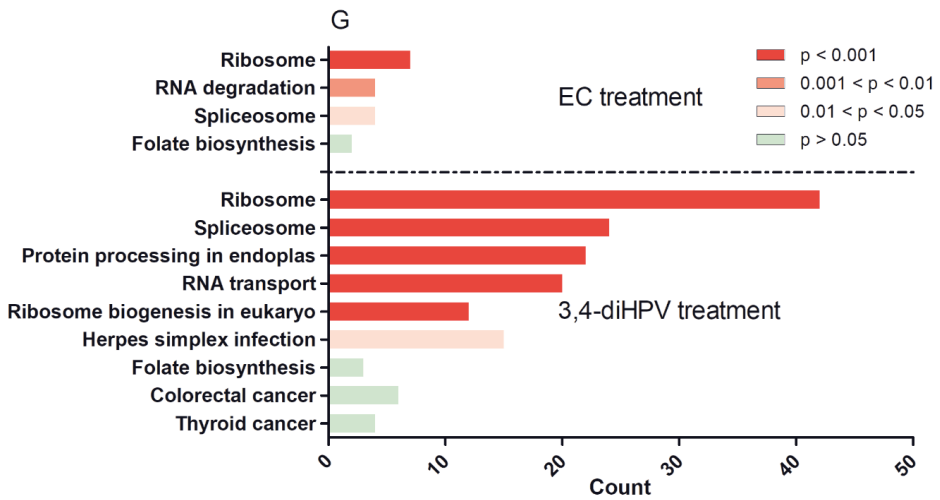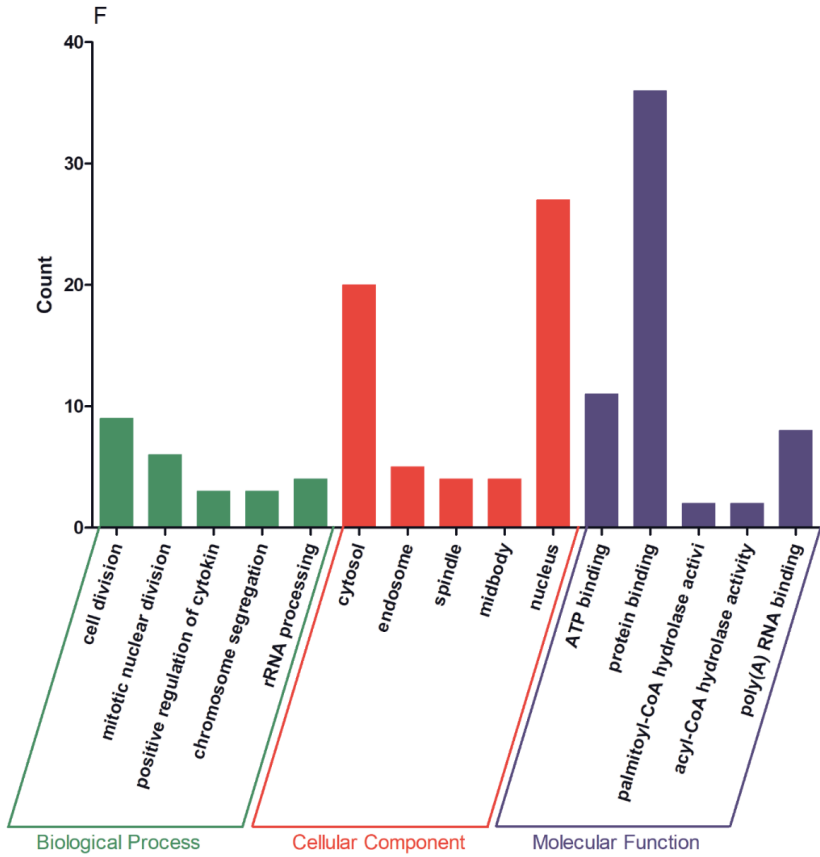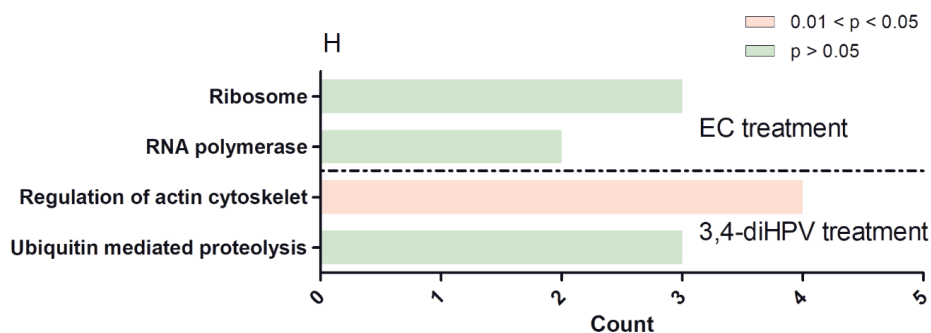
Figure 4. Numbers of DEPs identified by label-free proteomics upon treatment of Hepa1c1c7 cells (A) and Caco-2 cells (B) with either 30 μM EC (blue circle) or 30 μM 3,4-diHPV (yellow circle). GO enrichment of DEPs from 30 μM EC (C) and 30 μM 3,4-diHPV (D) treated Hep1c1c7 cells and from 30 μM EC (E) and 30 μM 3,4-diHPV (F) treated Caco-2 cells. The y-axis value reflects the number of proteins differentially regulated in respective GO terms. KEGG pathway enrichment analysis of DEPs from Hepa1c1c7 cells (G) and Caco-2 cells (H) treated with 30 μM of either EC or 3,4-diHPV.

3.5 RT-qPCR

To corroborate the potential Nrf2-activiation effects of EC and 3,4-diHPV, RT-qPCR was performed for confirmation of some Nrf2-regulated gene expression changes after exposure. Figure 5A presents the results for the relative RNA level for Nqo1, Ugt1a6 and Gclc in Hepa1c1c7 cells after exposure to 30 μM EC or 3,4-diHPV. EC exposure did not significantly affect the RNA level of any of the three genes in Hepa1c1c7 cells. While 3,4-diHPV significantly up-regulated the RNA level of Nqo1 and Ugt1a6 by 2.2-fold and 1.5-fold, respectively. In 3,4-diHPV exposed Hepa1c1c7 cells Gclc was slightly increased (1.2-fold) albeit not statistically significant. These results are well in line with the proteomics data. The fold change (FC) of NAD(P)H dehydrogenase [quinone] 1, UDP-glucuronosyltransferase 1 and glutamate cysteine ligase catalytic subunit (the corresponding proteins of the three genes) amounted to 2.6, 1.2 and 1.4 upon 3,4-diHPV treatment Hepa1c1c7 cells. While their FCs in EC treatment were between $1.0 - 1.1$, indicating no obvious alterations at protein level (Table S1 and Table S2 in Support Information2). On the other hand, the relative RNA level of TP53I3, MGST3 and HMOX-1 in Caco-2 cells was not significantly changed after either EC or 3,4-diHPV exposure, suggesting that in these cells the Nrf2 pathway may not be activated (Figure 5B).
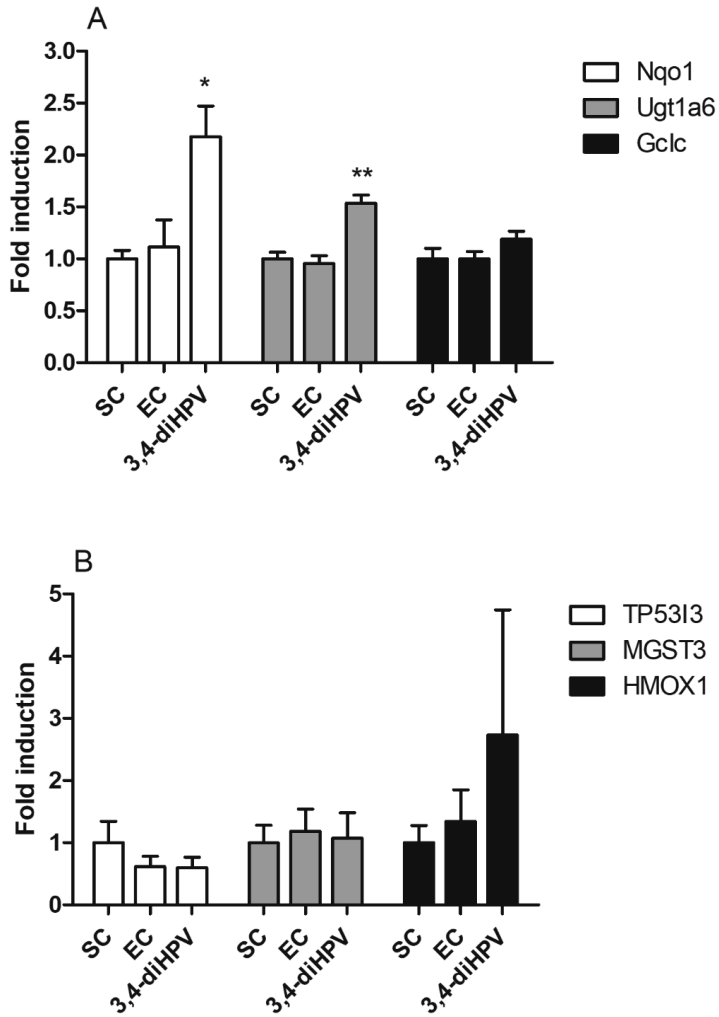
Figure 5. Relative RNA levels in Hepa1c1c7 cells (A) and Caco-2 cells (B) after exposure to the EC or 3,4-diHPV at 30 µM. Gene names are depicted as figure legends. The results were calculated as the ratio of the treatment and the solvent control (SC) and are presented as mean ± SEM, derived from at least three independent experiments.

4. Discussion

In the present study we have compared the inter- and intra-individual differences in human colonic microbial metabolism of EC. Subsequently, the bioactivity for activating Nrf2

signalling of both the parent compound EC and its dominant colonic metabolite 3,4-diHPV were investigated.

Polyphenols are considered as important micronutrients and are abundant in our diets. However, their bioavailability is low, as evidenced by the fact that their maximum plasma concentrations rarely exceed 1 µM after consumption of 80 – 100 mg quercetin equivalent.[32-33] Following the limited bioavailability substantial amounts of non-absorbable polyphenols are known to reach the colon where they are subject to further gut microbial transformations, including ring fission, dehydroxylation and decarboxylation, etc. The host microbial composition is known to vary substantially among people due to differences in age, gender, ethnic factors, lifestyle and diet, which in turn could cause inter-individual differences in gut microbial metabolism of polyphenols.[20, 34-36] Unlike the inter-individual differences, the intra-individual differences in colonic microbial composition and resulting metabolic conversions has scarcely been studied, as it is believed that the intestinal microbiota composition of an individual can be steady for years.[37-38]

The result of the time-dependent EC depletion in the present study, reveal only limited differences between or within individuals, with the data for individual 2, who appeared to be a slow metabolizer, showing only about 4-fold lower conversion at two hours fecal incubation time than what was observed for the other five individuals. This could be a reflection of the functional redundancy of gut microbiota providing the possibility for a reaction to be catalysed by multiple microbiota.[39] The formation of 3,4-diHPV from EC, which includes several reaction steps and reflects a balance between its formation and subsequent further conversion, showed larger inter- and intra-individual differences, than the decrease of EC, suggesting the reactions require specific groups of microbiota. So far, *Lactobacillus plantarum*, *Eggerthella lenta*, *Adlercreutzia equolifaciens* and *Eubacterium SDG-2* are the only identified microbiota that are able to open the C-ring of catechins to form diphenylpropan-2-ol, the precursor of 3,4-diHPV.[40-42] Subsequently, diphenylpropan-2-ol is converted into its A-ring fission metabolites, 3,4-diHPV and 4-hydroxy-5-(3',4'-dihydroxyphenyl)-valeric acid (4H-diHPVA), and this step is reported to be mediated by *Flavonifractor plautii*.[42] Interestingly, an obvious different metabolic pattern of 3,4-diHPV formation in individual 1 at collection 2 was found compared with this individual's collection 1 and 3, with much less 3,4-diHPV detected in the incubations of EC with the fecal sample from the 2nd collection. This indicates the intra-individual gut microbiome can be variable, while the limited differences observed for the fecal samples of the other individuals taken over time reflect the gut microbiome resilience in healthy individuals.[21]

At the 2nd collection, individual one's gut microbial ecosystem may have faced perturbations due to environmental factors, such as unhealthy diet, lifestyle, etc. As a result, the metabolic activity appeared different compared with the earlier and later samplings. However, this situation was probably a transient state, not reaching the tipping points, after which the microbial activity recovered to the initial state that also mimicked the final state.[37] Collectively, although the inter-individual difference in metabolic pattern appeared larger than the intra-individual differences, it is good to be aware of the possible variations caused by the latter when investigating the role of the gut microbiota in metabolism of food-borne compounds of interest.

Next, we investigated to what extent EC and 3,4-diHPV were able to activate the Nrf2 signalling pathway, often linked to (part of) the beneficial effects of catechin intake.[31, 43] The results of the CALUX reporter gene assay suggest that EC, in contrast to its metabolite 3,4-diHPV, was not effective as an Nrf2 activator. This is in agreement with findings of Muzolf-Panek and colleagues who investigated the induction of EpRE-mediated gene expression by several green tea catechins and found that EC along with ECG were inactive at all test concentrations.[44] However, Huang and colleagues concluded that EC is able to protect rats from monocrotaline (MCT) induced liver oxidative injury via activating Nrf2 signalling. For instance, they found that administration of 40 mg/kg EC could counteract the effect of MCT exposure of rats on the levels of Gst, Nrf2, Gclc, Gclm, Nqo1 and Hmox-1.[5] This protective effect of EC is likely, based on the findings of present study, mediated, at least in part, by its microbial metabolite, e.g., 3,4-diHPV, since EC is prone to microbial metabolism in the large intestine in *in vivo* condition. Moreover, other studies that claimed EC could activate the Nrf2 pathway in cells or rodents were all conducted with a pre-stimulated stress-model.[6, 45-46] While the present research provides insights in the Nrf2 activation by EC under non-stressed conditions.

Unlike EC, its major colonic metabolite 3,4-diHPV exerted significant induction of Nrf2-mediated luciferase expression in the CALUX reporter gene assay. The may be ascribed to the formation of semiquinone and quinone type metabolites upon (auto)oxidation of 3,4-diHPV, inducing oxidative and/or electrophilic stress, enabling them to activate the Nrf2.[8, 47-48] This was corroborated by the results that the presence of L-ascorbic acid in the exposure medium reduced the induction folds of Nrf2 signaling activation in 3,4-diHPV exposed U2OS Nrf2 CALUX cells, since it has been reported that L-ascorbic acid is able to inhibit the auto-oxidation of polyphenols.[49-51]

Following the studies with the U2OS Nrf2 CALUX reporter cells additional studies were performed on the Nrf2 mediated gene and protein expression in cells from the Hepa1c1c7 and

the Caco-2 cell lines, providing *in vitro* models for effects in liver and colon, respectively. Thus, both the Hepa1c1c7 and the Caco-2 cell line were used to quantify the EC and 3,4-diHPV induced RNA and protein level changes. From both RT-qPCR and proteomics results, the Nrf2 mediated genes and proteins were only positively regulated after 3,4-diHPV exposure but not after EC exposure, which is in line with the U2OS Nrf2 CALUX assay result. The DEP responses upon both EC and 3,4-diHPV treatments in Hepa1c1c7 cells were more pronounced than those observed in Caco-2 cells. This may indicate that, compared to colonic cells, hepatic cells are more sensitive to polyphenol-type stimuli. One of the explanations for this apparent difference may be related to the active efflux of polyphenols by the multidrug resistance-associated proteins 2 (MRP2) in Caco-2 cells decreasing the intracellular levels of these compounds.[52] Moreover, a substantially higher number (601) of DEPs were obtained in Hepa1c1c7 cells exposed to 3,4-diHPV than when exposed to EC, corroborating the more potent bioactivity of this intestinal microbial metabolite than of the parent catechin. The subsequent bioinformatical analysis also revealed several biological activities of 3,4-diHPV. However, it is worth noting that the Nrf2 pathway or Nrf2-regualted intermediary metabolisms were not among the most significantly enriched pathways indicated by the DEPs, which suggests the Nrf2 signalling may not represent the main target of either EC or 3,4-diHPV. Instead, the translation process was significantly enriched in Hepa1c1c7 cells by both compounds. This is in line with the KEGG enrichment results where spliceosome and ribosome, two important organelles involved in mRNA splicing and translation, were highly enriched. These results suggest the potential cell proliferation-promoting effect of EC and 3,4-diHPV at the test concentration. The promotion of cell proliferation by EC was already proven both in *in vivo* and *in vitro* studies and have been linked to the potential cellular protective effects of this compound.[53-54] However, barely any research on 3,4-diHPV regarding this effect is available so far, so that this provides an interesting topic for future research. Moreover, this metabolite is more bioavailable than its parent compound EC and presents an important biomarker *in vivo* for EC intake.[12, 14] It has been reported that valerolactones together with valeric acids and their phase 2 metabolites were excreted in quantities equivalent to 42% of the ingested EC, compared with just 20% of EC structurally-related metabolites.[12-13]

To conclude, the present study compared the inter- and intra-individual differences in microbial depletion of EC and formation of its major colonic metabolite 3,4-diHPV. Inter-individual differences appeared larger than the intra-individual differences. Unlike its parent compound EC, 3,4-diHPV appeared able to cause a concentration-dependent induction of Nrf2-mediated

gene expression in an Nrf2 reporter cell line. Furthermore, hepatic cells seemed to be more responsive than colonic cells to polyphenol exposure. The proteomics data of Hepa1c1c7 cells revealed that 3,4-diHPV was more potent than EC with more DEPs and enriched functional annotations. However, the data also indicated that the Nrf2 pathway may not represent a major target of 3,4-diHPV. Altogether, our results illustrate that the intestinal microbial metabolism of EC produces the important metabolite 3,4-diHPV, which enriches the bioactivities of the parent compound, increasing possibilities for the induction of Nrf2-mediated gene expression. As 3,4-diHPV is a major gut microbiota-derived metabolite of EC, both intra- and inter-differences in its formation from EC could affect the health-beneficial effects of EC consumption.

AUTHOR INFORMATION

Corresponding Author

Chen Liu - Division of Toxicology, Wageningen University and Research, Wageningen 6708 WE, The Netherlands; E-mail: chen.liu@wur.nl

Authors

Sjef Boeren - Laboratory of Biochemistry, Wageningen University and Research, Wageningen 6708 WE, The Netherlands

Ivonne M.C.M. Rietjens - Division of Toxicology, Wageningen University and Research, Wageningen 6708 WE, The Netherlands

Notes

The authors declare that there is no conflict of interest.

ABBREVIATIONS USED

LC-TQ-MS, liquid chromatograph triple quadrupole mass spectrometry; EC, (-)-epicatechin; 3,4-diHPP-2-ol, 1-(3',4'-dihydroxyphenyl)-3-(2'',4'',6''-trihydroxyphenyl)-2-propanol; 3,4-diHPV, 5-(3',4'-dihydroxyphenyl)-γ-valerolactone; LFQ, label-free quantitation; FDR, false discovery rate; FC, fold change; BP, biological process; CC, cellular component; MF, molecular function; DEPs, differentially expressed proteins; Keap1-Nrf2, Kelch-like ECH-associated protein 1-NF-E2-related factor 2; UGTs, UDP-glucuronosyltransferases; NQO1, NAD(P)H quinone dehydrogenase 1; FCS, foetal calf serum; NEAA, Nonessential amino acids

5. References

1.   Rodriguez-Mateos, A.; Cifuentes-Gomez, T.; Gonzalez-Salvador, I.; Ottaviani, J. I.; Schroeter, H.; Kelm, M.; Heiss, C.; Spencer, J. P., Influence of age on the absorption, metabolism, and excretion of cocoa flavanols in healthy subjects. *Molecular nutrition & food research* **2015,** *59* (8), 1504-1512.

2.   Qu, Z.; Liu, A.; Li, P.; Liu, C.; Xiao, W.; Huang, J.; Liu, Z.; Zhang, S., Advances in physiological functions and mechanisms of (−)-epicatechin. *Critical reviews in food science and nutrition* **2021,** *61* (2), 211-233.

3.   Ruijters, E. J.; Weseler, A. R.; Kicken, C.; Haenen, G. R.; Bast, A., The flavanol (-)-epicatechin and its metabolites protect against oxidative stress in primary endothelial cells via a direct antioxidant effect. *European journal of pharmacology* **2013,** *715* (1-3), 147-153.

4.   Prince, P. D.; Fischerman, L.; Toblli, J. E.; Fraga, C. G.; Galleano, M., LPS-induced renal inflammation is prevented by (−)-epicatechin in rats. *Redox biology* **2017,** *11*, 342-349.

5.   Huang, Z.; Jing, X.; Sheng, Y.; Zhang, J.; Hao, Z.; Wang, Z.; Ji, L., (-)-Epicatechin attenuates hepatic sinusoidal obstruction syndrome by inhibiting liver oxidative and inflammatory injury. *Redox biology* **2019,** *22*, 101117.

6.   Chang, C. F.; Cho, S.; Wang, J., (-)-Epicatechin protects hemorrhagic brain via synergistic Nrf2 pathways. *Annals of clinical and translational neurology* **2014,** *1* (4), 258-271.

7.   Bernatoniene, J.; Kopustinskiene, D. M., The role of catechins in cellular responses to oxidative stress. *Molecules* **2018,** *23* (4), 965.

8.   Yamamoto, M.; Kensler, T. W.; Motohashi, H., The KEAP1-NRF2 system: a thiol-based sensor-effector apparatus for maintaining redox homeostasis. *Physiological reviews* **2018,** *98* (3), 1169-1203.

9.   He, F.; Ru, X.; Wen, T., NRF2, a transcription factor for stress response and beyond. *International Journal of Molecular Sciences* **2020,** *21* (13), 4777.

10.   Clifford, M., Diet-derived phenols in plasma and tissues and their implications for health. *Planta medica* **2004,** *70* (12), 1103-1114.

11.   Schwedhelm, E.; Maas, R.; Troost, R.; Böger, R. H., Clinical pharmacokinetics of antioxidants and their impact on systemic oxidative stress. *Clinical pharmacokinetics* **2003,** *42* (5), 437-459.

12.   Ottaviani, J. I.; Borges, G.; Momma, T. Y.; Spencer, J. P.; Keen, C. L.; Crozier, A.; Schroeter, H., The metabolome of [2-14 C](−)-epicatechin in humans: implications for the assessment of efficacy, safety and mechanisms of action of polyphenolic bioactives. *Scientific reports* **2016,** *6* (1), 1-10.

13.   Borges, G.; Ottaviani, J. I.; van der Hooft, J. J.; Schroeter, H.; Crozier, A., Absorption, metabolism, distribution and excretion of (−)-epicatechin: A review of recent findings. *Molecular Aspects of Medicine* **2018,** *61*, 18-30.

14.   Ottaviani, J. I.; Fong, R.; Kimball, J.; Ensunsa, J. L.; Britten, A.; Lucarelli, D.; Luben, R.; Grace, P. B.; Mawson, D. H.; Tym, A., Evaluation at scale of microbiome-derived metabolites as biomarker of flavan-3-ol intake in epidemiological studies. *Scientific Reports* **2018,** *8* (1), 1-11.

15.   Chen, W.; Zhu, X.; Lu, Q.; Zhang, L.; Wang, X.; Liu, R., C-ring cleavage metabolites of catechin and epicatechin enhanced antioxidant activities through intestinal microbiotC-ring cleavage metabolites of catechin and epicatechin enhanced antioxidant activities through intestinal microbiot. *Food Research International* **2020,** *135*, 109271.

16.   Roowi, S.; Stalmach, A.; Mullen, W.; Lean, M. E.; Edwards, C. A.; Crozier, A., Green tea flavan-3-ols: colonic degradation and urinary excretion of catabolites by humans. *Journal of agricultural and food chemistry* **2010,** *58* (2), 1296-1304.

17.   Kohri, T.; Suzuki, M.; Nanjo, F., Identification of metabolites of (−)-epicatechin gallate and their metabolic fate in the rat. *Journal of agricultural and food chemistry* **2003,** *51* (18), 5561-5566.

18.   Urpi-Sarda, M.; Garrido, I.; Monagas, M.; Gomez-Cordoves, C.; Medina-Remon, A.; Andres-Lacueva, C.; Bartolome, B., Profile of Plasma and Urine Metabolites after the Intake of Almond [Prunus dulcis (Mill.) D.A. Webb] Polyphenols in Humans. *Journal of agricultural and food chemistry* **2009,** *57* (21), 10134-10142.

19.   González-Sarrías, A.; Espín, J. C.; Tomás-Barberán, F. A., Non-extractable polyphenols produce gut microbiota metabolites that persist in circulation and show anti-inflammatory and free radical-scavenging effects. *Trends in Food Science & Technology* **2017,** *69*, 281-288.

20.   Liu, C.; Vervoort, J.; Beekmann, K.; Baccaro, M.; Kamelia, L.; Wesseling, S.; Rietjens, I. M., Interindividual Differences in Human Intestinal Microbial Conversion of (−)-Epicatechin to Bioactive Phenolic Compounds. *Journal of agricultural and food chemistry* **2020,** *68* (48), 14168-14181.

21.   Lozupone, C. A.; Stombaugh, J. I.; Gordon, J. I.; Jansson, J. K.; Knight, R., Diversity, stability and resilience of the human gut microbiota. *Nature* **2012,** *489* (7415), 220-230.

22.   Liu, C.; Vervoort, J.; van den Elzen, J.; Beekmann, K.; Baccaro, M.; de Haan, L.; Rietjens, I. M., Interindividual Differences in Human In Vitro Intestinal Microbial Conversion of Green Tea (-)-Epigallocatechin-3-O-Gallate and Consequences for Activation of Nrf2 Mediated Gene Expression. *Molecular Nutrition & Food Research* **2021,** *65* (2), 2000934.

23.   Bäckhed, F.; Fraser, C. M.; Ringel, Y.; Sanders, M. E.; Sartor, R. B.; Sherman, P. M.; Versalovic, J.; Young, V.; Finlay, B. B., Defining a healthy human gut microbiome: current concepts, future directions, and clinical applications. *Cell host & microbe* **2012,** *12* (5), 611-622.

24.   van der Linden, S. C.; von Bergh, A. R.; van Vught-Lussenburg, B. M.; Jonker, L. R.; Teunis, M.; Krul, C. A.; van der Burg, B., Development of a panel of high-throughput reporter-gene assays to detect genotoxicity and oxidative stress. *Mutation Research/Genetic Toxicology and Environmental Mutagenesis* **2014,** *760*, 23-32.

25.   Wiechelman, K. J.; Braun, R. D.; Fitzpatrick, J. D., Investigation of the bicinchoninic acid protein assay: identification of the groups responsible for color formation. *Analytical biochemistry* **1988,** *175* (1), 231-237.

26.   Batth, T. S.; Tollenaere, M. X.; Rüther, P.; Gonzalez-Franquesa, A.; Prabhakar, B. S.; Bekker-Jensen, S.; Deshmukh, A. S.; Olsen, J. V., Protein aggregation capture on microparticles enables multipurpose proteomics sample preparation. *Molecular & Cellular Proteomics* **2019,** *18* (5), 1027-1035.

27.   Xiong, L.; Li, C.; Boeren, S.; Vervoort, J.; Hettinga, K., Effect of heat treatment on bacteriostatic activity and protein profile of bovine whey proteins. *Food Research International* **2020,** *127*, 108688.

28.   Cox, J.; Mann, M., MaxQuant enables high peptide identification rates, individualized ppb-range mass accuracies and proteome-wide protein quantification. *Nature biotechnology* **2008,** *26* (12), 1367-1372.

29.   Hayes, J. D.; Dinkova-Kostova, A. T., The Nrf2 regulatory network provides an interface between redox and intermediary metabolism. *Trends in biochemical sciences* **2014,** *39* (4), 199-218.

30.   Chun, K.-S.; Raut, P. K.; Kim, D.-H.; Surh, Y.-J., Role of chemopreventive phytochemicals in NRF2-mediated redox homeostasis in humans. *Free Radical Biology and Medicine* **2021,** *172*, 699-715.

31.   Talebi, M.; Talebi, M.; Farkhondeh, T.; Mishra, G.; İlgün, S.; Samarghandian, S., New insights into the role of the Nrf2 signaling pathway in green tea catechin applications. *Phytotherapy Research* **2021**.

32.   Manach, C.; Scalbert, A.; Morand, C.; Rémésy, C.; Jiménez, L., Polyphenols: food sources and bioavailability. *The American journal of clinical nutrition* **2004,** *79* (5), 727-747.

33.   Scalbert, A.; Williamson, G., Dietary intake and bioavailability of polyphenols. *The Journal of nutrition* **2000,** *130* (8), 2073S-2085S.

34.   Anesi, A.; Mena, P.; Bub, A.; Ulaszewska, M.; Del Rio, D.; Kulling, S. E.; Mattivi, F., Quantification of urinary phenyl-γ-valerolactones and related valeric acids in human urine on consumption of apples. *Metabolites* **2019,** *9* (11), 254.

35.   Mena, P.; Bresciani, L.; Brindani, N.; Ludwig, I. A.; Pereira-Caro, G.; Angelino, D.; Llorach, R.; Calani, L.; Brighenti, F.; Clifford, M. N., Phenyl-γ-valerolactones and phenylvaleric acids, the main colonic metabolites of flavan-3-ols: Synthesis, analysis, bioavailability, and bioactivity. *Natural product reports* **2019,** *36* (5), 714-752.

36.   Hollands, W. J.; Philo, M.; Perez-Moral, N.; Needs, P. W.; Savva, G. M.; Kroon, P. A., Monomeric Flavanols Are More Efficient Substrates for Gut Microbiota Conversion to Hydroxyphenyl-γ-Valerolactone Metabolites Than Oligomeric Procyanidins: A Randomized, Placebo-Controlled Human Intervention Trial. *Molecular nutrition & food research* **2020,** *64* (10), 1901135.

37.   Fassarella, M.; Blaak, E. E.; Penders, J.; Nauta, A.; Smidt, H.; Zoetendal, E. G., Gut microbiome stability and resilience: elucidating the response to perturbations in order to modulate gut health. *Gut* **2021,** *70* (3), 595-605.

38.   Faith, J. J.; Guruge, J. L.; Charbonneau, M.; Subramanian, S.; Seedorf, H.; Goodman, A. L.; Clemente, J. C.; Knight, R.; Heath, A. C.; Leibel, R. L., The long-term stability of the human gut microbiota. *Science* **2013,** *341* (6141).

39.   Blakeley-Ruiz, J. A.; Erickson, A. R.; Cantarel, B. L.; Xiong, W.; Adams, R.; Jansson, J. K.; Fraser, C. M.; Hettich, R. L., Metaproteomics reveals persistent and phylum-redundant metabolic functional stability in adult human gut microbiomes of Crohn's remission patients despite temporal variations in microbial taxa, genomes, and proteomes. *Microbiome* **2019,** *7* (1), 1-15.

40.   Sanchez-Patan, F.; Tabasco, R.; Monagas, M.; Requena, T.; Pelaez, C.; Moreno-Arribas, M. V.; Bartolome, B., Capability of Lactobacillus plantarum IFPL935 to catabolize flavan-3-ol compounds and complex phenolic extracts. *Journal of agricultural and food chemistry* **2012,** *60* (29), 7142-7151.

41.   Takagaki, A.; Nanjo, F., Bioconversion of (−)-epicatechin,(+)-epicatechin,(−)-catechin, and (+)-catechin by (−)-epigallocatechin-metabolizing bacteria. *Biological and Pharmaceutical Bulletin* **2015,** *38* (5), 789-794.

42.   Kutschera, M.; Engst, W.; Blaut, M.; Braune, A., Isolation of catechin-converting human intestinal bacteria. *Journal of applied microbiology* **2011,** *111* (1), 165-175.

43.   Fraga, C. G.; Oteiza, P. I.; Galleano, M., Plant bioactives and redox signaling:(−)-Epicatechin as a paradigm. *Molecular aspects of medicine* **2018,** *61*, 31-40.

44.   Muzolf-Panek, M.; Gliszczyńska-Świgło, A.; de Haan, L.; Aarts, J. M.; Szymusiak, H.; Vervoort, J. M.; Tyrakowska, B.; Rietjens, I. M., Role of catechin quinones in the induction of EpRE-mediated gene expression. *Chemical research in toxicology* **2008,** *21* (12), 2352-2360.

45.   Cheng, T.; Wang, W.; Li, Q.; Han, X.; Xing, J.; Qi, C.; Lan, X.; Wan, J.; Potts, A.; Guan, F., Cerebroprotection of flavanol (-)-epicatechin after traumatic brain injury via Nrf2-dependent and -independent pathways. *Free Radical Biology and Medicine* **2016,** *92*, 15-28.

46.   Lan, X.; Han, X.; Li, Q.; Wang, J., (−)-Epicatechin, a natural flavonoid compound, protects astrocytes against hemoglobin toxicity via Nrf2 and AP-1 signaling pathways. *Molecular neurobiology* **2017,** *54* (10), 7898-7907.

47.   Parvez, S.; Long, M. J.; Poganik, J. R.; Aye, Y., Redox signaling by reactive electrophiles and oxidants. *Chemical reviews* **2018,** *118* (18), 8798-8888.

48.   Na, H.-K.; Surh, Y.-J., Modulation of Nrf2-mediated antioxidant and detoxifying enzyme induction by the green tea polyphenol EGCG. *Food and Chemical Toxicology* **2008,** *46* (4), 1271-1278.

49.   Beekmann, K.; Rubió, L.; de Haan, L. H.; Actis-Goretta, L.; van der Burg, B.; van Bladeren, P. J.; Rietjens, I. M., The effect of quercetin and kaempferol aglycones and glucuronides on peroxisome proliferator-activated receptor-gamma (PPAR-γ). *Food & function* **2015,** *6* (4), 1098-1107.

50.   Grzesik, M.; Bartosz, G.; Stefaniuk, I.; Pichla, M.; Namieśnik, J.; Sadowska-Bartosz, I., Dietary antioxidants as a source of hydrogen peroxide. *Food chemistry* **2019,** *278*, 692-699.

51.   Chen, L.; Wang, W.; Zhang, J.; Cui, H.; Ni, D.; Jiang, H., Dual effects of ascorbic acid on the stability of EGCG by the oxidation product dehydroascorbic acid promoting the oxidation and inhibiting the hydrolysis pathway. *Food Chemistry* **2021,** *337*, 127639.

52.   Chu, K. O.; Pang, C. C., Pharmacokinetics and disposition of green tea catechins. *Pharmacokinetics and Adverse Effects of Drugs: Mechanisms and Risks Factors* **2018,** *17*.

53.   Vasconcelos, P. C. d. P.; Seito, L. N.; Di Stasi, L. C.; Akiko Hiruma-Lima, C.; Pellizzon, C. H., Epicatechin used in the treatment of intestinal inflammatory disease: an analysis by experimental models. *Evidence-Based Complementary and Alternative Medicine* **2012,** *2012*.

54.   Granado-Serrano, A. B.; Angeles Martín, M.; Izquierdo-Pulido, M.; Goya, L.; Bravo, L.; Ramos, S., Molecular mechanisms of (−)-epicatechin and chlorogenic acid on the regulation of the apoptotic and survival/proliferation pathways in a human hepatoma cell line. *Journal of Agricultural and Food Chemistry* **2007,** *55* (5), 2020-2027.

Supplementary Information

Cell viability results from WST-1 assay (Figure S1). U2OS Cytotox CALUX assay (Figure S2). PPI network analysis (Figure S3). The proteins identified and quantified in Hepa1c1c7 and Caco-2 cells (Table S1 and Table S2). Nrf2-asscociated proteins selected from whole protein datasets of Hepa1c1c7 and Caco-2 cells, respectively (Table S3 and Table S4). GO and KEGG pathway enrichment results in Hepa1c1c7 and Caco-2 (Support Information2).

Chapter 4
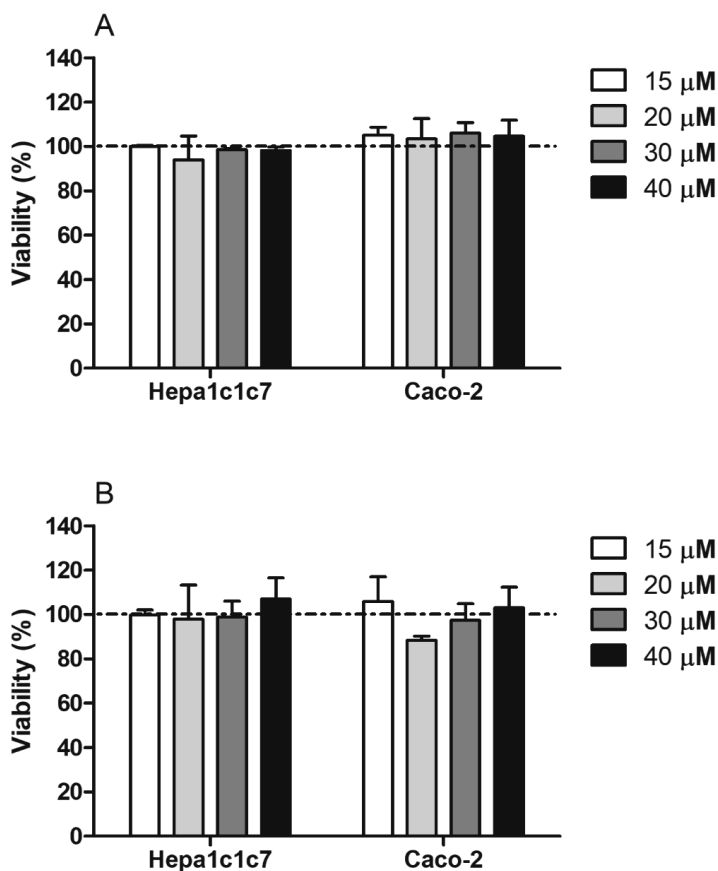
Figure S1. Cell viability test of Hepa1c1c7 cells and Caco-2 cells exposed to EC (A) and 3,4-diHPV (B) at different concentrations, conducted via WST-1 assay. All exposure with the presence of 0.5 mM ascorbic acid. The results are presented as mean ± SEM compared with solvent control, derived from at least three independent experiments.
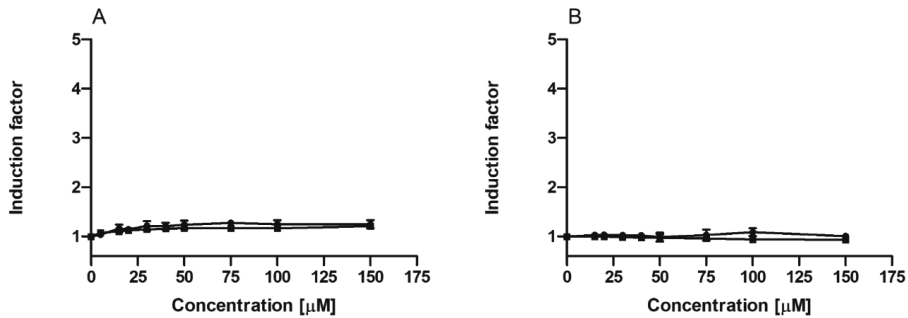
Figure S2. Induction of luciferase expression in U2OS Cytotox CALUX cells after 24 h exposure to EC (circles) and 3,4-diHPV (squares) with (Figure S2A) and without (Figure S2B) the presence of 0.5 mM L-ascorbic acid in the exposure medium. Results are presented as mean ± SEM compared with the solvent control, derived from three independent experiments.
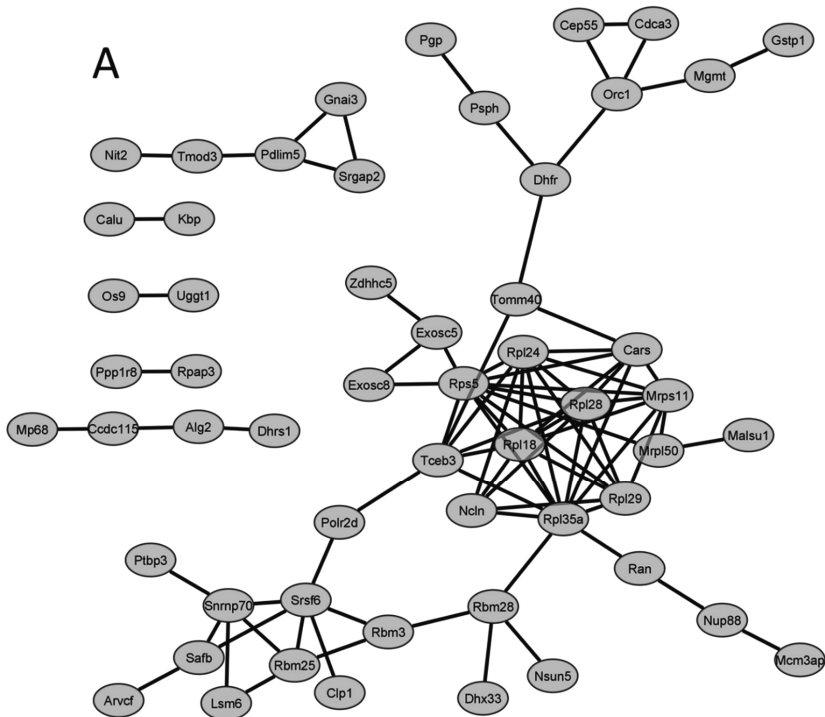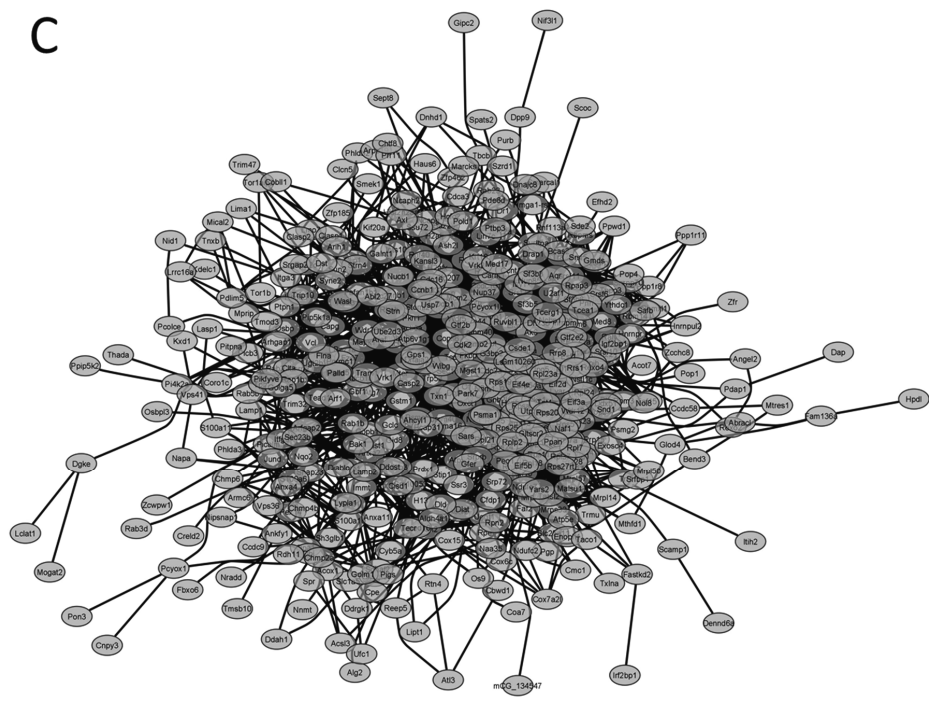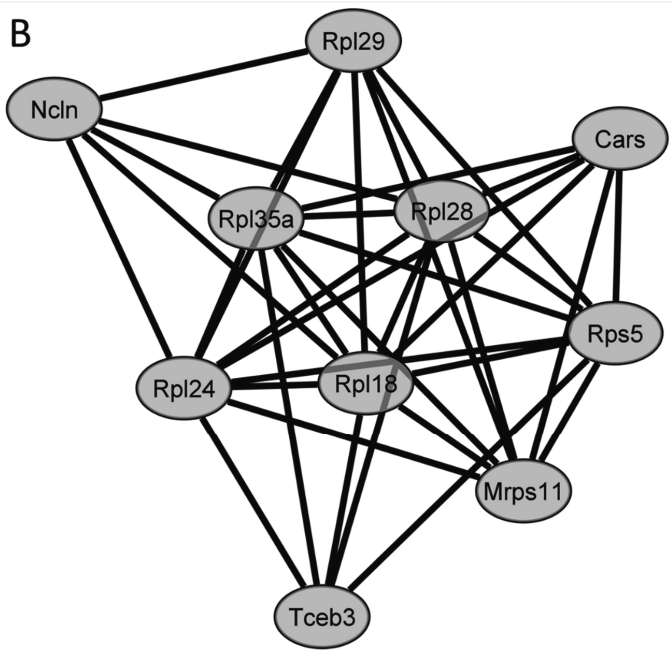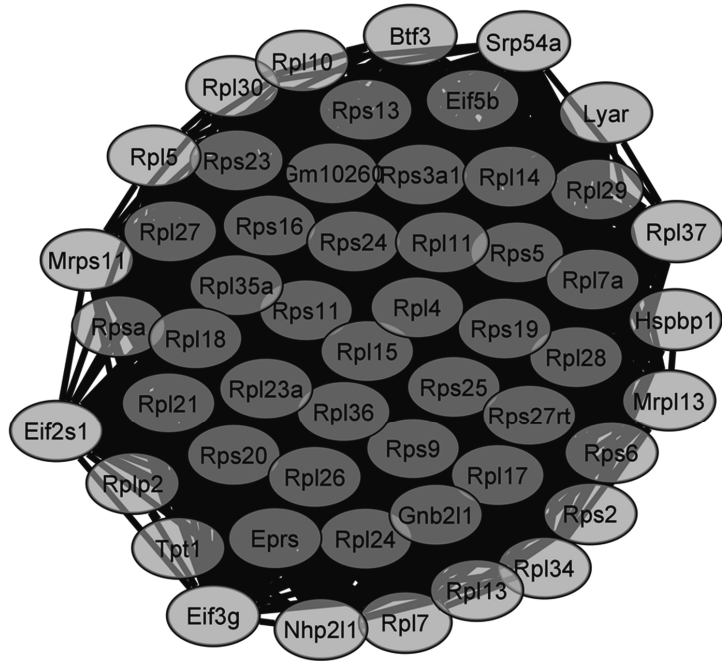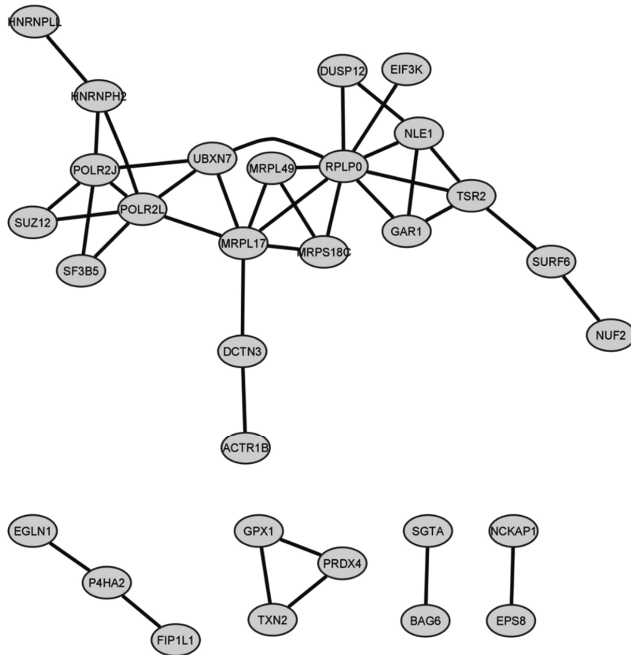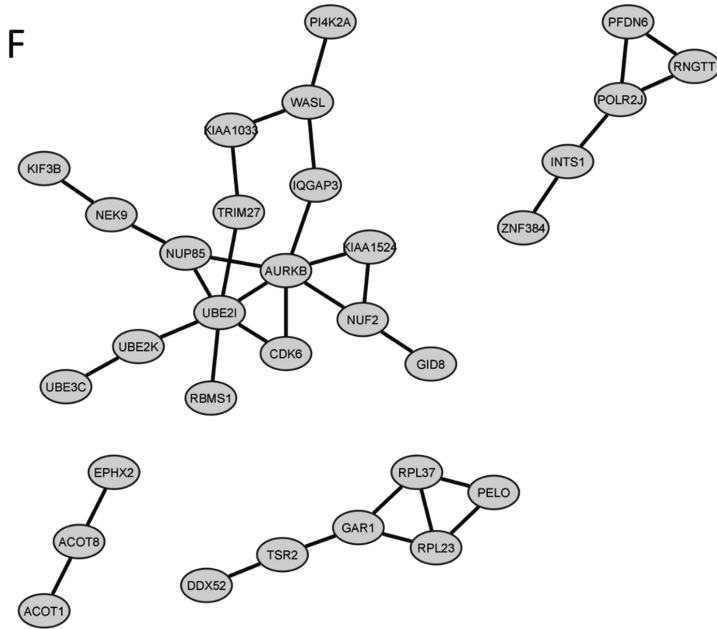
Figure S3. Protein-protein interaction (PPI) network analysis of DEPs in Hepa1c1c7 cells and Caco-2 cells after EC and 3,4-diHPV exposure. A and B: PPI network and its hub protein network of DEPs from EC treated Hepa1c1c7 cells. C and D: PPI network and its hub protein network of DEPs from 3,4-diHPV treated Hepa1c1c7 cells. E: PPI network of DEPs from EC treated Caco-2 cells. F: PPI network of DEPs from 3,4-diHPV treated Caco-2 cells.

5

Chapter 5

The gut microbial metabolite pyrogallol is a more potent regulator of Nrf2-associated gene expression than its parent compound green tea (-)-epigallocatechin gallate

Chen Liu, Sjef Boeren, Ignacio Miro Estruch, Ivonne M.C.M. Rietjens

Abstract

Scope: (-)-Epigallocatechin gallate (EGCG) is the most abundant catechin in green tea and has been reported to be responsible for multiple beneficial effects. However, EGCG is known to be converted by the gut microbiota when reaching the large intestine. The present study characterized the ability of EGCG and its major catechol moiety-containing microbial metabolites to induce Nrf2-mediated gene expression both at the transcriptional and translational levels.

Methods and Results: A reporter gene bioassay, label-free quantitative proteomics and an RT-qPCR were combined to investigate the regulation of Nrf2-related gene expression after exposure of cells in vitro to EGCG or its major microbial catechol moiety-containing metabolites (-)-epigallocatechin (EGC), gallic acid (GA) and pyrogallol (PG). The results show that at micromolar concentrations PG was a more potent inducer of Nrf2-mediated gene expression than EGCG. Bioinformatical analysis of the proteomics data indicated that Nrf2 pathway activation by PG could be related to glutathione metabolism, drug and/or xenobiotics metabolism, and the pentose phosphate pathway as the major pathways.

Conclusion: Taken together, our findings demonstrate that, especially in the gastrointestinal tract, microbial metabolites of EGCG including especially PG may contribute substantially to the Nrf2 signalling activation upon exposure to the parent compound or green tea.

Keywords: EGCG, Nrf2, proteomics, pyrogallol, t-BHQ

1. Introduction

Green tea is one of the most popular beverages that is welcomed both by Asian and Western cultures. Habitually consumption of green tea has been reported to have various health benefits, such as reduced risk of cardiovascular diseases, Alzheimer disease, anti-diabetes and anti-cancer effects.[1-2] These health-promoting properties are believed to be associated with the most abundant and bioactive green tea catechin (-)-epigallocatechin gallate (EGCG). However, as other polyphenols, EGCG has a poor bioavailability with only less than 1% of the total ingested amount being present in the systemic circulation.[3-4]

Upon ingestion of green tea or EGCG, only a small portion of the EGCG appears in the systemic circulation while the majority reaches the large intestine where it is degraded by intestinal microbiota.[5] The microbial conversion starts with the rapid degalloylation of the D-ring by microbial esterases which gives rise to gallic acid (GA) and (-)-epigallocatechin (EGC). Subsequently, these two metabolites are subject to further degradations. GA produces pyrogallol (PG) by decarboxylation, and PG can be further degraded into catechol, butyric acid and acetic acid.[6-7] Previous anaerobic fecal incubations of EGCG revealed EGC to be formed at a maximum level of 16.4% of the original EGCG.[6] Subsequent reductive cleavage in its C ring of EGC, gives rise to the formation of 1-(3',4',5'-trihydroxyphenyl)-3-(2'',4'',6''-trihydroxyphenyl)-2-propanol. This transient intermediate can be degraded to phenyl-γ-valerolactones, i.e., 5-(3',4',5'-trihydroxyphenyl)-γ-valerolactone (3,4,5-triHPV), 5-(3',4'-dihydroxyphenyl)-γ-valerolactone (3,4-diHPV) and 5-(3',5'-dihydroxyphenyl)-γ-valerolactone (3,5-diHPV).[6, 8] 3,5-DiHPV has been reported to be the dominant metabolite while 3,4,5-triHPV and 3,4-diHPV are detected in lower amounts and during shorter timeframes, with the latter compound being primarily formed from microbial conversion of (-)-epicatechin.[6, 8-10] The A-ring fission, lactonization, dehydroxylation, decarboxylation and beta-oxidation catalysed by the gut microbiome results in the formation of phenyl-γ-valerolactones and various smaller phenolic acids, which are more readily absorbed.[5, 11] The above metabolic pathways not only improve the overall bioavailability of EGCG or rather its metabolites, but may also contribute to the physiological bioactivities that are attributed to the parent compound. Therefore, bioactivities of EGCG but also of its microbial metabolites need to be taken into account when investigating the modes of action behind observed physiological effects induced by green tea or EGCG.

Among the cellular signalling pathways, the Kelch-like ECH associating protein 1/nuclear factor erythroid 2-related factor 2 (Keap1/Nrf2) system is often referred to as a pivotal pathway with vital regulatory roles in many physiological processes.[12] Studies have confirmed that several green tea catechins are able to facilitate the nucleus translocation of Nrf2.[13-14] As a result, this transcription factor, Nrf2, subsequently binds to the electrophile responsive element (EpRE) in the promotor region of a wide range of Nrf2 responsive genes, initiating the cellular defence system by transcription of a wide array of cytoprotective genes, including for example glutathione S-transferases (GSTs), glutathione reductases (GRs) and UDP-glucuronosyltransferases (UGTs) and many others.[12, 15]

The activation of the Nrf2 pathway is believed to be able to protect cells from both oxidative and electrophilic stresses that originate from either exogenously or endogenously formed reactive oxygen species and/or electrophiles.[16-17] However, as discussed above, the catechins are hardly bioavailable and only remain intact for very limited time after they are passed to the colon where they are converted by the microbiota. Therefore, the aim of the present study was to characterize the bioactivity of the microbial metabolites formed and to compare these activities to those of the parent catechin taking EGCG as the model compound. The microbial EGCG metabolites to be tested in the present study were chosen based on i) abundance in their formation during a 6 hour anaerobic fecal incubation of EGCG,[6] and ii) the presence of a catechol moiety, the latter because such a structural element is known to be essential for efficient Nrf2 activation potency.[13, 18-19] Especially this second criterium is not fulfilled for 3,5-diHPV, the dominant EGCG metabolites in anaerobic fecal incubations with EGCG.[6] GA, which does contain a catechol moiety, has been abundantly quantified in the earlier hours of in vitro anaerobic fecal incubations of EGCG, with a peak occurrence amounting to 33.9% (mol/mol) of the initial amount of EGCG.[6] GA is further decarboxylated to PG,[5, 20] which was quantified in a substantial amount from 3 to 6 h in in vitro anaerobic fecal incubations of EGCG, reaching a plateau amounting to 31.7% of the EGCG added to the incubation.[6] PG has also been reported to be one of the main metabolites in urinary excretion after green tea consumption by human volunteers.[21] So far, more than hundreds of Nrf2-mediated genes have been reported in in vitro and in vivo studies.[22-23] However, a complete picture of what Nrf2-related proteins are affected after exposure to EGCG and/or its microbial metabolites is still waiting to be unveiled.

To this end, the activity of EGCG and several of its selected catechol moiety containing microbial metabolites including EGC, GA and PG were quantified in an Nrf2 reporter gene assay, and also by RT-qPCR and label-free quantitative proteome analysis of exposed U2OS

cells or Hepa1c1c7 cells. Results obtained will provide valuable leads on the importance of intestinal microbial metabolites of EGCG regarding the activation of the Nrf2-mediated cellular defence system. These results will also provide insights into the potential role of the microbiome metabolites in the mode of action underlying the potential pharmacological/physiological effects of green tea and/or EGCG intake.

2. Experimental Section

2.1 Chemicals and reagents

EGCG, EGC, GA, PG, t-BHQ, L-ascorbic acid, curcumin were ordered from Sigma-Aldrich (Zwijndrecht, The Netherlands). Trypsin, penicillin/streptomycin (P/S), geneticin (G148) and non-essential amino acids (NEAA) were obtained from Invitrogen Corporation (Breda, The Netherlands). Dimethyl sulfoxide (DMSO) was purchased from Acros Organic (New Jersey, USA). Fetal bovine serum (FBS) was bought from Capricorn Scientific (Ebsdorfergrund, Germany). Minimum Essential Medium (MEM) Alpha, Dulbecco's Modified Eagle Medium with 1:1 F-12 Nutrient Mixture (DMEM/F-12), and phosphate buffered saline (PBS) were supplied by Gibco (Paisley, UK).

2.2 Cell lines

The U2OS-Nrf2 CALUX cells (Biodetection Systems, Amsterdam) were derived from human osteoblastic cells, transfected with a reporter construct carrying a luciferase reporter gene under transcriptional control of four different EpRE sequences.[24] The cells were cultured with DMEM/F-12 culture medium, supplemented with 1% (v/v) P/S, 1% (v/v) NEAA and 10% (v/v) FBS. The U2OS-Cytotox CALUX cells (Biodetection Systems, Amsterdam) carry a luciferase reporter gene under transcriptional control of a constitutive promoter. As a result, the cells are able to produce an invariant luciferase expression. The Hepa1c1c7 cell line is a murine hepatoma cell line and was cultured in MEM-Alpha supplemented with 1% (v/v) P/S and 10% (v/v) FBS. Controlled culturing conditions were provided as previously established.[6] 200 µg/ml G418 was added to the culture medium once a week in order to maintain the selection pressure for aforementioned cells lines.

2.3 Reporter gene assay

The bioactivity of EGCG, EGC, GA, PG and t-BHQ in inducing Nrf2 gene transcription were checked by measuring the luciferase activity in the U2OS-Nrf2 CALUX cells.[24] All assay medium contained freshly made 0.5 mM L-ascorbic acid to inhibit the auto-oxidation of test

compounds.[25-27] A total of five exposure concentrations were applied for all compounds, ranging from 5 µM to 75 µM (added from 200-times concentrated stock solutions in DMSO). 20 µM curcumin served as positive control.

To investigate the cytotoxicity (which could cause false negative results) and whether luciferase stabilisation (false positive results) occurred during the exposure to test compounds, a parallel U2OS-Cytotox CALUX assay was performed. This assay was performed using the same conditions as described above for the U2OS-Nrf2 CALUX assay. Results of both assays are presented as the induction factor (IF) compared to the solvent control (0.5% DMSO in exposure medium). Results from at least three independent biological replicates were obtained for all compounds.

2.4 Cell viability assay

The WST-1 assay was applied to assess the viability of Hepa1c1c7 cells after exposure to the compounds tested. Exposure concentrations leading to viabilities higher than 80% are considered as non-cytotoxic. In brief, the cells were seeded in the inner 60 wells of a transparent 96 well plate at a density of 2×10^4 cells per well in 100 µl culture medium. The subsequent exposure procedure was same as described above for the CALUX assay. For the WST-1 assay, 6 µL WST-1 solution was transferred into each exposure well followed by 60 min incubation at 37 °C. The amount of formazan formed from WST-1 directly correlates to the number of viable cells and was quantified by measuring the absorbance at 440 and 620 nm with a microplate reader. The result was calculated by using the values at 440 nm to subtract their corresponding values at 620 nm. The viability (%) of the solvent control was set as 100%.

2.5 Sample preparation and liquid chromatography mass spectrometry (LC-MS) analysis for label-free quantitative proteomics

To prepare cell samples, Hepa1c1c7 cells were seeded at a density of 6×10^5 cells/mL in T25 flasks one day before exposure. Subsequently, cells were exposed to assay medium containing 30 µM EGCG, EGC, GA, PG or t-BHQ for 24 h in the presence of 0.5 mM L-ascorbic acid. The concentration of test compounds used were shown to not cause a significant decrease in cell viability (Fig. S1 in Supplementary material) and is not too high to achieve. Afterwards, cells were washed twice with PBS after which 1.5 mL 100 mM Tris-HCl, pH 8 was added into the flask. The cells then were scraped and homogenised followed by centrifuging for three minutes at 1×10^4 rpm (9391 rcf). Supernatants were discarded and cell pellets were washed twice with 1 mL 100 mM Tris-HCl, pH 8. In the end, the cell pellets were sonicated and

dissolved in 100 µL 100 mM Tris-HCl, pH 8. The concentration of protein in the samples were determined by the Bicinchoninic Acid (BCA) method.[28] To obtain peptide samples a total of 100 µg protein from each sample was subjected to sample preparation via the protein aggregation capture (PAC) method.[29] A final concentration of 0.1 µg/µL peptides was prepared for all samples and these samples were stored immediately at -20 °C until further analysis. Four independent biological replicates were collected for all treatments.

Three ul of peptide samples were loaded directly onto a 0.10×250 mm ReproSil-Pur 120 C18-AQ 1.9 µm beads analytical column (prepared in-house) at a constant pressure of 825 bar (flow rate of circa 600 nL/min) with buffer 1 mL/L formic acid in water and eluted at a flow of 0.5 µL/min with a 50 min linear gradient from 9% to 34% acetonitrile in water with 1 mL/L formic acid with a Thermo EASY nanoLC1000 (Thermo, Waltham, MA, USA). An electrospray potential of 3.5 kV was applied directly to the eluent via a stainless steel needle fitted into the waste line of a micro cross that was connected between the nLC and the analytical column. On the connected Orbitrap Exploris 480 (Thermo electron, San Jose, CA, USA), MS and MSMS AGC targets were set to 300%, 100% respectively or maximum ion injection times of 50 ms (MS) and 30 ms (MSMS) were used. HCD fragmented (isolation width 1.2 m/z, 28% normalized collision energy) MSMS scans in a cycle time of 1.1 recording the most abundant 2-5+ charged peaks in the MS scan in data dependent mode (Resolution 15000, threshold 2e4, 15 s exclusion duration for the selected m/z +/- 10 ppm).

For identifications and relative quantifications of the peptides, the MaxQuant software package (1.6.3.4) was used. Data were filtered to show only proteins reliably identified by minimally two peptides of which at least one is unique and one is unmodified and a false discovery rate (FDR) of less than 1% on both protein and peptide level. Reversed hits were deleted from the MaxQuant result table. Zero label-free quantitation (LFQ) intensity values were replaced by a value of $10^{6.5}$ (a value slightly lower than the lowest measured value) to make sensible ratio calculations possible.

2.6 Data analysis and bioinformatics

After obtaining the whole protein dataset of all groups, a manual search for Nrf2-related proteins was conducted, based on recent publications.[12, 15, 22-23, 30-31] The protein fold change (FC) was calculated as the ratio of the average LFQ intensities of a specific treatment and the control. The Nrf2-related proteins thus identified were derived and together with their respective FCs for the different treatments were further subjected to a PCA analysis and

heatmap plotting by ClustVis (https://biit.cs.ut.ee/clustvis/). Furthermore, R 3.6.0 (R Core Team 2019) was used to do a Student's t-test for analysing the statistical significance of differences between the control and different treatments. The differentially expressed proteins (DEPs) in different treatments were selected based on the FCs ($\geqslant 1.2$ or $\leqslant 0.8$) with a P-value of < 0.05. In the next step, the DEPs in each treatment were used as input to do gene ontology enrichment analysis (Biological Process (BP), Cellular Component, (CC) and Molecular Function (MF)) and KEGG pathway enrichment via the DAVID functional annotation tool (https://david.ncifcrf.gov/tools.jsp). The derived results were subjected to Bioinformatics (http://www.bioinformatics.com.cn) for visualization. Additionally, DEPs were also used for PPI network analysis which was performed via the STRING database (https://string-db.org/) and results thus obtained were visualized using Cytoscape 3.8.2 (Seattle, USA). Hub protein networks were further produced by the plug-in software MCODE in Cytoscape 3.8.2.

2.7 RT-qPCR

To study the Nrf2 activation at RNA level, RT-qPCR was carried out. To do so, Hepa1c1c7 cells were seeded in a 6-well plate at a density of 2.4×10^5 cells/mL in 2.5 mL culture medium per well and left to attach for 24 h followed by another 24 h of exposure to 30 µM EGCG, EGC, GA, PG or t-BHQ in the presence of 0.5 mM L-ascorbic acid. After exposure, cells were washed twice with ice-cold PBS and lysed with RLT lysis buffer (Qiagen, Venlo, The Netherlands). The QIAshredder and RNeasy kits (Qiagen, Venlo, The Netherlands) were used to extract high quality RNA from cell samples. Subsequently, the RNA concentrations, A260/A280 and A260/230 were quantified via Nanodrop One (Thermoscientific, Delaware, USA). Afterwards, RNA was reverse-transcribed into cDNA using the QuantiTect Reverse Transcription Kit (Qiagen, Venlo, The Netherlands). Gapdh was chosen as the reference gene. The relative transcription level of NAD(P)H dehydrogenase [quinone] 1 (Nqo1), Glutathione s-transferase A3 (Gsta3), Glutamate-cysteine ligase catalytic subunit (Gclc) and UDP glucuronosyltransferase family 1 member a6 (Ugt1a6) were checked by RT-qPCR using SYBR Green-based method (Qiagen, Venlo, The Netherlands). The Rotor-Gene 6000 cycler (Qiagen, Venlo, The Netherlands) recorded cycle threshold (Ct) values of all samples and these data were used to calculate relative RNA level by the $2^{-\Delta\Delta Ct}$ method. Primers were commercial QuantiTect Pimer Assays ordered from Qiagen (Venlo, The Netherlands), namely Mm_Gapdh_3_SG, Mm_Nqo1_1_SG, Mm_Gsta3_va.1_SG, Mm_Gclc_1_SG and Mm_Ugt1a6_1_SG.

2.8 Dosage Information

The concentration of EGCG used in U2OS Nrf2 CALUX assay ranged between 5 and 75 µM. One cup of green tea contains 110 mg EGCG.[32-33] It was estimated that 52% of the dose could reach the large intestine, and a large intestinal volume of 371 mL for a 70 kg person.[34] Thus, the concentration of EGCG in the large intestine may reach 336 µM. The concentration of all compounds used in the proteomics and RT-qPCR was 30 µM, which did not cause an obvious decrease in viabilities (less than 20% compare with control) of Hepa1c1c7 cells, is considered as non-cytotoxic.

2.9 Statistical analysis

Data are presented as mean ± SEM. All experiments mentioned in the present study were conducted in at least three independent biological replications. GraphPad Prism 5.0 (San Diego, USA) was used to plot line charts and histograms. One-way ANOVA was performed on data of relative RNA levels in Hepa1c1c7 cells after exposure to the selected model compounds in RT-qPCR experiments. For the U2OS-Nrf2 CALUX reporter gene assay, two-way ANOVA was performed to evaluate induction factors by the compound (EGCG or PG) and exposure concentrations, and their interactions. Both data of the U2OS-Nrf2 CALUX reporter gene assay and RT-qPCR analysis were evaluated for equal variances and homogeneity of variance using the Shapiro-Wilk and Levene tests, respectively. Logarithmic transformation or taking the reciprocal were performed for variables with unequal variance. Statistical significance was determined at P-values < 0.05.

3. Results

3.1 Activation of Nrf2-mediated luciferase expression by EGCG and its metabolites

The concentration response curves of luciferase activity induced by EGCG, EGC, GA, PG and t-BHQ are presented in Fig. 1A. At moderate concentrations (0 - 30 µM), PG and t-BHQ already induced significant increases in luciferase expression. For instance, at 15 µM PG and t-BHQ the induction factor (IF) values amounted to 2.1 and 1.9, respectively. At 30 µM PG and t-BHQ the induction was 3.3 and 2.6-fold. On the other hand, EGCG was less active, with an IF of 1.0 and 1.6 at 15 and 30 µM, respectively. Two-way ANOVA of IFs induced by EGCG and PG further indicates both the compound and concentration significantly affect the IF values (P < 0.0001). Moreover, the metabolite PG was more capable of inducing Nrf2 activation than EGCG especially at concentrations ranging between 15 to 50 µM (P < 0.05). GA and EGC were

inactive at all test concentrations. The average IF of the positive control (20 µM curcumin) was 42.3, indicating the assay worked well. Results of the U2OS-Cytotox CALUX assays showed no luciferase stabilisations for all five compounds at all tested concentrations except for EGCG showing a slight increase (1.7 fold) in luciferase activity at 50 and 75 µM (Fig. 1B). The IFs for the Nrf2 CALUX assay at these two concentrations for EGCG were corrected for this response in the Cytotox CALUX assay. No cytotoxicity was found for EGCG, EGC, GA and PG until the maximum concentration tested. However, the U2OS cells seem to be much more susceptible to the cytotoxicity of t-BHQ, with an IF dropping from 15 µM (0.87) and decreasing to 0.28 at 75 µM (Fig. 1B).
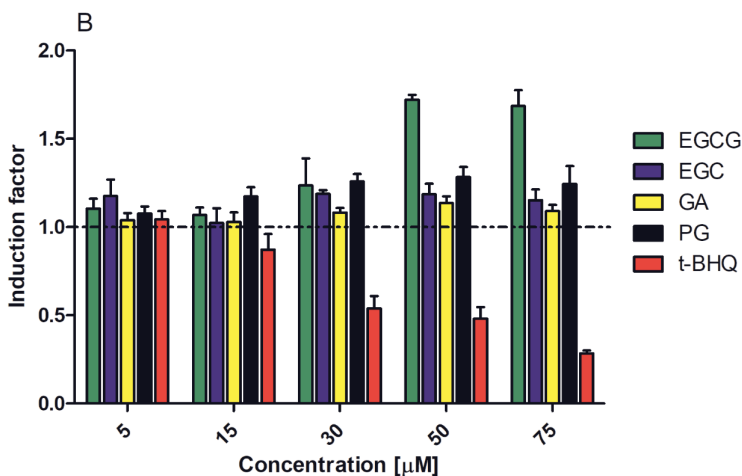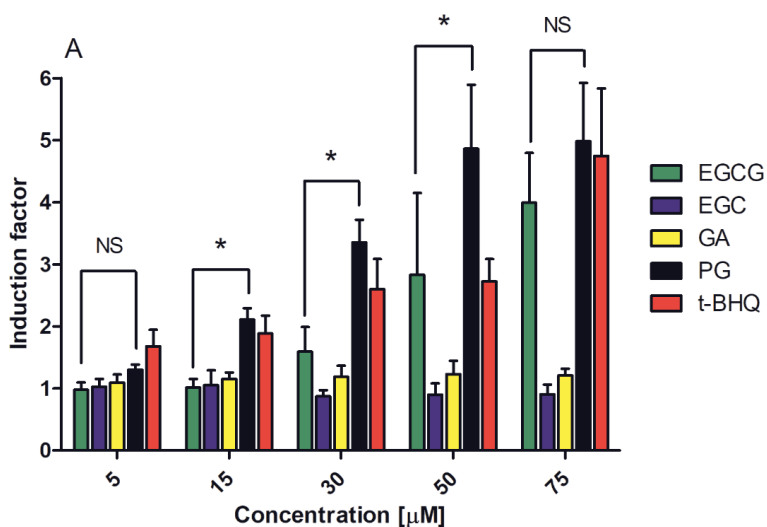
Figure 1. Induction of luciferase activity in U2OS-Nrf2 CALUX reporter cells (A) and in U2OS-Cytotox CALUX cells (B) after 24 h exposure to EGCG, EGC, GA, PG and t-BHQ. The results are presented as mean ± SEM compared to solvent control, derived from at least three independent experiments. Two-way ANOVA with Bonferroni multiple comparisons were performed to evaluate Nrf2 induction factors induced by EGCG and PG at various concentrations. Statistical differences between different treatments are demonstrated (*, $P < 0.05$). NS, not significant.

3.2 Nrf2-related protein expression in Hepa1c1c7 cells

Based on the results from Fig. 1A, at 30 µM both PG and t-BHQ were able to induce an induction that was substantially above the 2-fold threshold which was considered as a positive response in the U2OS-Nrf2 CALUX reporter gene assay. Therefore, to further study the changes of Nrf2-associated gene expression 30 µM was selected as the concentration tested in the proteomics study. In total, 3973 proteins were detected in all samples and their fold changes (FCs) compared to solvent control were calculated (Table S1). Furthermore, a manual selection of literature reported Nrf2-related proteins provided a list of 97 proteins (Table S2). The FCs for these 97 proteins were used as input for a PCA and clustering analysis. The PCA explained 63.9% of the variation in the protein profiles with PC1 and PC2 (Fig. 2A). PC1 accounted for a major part of the variation (48.0%) in the dataset, where PC2 captured 15.9% of the overall variation. On the PCA plot, EGCG, EGC, GA and control groups locate close to one another, indicating the inactivity of EGCG, EGC and GA in activating Nrf2 mediated protein expression at 30 µM. In contrast, PG and t-BHQ treatments separated far away from the controls and the other treatments in the PCA graph, suggesting, that these two treatments caused differential changes in the expression levels of Nrf2-related proteins. The hierarchic clustering of the treatments based on the protein dataset was visualized by a heat map (Fig. 2B). In agreement with the results of the PCA analysis, the PG and t-BHQ treatments separate from the EGCG, EGC, GA and control groups. This is mainly due to the upregulation of proteins in both the PG and t-BHQ treatments in contrast to the non-activation in the other treatments. These upregulated proteins are presented in red colour in the heatmap in Fig. 2B. For instance, the FCs of Aldehyde dehydrogenase family 3, subfamily A1 (Aldh3a1, protein ID: P47739) in PG and t-BHQ treatments are 1.9 ($p < 0.001$) and 2.5 ($p < 0.001$) respectively, while they are 1.0 (all not significant) in the other groups. The FCs of NAD(P)H dehydrogenase [quinone] 1 (Nqo1, protein ID: Q64669) in PG and t-BHQ treatments were 3.1 ($p < 0.05$) and 4.3 ($p < 0.05$),

respectively, while ranging from 0.9 to 1.1 (all not significant) in EGCG, EGC, GA treated and control groups.
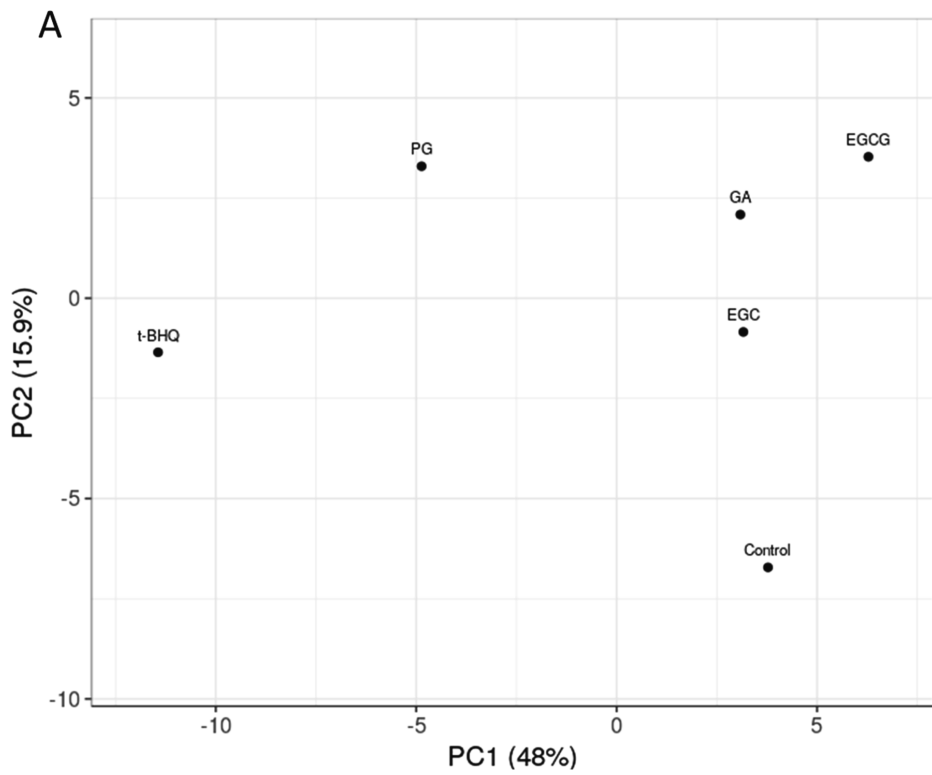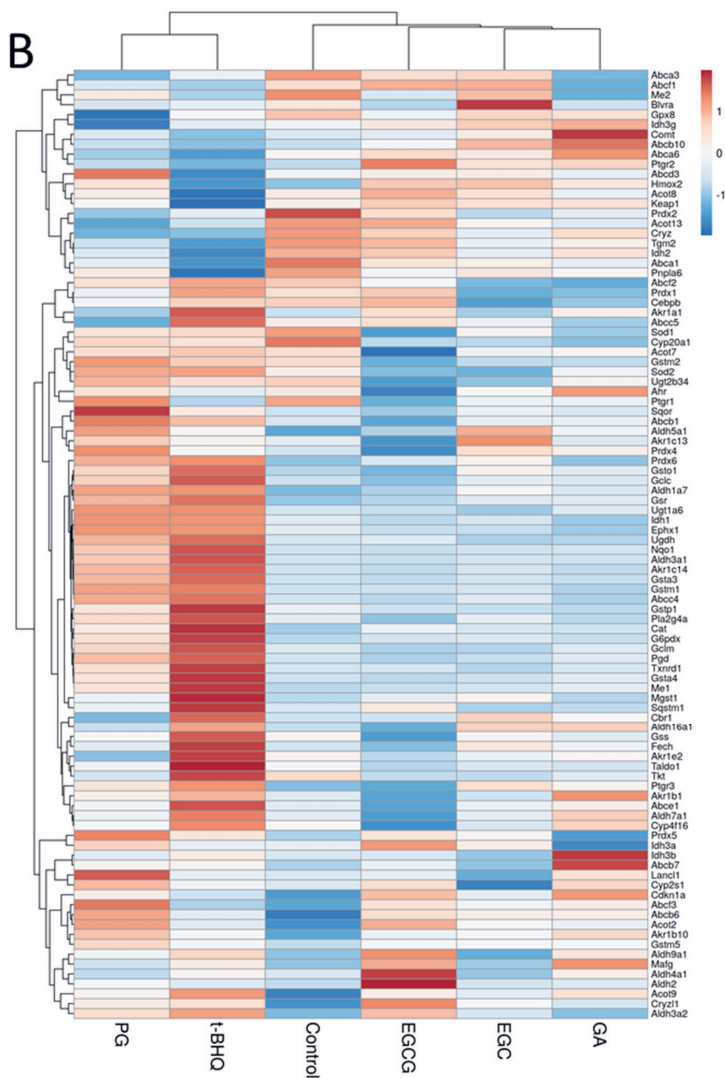
Figure 2. PCA (A) and heatmap (B) based on the FCs of 97 Nrf2-related proteins in different treatments of Hepa1c1c7 cells.

3.3 Differentially expressed proteins (DEPs) and functional enrichment analysis

By comparing the treated groups with the solvent control group, a total of number of 213, 151, 180 and 227 DEPs were identified for EGCG, EGC, GA and PG treatments (Fig. 3A). As the Nrf2-activator, t-BHQ treatment had the highest number of DEPs, which was 419 including 161 up-regulated and 258 down-regulated DEPs. EGCG treatment resulted in 93 up-regulated

and 120 down-regulated DEPs, EGC treatment resulted in 72 up-regulated and 79 down-regulated DEPs, GA treatment resulted in 93 up-regulated and 87 down-regulated DEPs, and PG treatment had 103 up-regulated and 124 down-regulated DEPs. Subsequently, GO enrichment and KEGG pathway enrichment analyses were performed for DEPs detected in different treatments. The GO enrichment analysis consisted of three parts: biological process (BP), molecular function (MF) and cellular components (CC). The enrichment results of the three parts were plotted as bubble charts where the x-axis presents the fold enrichment and the y-axis the $-\log_{10}$ (P-value) of different annotations. The size of the circles positively correlates with the number of DEPs that falls into the term (Fig. S2). In line with results presented in Fig. 2, Nrf2-associated terms were only enriched in PG and t-BHQ treated cells. For instance, glutathione metabolic process, and oxidation-reduction process were both observed upon PG and t-BHQ treatments in terms of BP. Oxidoreductase activity, and glutathione binding were both obtained in PG and t-BHQ treatments for MF (Fig. S2). Furthermore, KEGG pathway analysis enables the better understanding of the relationship among different DEPs (Fig. S3 and Fig. 3B, C). Fig. 3B and Fig. 3C present the top 10 most significantly enriched KEGG terms in PG and t-BHQ treated cells, respectively. Glutathione metabolism is the term that was enriched most significantly in both treatments. Moreover, Metabolism of xenobiotics by cytochrome P450 and Drug metabolism – cytochrome P450, which are the 2nd and 3rd significant pathways enriched in PG treatment, were also found in t-BHQ treated cells. These findings suggest that PG and t-BHQ shared some common characteristics regarding the glutathione synthesis or metabolism which are the vital consequence of Nrf2 activation. While other tested compounds at 30 µM were not able to trigger biological process and pathways that are critical to Nrf2 signalling.
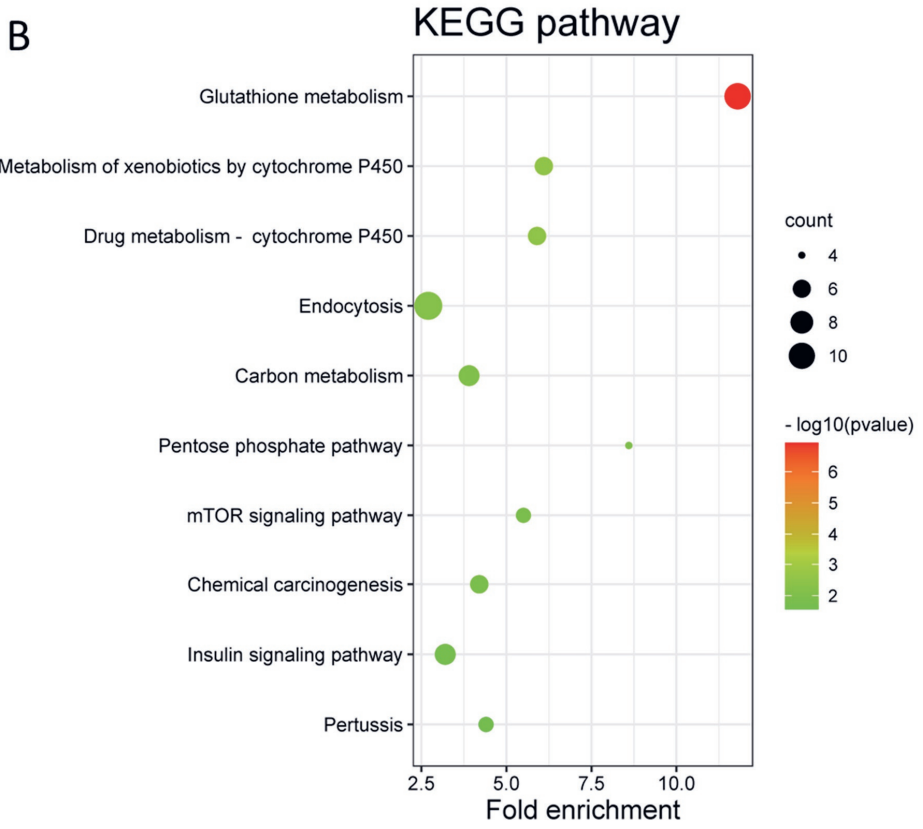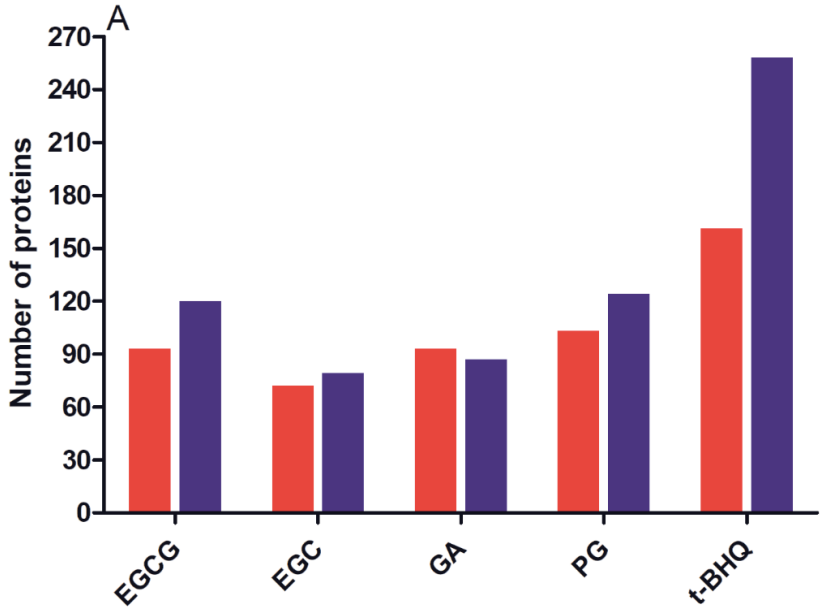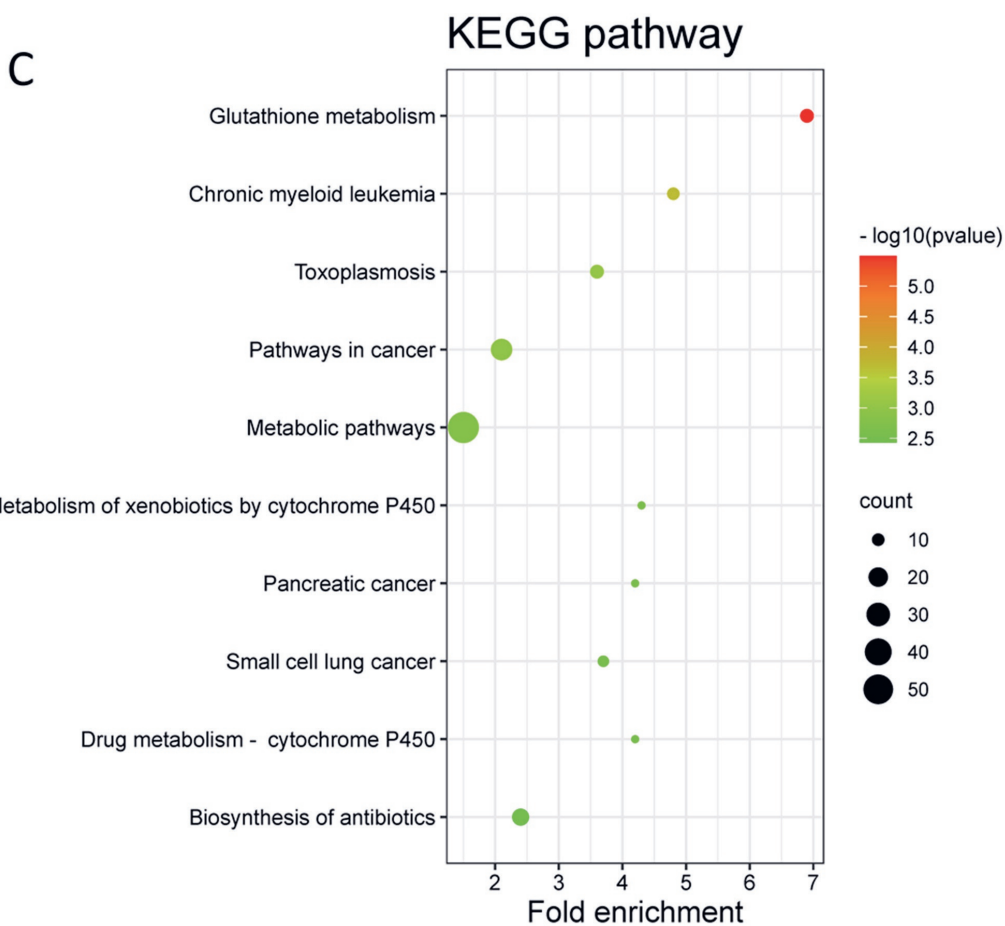
Figure 3. Numbers of DEPs derived from different treatments compared with the solvent control (A). Red and blue bars represent up- and down-regulating, respectively. KEGG pathway enrichment analysis of DEPs for Hepa1c1c7 cells treated with 30 µM of PG (B) and t-BHQ (C). Only top 10 enriched terms were plotted on the graphs and the complete results of enrichment analysis can be found in Table S3 in Supplementary materials.

3.4 Protein-protein interaction (PPI) network analysis

Fig. 4 shows the results of the PPI network analysis for the PG and t-BHQ treatments. PPI results of the other treatments can be found in Fig. S4 in the Supplementary materials. The PPI interaction network of the PG treatment comprises 175 nodes and 443 edges (Fig. 4A).

Meanwhile, as more DEPs were enriched after t-BHQ treatment, the PPI interaction network of t-BHQ treatment resulted in 375 nodes and 1787 edges (Fig. 4C). To further visualize the essential proteins among the complex PPI networks, the hub protein networks were produced via the MCODE plugin in the Cytoscape software. Several hub proteins were detected in both PG and t-BHQ PPI networks. These hub protein networks are ranked according to their network scores which are calculated by algorithms of MCODE. The analysis revealed that nine out of ten nodes from the top one hub protein network of the PG treatment (Fig. 4B) were also found in the second high-scored hub protein network of the t-BHQ treatment (Fig. 4D), and all of these hub proteins are Nrf2-asscociated proteins. Specifically, 10 nodes (Gclc, Gstm1, Gpx8, Gsr, Gsta3, Gsta4, Gstp1, Cryz, Gsto1 and Nqo1) connected by 42 edges are depicted in the PG hub protein network (Fig. 4B). 15 nodes (Gclc, Gstm1, Gsr, Gsta3, Gsta4, Gstp1, Cryz, Gsto1, Nqo1, Gss, Txnrd1, Aldh3a, Mgst1, Cyp1a1 and Cat) connected by 85 edges are presented in the t-BHQ hub protein network depicted in Fig. 4D. These data suggest that the Nrf2 signalling activation is an important response following exposure to PG or t-BHQ.
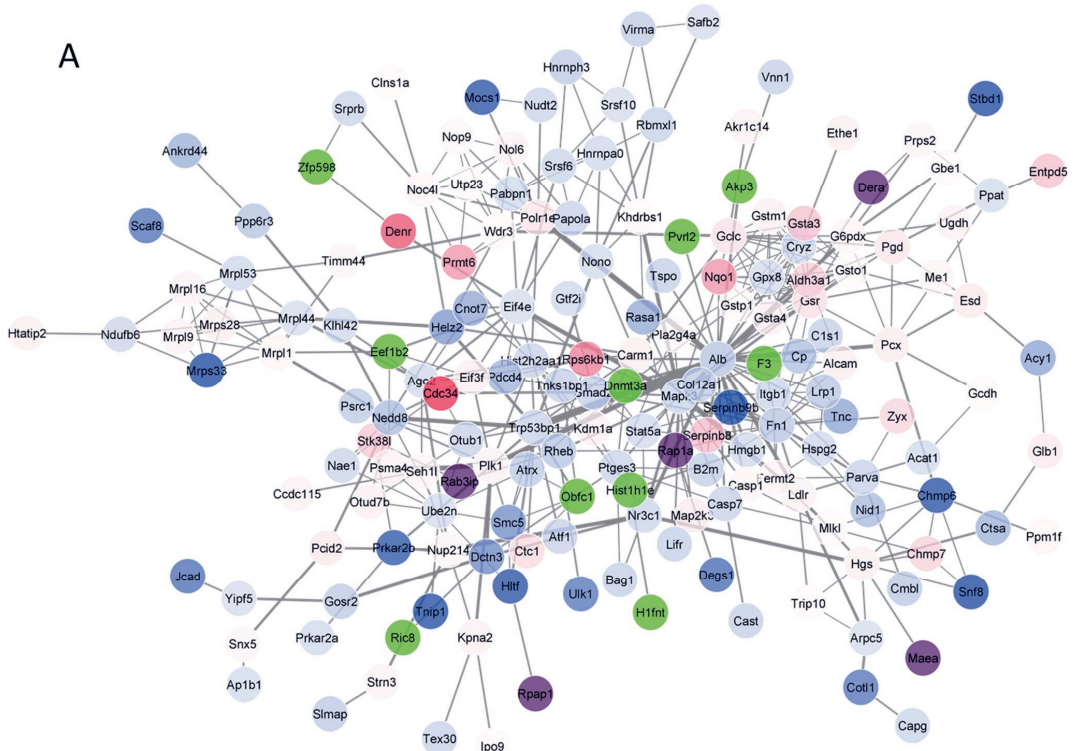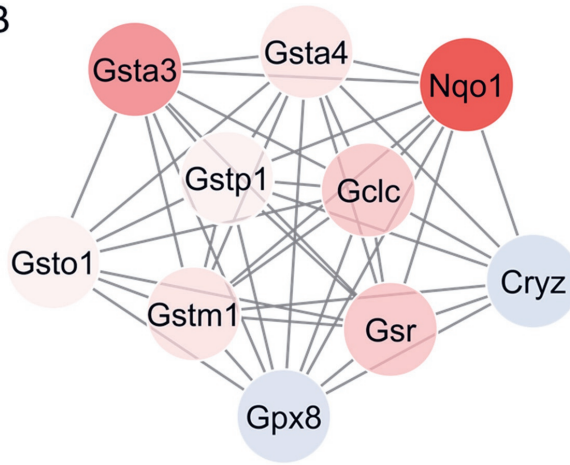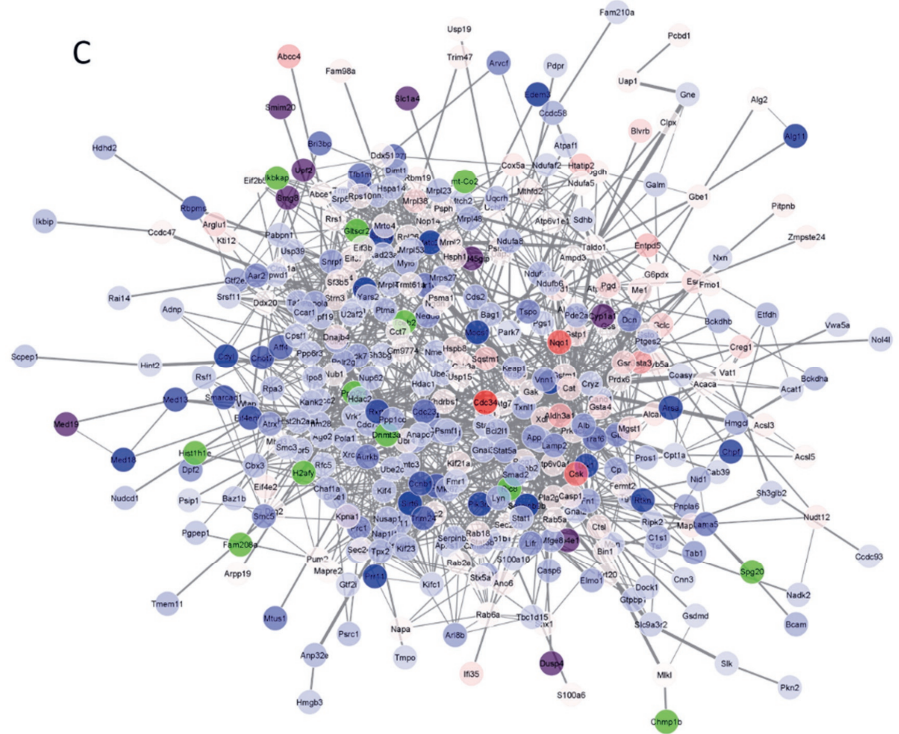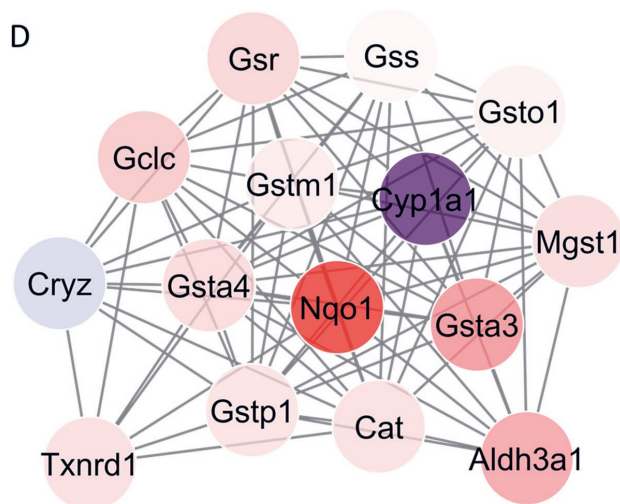
Figure 4. Protein-protein interaction (PPI) of DEPs for the PG (A) and t-BHQ (C) treatments and hub proteins derived from the PPI of the PG (B) and t-BHQ (D) treatments. The colour indicates the expression level of DEPs, with red indicating up-regulation, and blue indicating down-regulation (green coloured proteins were not in the DEPs but interacting with some of the DEPs, purple coloured proteins were highly induced proteins with an FC > 7) The widths of the edges are positively correlated with Edge Betweennesses.

3.5 A further analysis of "target" proteins from PG and t-BHQ treatments

Since the same KEGG terms (Glutathione metabolism, Metabolism of xenobiotics by cytochrome P450 and Drug metabolism - cytochrome P450) were enriched both in PG and t-BHQ treatments and given that the hub proteins were all Nrf2-related proteins, these proteins, together with their gene names and FCs were summarized in Table S4. In total, 22 proteins were obtained. In the EGCG, EGC and GA treatments all these proteins remained unchanged with protein intensity FCs ranging from 0.8 to 1.2. However, their FCs range from 0.8 to 3.1 in the PG group and from 0.8 to 4.3 in the t-BHQ group. PCA and hierarchic clustering analysis were processed based on the FCs of the 22 proteins in different treatments of Hepa1c1c7 cells. The PCA explained a total of 94.0% of the variation in the protein dataset with two PCs (PC1 and PC2) (Fig. S5A). The PC1 accounts for a majority of the total variation (85.2%) in the dataset, where the PC2 captures only 8.8% of the overall variation. From the PCA plot, it follows that the EGCG, EGC, GA and control groups are close to each other while the PG treatment are separated far from them and the t-BHQ group locates even further away.

Meanwhile, on the heatmap (Fig. S5B), almost all proteins were up-regulated in the PG and t-BHQ groups (except quinone oxidoreductase and probable glutathione peroxidase 8 in both groups and cytochrome P450 1A1 in the PG group) in contrast to the responses observed for all the proteins in the other exposure groups. This difference makes that the PG and t-BHQ groups cluster together while all other groups are in another cluster. The findings here are in line with the analysis for the 97 Nrf2-related proteins in section 3.3 but also show a more vivid contrast between the PG, t-BHQ treatments and the other groups. Taken all together, the results reveal that at moderate concentrations, EGCG is not potent enough to trigger the Nrf2 signalling while its microbial metabolite, PG, seems able to activate the cascade in Hepa1c1c7 cells.

3.6 RT-qPCR analysis

To further corroborate the effects of PG, the Nrf2-mediated gene expression was investigated by RT-qPCR. Four well-known Nrf2-regulated genes were selected.[12, 23] Their corresponding protein names, protein IDs and protein intensity FCs can be found in the Tables S2 or S4. The RT-qPCR results are presented in Fig. 5 and are well in line with the proteomics data. Only PG and t-BHQ exposed Hepa1c1c7 cells showed up-regulated (1.5 – 10.2 folds) gene expressions for all four genes while gene expressions in the EGCG, EGC or GA exposed cells were not affected (< 1.5 folds) compared to the solvent control (Fig. 5). Although proteomics results and RT-qPCR results share increased gene and protein expression characteristics, it is worth to mention that relative RNA levels not always exactly align with the respective protein levels from proteomics results in terms of the fold changes observed. For example, the relative RNA level of Gsta3 was 10.2 (Fig. 5B) while the FC of glutathione S-transferase A3 (the corresponding protein) amounted to 2.7. This can be due to, for example, saturation in mRNA translation efficiency and/or post-translational modifications via miRNAs, etc. Nevertheless, both our proteomics and RT-qPCR results corroborate the hypothesis that the microbial metabolite, PG, was more potent in inducing Nrf2 signalling compared to the parent compound EGCG.
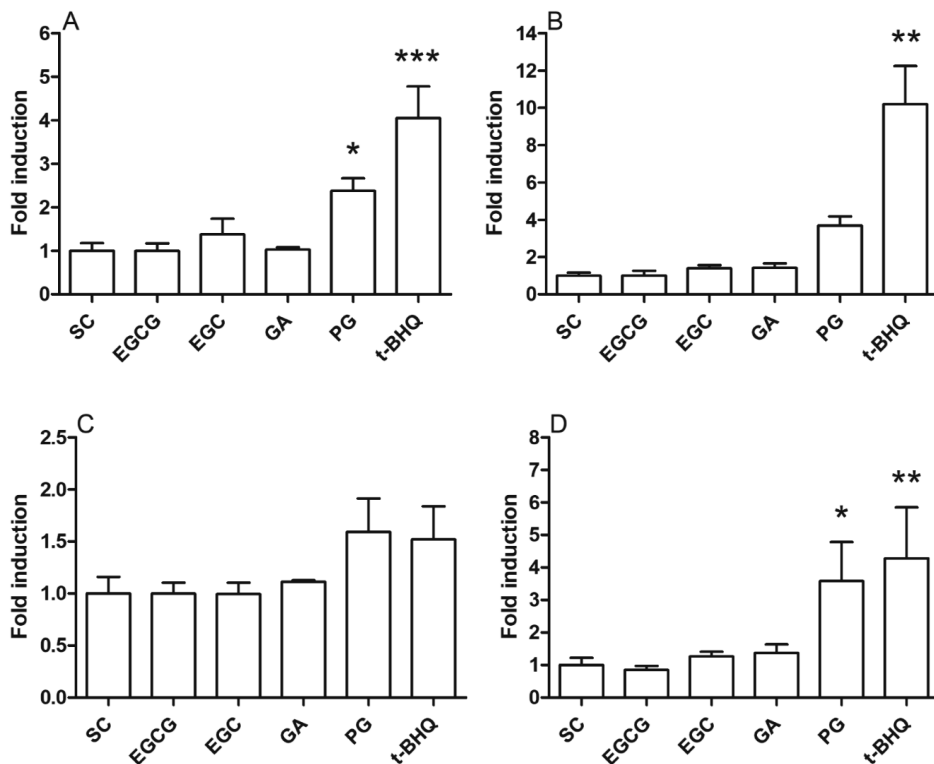
Figure 5. Relative RNA levels in Hepa1c1c7 cells after exposure to the selected model compounds at 30 µM. Graphs A to D each represents the results for one gene. A: Nqo1; B: Gsta3; C: Gclc; D: Ugt1a6. The results were calculated relative to solvent control (SC) and are presented as mean ± SEM, derived from four independent experiments. One-way ANOVA with Bonferroni post-test was performed. Statistical significances compared to SC are indicated by asterisk(s) (*, $0.01 < P < 0.05$; **, $0.001 < P < 0.01$, ***, $0.0001 < P < 0.001$).

4. Discussion

Employing an Nrf2 reporter gene assay, RT-qPCR and label-free quantitative proteomics, our current study characterized the differences between EGCG, and its microbial metabolites EGC, GA and PG in inducing Nrf2-mediated gene expression both at the transcriptional and translational level. The results indicate that both the parent compound EGCG and especially its catechol moiety containing metabolite PG are able to induce Nrf2-mediated gene expression.

However, at the micromolar exposure concentration, especially PG rather than EGCG appeared able to alter Nrf2-related gene expression.

EGCG is one of the most popular polyphenols that is intensively investigated by numerous researchers due to its versatile pharmacological benefits. It accounts for more than 50% of the total catechin content in green tea.[35] As other flavonoids, EGCG has a molecular structure comprised of two phenyl rings (A ring and B ring) which are connected by a heterocyclic ring (C ring). In addition, a galloyl moiety connects to the C ring in the 3-position which is known as the D ring of EGCG. Therefore, EGCG has the highest number of (eight) free hydroxy groups compared to other catechins, which is often considered as the reason for its potent bioactivities.[3, 36] For example, Dey and co-workers found EGCG being superior to (+)-catechin in alleviating high fat diet-induced nonalcoholic steatohepatitis in C57BL/6J mice at the same dose level.[37] The estimated concentration (336 µM) of EGCG in the large intestinal lumen appears an order of magnitude higher than concentrations of EGCG already inducing Nrf2 mediated enzyme activity. This corroborates that EGCG will activate Nrf2 activation especially in the intestine. The order of magnitude difference in the estimated and active concentration even leaves room for processes like diffusion through the mucus layer or binding of EGCG to intestinal content that may result in the actual concentration at the enterocytes to be lower than the 336 µM calculated based on the dose level and the intestinal volume. Interestingly, in the present study, we revealed that PG, which is one of the major microbial metabolites formed from EGCG both in in vitro and in vivo studies,[6, 21] exhibits a more potent ability in inducing the Nrf2 signalling pathway. It has been recognized that the parent compound EGCG possesses very limited transepithelial absorption and transport and obvious efflux is rather mediated by multidrug resistance proteins.[5, 38-39] Additionally, Grzesik and colleagues analysed the auto-oxidation of 54 dietary antioxidants. They found that both EGCG and PG could generate hydrogen peroxide in DMEM medium with PG being more potent than EGCG.[27] This might provide another explanation for the difference in the potency for Nrf2 mediated induction, since it suggests that the pro-oxidant activity, accompanied by the formation of ROS and reactive quinone metabolites, is more efficient with PG than EGCG. These products of pro-oxidant chemistry of the polyphenols, especially the ones with a catechol type moiety,[13, 18-19, 36] could either directly react with cysteine residues of Keap1 causing the dissociation of Nrf2 or conjugate with reduced GSH thereby leading to cellular oxidative stress and an indirect triggering of Nrf2 pathway activation.[13, 40]

It is worth to note that the blood concentrations of EGCG in human volunteers were reported to range between sub-micromolar to less than 10 μM upon intake of EGCG, EGCG-containing supplements or green tea.[41-44] Literature also reports PG conjugates in plasma reaching 2.6 μM after drinking black tea.[24] To what extent these conjugated forms will be deconjugated within tissues remains to be elucidated. Nevertheless, it is concluded from a comparison of these in vivo concentrations to the concentration response data of the present study that in vivo Nrf2-mediated gene expression may occur in the intestinal tissue while being less likely at the systemic concentrations of EGCG and PG reported so far. Thus, the systemic health benefits of EGCG may arise from other Nrf2-independent modes of action. For instance, Li and colleagues conducted a study on protective effects of catechin-rich green tea extract (GTE) against high fat diet-induced nonalcoholic steatohepatitis in wild-type and Nrf2-knock-out mice.[45] They revealed that GTE reduced hepatic steatosis and injury and lowered mRNA expression of hepatic lipid uptake and lipogenic genes regardless of Nrf2 status. Additionally, GTE also lowered NFκB phosphorylation and TNF-α and MCP1 mRNA levels in Nrf2-knock-out mice. Thus, the authors concluded that anti-inflammatory and hypolipidemic activities of GTE during nonalcoholic steatohepatitis likely occur through an Nrf2-independent mechanism.[45] However, the concentrations of green tea catechins in the intestinal tract likely amount to higher levels compared to their systemic concentrations, and may reach levels that are able to exert local bioactivities. Local intestinal effects were also reported for GTE which was shown able to improve gut barrier function, increase gut microbial diversity and decrease the Firmicutes:Bacteroidetes ratio in high fat diet-fed mice.[46-47]

When EGCG is ingested, the ester bond that links the D ring is rapidly cleaved by intestinal microbiota which liberates GA from EGCG.[6] GA was inactive at all concentrations tested in the current study. However, it is worth to note that this compound was identified as an Nrf2 inducer in our previous work when the reporter gene assay was performed in the absence of L-ascorbic acid,[6] while all the exposure medium in the present study was with fresh-made 0.5 mM L-ascorbic acid. To check the difference, Nrf2 CALUX cells exposed to GA in the absence of L-ascorbic acid was conducted, and a concentration-dependent increase in luciferase expression was observed (Fig. S6 in Supplementary materials). The decision of including L-ascorbic acid for co-exposure in this study is not only due to the fact that the L-ascorbic acid is highly abundant in human plasma but also it is able to improve the stability of polyphenols.[26-27, 48]

Nrf2 is a master regulator that lies at the centre of the complex cellular regulatory network mediating a vast array of cytoprotective genes. While most research schemes focus on the role

of single or limited gene(s) or protein(s), such information cannot effectively reflect the molecular functional network as a whole picture. In the current study, with the help of proteome technics, we were able to monitor the differences in the expression levels of a substantial amount of proteins between control and different chemical exposed groups. Among EGCG and the metabolites tested, especially PG appeared able to induce significant changes of Nrf2-mediated gene expression at protein level. Glutathione metabolism, Metabolism of xenobiotics by cytochrome P450 and Drug metabolism-cytochrome P450, which are three well-accepted Nrf2-related pathways that are involved in cellular antioxidant and detoxification mechanisms, were the top three most significant altered pathways after 24 h of exposure to 30 μM PG. In the meantime, these three pathways were also among the top 10 most significantly enriched pathways observed upon treatment of the cells with the reference compound t-BHQ. These results support the theory that Nrf2 pathway activation regulates detoxication and antioxidant enzymes.[12, 15, 22-23] For example, the rate-limiting entities in glutathione biosynthesis, glutamate-cysteine ligase catalytic subunit (Gclc) and glutamate-cysteine ligase modifier subunit (Gclm), were up-regulated 1.6 and 2.3 fold after the PG treatment, and 1.9 and 3.5 fold after the t-BHQ treatment. Other thiol-reducing enzymes, e.g., thioredoxin reductase 1 (Txnrd1) were also positively regulated after PG or t-BHQ treatment.

When we further combined the proteins in the three pathways and those from the hub proteins of PG and t-BHQ treatments, a list of 22 common proteins was the result (Table S4). Though it has been estimated that over 200 proteins are Nrf2-mediated,[23] we conclude that stimulation of the Nrf2 pathway by different chemicals may result in different protein profile fingerprints. Secondly, most of the protein level changes in PG or t-BHQ treatments were relatively mild, with FCs smaller than 1.5. With only few exceptions, for example, Nqo1 which appeared to be the most up-regulated Nrf2-mediated protein both after PG and t-BHQ treatments, with an FC of 3.1 and 4.3, respectively. It is one of the major quinone reductases of mammalian cells and generally recognized as an extremely effective cellular detoxification enzyme which can catalyze the two-electron reduction of quinones to generate hydroquinones. In some cases, the hydroquinones are more stable and easier to be conjugated and excreted, thereby ameliorating endogenous perturbations.[49] Besides, Nqo1 can also exert its protective functions via for example generation of vitamin E and ubiquinone, and inhibition of 20S proteasomal degradation.[49-50] It is considered as the cellular redox switch which is able to ameliorate oxidative stress by multiple mechanisms.[49, 51]

The Nrf2 activation builds an interface between cellular redox and intermediary metabolism. It regulates the NADPH synthesis and utilization.[23, 52] This was corroborated by the results of the present study indicating that all the four reported NADPH generating enzymes (G6pdx, Pgd, Me1 and Idh1) were up-regulated after PG and t-BHQ treatments. NADPH can serve as the cofactor for various drug metabolizing and antioxidant enzymes, including Glutathione reductase (Gsr), Nqo1, Aldo-keto reductase (Akr), and many others.[53] NADPH is essential for them to exert their protective roles during stressed conditions. Another intermediary metabolism that has been demonstrated to be one of the major cellular regulators of redox homeostasis and biosynthesis is the pentose phosphate pathway (PPP), also known as pentose phosphate shunt.[54] This pathway was enriched only in PG and t-BHQ treatments, once again, suggesting the potent bioactivity of PG and t-BHQ in activation of the Nrf2 pathway. The up-regulated G6pdx and Pgd (due to Nrf2 activation) facilitate the oxidative branching of the PPP, therefore directing the carbon flux towards the PPP instead of glycolysis.[54] Importantly, the oxidative branch of the PPP is the primary contributor to the cytosolic NADPH generation in mammalian cells, playing a vital role in cellular detoxication and antioxidation.[55] Moreover, Nrf2 activation could also positively regulate the expression of Transketolase (Tkt) and Transaldolase (Taldo), two important enzymes in the nonoxidative branch of the PPP, thereby promoting the PPP.[23, 54] However, it is notable to mention that only in the t-BHQ treatment the Tkt and Taldo protein levels were increased in the current study. Lastly, other physiological pathways, e.g., the mTOR signaling pathway and the insulin signaling pathway were also significantly enriched after the PG treatment. Whether or how these pathways are involved in an Nrf2-mediated regulatory network is of interest to explore. Studies on illustrating potential crosstalk between those pathways and the Nrf2 pathway may shed light on the sophisticated mechanisms behind the observed health-related physiological effects.

In conclusion, this study revealed the different characteristics of EGCG, EGC, GA and PG in terms of their ability to activate Nrf2-mediated gene expression. By using proteomic technics, for the first time, we obtained an extended picture of protein changes after treatment of the cells with EGCG and its major microbial catechol moiety containing metabolites. It was shown that the microbial metabolite PG is more potent than its parent compound EGCG in inducing Nrf2 pathway activation. Certain intermediary metabolic pathways, e.g., glutathione metabolism, xenobiotics and drug metabolism and the PPP, which are positively regulated after Nrf2 pathway activation, may contribute to the cytoprotective functions of green tea polyphenols. Altogether, our results illustrate the pivotal role of intestinal microbial metabolites of EGCG in

inducing Nrf2-associated beneficial gene expression. This finding may contribute to the observed health-promoting effects which have previously been attributed to EGCG or green tea consumption.

Abbreviations: EGCG, (-)-epigallocatechin gallate; EGC, (-)-epigallocatechin; GA, gallic acid; PG, pyrogallol; t-BHQ, *tert*-butylhydroquinone; Keap1/Nrf2, Kelch-like ECH associating protein 1/nuclear factor erythroid 2-related factor 2; EpRE, electrophile responsive element; LC-TQ-MS, liquid chromatograph triple quadrupole mass spectrometry; GSTs, glutathione S-transferases; GRs, glutathione reductases; UGTs, UDP-glucuronosyltransferases; PCA, principle component analysis; KEGG, Kyoto Encyclopedia of Genes and Genomes; DEPs, differentially expressed proteins; PPI, protein-protein interaction; NEAA, non-essential amino acids; FBS, fetal bovine serum; PAC, protein aggregation capture; LFQ, label-free quantitation; FDR, false discovery rate; BP, Biological Process; CC, Cellular Component; MF, Molecular Function; Gclc, glutamate-cysteine ligase catalytic subunit; PPP, pentose phosphate pathway.

Acknowledgement

Author Contributions

C.L. and S.B. performed experiments. I.M.E provided technical support. C.L. and S.B. interpreted data. C.L. wrote the manuscript. I.M.C.M.R. designed the scope of the manuscript and revised the manuscript. All authors read and approved the final manuscript.

Conflict of interest

The authors declare that there is no conflict of interest.

5. References

1.   Kakutani, S.; Watanabe, H.; Murayama, N., Green tea intake and risks for dementia, Alzheimer's disease, mild cognitive impairment, and cognitive impairment: a systematic review. *Nutrients* **2019,** *11* (5), 1165.

2.   Cabrera, C.; Artacho, R.; Giménez, R., Beneficial effects of green tea—a review. *Journal of the American College of Nutrition* **2006,** *25* (2), 79-99.

3.   Gan, R.-Y.; Li, H.-B.; Sui, Z.-Q.; Corke, H., Absorption, metabolism, anti-cancer effect and molecular targets of epigallocatechin gallate (EGCG): An updated review. *Critical reviews in food science and nutrition* **2018,** *58* (6), 924-941.

4.   Lee, M.-J.; Maliakal, P.; Chen, L.; Meng, X.; Bondoc, F. Y.; Prabhu, S.; Lambert, G.; Mohr, S.; Yang, C. S., Pharmacokinetics of tea catechins after ingestion of green tea and (−)-epigallocatechin-3-gallate by humans: formation of different metabolites and individual variability. *Cancer Epidemiology and Prevention Biomarkers* **2002,** *11* (10), 1025-1032.

5.   Monagas, M.; Urpi-Sarda, M.; Sánchez-Patán, F.; Llorach, R.; Garrido, I.; Gómez-Cordovés, C.; Andres-Lacueva, C.; Bartolomé, B., Insights into the metabolism and microbial biotransformation of dietary flavan-3-ols and the bioactivity of their metabolites. *Food & function* **2010,** *1* (3), 233-253.

6.   Liu, C.; Vervoort, J.; van den Elzen, J.; Beekmann, K.; Baccaro, M.; de Haan, L.; Rietjens, I. M., Interindividual Differences in Human In Vitro Intestinal Microbial Conversion of Green Tea (‑)‑Epigallocatechin‑3‑O‑Gallate and Consequences for Activation of Nrf2 Mediated Gene Expression. *Molecular Nutrition & Food Research* **2021,** *65* (2), 2000934.

7.   Gross, G.; Jacobs, D. M.; Peters, S.; Possemiers, S.; van Duynhoven, J.; Vaughan, E. E.; Van de Wiele, T., In vitro bioconversion of polyphenols from black tea and red wine/grape juice by human intestinal microbiota displays strong interindividual variability. *Journal of agricultural and food chemistry* **2010,** *58* (18), 10236-10246.

8.   van Duynhoven, J.; van der Hooft, J. J.; van Dorsten, F. A.; Peters, S.; Foltz, M.; Gomez-Roldan, V.; Vervoort, J.; de Vos, R. C.; Jacobs, D. M., Rapid and sustained systemic circulation of conjugated gut microbial catabolites after single-dose black tea extract consumption. *Journal of proteome research* **2014,** *13* (5), 2668-2678.

9.   Liu, C.; Vervoort, J.; Beekmann, K.; Baccaro, M.; Kamelia, L.; Wesseling, S.; Rietjens, I. M., Interindividual differences in human intestinal microbial conversion of (−)-epicatechin to bioactive phenolic compounds. *Journal of agricultural and food chemistry* **2020,** *68* (48), 14168-14181.

10.   Kohri, T.; Matsumoto, N.; Yamakawa, M.; Suzuki, M.; Nanjo, F.; Hara, Y.; Oku, N., Metabolic fate of (−)-[4-3H] epigallocatechin gallate in rats after oral administration. *Journal of agricultural and food chemistry* **2001,** *49* (8), 4102-4112.

11.   Liu, Z.; de Bruijn, W. J.; Bruins, M. E.; Vincken, J.-P., Reciprocal interactions between epigallocatechin-3-gallate (EGCG) and human gut microbiota in vitro. *Journal of Agricultural and Food Chemistry* **2020,** *68* (36), 9804-9815.

12.   Yamamoto, M.; Kensler, T. W.; Motohashi, H., The KEAP1-NRF2 system: a thiol-based sensor-effector apparatus for maintaining redox homeostasis. *Physiological reviews* **2018,** *98* (3), 1169-1203.

13.   Muzolf-Panek, M.; Gliszczyńska-Świgło, A.; de Haan, L.; Aarts, J. M.; Szymusiak, H.; Vervoort, J. M.; Tyrakowska, B.; Rietjens, I. M., Role of catechin quinones in the induction of EpRE-mediated gene expression. *Chemical research in toxicology* **2008,** *21* (12), 2352-2360.

14.   Talebi, M.; Talebi, M.; Farkhondeh, T.; Mishra, G.; İlgün, S.; Samarghandian, S., New insights into the role of the Nrf2 signaling pathway in green tea catechin applications. *Phytotherapy Research* **2021**.

15.   He, F.; Ru, X.; Wen, T., NRF2, a transcription factor for stress response and beyond. *International journal of molecular sciences* **2020,** *21* (13), 4777.

16. Park, H. J.; DiNatale, D. A.; Chung, M.-Y.; Park, Y.-K.; Lee, J.-Y.; Koo, S. I.; O'Connor, M.; Manautou, J. E.; Bruno, R. S., Green tea extract attenuates hepatic steatosis by decreasing adipose lipogenesis and enhancing hepatic antioxidant defenses in ob/ob mice. *The Journal of nutritional biochemistry* **2011,** *22* (4), 393-400.

17. Park, H. J.; Lee, J.-Y.; Chung, M.-Y.; Park, Y.-K.; Bower, A. M.; Koo, S. I.; Giardina, C.; Bruno, R. S., Green tea extract suppresses NFκB activation and inflammatory responses in diet-induced obese rats with nonalcoholic steatohepatitis. *The Journal of nutrition* **2012,** *142* (1), 57-63.

18. Thavasi, V.; Leong, L. P.; Bettens, R. P. A., Investigation of the influence of hydroxy groups on the radical scavenging ability of polyphenols. *The journal of physical chemistry A* **2006,** *110* (14), 4918-4923.

19. Lee-Hilz, Y. Y.; Boerboom, A.-M. J.; Westphal, A. H.; van Berkel, W. J.; Aarts, J. M.; Rietjens, I. M., Pro-oxidant activity of flavonoids induces EpRE-mediated gene expression. *Chemical research in toxicology* **2006,** *19* (11), 1499-1505.

20. Yoshida, H.; Yamada, H., Microbial production of pyrogallol through decarboxylation of gallic acid. *Agricultural and biological chemistry* **1985,** *49* (3), 659-663.

21. van der Hooft, J. J.; de Vos, R. C.; Mihaleva, V.; Bino, R. J.; Ridder, L.; de Roo, N.; Jacobs, D. M.; van Duynhoven, J. P.; Vervoort, J., Structural elucidation and quantification of phenolic conjugates present in human urine after tea intake. *Analytical Chemistry* **2012,** *84* (16), 7263-7271.

22. Tonelli, C.; Chio, I. I. C.; Tuveson, D. A., Transcriptional regulation by Nrf2. *Antioxidants & redox signaling* **2018,** *29* (17), 1727-1745.

23. Hayes, J. D.; Dinkova-Kostova, A. T., The Nrf2 regulatory network provides an interface between redox and intermediary metabolism. *Trends in biochemical sciences* **2014,** *39* (4), 199-218.

24. van der Linden, S. C.; von Bergh, A. R.; van Vught-Lussenburg, B. M.; Jonker, L. R.; Teunis, M.; Krul, C. A.; van der Burg, B., Development of a panel of high-throughput reporter-gene assays to detect genotoxicity and oxidative stress. *Mutation Research/Genetic Toxicology and Environmental Mutagenesis* **2014,** *760*, 23-32.

25. Beekmann, K.; Rubió, L.; de Haan, L. H.; Actis-Goretta, L.; van der Burg, B.; van Bladeren, P. J.; Rietjens, I. M., The effect of quercetin and kaempferol aglycones and glucuronides on peroxisome proliferator-activated receptor-gamma (PPAR-γ). *Food & function* **2015,** *6* (4), 1098-1107.

26. Chen, L.; Wang, W.; Zhang, J.; Cui, H.; Ni, D.; Jiang, H., Dual effects of ascorbic acid on the stability of EGCG by the oxidation product dehydroascorbic acid promoting the oxidation and inhibiting the hydrolysis pathway. *Food Chemistry* **2021,** *337*, 127639.

27. Grzesik, M.; Bartosz, G.; Stefaniuk, I.; Pichla, M.; Namieśnik, J.; Sadowska-Bartosz, I., Dietary antioxidants as a source of hydrogen peroxide. *Food chemistry* **2019,** *278*, 692-699.

28. Wiechelman, K. J.; Braun, R. D.; Fitzpatrick, J. D., Investigation of the bicinchoninic acid protein assay: identification of the groups responsible for color formation. *Analytical biochemistry* **1988,** *175* (1), 231-237.

29. Batth, T. S.; Tollenaere, M. X.; Rüther, P.; Gonzalez-Franquesa, A.; Prabhakar, B. S.; Bekker-Jensen, S.; Deshmukh, A. S.; Olsen, J. V., Protein aggregation capture on microparticles enables multipurpose proteomics sample preparation. *Molecular & Cellular Proteomics* **2019,** *18* (5), 1027-1035.

30. Chun, K.-S.; Raut, P. K.; Kim, D.-H.; Surh, Y.-J., Role of chemopreventive phytochemicals in NRF2-mediated redox homeostasis in humans. *Free Radical Biology and Medicine* **2021,** *172*, 699-715.

31. Zhan, X.; Li, J.; Zhou, T., Targeting Nrf2-mediated oxidative stress response signaling pathways as new therapeutic strategy for pituitary adenomas. *Frontiers in Pharmacology* **2021,** *12*.

32. Stalmach, A.; Mullen, W.; Steiling, H.; Williamson, G.; Lean, M. E.; Crozier, A., Absorption, metabolism, and excretion of green tea flavan‐3‐ols in humans with an ileostomy. *Molecular nutrition & food research* **2010,** *54* (3), 323-334.

33. Roowi, S.; Stalmach, A.; Mullen, W.; Lean, M. E.; Edwards, C. A.; Crozier, A., Green tea flavan-3-ols: colonic degradation and urinary excretion of catabolites by humans. *Journal of agricultural and food chemistry* **2010,** *58* (2), 1296-1304.

34.   Brown, R. P.; Delp, M. D.; Lindstedt, S. L.; Rhomberg, L. R.; Beliles, R. P., Physiological parameter values for physiologically based pharmacokinetic models. *Toxicology and industrial health* **1997,** *13* (4), 407-484.

35.   Singh, B. N.; Shankar, S.; Srivastava, R. K., Green tea catechin, epigallocatechin-3-gallate (EGCG): mechanisms, perspectives and clinical applications. *Biochemical pharmacology* **2011,** *82* (12), 1807-1821.

36.   Cai, Y.-Z.; Sun, M.; Xing, J.; Luo, Q.; Corke, H., Structure–radical scavenging activity relationships of phenolic compounds from traditional Chinese medicinal plants. *Life sciences* **2006,** *78* (25), 2872-2888.

37.   Dey, P.; Olmstead, B. D.; Sasaki, G. Y.; Vodovotz, Y.; Yu, Z.; Bruno, R. S., Epigallocatechin gallate but not catechin prevents nonalcoholic steatohepatitis in mice similar to green tea extract while differentially affecting the gut microbiota. *The journal of nutritional biochemistry* **2020,** *84*, 108455.

38.   Zhang, L.; Zheng, Y.; Chow, M. S.; Zuo, Z., Investigation of intestinal absorption and disposition of green tea catechins by Caco-2 monolayer model. *International journal of pharmaceutics* **2004,** *287* (1-2), 1-12.

39.   Liu, Z.; Bruins, M. E.; Ni, L.; Vincken, J.-P., Green and black tea phenolics: Bioavailability, transformation by colonic microbiota, and modulation of colonic microbiota. *Journal of Agricultural and Food Chemistry* **2018,** *66* (32), 8469-8477.

40.   Na, H.-K.; Surh, Y.-J., Modulation of Nrf2-mediated antioxidant and detoxifying enzyme induction by the green tea polyphenol EGCG. *Food and Chemical Toxicology* **2008,** *46* (4), 1271-1278.

41.   Chow, H. S.; Cai, Y.; Alberts, D. S.; Hakim, I.; Dorr, R.; Shahi, F.; Crowell, J. A.; Yang, C. S.; Hara, Y., Phase I pharmacokinetic study of tea polyphenols following single-dose administration of epigallocatechin gallate and polyphenon E. *Cancer Epidemiology and Prevention Biomarkers* **2001,** *10* (1), 53-58.

42.   Naumovski, N.; Blades, B. L.; Roach, P. D., Food inhibits the oral bioavailability of the major green tea antioxidant epigallocatechin gallate in humans. *Antioxidants* **2015,** *4* (2), 373-393.

43.   Chow, H. S.; Cai, Y.; Hakim, I. A.; Crowell, J. A.; Shahi, F.; Brooks, C. A.; Dorr, R. T.; Hara, Y.; Alberts, D. S., Pharmacokinetics and safety of green tea polyphenols after multiple-dose administration of epigallocatechin gallate and polyphenon E in healthy individuals. *Clinical cancer research* **2003,** *9* (9), 3312-3319.

44.   Chow, H. S.; Hakim, I. A.; Vining, D. R.; Crowell, J. A.; Ranger-Moore, J.; Chew, W. M.; Celaya, C. A.; Rodney, S. R.; Hara, Y.; Alberts, D. S., Effects of dosing condition on the oral bioavailability of green tea catechins after single-dose administration of Polyphenon E in healthy individuals. *Clinical cancer research* **2005,** *11* (12), 4627-4633.

45.   Li, J.; Sapper, T. N.; Mah, E.; Rudraiah, S.; Schill, K. E.; Chitchumroonchokchai, C.; Moller, M. V.; McDonald, J. D.; Rohrer, P. R.; Manautou, J. E., Green tea extract provides extensive Nrf2‐independent protection against lipid accumulation and NFκB pro‐inflammatory responses during nonalcoholic steatohepatitis in mice fed a high‐fat diet. *Molecular nutrition & food research* **2016,** *60* (4), 858-870.

46.   Dey, P.; Sasaki, G. Y.; Wei, P.; Li, J.; Wang, L.; Zhu, J.; McTigue, D.; Yu, Z.; Bruno, R. S., Green tea extract prevents obesity in male mice by alleviating gut dysbiosis in association with improved intestinal barrier function that limits endotoxin translocation and adipose inflammation. *The journal of nutritional biochemistry* **2019,** *67*, 78-89.

47.   Hodges, J. K.; Sasaki, G. Y.; Bruno, R. S., Anti-inflammatory activities of green tea catechins along the gut–liver axis in nonalcoholic fatty liver disease: Lessons learned from preclinical and human studies. *The Journal of Nutritional Biochemistry* **2020,** *85*, 108478.

48.   Schwedhelm, E.; Maas, R.; Troost, R.; Böger, R. H., Clinical pharmacokinetics of antioxidants and their impact on systemic oxidative stress. *Clinical pharmacokinetics* **2003,** *42* (5), 437-459.

49.   Ross, D.; Siegel, D., The diverse functionality of NQO1 and its roles in redox control. *Redox Biology* **2021**, 101950.

50.   Ross, D.; Siegel, D., Functions of NQO1 in cellular protection and CoQ10 metabolism and its potential role as a redox sensitive molecular switch. *Frontiers in physiology* **2017,** *8*, 595.

Chapter 5

51. Dinkova-Kostova, A. T.; Talalay, P., NAD (P) H: quinone acceptor oxidoreductase 1 (NQO1), a multifunctional antioxidant enzyme and exceptionally versatile cytoprotector. *Archives of biochemistry and biophysics* **2010,** *501* (1), 116-123.

52. Wu, K. C.; Cui, J. Y.; Klaassen, C. D., Beneficial role of Nrf2 in regulating NADPH generation and consumption. *Toxicological Sciences* **2011,** *123* (2), 590-600.

53. Ju, H.-Q.; Lin, J.-F.; Tian, T.; Xie, D.; Xu, R.-H., NADPH homeostasis in cancer: Functions, mechanisms and therapeutic implications. *Signal transduction and targeted therapy* **2020,** *5* (1), 1-12.

54. Ge, T.; Yang, J.; Zhou, S.; Wang, Y.; Li, Y.; Tong, X., The role of the pentose phosphate pathway in diabetes and cancer. *Frontiers in Endocrinology* **2020,** *11*, 365.

55. Cho, E. S.; Cha, Y. H.; Kim, H. S.; Kim, N. H.; Yook, J. I., The pentose phosphate pathway as a potential target for cancer therapy. *Biomolecules & therapeutics* **2018,** *26* (1), 29.

Supporting Information
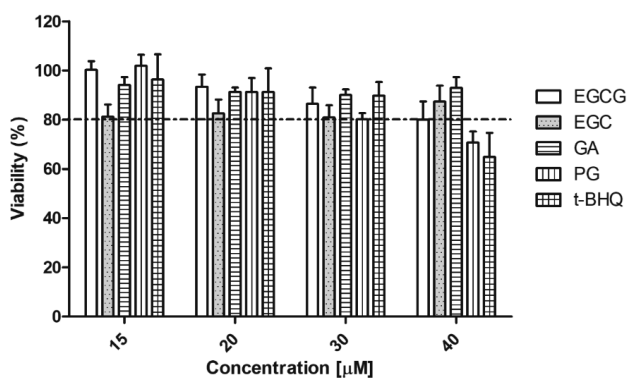
Figure S1. WST-1 assay in Hepa1c1c7 cells.

A

Biological process

B

Cellular component

Molecular function

Biological process

Cellular component

E

Molecular function

F
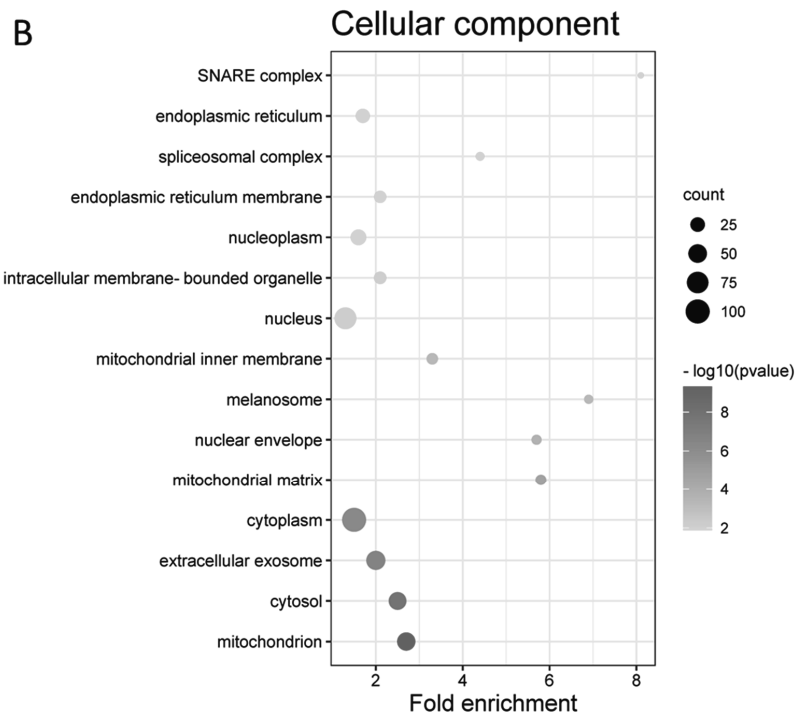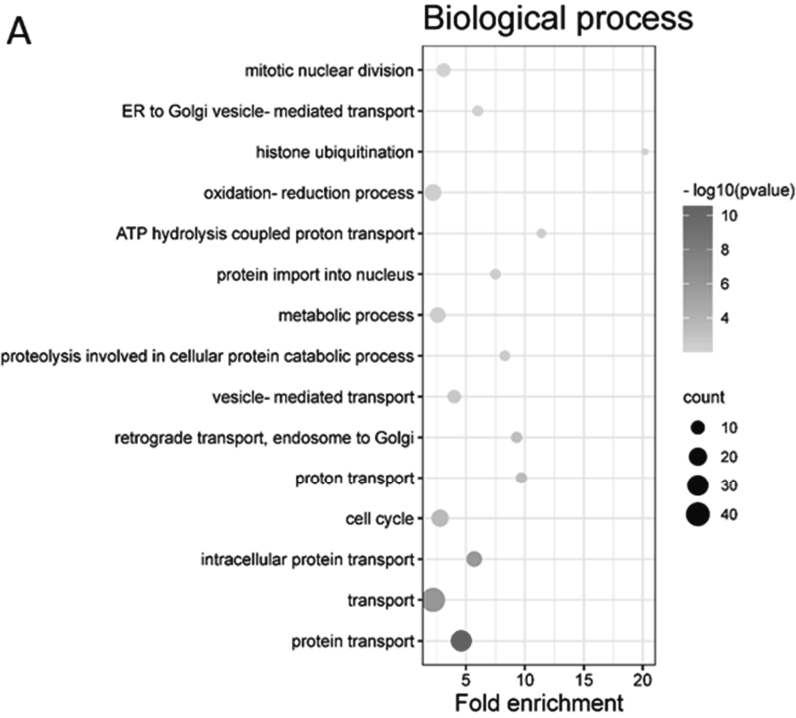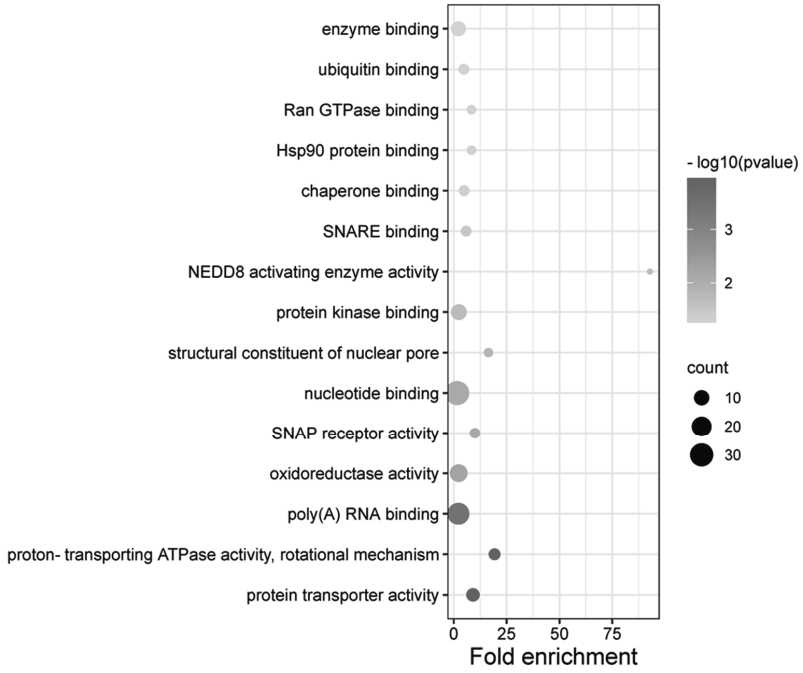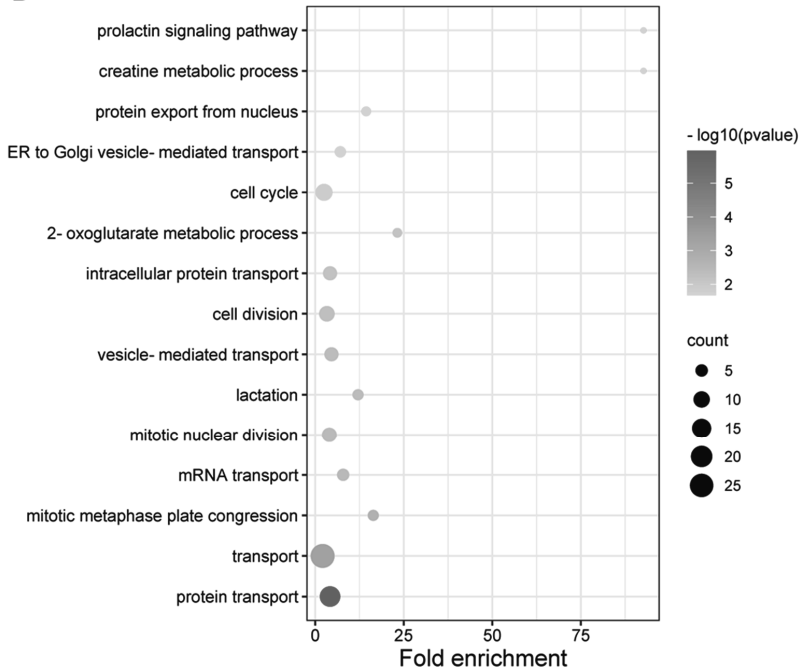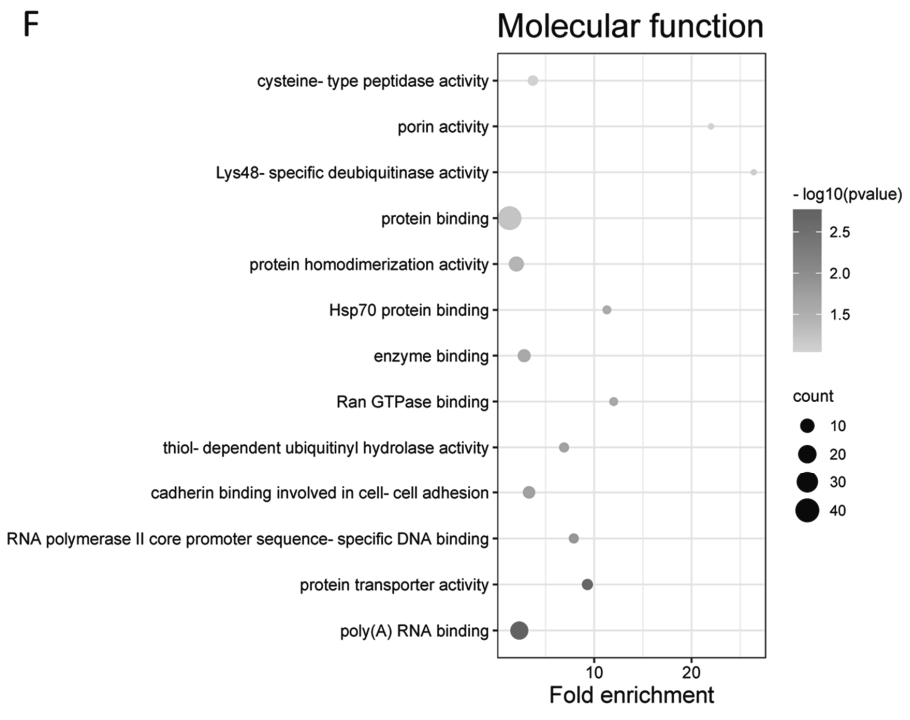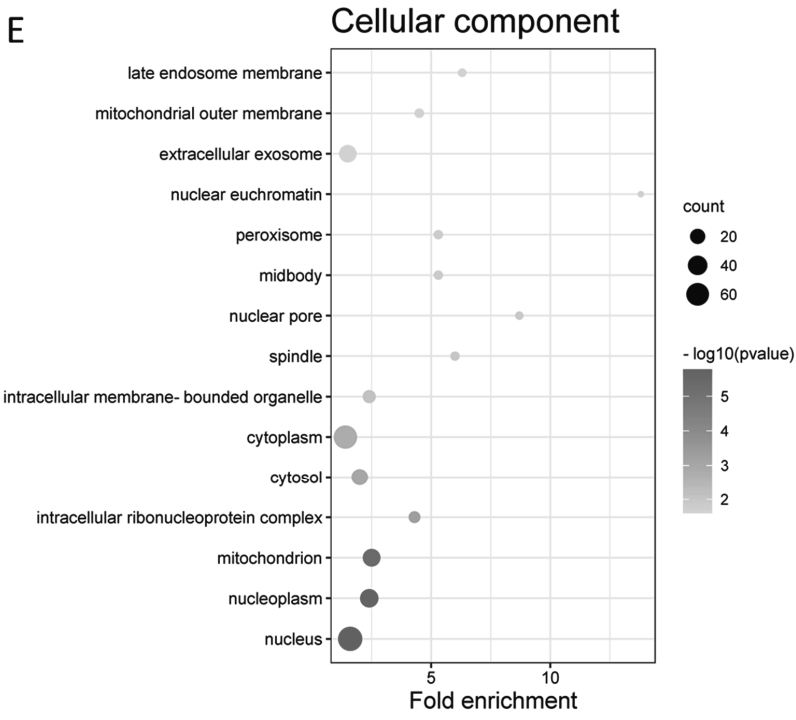
G Biological process

H Cellular component

Molecular function

Biological process

K
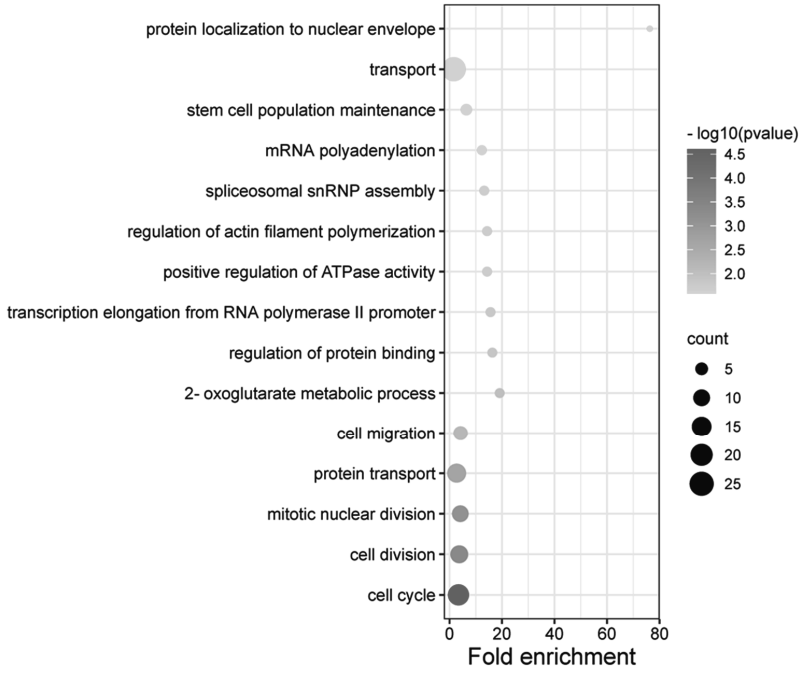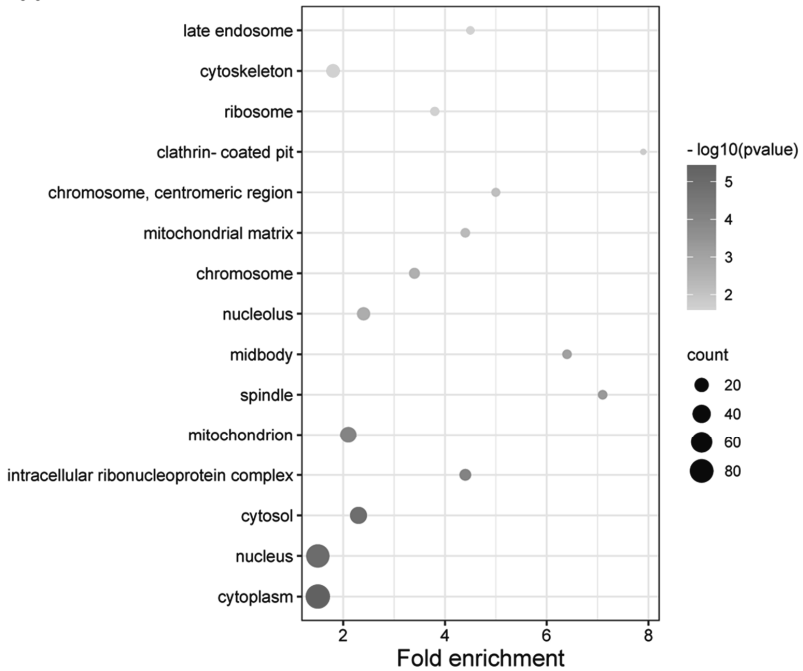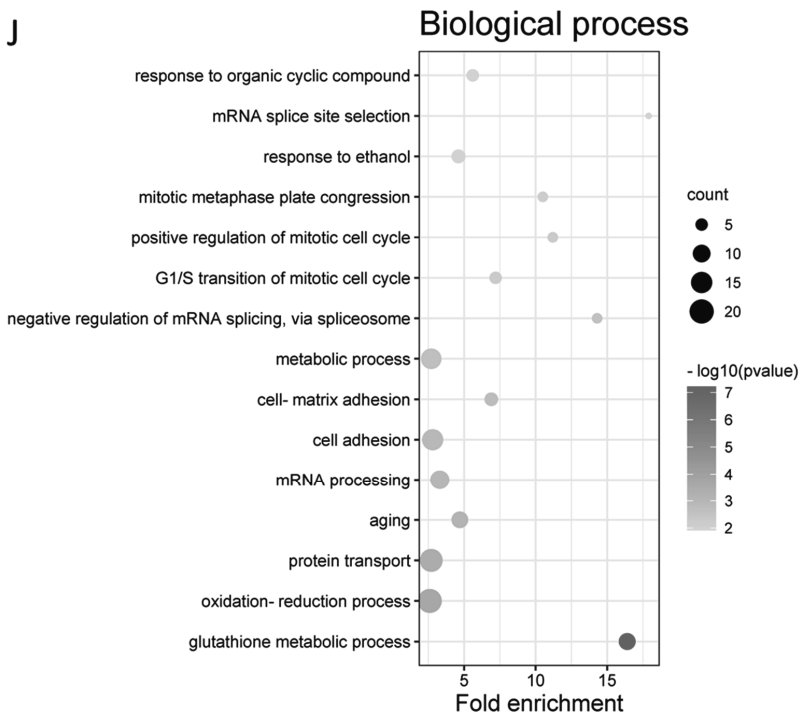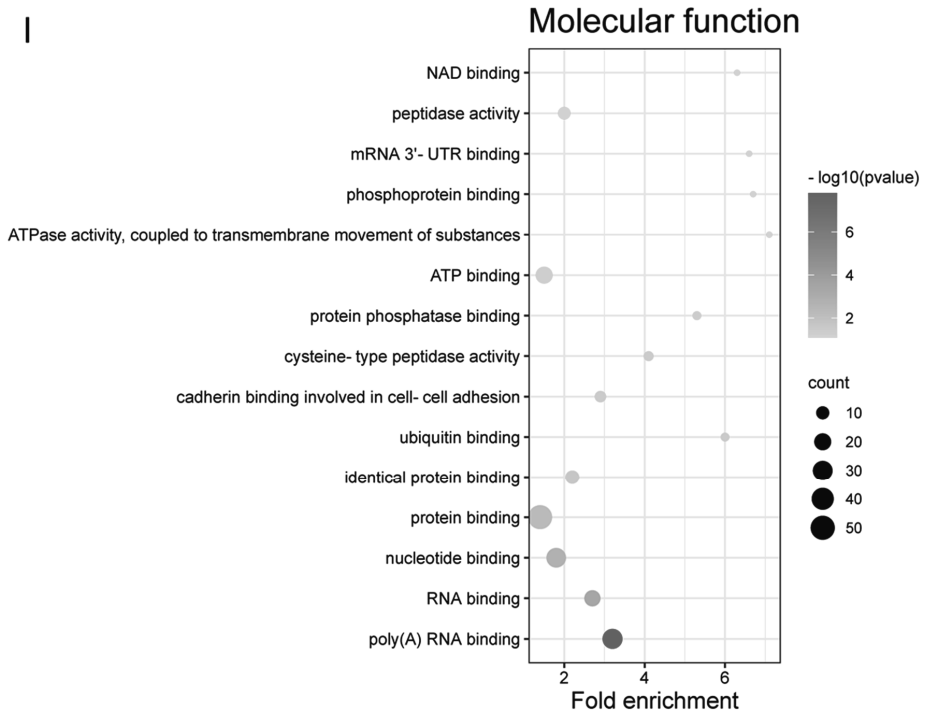
Cellular component
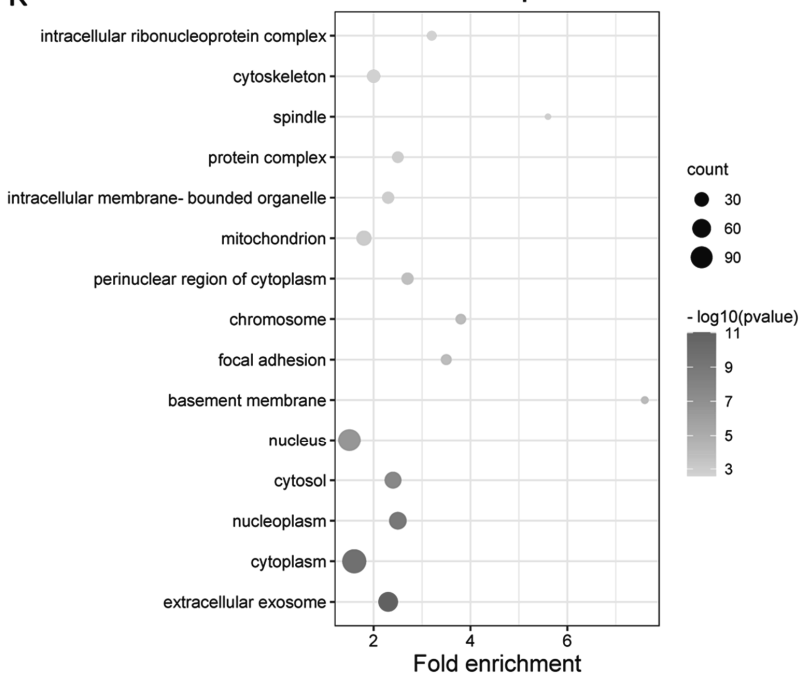
Fold enrichment

L

Molecular function
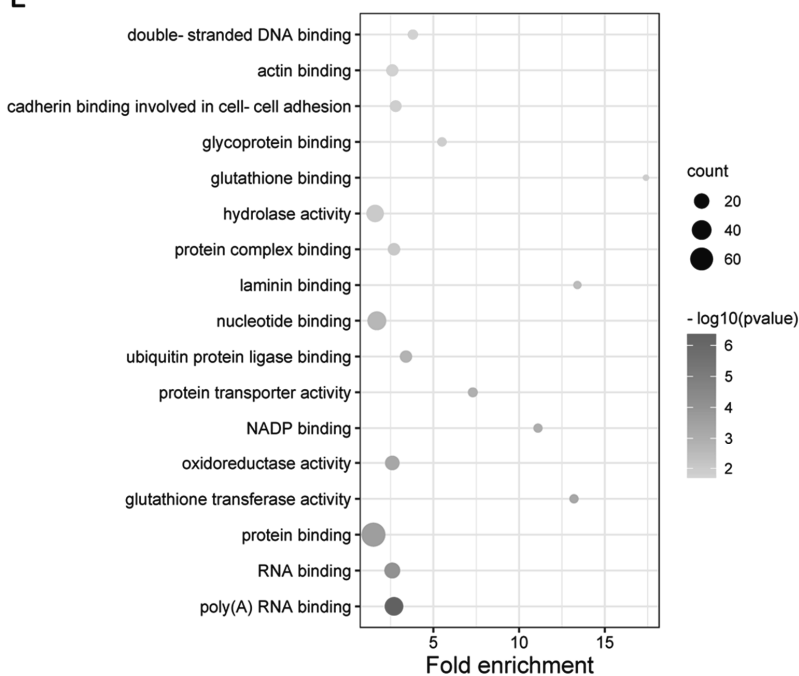
Fold enrichment

M

Biological process
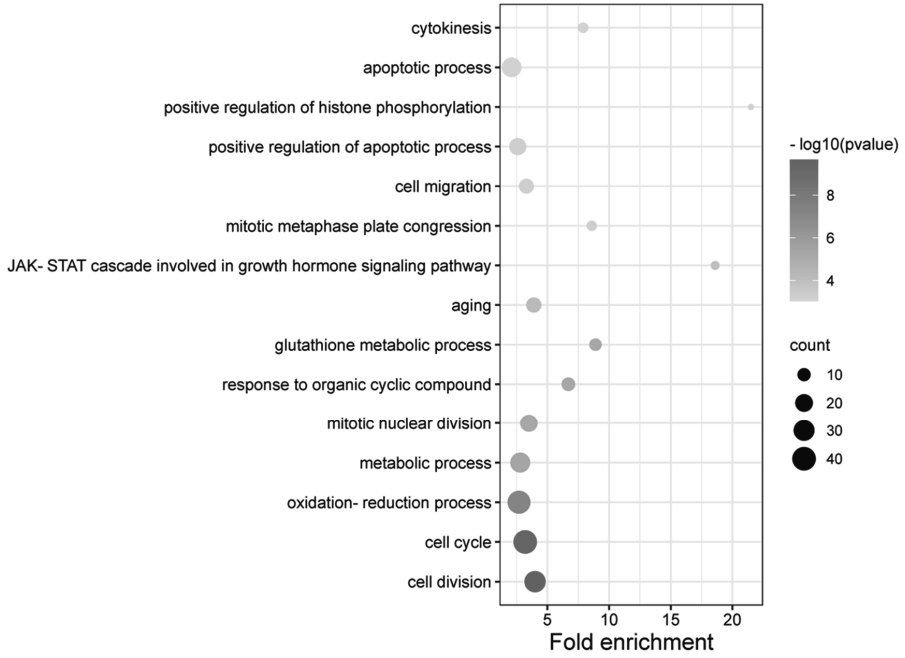
N

Cellular component
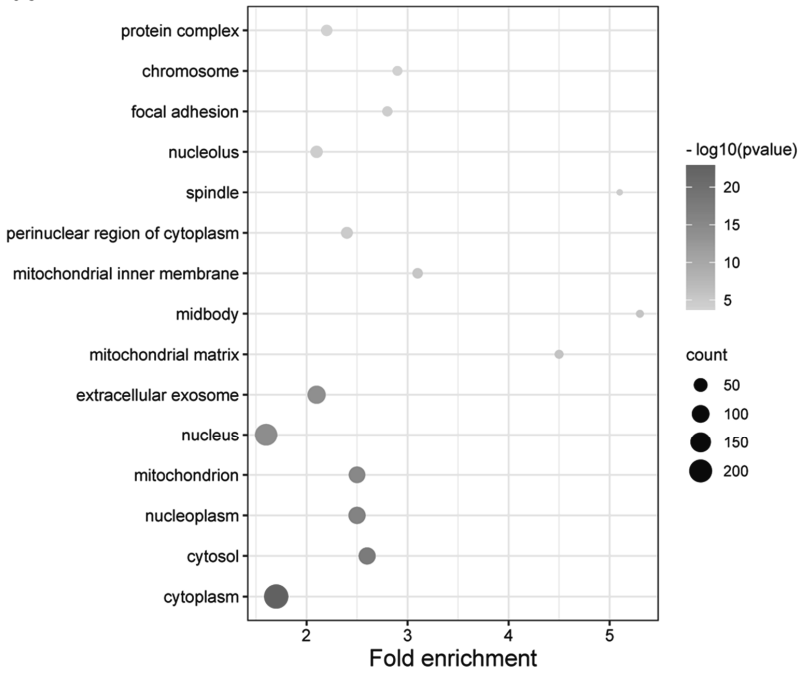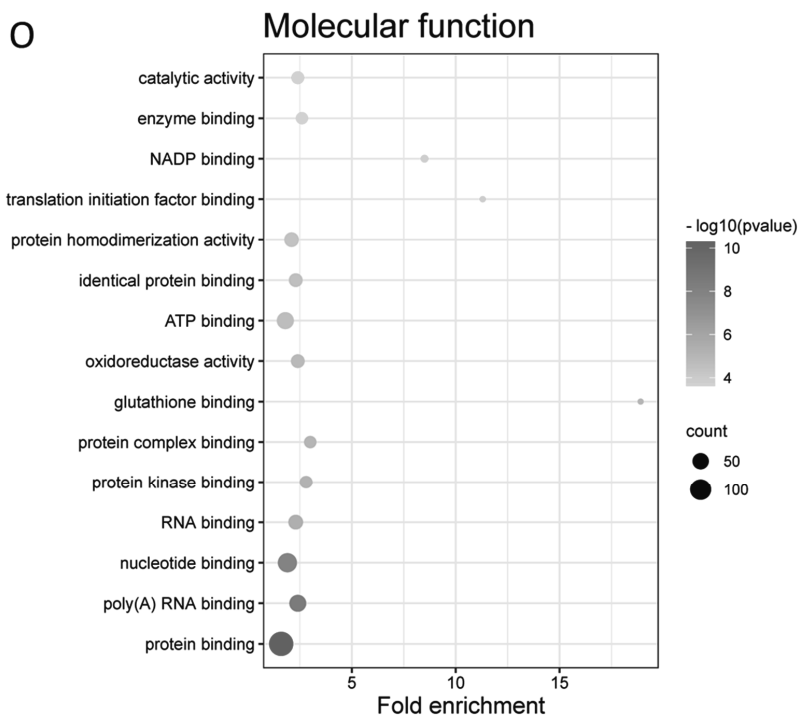
Figure S2. GO functional enrichment analysis of differentially expressed proteins (DEPs) from different treatments. Top 15 most significantly enriched terms of biological process (BP), cellular compartment (CC) or molecular function (MF) are included. A – C: EGCG treatment; D – F: EGC treatment; G – I: GA treatment; J – L: PG treatment; M – O: t-BHQ treatment.

KEGG pathway

A

Purine metabolism
Alzheimer's disease
Alanine, aspartate and glutamate metabolism
Lysosome
Phagosome
Endocytosis
Collecting duct acid secretion
Pyrimidine metabolism
Riboflavin metabolism
Tryptophan metabolism
SNARE interactions in vesicular transport
Synaptic vesicle cycle
Fatty acid degradation
Oxidative phosphorylation
Metabolic pathways

Fold enrichment

count
10
20
30

- log10(pvalue)
3
2

B

KEGG pathway

Metabolic pathways
Huntington's disease
HTLV- I infection
RNA transport
Peroxisome
Lysosome
Pyrimidine metabolism

Fold enrichment

- log10(pvalue)
2.00
1.75
1.50
1.25

count
4
6
8
10
12
14
16

Figure S3. KEGG pathway enrichment analysis of differentially expressed proteins (DEPs) from different treatments. A: EGCG treatment; B: EGC treatment; C: GA treatment.

A

B

195
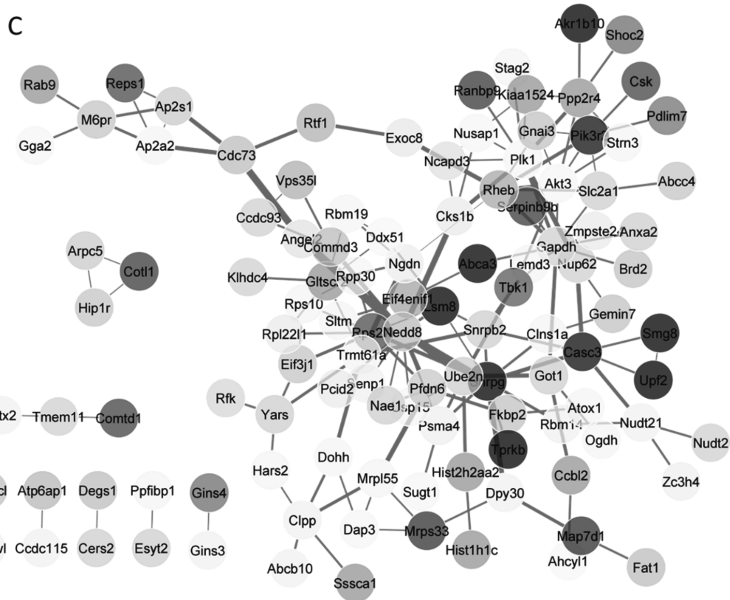
Figure S4. Protein-protein integration (PPI) of DEPs for the EGCG (A), EGC (B) and GA (C) treatments. The colour indicates the expression level of DEPs, with red indicating up-regulation, and blue indicating down-regulation.
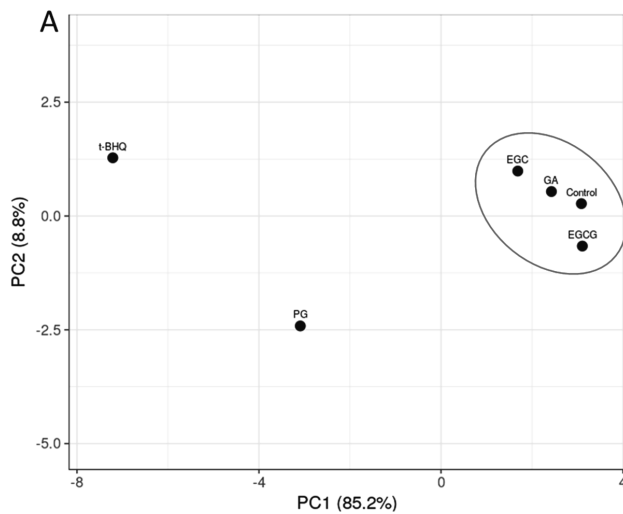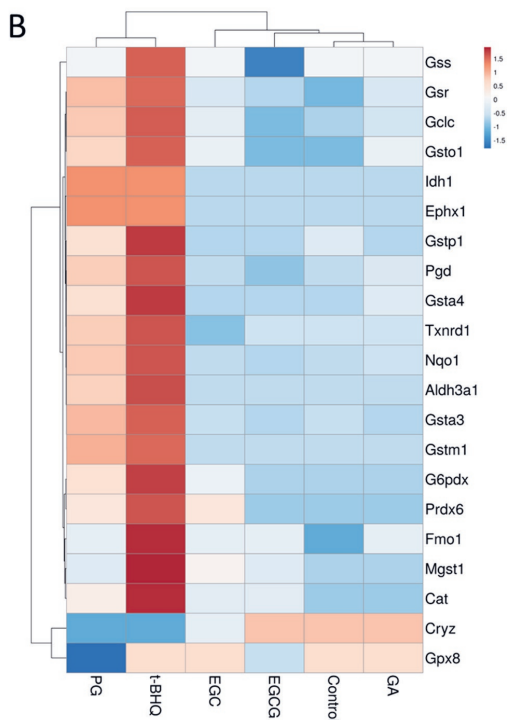
Figure S5. PCA (A) and heatmap (B) based on the FCs of 22 selected proteins in different treatments of Hepa1c1c7 cells.
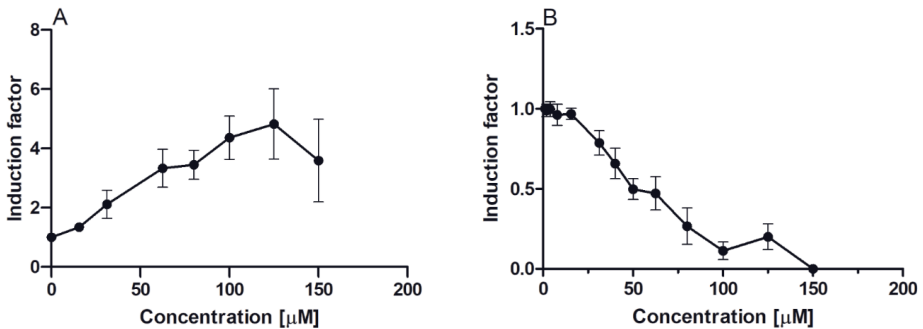
Figure S6. Induction of luciferase activity in U2OS-Nrf2 CALUX reporter cells (A) and in U2OS-Cytotox CALUX cells (B) after 24 h exposure to GA without the presence of L-ascorbic acid. The results are presented as mean ± SEM compared to solvent control, derived from at least three independent experiments.

6

Chapter 6

Use of physiologically based kinetic modeling-based reverse dosimetry to predict *in vivo* Nrf2 activation by EGCG and its colonic metabolites in humans

Chen Liu, Jolijn van Mil, Annelies Noorlander, Ivonne M.C.M. Rietjens

Abstract

(-)-Epigallocatechin gallate (EGCG) is reported to be able to induce Nrf2-mediated gene expression. However, its bioavailability is poor and it is prone to microbial metabolism when reaching the colon. This study aimed to develop a combined *in vitro – in silico* approach to predict Nrf2 activation by EGCG and its major colonic metabolites gallic acid (GA) and pyrogallol (PG) in humans. To this end, a human physiologically based kinetic (PBK) model for EGCG was developed, with sub-models for GA and PG and an intestinal compartment that included microbial metabolism to enable prediction of the kinetics of EGCG and also of GA and PG. The Nrf2 activation by these compounds was characterized using an U2OS-Nrf2 CALUX reporter gene assay and the resulting *in vitro* concentration-response curves were used to extrapolate the *in vitro* data to an *in vivo* dose-response curve for EGCG mediated Nrf2 induction in humans using PBK modeling-based reverse dosimetry. Results obtained show, by comparing to literature data, that the developed PBK model could adequately predict *in vivo* time-dependent blood concentrations of EGCG after either a single or repeated oral administration(s) of EGCG under both fasting and non-fasting conditions. The predicted *in vivo* dose response curve revealed that at daily intake levels of green tea or EGCG supplements, the resulting blood C_{max} of EGCG was in the sub-micromolar range, concentrations at which Nrf2 activation was shown to be limited. Moreover, blood C_{max} values of GA and PG upon intake of EGCG were predicted to be less than 1.5% of the C_{max} of EGCG, indicating that in spite of their higher potential for Nrf2 activation, their contribution to the overall systemic Nrf2 pathway induction upon EGCG exposure is expected to be limited. In contrast, concentrations of these metabolites in the intestinal tract may reach levels that are, expressed in EGCG equivalents for Nrf2 induction, higher than that of EGCG, and also high enough to activate Nrf2 gene transcription. Taken together, combining *in vitro* data with a human PBK model allowed the prediction of a dose-response curve for EGCG induced Nrf2-mediated gene expression in humans, and provided insight into the contribution of gut microbial metabolites to this effect. It also provided a proof-of-principle for a novel approach methodology (NAM) to study the *in vivo* effects of bioactive phytochemicals without the need for human intervention studies.

Keywords: EGCG, gallic acid, pyrogallol, microbial metabolism, novel approach methodology, Nrf2, PBK model, reverse dosimetry

1. Introduction

Green tea has been considered a traditional Chinese medicine and a healthful beverage since ancient times.[1] The biological activities of green tea are often related to the active ingredients: green tea catechins, which account for up to 40% dry weight of green tea.[2] Among the tea catechins, (-)-epigallocatechin gallate (EGCG) is the most bioactive and abundant catechin, making up 48 - 60% of the total catechin constituents.[2-3] Nowadays, EGCG has become one of the most promising dietary supplements. Many health beneficial effects have been associated with this catechin, e.g., antimutagenic, antioxidant, anti-hypertensive, anticarcinogenic, and antibacterial activities, reduced risk of cardiovascular disease, antiviral effects and solar ultraviolet protection, etc.[4-9] The mechanisms behind these health-promoting effects can be complicated and have not been fully elucidated. However, among others, the Kelch-like ECH-associated protein 1/Nuclear factor E2-related factor 2 (Keap1/Nrf2) regulatory network has often been reported to play a role.[10-12]

Under homeostatic conditions, the abundance of the Nrf2 protein within cells is strictly regulated by Keap1. The mode of action underlying EGCG mediated Nrf2 activation has been related to either the generation of H_2O_2 or the formation of its reactive quinone intermediates.[13-14] Both H_2O_2 and quinone metabolites are able to directly inactivate Keap1 or oxidize intracellular GSH resulting in transient oxidative stress causing oxidation or modification of thiol groups of Keap1.[15] As a result, the Nrf2 protein is dissociated from the Keap1 homodimer and translocates into the nucleus where it forms a heterodimer with sMaf proteins and binds to the ARE/EpRE to induce transcription of a wide array of cytoprotective genes.[12]

However, the bioavailability of EGCG is low, being less than 1% of total intake.[16] After EGCG has been ingested, only a very small portion appears in the systemic circulation while the majority of ingested EGCG is passed on to the large intestine where it is prone to intensive microbial metabolism.[17-18] Gallic acid (GA) and pyrogallol (PG) are two major microflora-derived metabolites of EGCG (**Figure 1**), and they have been reported to be more potent inducers of Nrf2-mediated gene expression compared to the parent compound EGCG.[19] Nevertheless, *in vivo* kinetics of GA and PG after EGCG intake have not been studied yet, so it remains to be investigated to what extent these two colonic metabolites contribute to the Nrf2 activation upon *in vivo* EGCG administration.
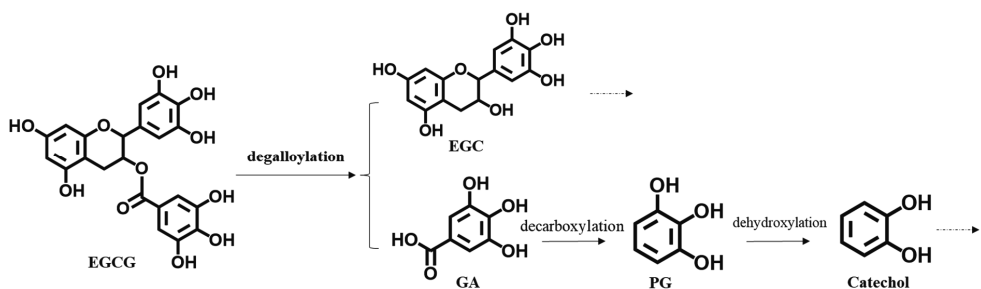
Figure 1. Pathways of human intestinal microbial metabolism of EGCG. Dashed arrows indicate further microbial degradations.

Current studies on EGCG and its biological activities are mostly done in animal or cell-based *in vitro* models.[20-22] The limitations of animal models are obvious as they are often considered costly, time-consuming, unethical and, most importantly, not always adequately representing the human physiological situation because of the existence of interspecies differences.[23] On the other hand, though *in vitro* cell-based assays can be efficient, ethical and relatively economically sustainable, quantitative *in vitro* to *in vivo* extrapolation (QIVIVE) sometimes can be challenging, for example because the *in vitro* models do not take *in vivo* kinetics into account. These challenges may be overcome using a combined *in vitro* and physiologically based kinetic (PBK) modeling-based reverse dosimetry approach. When the PBK model would include gut microbial metabolism this *in vitro* - PBK modeling approach could provide a novel approach methodology (NAM) to characterize the *in vivo* kinetics of EGCG including its gut microbial metabolism, and predict whether systemic exposure of the host to EGCG could result in internal concentrations of EGCG and/or of its metabolites that could activate Nrf2 mediated gene expression. Previously, the PBK modeling-based reverse dosimetry approach has been proved to be an efficient *in vitro* - *in silico* way to adequately perform QIVIVE for several model compounds,[24] contributing to the development of non-animal-based methods towards NAMs. Thus, it is of interest to apply such an *in vitro* - *in silico* approach for quantitative translation of *in vitro* EGCG concentration-response curves of Nrf2 activation to *in vivo* dose-response curves, taking the activity of its gut microbial metabolites into account, and to subsequently compare these data to estimated daily consumption levels of EGCG supplements or green tea.

The aim of the present study was to develop a PBK model in humans including a separate microbial metabolism compartment to predict *in vivo* kinetics of EGCG and to gain insight in the role of the gut microbiota in the bioactivation of EGCG. To characterise the PBK model parameters for the gut microbial conversion of EGCG, *in vitro* anaerobic fecal incubations were performed, previously shown to be an adequate way to generate kinetic PBK model parameters of colonic metabolism, including the respective kinetic constants V_{max} and K_m for microbial conversions.[25-26] Model predictions for blood levels of EGCG were evaluated against available *in vivo* kinetic data from literature. Subsequently, PBK modeling-based reverse dosimetry was used to extrapolate the *in vitro* concentration-response curves from U2OS-Nrf2 CALUX reporter gene assays to *in vivo* dose-response curves for Nrf2 activation by EGCG in humans, taking the concentrations and relative activity of its major colonic metabolites GA and PG into account.

2. Materials and Methods

2.1 Chemicals and Reagents

EGCG, EGC, GA, PG and curcumin were ordered from Sigma-Aldrich (Zwijndrecht, The Netherlands). Geneticin (G148), penicillin/streptomycin (P/S), trypsin and non-essential amino acids (NEAA) were obtained from Invitrogen Corporation (Breda, The Netherlands). Dimethyl sulfoxide (DMSO) was purchased from Acros Organic (New Jersey, USA). Methanol and acetonitrile (ACN) were obtained from Biosolve BV (Valkenswaard, The Netherlands). Dulbecco's Modified Eagle Medium with 1:1 F-12 Nutrient Mixture (DMEM/F-12), phosphate buffered saline (PBS) and dextran-coated charcoal-treated fetal calf serum (DCC-FCS) were supplied by Gibco (Paisley, UK). Fetal bovine serum (FBS) was bought from Capricorn Scientific (Ebsdorfergrund, Germany). Formic acid was purchased from VWR CHEMICA (Amsterdam, The Netherlands) and acetic acid was ordered from Merck KGaA (Darmstadt, Germany).

2.2 PBK Modeling-based Reverse Dosimetry Approach

The PBK modeling-based reverse dosimetry approach was used to predict *in vivo* dose-dependent Nrf2 pathway induction by EGCG taking the activity of its microbial metabolites GA and PG into account. This approach consisted of the following five steps: (1) development of a human PBK model for EGCG including its intestinal microbial metabolism and sub-models for GA and PG to allow the prediction of not only kinetics of EGCG but also of GA and PG, (2) evaluation of the PBK model by comparison of predictions made with *in vivo* data, (3)

establishment of *in vitro* concentration-response curves for EGCG, GA and PG using the *in vitro* U2OS-Nrf2 CALUX reporter gene assay, (4) extrapolation of the *in vitro* concentration-response curve to an *in vivo* dose-response curve using PBK model based reverse dosimetry taking the relative potency of GA and PG into account, (5) evaluation of the predicted dose-response data by comparison to *in vivo* data including comparison to dietary intake levels of EGCG from supplements and/or use of green tea.

2.3 Development of A PBK Model for *In Vivo* EGCG, GA and PG Kinetics in Humans

The conceptual PBK model of EGCG, including sub-models for GA and PG, for humans is presented in **Figure 2**. The model is modified from PBK models developed and evaluated previously for zearalenone and daidzein also taking gut microbial metabolism into account.[26-27] The model includes a separate compartment for liver as biliary excretion and metabolizing compartment, and compartments for stomach, fat, kidney, blood, small intestinal lumen, small intestine tissue, large intestinal lumen, slowly perfused tissue (muscle, skin, bone) and rapidly perfused tissue. The model includes a stomach emptying process,[28] and the small intestinal lumen was divided into seven sub-compartments enabling the description of the transition within the small intestine.[29] The large intestinal lumen contains fecal microbiota which allows the description of colonic microbial metabolism of EGCG. The model contains two sub-models, one for microflora-derived GA, formed from EGCG, and another one for the microbial metabolite PG, formed from GA. The PBK model thus defined enables the definition of systemic blood concentrations of both the parent compound EGCG and of its microbial metabolites GA and PG after oral dosing of EGCG. Moreover, considering that EGCG is usually administered by green tea drinkers on a daily basis, the PBK model was also developed to predict kinetics upon repeated dosing of EGCG. The physiological and anatomical parameters in the model, such as tissue volumes and blood flows were taken from literature[30] and are depicted in **Table 1**. The physicochemical parameters, such as tissue/blood partition coefficients, are presented in **Table 2**, and were calculated based on the quantitative property – property relationship (QPPR) approach.[31] The input parameters for this method is the logarithmic octanol-water partition coefficient (LogP) obtained from ChemDraw 18.0 (PerkinElmer, MA, USA). The LogP values are 2.07, 0.42 and 0.82 for EGCG, GA and PG, respectively.

Table 1. Physiological parameters used in the PBK model for EGCG and its microbial metabolites GA and PG based on Brown et al.[30]

Physiological parameters	Symbol	Value	Physiological parameters	Symbol	Value
Body weight [kg]	BW	70	Cardiac output [L/h]	QC	347.9
Tissue volumes (fraction of body weight)			**Blood flow to tissue (fraction cardiac output)**		
Small intestine	VSIc	0.009	Small intestine	QIc	0.181
Liver	VLc	0.026	Liver	QLc	0.046
Kidney	VKc	0.004	Kidney	QKc	0.175
Fat	VFc	0.214	Fat	QFc	0.052
Rapidly perfused tissue	VRc	0.068	Rapidly perfused tissue	QRc	0.255
Slowly perfused tissue	VSc	0.58	Slowly perfused tissue	QSc	0.291
Large intestine	VLIc	0.005			
Gastrointestinal tract contents	VGIc	0.014			
Blood	VBc	0.079			

Table 2. Physicochemical parameters used in the PBK model. Tissue/blood partition coefficients of EGCG, GA and PG were calculated based on the QPPR approach by DeJongh et al.[31]

Tissue/Blood partition coefficients	EGCG	GA	PG
Small intestine	2.68	0.72	0.85
Liver	2.68	0.72	0.85
Kidney	1.49	0.85	0.91
Rapidly perfused tissue	2.68	0.72	0.85
Slowly perfused tissue	1.94	0.82	0.90
Fat	55.57	1.96	5.18

Chapter 6
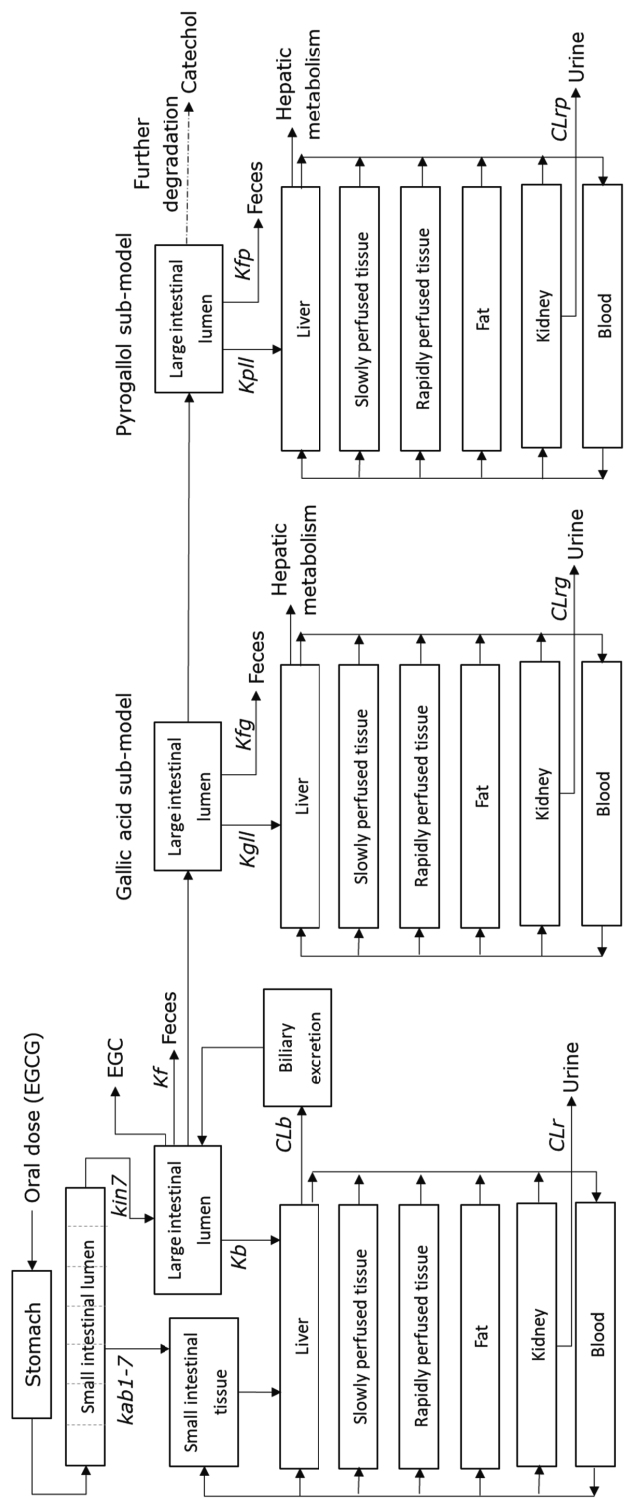
Figure 2. Schematic presentation of the main PBK model for EGCG including sub-models for the bioactive metabolites GA and PG.

The apparent permeability coefficients (P_{app}) were used to define the intestinal absorption of EGCG from the small intestinal lumen into the liver via the small intestine tissue and portal vein or to describe the uptake of GA and PG from the large intestinal lumen directly to the liver. The P_{app} values of EGCG, GA and PG were calculated using the quantitative structure-activity relationship (QSAR) method with the formula: Log ($P_{appCaco-2}$) = –4.36 – 0.010 × TPSA where TPSA stands for the topological polar surface area for which the values were derived using ChemDraw 18.0 (PerkinElmer, MA, USA).[32] The *in vivo* P_{app} values were estimated by using the formula: Log ($P_{app, in vivo}$) = 0.6836 × Log ($P_{appCaco-2}$) – 0.5579.[33] However, it is reported that the absorption rate of EGCG under fasting conditions can be higher than under non-fasting conditions.[34-35] Therefore, to allow for the higher rate of uptake of EGCG under fasting conditions, the $P_{appCaco-2}$ value of EGCG under fasting conditions was model-fitted by comparing the predicted time-dependent blood concentration curve to the *in vivo* data from Chow et al., for the dose dependent C_{max} for EGCG upon oral dosing EGCG under fasting conditions,[34] yielding a value of 9.9×10^{-6} cm/s. The intestinal absorption rate of EGCG in the small intestine was subsequently determined using the following equation: absorption rate (μmol/h) = $P_{app, in vivo}$ (cm/h) × surface area of the human small intestine (cm^2) × luminal concentration of EGCG (mM = μmol/cm^3).[26, 36] The surface areas of human small and large intestine were 7200 and 4700 cm^2.[26] The luminal concentrations of EGCG in the small intestine and large intestine were calculated by dividing the amount of EGCG by the volume of the small or large intestines, respectively. The transport of GA and PG formed by intestinal microbiota was modeled to go directly from the large intestinal lumen to the liver. The calculations of $P_{app, in vivo}$ and the absorption rates of GA and PG were performed in the same way as described above for EGCG using the $P_{appCaco-2}$ values for GA and PG calculated using the above-mentioned QSAR formula, as no kinetic data for further refinement of their $P_{appCaco-2}$ values by fitting to experimental data were available.

For EGCG, its elimination is mostly through biliary excretion to the colon while its renal excretion was reported in undetectable low level, thus could be ignored.[37] Therefore, the renal clearance of EGCG (CLr) in the kidney compartment was set to 0. The biliary excretion clearance of EGCG (CLb) was not available from literature. Therefore, this value was obtained by fitting the predicted time-dependent blood concentration curve to the *in vivo* data from Chow et al.[38] In contrast to EGCG, the microbial metabolites GA and PG are largely excreted through renal excretion.[39-40] The value of renal clearance of GA used in the model was obtained from an *in vivo* study conducted by Shahrzad et al. who investigated the pharmacokinetics of GA

upon oral administration by human volunteers.[39] Since data on the *in vivo* kinetics of PG in human are not available, the renal clearance parameter of PG was assumed to be the same as that for GA.

2.4 Determination of Model Parameter Values for Microbial Metabolism

To obtain the kinetic constants (V_{max} and K_m) for the microbial conversions, *in vitro* anaerobic fecal incubations were performed. The protocol was essentially the same as previously described.[19] The protocol for the collection of human fecal samples was evaluated by the Medical Ethical Reviewing Committee of Wageningen University (METC-WU), who concluded that the study design did not to require further evaluations based on the Dutch Medical Research Involving Human Subjects Act. In brief, feces were collected from 14 healthy individuals aged between 19 and 65 who were not taking antibiotics for at least three months, including nine females (none of them were pregnant) and five males. After volunteers' donations, feces were immediately collected and diluted with an anaerobic solution of 10% (v/v) glycerol in PBS to obtain a final fecal concentration of 20% (w/v) in fecal slurries under an anaerobic atmosphere (85% N_2, 10% CO_2, and 5% H_2) (BACTRON300 anaerobic chamber (Cornelius, USA)). A pooled sample used in the present study was obtained by mixing equal volumes of the 14 fecal suspensions and was subsequently aliquoted. Conditions for anaerobic incubations with human fecal samples were optimized to achieve linear depletion of the substrate and linear formation of metabolites over time and concentration of feces. An experimental incubation of 50 µL contained parent compound added from a 100-times concentrated stock solution in methanol (final concentration 70 µM) (or 1% methanol referred to as "negative control"), 4 to 60 mg pooled feces/mL (final concentrations) and complementary 34.5 to 48.5 µL anaerobic PBS. Incubations of parent compounds without fecal slurries were included as blank control. After incubating in an atmosphere of 85% N_2, 10% CO_2, and 5% H_2, at 37 °C for 15, 30 and 50 minutes in the anaerobic chamber, the reaction was terminated by adding one volume of ice-cold methanol. Subsequently, samples were put on ice for 15 min, followed by centrifugation at 21500 × g (VWR, Hitachi Koki Co., Ltd.) for 15 min at 4 °C. The supernatant of each sample was collected and stored immediately at −80 °C until liquid chromatography triple quadrupole mass spectrometry (LC-TQ-MS) analysis. Optimized conditions at which conversion appeared linear with time and the amount of fecal sample, consisting of 20 mg feces/mL and an incubation time of 30 minutes, were used for incubations to derive kinetics of microbial conversions.

To obtain the kinetic constants (V_{max} and K_m, explained in detail in the next section) for the microbial conversion of EGCG to GA and PG, anaerobic incubations were carried out with a range of EGCG concentrations from 2.2 to 280 µM (final concentrations) (added from 100-times concentrated stock solutions in methanol). Incubations were conducted the same way as described above. Also, negative controls and blank controls were conducted as described above. The incubations were performed in triplicate.

2.5 Kinetic Analysis of the Data from the *In Vitro* Fecal Incubations

The apparent maximum velocity (V_{max}, expressed in µmol/h/g feces) and apparent Michaels-Menten constant (K_m, expressed in µM) were used to describe the human colonic microbial metabolism for EGCG, GA and PG. The curves for the concentration-dependent metabolite formation were fitted to the Michaelis-Menten equation ($v = V_{max}*[S] / (K_m + [S])$) using GraphPad Prism 5.04 (GraphPad software, CA, USA). The V_{max} expressed in µmol/h/g feces, was scaled to the whole body using a fecal fraction of body weight of 0.0018.[41]

2.7 Hepatic Clearance of GA and PG

For the reverse dosimetry, it was assumed that the Nrf2 pathway is induced by aglycones and not by their conjugates because the free hydroxy groups are essential for the Nrf2 activation.[14-15] Thus, the current PBK model includes an overall hepatic metabolism/clearance of GA and PG in the respective sub-models. Upon oral intake of EGCG, the hepatic metabolism is limited and could be ignored because EGCG is mainly excreted through biliary excretion and/or passed on to the colon.[37] With respect to metabolism/clearance in the liver, in the GA and PG sub-models, the metabolism of GA and PG in the liver is described based on substrate depletion in incubations with a range of cofactors for potentially involved biotransformation enzymes[36] as their detailed hepatic metabolic profiles have not been entirely elucidated yet. The *in vitro* hepatic clearance (CL_{int}) values of GA and PG were assumed to be the same and estimated to be 300 µL/min/mg/protein according to the studies of Zhang et al. for a generic PBK model.[36, 42]

The PBK model equations were coded and numerically integrated in Berkeley Madonna 9.1.18 (UC Berkeley, CA, USA) using the Rosenbrock's algorithm for stiff systems. The model script is presented in the Supporting Information2.

2.8 LC-TQ-MS Analysis

EGCG, EGC, GA and PG in the incubation samples were measured using a Shimadzu LC-TQ-MS 8045 (Shimadzu, Benelux, B.V. The Netherlands). Liquid chromatographic separation was conducted on a Waters Acquity UPLC BEH C18 column (2.1 × 50 mm; 1.7 μm) at 40 °C. A previously optimized method was used to qualitatively and quantitatively identify these compounds.[19] Briefly, mobile phase A was composed of water : acetic acid (999 : 1, v/v), and mobile phase B was methanol. The flow rate was 0.4 mL/min with the following gradient: 0 - 0.5 min: 5% B, 0.5 - 5 min: 5 - 25% B, 5 - 6 min: 25 - 100% B, 6 - 7 min: 100% B, 7 - 8 min: 100 - 5% B, 8 - 13 min: 5% B. Authentic chemical standards of EGCG, GA and PG were used for identification and defining calibration curves for quantifications. Notably, in fecal incubation samples, concentrations of test compounds were calculated by subtracting the concentrations quantified from the concentrations detected in corresponding negative controls incubated without adding test compounds in order to correct for potential background levels of polyphenols in the fecal sample.

2.9 PBK Model Evaluation

The performance of the developed PBK model was evaluated by comparison of model predicted time-dependent blood concentrations of EGCG to available time-dependent blood concentrations reported in literature upon single oral administrations of 2.00, 2.86, 5.71, 8.57, 11.43, 17.14 mg/kg bw of EGCG (or Polyphenon E containing a known amount of EGCG) to human volunteers under non-fasting conditions,[34, 38, 43-44] and of 5.71, 7.14, 11.43, 17.14 mg/kg bw of EGCG (or Polyphenon E containing a known amount of EGCG) to human volunteers under fasting conditions.[34-35] Since the PBK model developed predicts EGCG, GA and PG blood concentrations, the plasma concentrations from *in vivo* studies were converted to blood concentrations assuming that the blood to plasma partition ratio (BP) of GA and PG is 0.55 i.e., $C_{blood} = C_{plasma}*0.55$.[45] For EGCG, the BP value was 0.91 taken from a research article of Law et al., thus $C_{blood\ EGCG} = C_{plasma\ EGCG}*0.91$.[46]

2.10 Sensitivity Analysis PBK Model

To further identify the parameters that affect the predicted maximal blood concentrations (C_{max}) to the largest extent, sensitivity coefficients (SCs) were characterized according to the following equation: SC = (C' - C)/(P' - P) × (P/C), in which C stands for the initial value of the model output, C' represents the modified value after changing the parameter value, P and P' are the initial and modified parameter values, respectively.[47] A 5% increase of the input parameter value was applied to assess the effect of a change in parameter on the prediction of the C_{max} of

EGCG, GA and PG. Each parameter change was analyzed individually by changing only one parameter at a time and keeping the other parameters at the initial levels, keeping total blood flow and body weight at 100%. The larger the SC value, the higher the impact of the respective parameter on the predictions for C_{max} of EGCG, GA and PG. The sensitivity analysis was conducted for a single oral administration of 2.86 or 5.71 or 8.57 mg/kg bw EGCG under the non-fasting condition, which were the dose levels from the *in vivo* kinetic study and also represent the amount of EGCG consumed via drinking around two or four or six cups of green tea.[38]

2.11 Determination of Nrf2 Activation by EGCG, GA and PG in the *In Vitro* U2OS-Nrf2 CALUX Reporter Gene Assay

The U2OS-Nrf2 CALUX reporter gene assay (Biodetection Systems, Amsterdam) was performed to assess the potency of EGCG, GA and PG to activate the Nrf2 signaling pathway. The U2OS-Nrf2 CALUX cells were derived from human osteoblastic cells transfected with a reporter construct carrying a luciferase reporter gene under transcriptional control of four EpRE sequences,[48] which can be used to measure the luciferase expression after exposure to test compounds. The cell culturing and subsequent bioassays were conducted mainly as described before.[19] In brief, U2OS-Nrf2 CALUX cells were cultured in a black 96-well microplate with a clear bottom (Greiner bio-one) at a density of 2×10^4 cells in 100 µL culture medium per well (2×10^5 cells/mL) for 24 hours. The culture medium was then replaced with exposure medium containing model compounds at different concentrations for another 24 hours of exposure. Eight exposure concentrations were applied for EGCG, GA and PG, ranging from 15.6 µM to 160 µM, diluted from 200 times concentrated stock solutions in DMSO. After finishing exposure, the luciferase activity of each well was measured upon injecting 100 µl flash mix (2.67 mM $MgSO_4$, 1.07 mM $(MgCO_3)_4Mg(OH)_2 \cdot 5H_2O$, 20 mM Tricine, 0.1 mM EDTA, 5.0 mM ATP; 2.0 mM DTT, 470 µM D-luciferine, pH 7.8) and the resulting relative light units (RLUs) of each well were recorded using a luminometer (GloMax-Multi Detection System-Promega).

Additionally, a paralleled U2OS-Cytotox CALUX assay (Biodetection Systems, Amsterdam) was performed to investigate the potential luciferase stabilisation and cytotoxicity after the exposure to EGCG, GA or PG. The assay was performed under the same conditions as described above for the U2OS-Nrf2 CALUX assay. Results of both CALUX assays are presented as the induction factor (IF) compared to the solvent control. At least three independent assays were carried out for all model compounds.

From the concentration response curves an estimate for the difference in relative potency between EGCG, GA and PG was made by estimating the concentration needed to reach an IF of 2, 3 and 4-fold. The average relative potency (REP) values of GA and PG were expressed relative to the REP value for the parent compound EGCG set at 1.0, in order to allow expression of concentrations in ECGC equivalents.

2.12 Quantitative Extrapolation of *In Vitro* Concentration-response Data into An *In Vivo* Dose-response Curve Using the PBK Model Developed

In vivo dose-dependent Nrf2 activation by EGCG, GA and PG was assumed to be dependent on their maximum unbound concentrations (C_{max}) reached in the plasma. The effective concentrations of unbound EGCG in the *in vitro* assays expressed in EGCG equivalents were set equal to the unbound *in vivo* plasma C_{max} expressed in EGCG equivalents. Based on this, the PBK modeling-based reverse dosimetry approach was applied to predict the dose levels that would be required to reach the C_{max} in plasma expressed in EGCG equivalents. A correction for protein binding was applied since only the unbound fraction (f_{ub}) of the model compounds was assumed to be responsible for the Nrf2 pathway activation. Thus, in this reverse dosimetry approach, the unbound fraction of EGCG in the *in vitro* medium was linked to the *in vivo* freely available (unbound) C_{max} in human plasma expressed in EGCG equivalents. This unbound C_{max} in human plasma expressed in EGCG equivalents was calculated by the following equations: $C_{in\ vitro,\ EGCG} * f_{ub,\ in\ vitro,\ EGCG} = C_{unbound,\ plasma,\ EGCG\ equivalents}$ where $C_{unbound,\ plasma,\ EGCG\ equivalents} = (C_{blood,\ EGCG} / BP_{EGCG}) * f_{ub,\ in\ vivo,\ EGCG} * REP_{EGCG} + (C_{blood,\ GA} / BP_{GA}) * f_{ub,\ in\ vivo,\ GA} * REP_{GA} + (C_{blood,\ PG} / BP_{PG}) * f_{ub,\ in\ vivo,\ PG} * REP_{PG}$. In these equations $C_{in\ vitro,\ EGCG}$ and $f_{ub,\ in\ vitro,\ EGCG}$ are the *in vitro* concentration and unbound fraction of EGCG in the medium. $C_{blood,\ EGCG}$, $C_{blood,\ GA}$ and $C_{blood,\ PG}$ are *in vivo* blood concentrations of EGCG, GA and PG, respectively. BP_{EGCG}, BP_{GA} and BP_{PG} are the respective blood to plasma partition ratios' of EGCG, GA and PG, $f_{ub,\ in\ vivo,\ EGCG}$, $f_{ub,\ in\ vivo,\ GA}$ and $f_{ub,\ in\ vivo,\ PG}$ are the *in vivo* plasma unbound fraction of EGCG, GA and PG, respectively. REP_{EGCG}, REP_{GA} and REP_{PG} are the REP values of EGCG (defined as 1.0), GA and PG (defined based on their relative potency in the U2OS-Nrf2 CALUX assay), respectively, and BP_{EGCG}, BP_{GA} and BP_{PG} are 0.91, 0.55 and 0.55, respectively, as described above.[45-46] $f_{ub,\ in\ vivo,\ EGCG}$, $f_{ub,\ in\ vivo,\ GA}$ and $f_{ub,\ in\ vivo,\ PG}$ were calculated with online QIVIVE tools (https://wfsr.shinyapps.io/wfsrqivivetools/) and amounted to 0.121, 0.214 and 0.550, respectively.[49-50] The $f_{ub,\ in\ vitro,\ EGCG}$ value was calculated to be 0.451, using the method reported by van Tongeren et al., assuming a linear relation between the fraction unbound and the protein content in a biological matrix, with the fraction unbound being 1.0 in the absence of protein.[51]

The protein content of human plasma is around 8% while the exposure medium of the U2OS-Nrf2 CALUX assay used in the present study contained 5% DCC-FCS.[52] Based on this assumption, the $f_{ub, in vitro}$ values of the model compounds were calculated using the following equation: $f_{ub, in vitro} = 1 - (1 - f_{ub, in vivo})/ 8\% * 5\%$ where $f_{ub, in vitro}$ and $f_{ub, in vivo}$ are the *in vitro* unbound fraction of the model compound in the medium and the *in vivo* plasma unbound fraction of the model compound, respectively.

Following the approach described, the PBK model was used to determine the dose level that would result in the unbound C_{max} expressed in EGCG equivalents, translating each *in vitro* exposure concentration into an *in vivo* dose level so that the *in vitro* EGCG concentration-response curves was translated into and *in vivo* EGCG dose-response curve, taking the contributions of EGCG and its major colonic metabolites GA and PG into account.

2.13 Benchmark Dose Modeling of PBK Model Predicted *In Vivo* Dose-response Curves

BMD analysis was performed to determine the point of departure (POD) from the PBK model predicted dose-response curves. To this end, the European Food Safety Authority (EFSA) online BMD analysis tool (https://r4eu.efsa.europa.eu/app/bmd) integrated with the R package PROAST version 70.0 was used to characterize the benchmark dose that resulted in an extra 10% response above background compared to the control, with lower and upper 90% confidence limit were defined as $BMDL_{10}$ and $BMDU_{10}$, respectively.

3. RESULTS

3.1 Kinetic Constants for Microbial Metabolism of EGCG, GA and PG

To determine the V_{max} and K_m for the microbial conversion of EGCG, GA and PG, anaerobic incubations of EGCG, GA or PG were performed with human fecal samples. **Figure 3A** shows the time-dependent formation of GA in anaerobic fecal microbial incubations with EGCG (70 μM) at different concentrations of feces, i.e., 4, 10, 20, 40 and 60 mg feces/mL. At low fecal concentrations, i.e., 4 and 10 mg feces/mL, the formation of GA from EGCG appeared to show a lag phase. With the increase of the fecal concentration the metabolism of EGCG started immediately and showed linearity in formation of GA over time for at least 50 min at both 20 and 40 mg feces/mL of fecal concentration. **Figure 3B** shows the fecal concentration-dependent formation of GA from EGCG (70 μM) at different incubation times. These graphs reveal that the formation of GA from EGCG is linear with the fecal concentration up to and including at least 40 mg feces/mL. Based on these data 20 mg feces/mL and 30 minutes of incubation were

selected as the optimized conditions for subsequent anaerobic fecal incubations to obtain microbial conversion kinetics for the PBK model.

Figure 3C presents the EGCG concentration-dependent formation rates of EGC and GA in anaerobic human fecal incubations. Both product formations show Michaelis Menten kinetics. Comparison of the concentration dependent formation of EGC to that for GA reveals a significant difference in the EGCG concentration dependent formation rate of EGC and GA. This is of interest given that EGC and GA are both formed from EGCG in the same reaction (**Figure 1**), being the first step of EGCG microbial conversion. The discrepancy can be ascribed to the swift further metabolic conversion of GA to PG, while the EGC formed was assumed not to be substantially further degraded in the available incubation time. Based on this assumption the rate of formation of PG was calculated from the difference in rate of formation of EGC minus the rate of formation of GA (**Figure 3C**). This provides apparent kinetic constants for PG as a function of the EGCG concentration and for a first approximation these were assumed to be the same as the kinetic constants for PG formation from GA. The EGCG concentration dependent metabolite formation curves thus obtained were fitted to the Michaelis-Menten equation, to obtain the apparent V_{max}, K_m and respective catalytic efficiencies (k_{cat}, calculated as V_{max}/K_m) for the formation of EGC, GA and PG. The kinetic constants thus obtained are presented in **Table 3**. Kinetic parameters for catechol formed from microbial degradation of PG were assumed to be the same as kinetic parameters of PG formation from GA (**Table 3**).

Table 3. Apparent kinetic parameters for formation of EGCG gut microbial metabolites in anaerobic fecal incubations.

	EGC from EGCG	GA from EGCG	PG from GA	Catechol from PG[a]
V_{max} [μmol/h/g feces]	3.07	0.87	2.43	2.43
K_m [μM]	41.61	11.13	68.70	68.70
k_{cat} [mL/h/g feces]	73.78	78.17	35.37	35.37

[a]Kinetics are assumed to be similar to those for microbial conversion of GA to PG
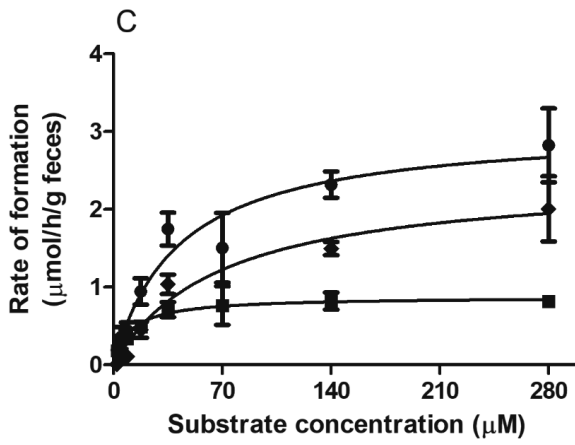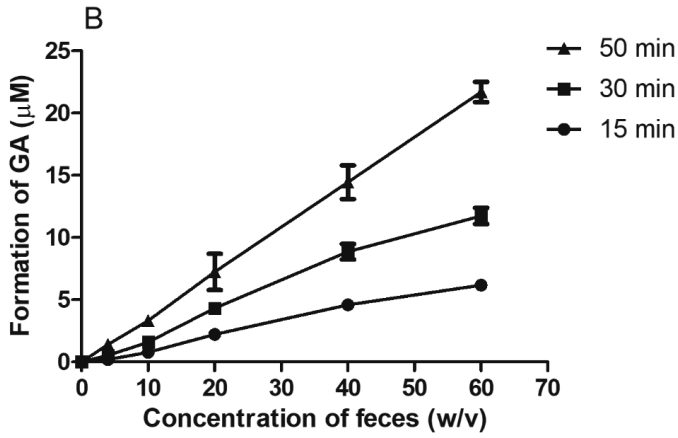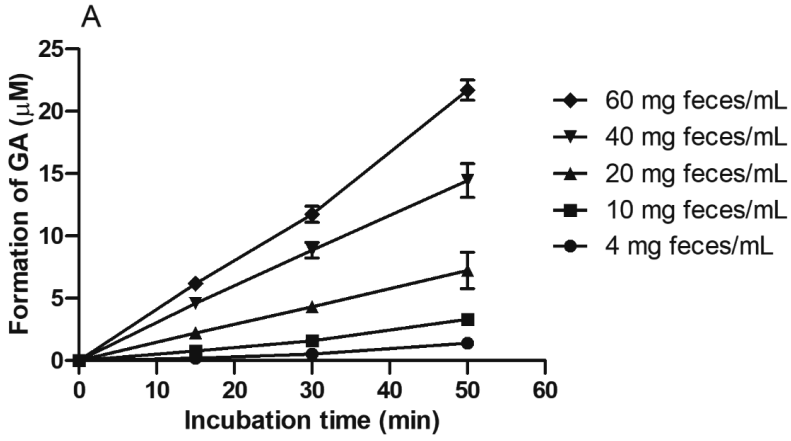
Figure 3. Time-, fecal concentration- and EGCG- concentration dependent (rate of) metabolite formation in *in vitro* anaerobic fecal incubations of EGCG, including the time-dependent (A) and the fecal concentration dependent (B) formation of GA from microbial conversion of EGCG (starting concentration 70 μM), and the EGCG concentration-dependent (C) rate of formation of EGC (circles), GA (squares) and PG (diamonds) (the latter calculated as the rate of formation of EGC minus the rate of formation of PG) in anaerobic human fecal incubations. Data are presented as mean ± SEM of quadruplicate experiments.

3.2 PBK Model Evaluation

To evaluate the model predictions, the predicted time-dependent blood concentrations of EGCG were compared with *in vivo* kinetic data upon oral administration of EGCG at various dose levels to humans both under fasting and non-fasting conditions.[34-35, 38, 43-44] **Figure 4** depicts the blood concentrations of EGCG reported in the *in vivo* studies with human volunteers orally taking a single dose of EGCG (symbols) under non-fasting conditions, as compared with model-predicted values (lines). The results indicate that the model was able to adequately predict the time-dependent blood concentrations of EGCG at various dose levels under non-fasting conditions. The C_{max} and T_{max} of free EGCG in blood predicted upon single oral intake was compared to the C_{max} and T_{max} reported *in vivo* (**Table 4**). At medium dose levels (until 8.57 mg/kg bw), the model was able to predict the kinetics well, with a ratio between 0.73 to 1.14 and 0.85 to 1.71 for predicted C_{max}/*in vivo* C_{max} and predicted T_{max}/*in vivo* T_{max}, respectively. Moreover, the mean values for predicted C_{max}/*in vivo* C_{max} and predicted T_{max}/*in vivo* T_{max} are 0.83 and 1.06 for all dose levels in the studies compared (**Table 4**). However, it is worth noting that at the highest dose, i.e., 17.14 mg/kg bw, the model predictions were somewhat less accurate. This may be due to saturation of pre-systemic elimination upon oral administration of EGCG at high dose levels in the *in vivo* study.[37-38] Moreover, some literature studies reporting *in vivo* data at similar dose levels of EGCG were contradictory. For example, discrepancies were found in two studies conducted by Chow et al. reporting *in vivo* kinetics after dosing 11.43 mg/kg bw.[34, 38] The predictions of the current model at a dose of 11.43 mg/kg bw were in line with their second study[44] (**Figure 4G**) and their third study[34] (**Figure 4I**) but not with results of the first study[38] (**Figure 4E**) for which the experimental blood concentrations were higher in spite of the similar dosing regimen. Furthermore, adverse effects, such as nausea and headache were found at high EGCG dosing level among volunteers in *in vivo* studies, indicating the inappropriateness of using such high dose levels in real life.[34]

Table 4. C_{max} and T_{max} of EGCG obtained from *in vivo* data (a single dose under non-fasting conditions) and predicted by the PBK model in human blood upon a single oral administration.

Dose (mg/kg bw)	*In vivo* C_{max} (µM)	Predicted C_{max} (µM)	Predicted C_{max}/*In vivo* C_{max}	*In vivo* T_{max} (h)	Predicted T_{max} (h)	Predicted T_{max}/*In vivo* T_{max}	References
2.00	0.07	0.08	1.14	1.61	2.75	1.71	[43]
2.86	0.15	0.11	0.73	2.12	2.45	1.16	[38]
5.71	0.22	0.23	1.05	1.81	2.62	1.45	[38]
5.71	0.27	0.23	0.85	3.07	2.62	0.85	[44]
5.71	0.28	0.23	0.82	2.05	2.62	1.28	[34]
8.57	0.34	0.34	1.00	3.00	2.69	0.90	[38]
11.43	0.87	0.46	0.53	4.00	2.63	0.66	[38]
11.43	0.47	0.46	0.98	3.74	2.63	0.70	[44]
11.43	0.58	0.46	0.79	2.58	2.63	1.02	[34]
17.14	1.83	0.68	0.38	2.92	2.61	0.89	[34]
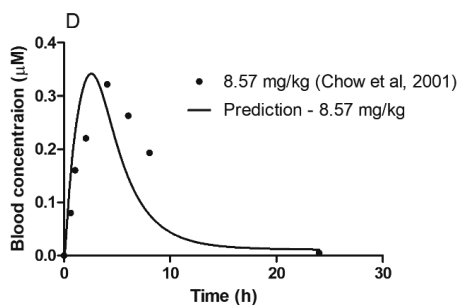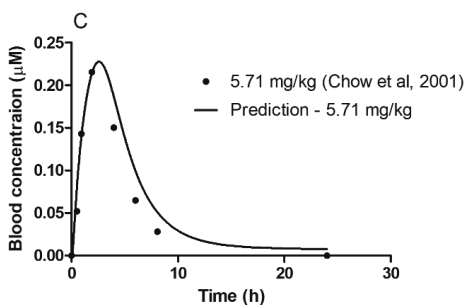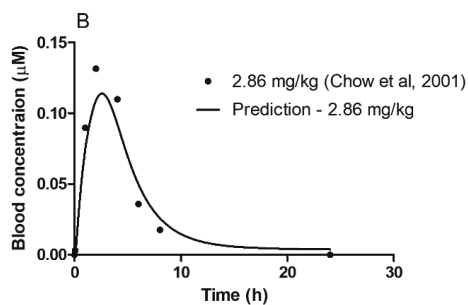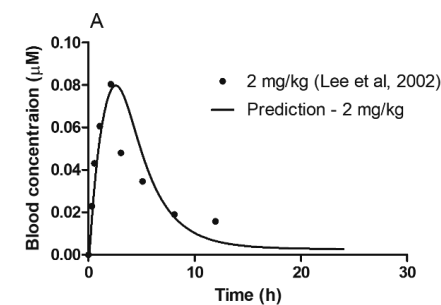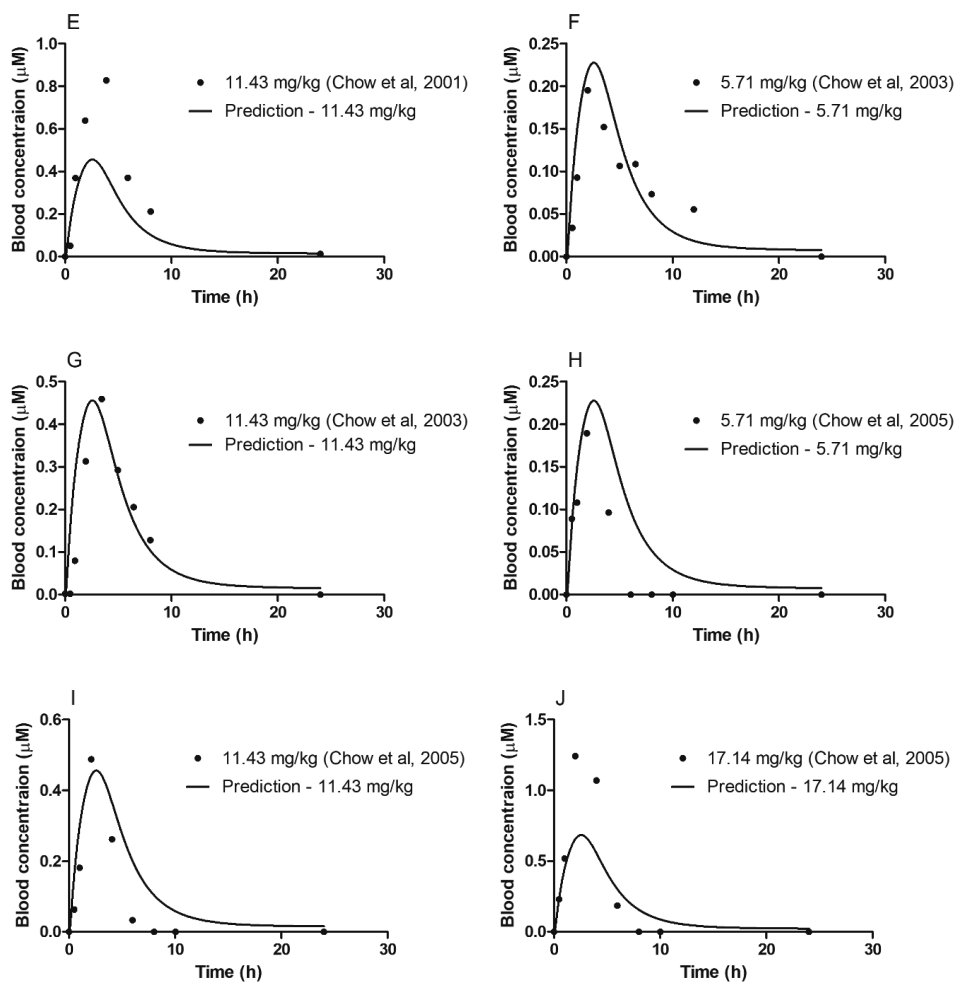
Figure 4. Comparison of predicted and reported time-dependent blood concentrations of free EGCG upon a single oral administration of EGCG to human volunteers at different dose levels under non-fasting conditions.[34, 38, 43-44] Note that the experimental data from Chow et al., 2001 (E) do not match the experimental data from Chow et al., 2003 (G) and Chow et al., 2005 (I) at a similar dose level.

In addition, the model performance of predicting EGCG kinetics upon repeated oral administration of EGCG to humans at different dose levels under non-fasting conditions was evaluated by comparing predictions made to *in vivo* human data obtained from literature reporting on repeated dosing regimens.[44] The results obtained are presented in **Figure 5**, and reveal that the model accurately predicts the change of EGCG blood concentrations during the

last 12 or 24 h upon repeated oral EGCG exposure as described in the study of Chow et al.,[44] especially for the prediction of the C_{max} upon dosing 5.71 mg/kg bw EGCG twice a day at an interval of 12 h for four consecutive weeks. The ratios for predicted C_{max}/*in vivo* C_{max} and T_{max}/*in vivo* T_{max} of blood EGCG on the last treatment day are 0.89 and 1.58, respectively (**Figure 5A**). While for the prediction of the higher dose, i.e., a daily exposure to EGCG at 11.43 mg/kg bw for four consecutive weeks, the ratios for predicted C_{max}/*in vivo* C_{max} and T_{max}/*in vivo* T_{max} of blood EGCG on the last treatment day amounted to 0.65 and 1.03, respectively (**Figure 5B**).
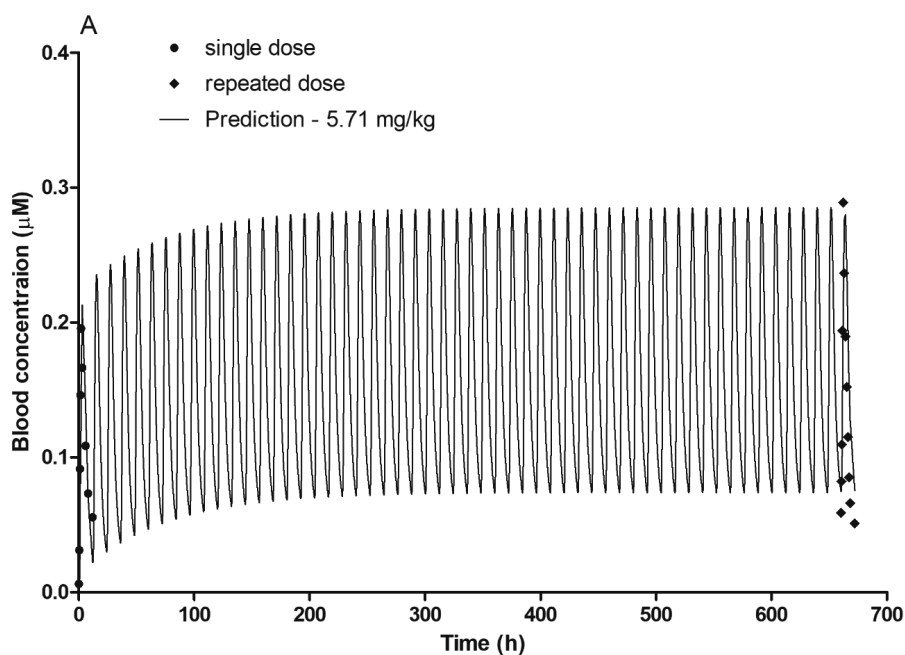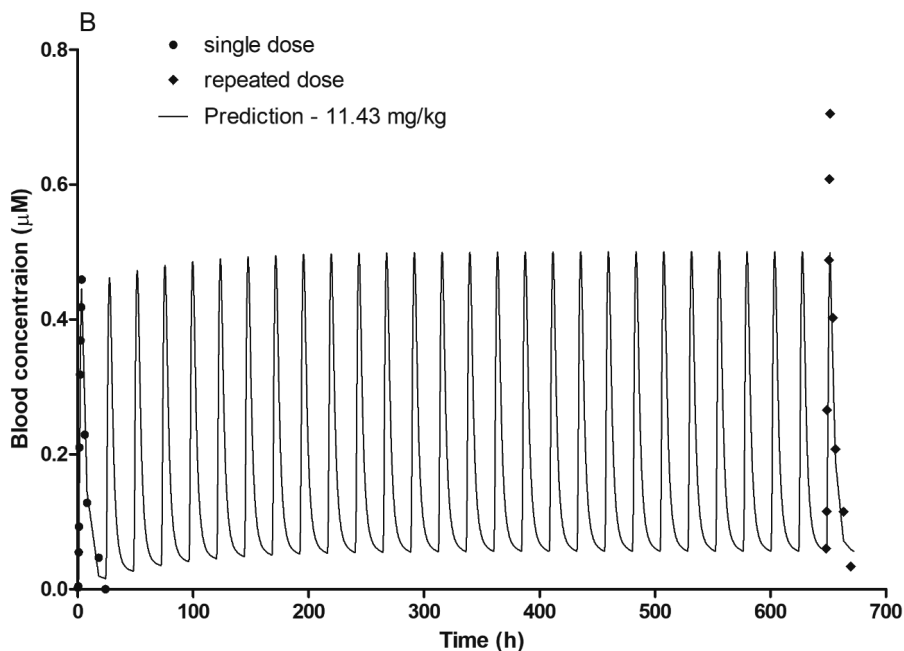
Figure 5. Human blood concentration–time curves of EGCG predicted with the PBK model (lines) and *in vivo* data (symbols) from literature[44] after a repeated oral dose of 5.71 mg/kg bw per 12 hours for four weeks (A), and of 11.43 mg/kg bw per 24 hours for four weeks (B). The circular symbols represent the *in vivo* data after the first dose at the beginning of study and the diamond symbols represent the *in vivo* data from the last treatment day of the study.

Next, the model performance for predicting blood concentration of EGCG after a single oral administration of EGCG (or Polyphenon E) to humans at different levels under fasting conditions was evaluated by comparing data obtained from human intervention studies conducted under fasting conditions.[34-35] After fitting the $P_{appCaco-2}$ value of EGCG, the absorption rate constant kabin increased to 0.39 compared to 0.05 L/h under non-fasting conditions. **Figure 6** depicts the blood concentrations of EGCG reported in the *in vivo* studies with human volunteers orally taking a single dose of EGCG (symbols) under fasting conditions, as compared with model-predicted values (lines). The results indicate that the model was able to also adequately predict the time-dependent blood concentrations of EGCG at various dosing levels under fasting conditions. The C_{max} and T_{max} of free EGCG in blood predicted was comparable to the C_{max} and T_{max} reported *in vivo* (**Table 5**). The mean values for predicted C_{max}/*in vivo* C_{max} and predicted T_{max}/*in vivo* T_{max} are 0.83 and 1.56 for all comparisons made

(**Table 5**). Similar to what was observed for non-fasting conditions, at the highest dose, i.e., 17.14 mg/kg bw, the model predictions were somewhat less accurate than predictions for lower dose levels, with a ratio of 0.59 for the predicted C_{max}/*in vivo* C_{max}.
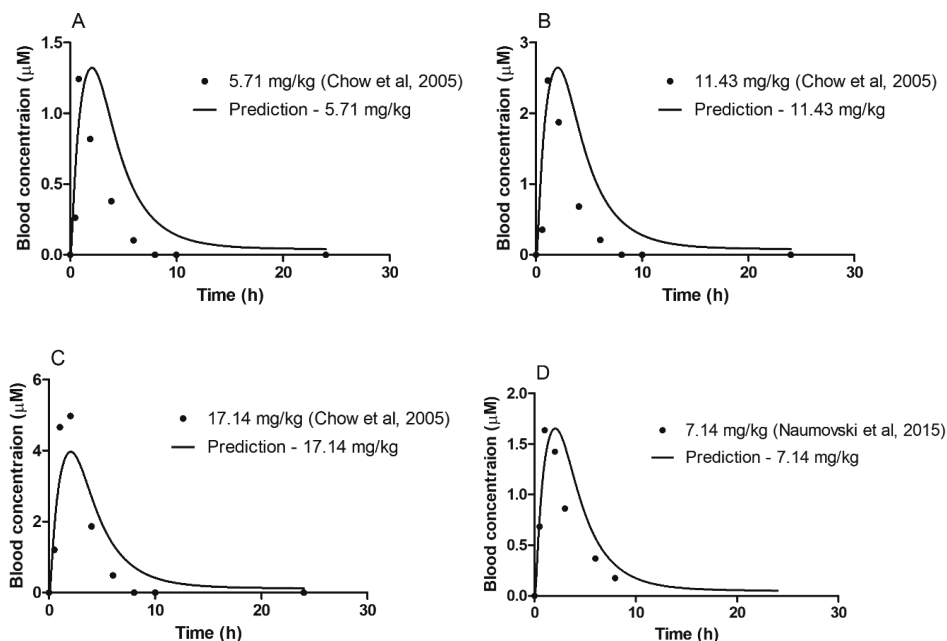
Figure 6. Comparison of predicted and reported time-dependent blood concentrations of free EGCG upon a single oral administration of EGCG at different dose levels under fasting conditions.[34-35]

Table 5. C_{max} and T_{max} of EGCG obtained from *in vivo* data (a single dose under fasting conditions) and predicted by the PBK model in human blood upon a single oral administration.

Dose (mg/kg bw)	*In vivo* C_{max} (μM)	Predicted C_{max} (μM)	Predicted C_{max}/*In vivo* C_{max}	*In vivo* T_{max} (h)	Predicted T_{max} (h)	Predicted T_{max}/*In vivo* T_{max}	References
5.71	1.59	1.32	0.83	1.57	1.93	1.23	34
7.14	1.64	1.65	1.01	1.00	2.16	2.16	35
11.43	3.02	2.64	0.87	1.39	2.19	1.58	34
17.14	6.69	3.96	0.59	1.51	1.94	1.28	34

3.3 PBK Model Prediction of Intestinal Lumen Concentrations of the Model Compounds

Given that EGCG and GA or PG may also exert an effect on the intestinal cells upon their formation in the large intestine, **Figure 7** presents the model predicted human large intestinal lumen concentrations of EGCG, GA and PG after a single dose of 2.86 mg/kg bw EGCG under fasting (**Figure 7A**) and non-fasting conditions (**Figure 7B**) and of 5.71 mg/kg bw EGCG under fasting (**Figure 7C**) and non-fasting conditions (**Figure 7D**). The maximum concentrations of the model compounds reached in the large intestine were predicted to be much higher than the C_{max} values reached in blood after the same dose of administration. For instance, after a single oral administration of 2.86 mg/kg bw EGCG under fasting conditions, the model predicted maximum concentrations of EGCG, GA and PG in the large intestinal lumen to be 15.6, 13.2 and 9.8 µM, respectively, at 3 hours upon intake (**Figure 7A**), being 23.6, 13200 and 4900-fold higher than the predicted C_{max} in blood resulting from the same dose level. When dosing the same amount of EGCG under non-fasting conditions, the model predicted maximum concentrations of EGCG, GA and PG in the large intestinal lumen to be 23.0, 15.6 and 11.4 µM, respectively, being higher than the large intestinal lumen concentrations predicted under fasting conditions (**Figure 7B**). The higher levels predicted under the non-fasting condition could be explained by the fact that the absorption of EGCG was slower under the non-fasting condition which results in a higher amount of unabsorbed EGCG reaching the large intestine. Similar results were also found at a higher oral dose level i.e., 5.71 mg/kg bw EGCG, the model predicted maximum concentrations of EGCG, GA and PG in the large intestinal lumen amounted to respectively 86.5, 21.8 and 15.9 µM under the non-fasting condition, being 376.1, 10900 and 5300-fold higher than the C_{max} in blood predicted at the same dose level (**Figure 7D**).
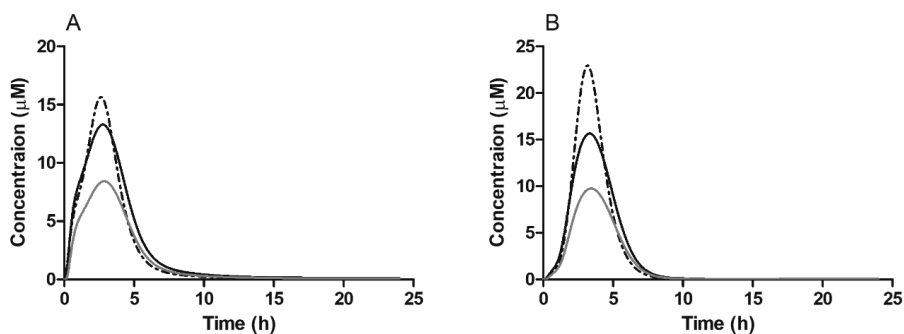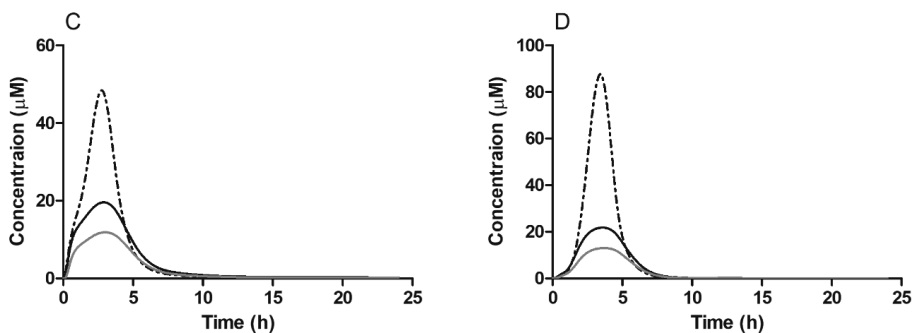
Figure 7. PBK model predicted time-dependent concentration of EGCG (dashed line), GA (black line) and PG (grey line) in the human large intestinal lumen after a single oral administration of 2.86 mg/kg bw EGCG under fasting (A) and non-fasting (B) conditions or of 5.71 mg/kg bw EGCG under fasting (C) and non-fasting conditions (D).

3.4 Sensitivity Analysis of PBK Model

The performance of the model was further evaluated through a sensitivity analysis to assess the most influential parameters affecting the predictions of the blood C_{max} of EGCG, GA and PG upon a single oral administration of either 2.86, 5.71 or 8.57 mg/kg bw under non-fasting conditions. The parameters with an absolute value of the normalized sensitivity coefficient (SC) higher than 0.1 for at least one dose are displayed in **Figure 8**. The results indicate that the prediction of C_{max} of EGCG in the present model is most sensitive to parameters including the fraction of blood flow to small intestine (QIc), the fraction of blood flow to rapidly and slowly perfused tissues (QRc and QSc), and the surface area of each compartment of the small intestine (SAin). The most sensitive chemical-specific parameters for the prediction of the blood C_{max} of EGCG appeared to be the *in vitro* apparent permeability coefficient of EGCG (PappCaco2EGCG) (**Figure 8A**). For the prediction of C_{max} of GA, parameters including body weight (BW), fraction of liver tissue (VLc) and kinetic constants for gut microbial formation of GA and PG (i.e., VmaxLIGAc, VmaxLIPGc and KmLIPG) as well as kinetic constants for hepatic metabolism of GA (CLintS9GA) are of influence (**Figure 8B**). Similarly, the prediction of the C_{max} of PG appeared to be mainly affected by BW, VLc, fraction of blood flow to liver (QLc), kinetic constants for gut microbial formation of GA and catechol (VmaxLIGAc and VmaxLICtc) and the hepatic clearance of PG from S9 fractions (CLintS9GA) (**Figure 8C**).
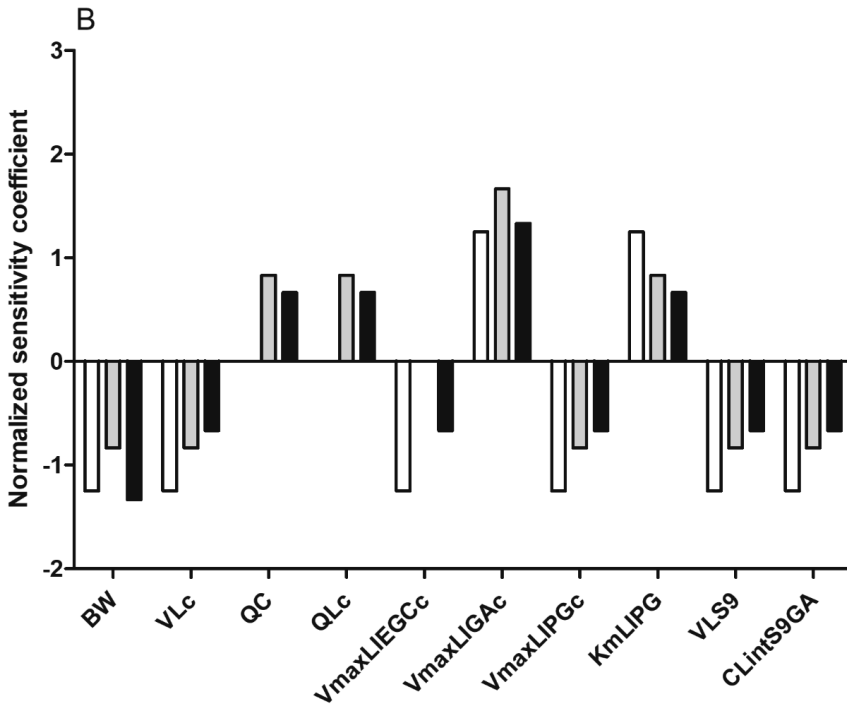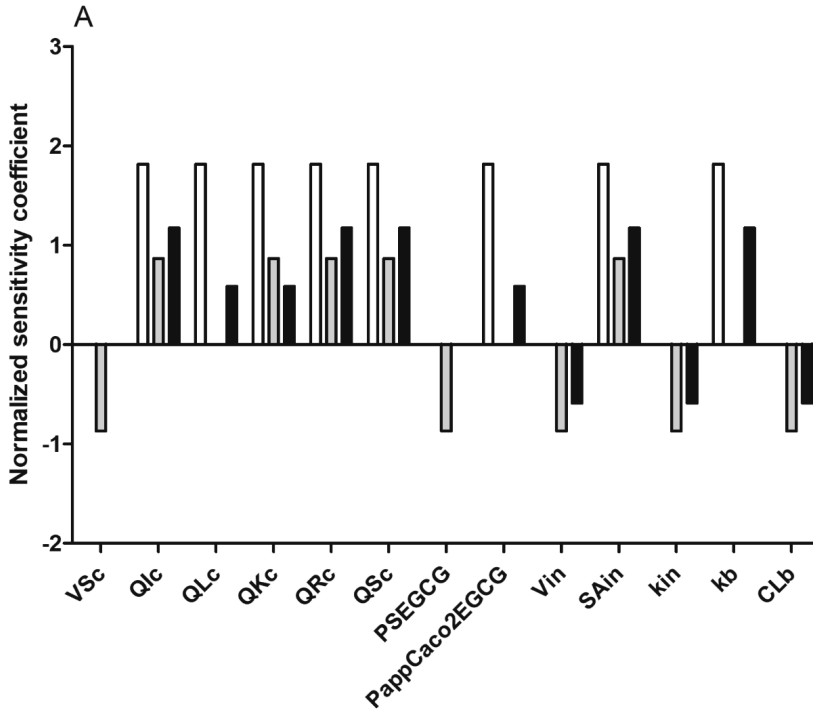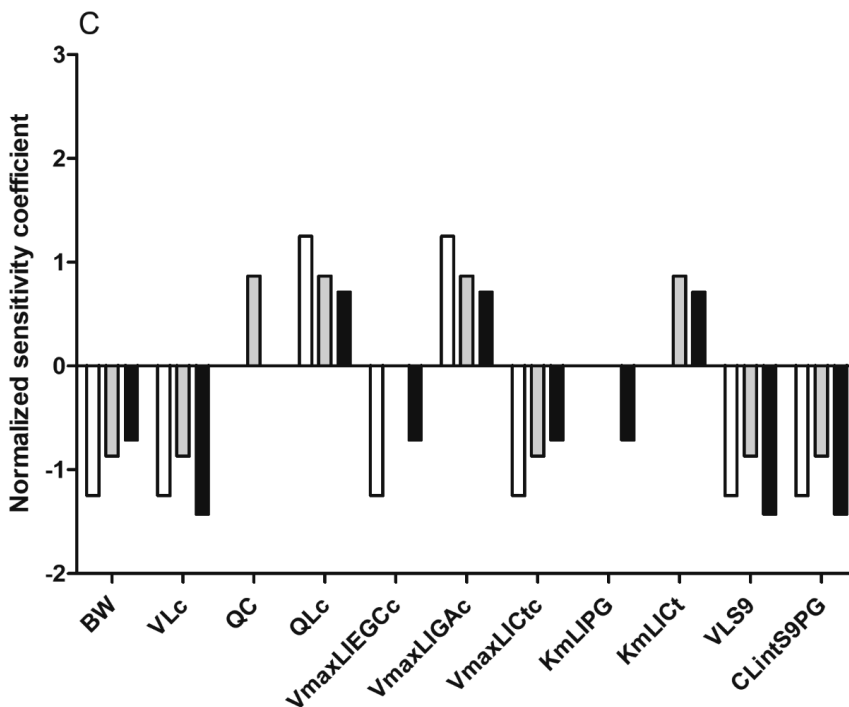
Figure 8. Normalized sensitivity coefficients for the parameters of the PBK model for the prediction of blood C_{max} of EGCG (A), GA (B) and PG (C) after a single oral administration of 2.86 (white bars), 5.71 (grey bars) and 8.57 (black bars) mg/kg bw EGCG under non-fasting conditions. VSc, fraction of slowly perfused tissue; QIc, fraction of blood flow to small intestine; QLc, fraction of blood flow to liver; QRc, fraction of blood flow to rapidly perfused tissue; QSc, fraction of blood flow to slowly perfused tissue; PSEGCG, slowly perfused tissue/blood partition coefficient of EGCG; PappCaco2EGCG, *in vitro* apparent permeability coefficient of EGCG; Vin, volume for each compartment of the small intestine; SAin, surface area of each compartment of the small intestine; kin, transfer rate to next compartment within the small intestine; kb, transfer rate of EGCG from the large intestinal lumen to liver; CLb, biliary clearance of EGCG; BW, body weight; VLc, fraction of liver tissue; QC, cardiac output; VmaxLIEGCc, V_{max} of EGC by the large intestinal lumen; VmaxLIGAc, V_{max} of GA by the large intestinal lumen; VmaxLIPGc, V_{max} of PG by the large intestinal lumen; KmLIPG, K_m for formation of PG by the large intestinal lumen; VLS9, liver S9 protein yield; CLintS9GA, hepatic clearance of GA derived from S9 fractions; VmaxLICtc, V_{max} of catechol by the large intestinal lumen; KmLICt, K_m for formation of catechol by the large intestinal lumen; CLintS9PG, hepatic clearance of PG derived from S9 fractions.

3.5 *In Vitro* Concentration-response Curves from the U2OS-Nrf2 CALUX Reporter Gene Assay

Figure 9 presents the concentration-dependent induction of luciferase expression after 24 h exposure of U2OS-Nrf2 CALUX cells to EGCG, GA or PG. GA and PG display higher potency compared to the parent compound EGCG in activation of the Nrf2-mediated luciferase expression. Given that the concentration-response curves were not parallel, the concentrations of EGCG, GA and PG to reach an IF of 2, 3 and 4-fold were used to obtain an averaged rough estimate of the relative potency (REP) values of GA and PG compared to the parent compound EGCG. The REP values of GA (REP_{GA}) and PG (REP_{PG}) thus calculated amounted for both GA and PG to 2.1 relative to the REP for EGCG set at 1.0. The maximum induction factors (IFs) observed for EGCG, GA and PG were 6.1, 4.8 and 10.9, respectively. Results of the U2OS-Cytotox CALUX assay confirmed that the luciferase inductions by the test compounds were not due to stabilisation of the luciferase reporter protein (**Figure S1** in Supporting Information1).
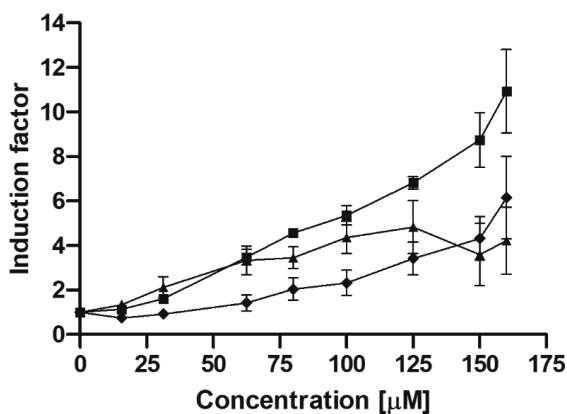
Figure 9. Induction of luciferase expression in U2OS-Nrf2 CALUX reporter cells after 24 h exposure to EGCG (diamonds), GA (triangles) or PG (squares). Results are presented as mean ± SEM compared with the solvent control, derived from at least three independent experiments.

3.6 Contributions of EGCG, GA and PG to Plasma and Intestinal EGCG Equivalents

Figure 10A presents the time-dependent blood concentrations of EGCG (black line), GA (blue dashed line) and PG (red dashed line) after a single oral dose of 2.86 mg/kg bw EGCG under

non-fasting conditions. The results obtained reveal that the blood concentrations of GA and PG upon dosing of EGCG are relatively low, with a C_{max} amounting to respectively 1.1% and 1.2% of the C_{max} of EGCG. To further illustrate the potential relative contributions of EGCG, GA and PG to EGCG-induced Nrf2 activation in humans, **Figure 10B** presents the calculated dose-dependent C_{max} values of EGCG, GA and PG expressed in unbound EGCG equivalents. The results thus obtained demonstrate that the contribution of EGCG to the plasma C_{max} expressed in unbound EGCG equivalents is substantially higher than the contributions of GA and PG, in spite of their higher REP values. Expressed in EGCG equivalents the contribution of GA and PG amounted to respectively 2.9 to 8.8% and 6.7 to 24.8% of the total C_{max} expressed in unbound EGCG equivalents at concentrations decreasing from 20 to 0.2 mg/kg bw with the contribution being higher at lower dose levels. **Figure 10C** presents the model predicted human large intestinal lumen concentrations of EGCG, GA and PG expressed in EGCG equivalents after a single dose of 2.86 mg/kg bw EGCG under non-fasting conditions. At this dose level the predicted C_{max} of EGCG, GA and PG reached in the large intestinal tract expressed in EGCG equivalents are 22.96, 32.72 and 20.32 μM, respectively. **Figure 10D** presents the dose dependent predicted C_{max} of EGCG, GA and PG reached in the large intestinal tract expressed in EGCG equivalents. Expressed in EGCG equivalents the contribution of GA and PG amounted to respectively 2.4 to 50.4% and 1.4 to 35.1% of the total EGCG equivalents at concentrations decreasing from 20 to 0.2 mg/kg bw with the contribution being higher at lower dose levels. This reveals that in the intestines the contributions of GA and PG to the total Nrf2 inducing potential expressed in EGCG equivalents are substantial and may even exceed (when dosing levels are within 4 mg/kg bw which is equal to two to three cups of green tea consumption) that of EGCG itself.
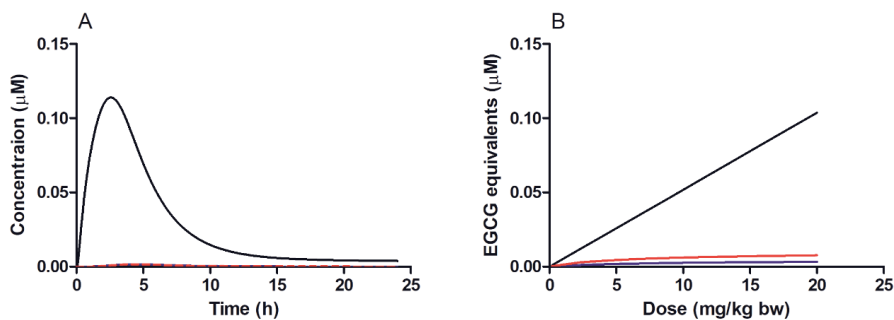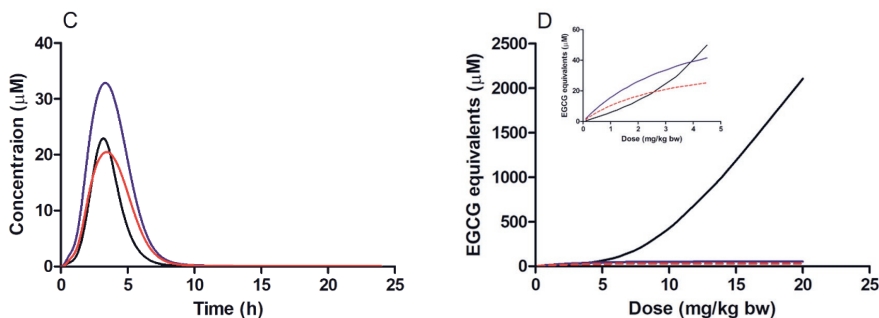
Figure 10. Predicted time-dependent blood concentrations (A) of EGCG (black line), GA (blue dashed line) and PG (red dashed line), dose-dependent relative contribution (B) of EGCG (black line), GA (blue line) and PG (red line) to the plasma Cmax expressed in unbound EGCG equivalents, time-dependent large intestinal lumen concentrations (C) of EGCG (black line), GA (blue line) and PG (red line) expressed in EGCG equivalents after a single oral dose of 2.86 mg/kg bw EGCG under non-fasting conditions and dose-dependent relative contribution (D) of EGCG (black line), GA (blue line) and PG (red dashed line) to the large intestinal C_{max} expressed in EGCG equivalents.

3.7 Translation of the *In Vitro* Concentration-response Curve for EGCG Mediated Nrf2 Induction to An In Vivo Dose-Response Curve and BMD Analysis

Using the developed PBK model, the *in vitro* concentration-response curve for Nrf2 pathway activation by EGCG was converted to an *in vivo* dose-response curve, taking the contributions of its major colonic metabolites GA and PG into account (**Figure 11**). **Figure S2** presents the fitted bootstrap curves from the benchmark dose modeling (BMD) analysis on the data presented in **Figure 11**. The analysis defined the $BMDL_{10}$ and $BMDU_{10}$ as 308 and 4260 mg/kg bw/day for a single oral dose intake of EGCG, and as 277 and 3830 mg/kg bw/day for repeated oral administrations of EGCG under non-fasting conditions. Under fasting conditions, the $BMDL_{10}$ and $BMDU_{10}$ were defined as 55.2 and 763 mg/kg bw/day for a single oral administration of EGCG, and as 50.5 and 698 mg/kg bw/day for repeated oral administrations of EGCG. Furthermore, BMD analysis of *in vitro* concentration-response data was also performed to calculate the benchmark concentration of EGCG resulting in a 10% increase (BMC_{10}) in Nrf2 activation *in vitro* with lower 90% confidence limit ($BMCL_{10}$) and upper 90% confidence limit ($BMCU_{10}$) (**Figure S3**). These nominal $BMCL_{10}$ (3.69 μM) and $BMCU_{10}$ (51.10 μM) values were converted to *in vitro* free $BMCL_{10}$ and $BMCU_{10}$ values by multiplying with 0.451 ($f_{ub, in vitro, EGCG}$), resulting in values of 1.66 and 23.05 μM, respectively. The

calculated BMD_{10} and free BMC_{10} concentration ranges thus obtained were compared to estimated intake dose levels and the PBK model predicted C_{max} expressed in free EGCG equivalents, respectively, upon different dietary exposure scenarios: (1) one to ten cups of green tea, with one cup of 300 mL green tea containing about 110 mg EGCG;[17] (2) one to ten Polyphenon E capsules, each contains 200 mg of EGCG; (3) one to ten capsules (recommended dose level) of an EGCG supplement, containing 175 mg EGCG both under fasting and non-fasting conditions (**Figure 12A** and **B**). **Figure 12C** also presents the estimated combined concentrations of EGCG, GA and PG expressed in EGCG equivalents, calculated taking their respective REP values into account, in the large intestinal lumen at one to ten cups/capsules of green tea/EGCG supplements under both fasting and non-fasting conditions. The results obtained thus reveal that even at the highest EGCG exposure scenarios, the estimated intake levels were still lower than the $BMDL_{10}$ for both single and repeated dose administrations under both fasting and non-fasting conditions (**Figure 12A**) and the predicted unbound plasma C_{max} of EGCG equivalents from different dietary intakes were also lower than the free *in vitro* $BMCL_{10}$ value of EGCG for Nrf2 activation (**Figure 12B**). This indicates that at these intake scenario's systemic C_{max} values expressed in EGCG equivalents will not be high enough to result in Nrf2 activation. However, upon administration of one to ten cups/capsules of green tea/EGCG supplements the predicted EGCG equivalents reached in the large intestinal lumen ranged between 37.2 to 3941.2 µM, concentrations that are substantially higher than the nominal $BMCL_{10}$ (3.69 µM) (**Figure 12C**). These results suggest that the concentrations expressed in EGCG equivalents reached in the large intestinal lumen after realistic amounts of green tea or EGCG supplement consumption may potentially activate Nrf2 mediated gene expression in intestinal cells.
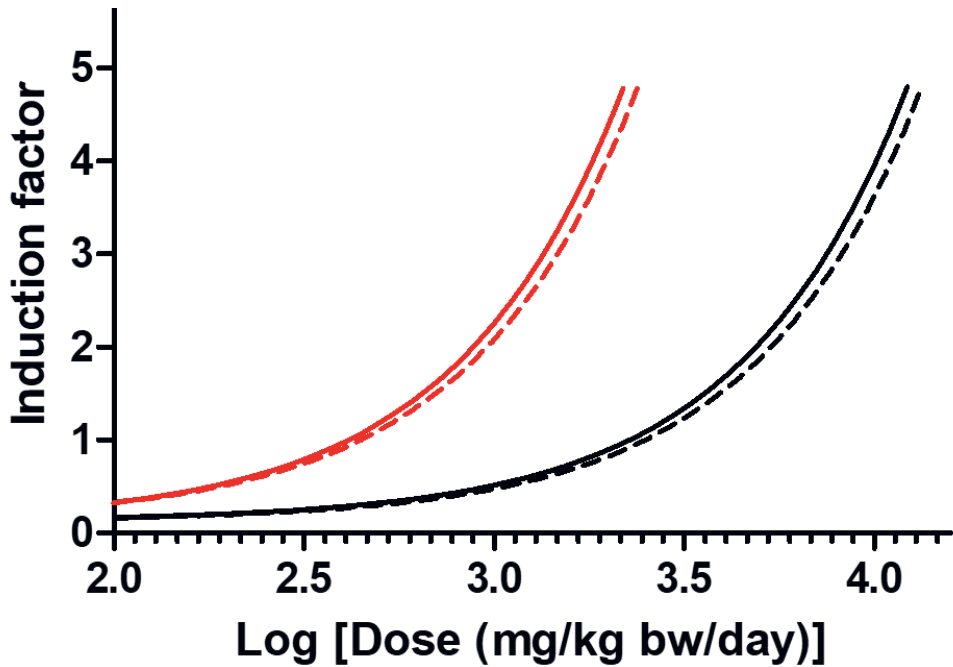
Figure 11. Predicted *in vivo* dose-response curves for Nrf2 induction by a single (dashed line) or repeated (solid line) oral administration of EGCG in humans under fasting (red curves) non-fasting (black curves) conditions obtained by PBK modeling-based reverse dosimetry of the concentration-response curve for EGCG presented in Figure 9.
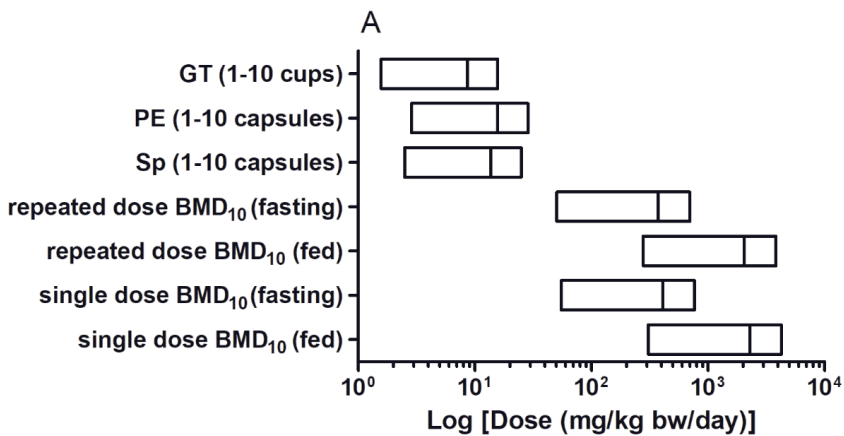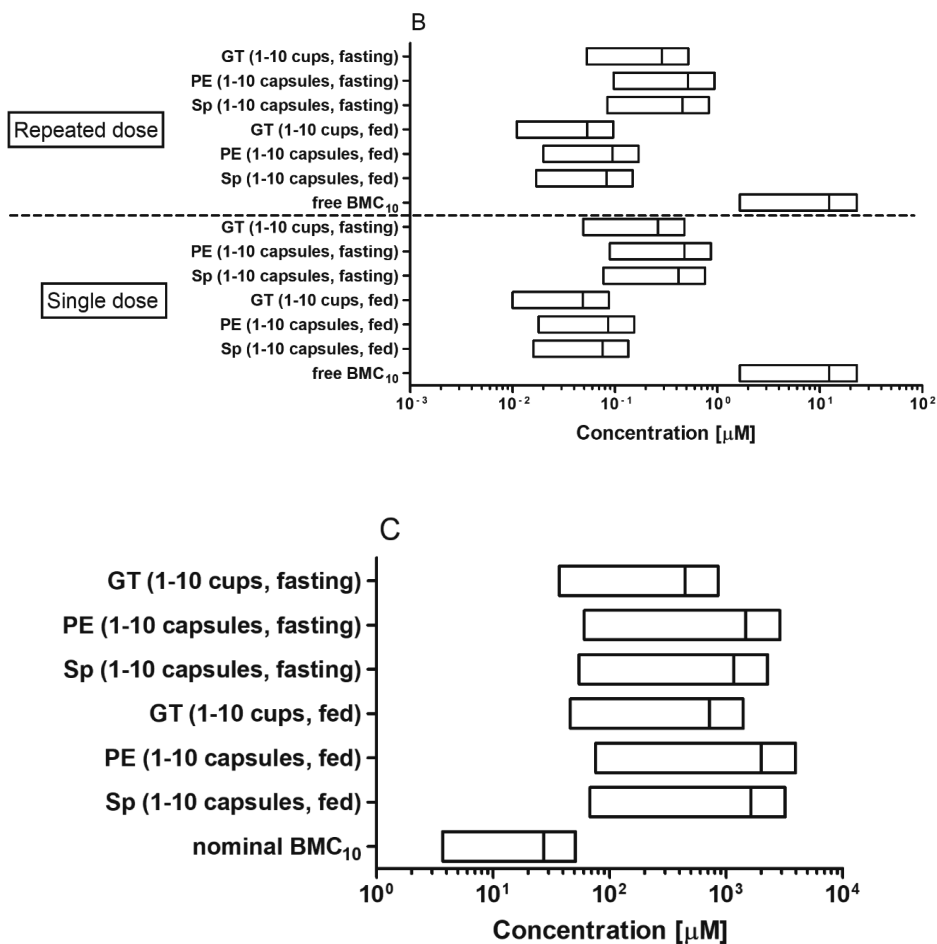
Figure 12. Comparison of estimated intake dose levels of different dosing scenarios to the predicted BMD$_{10}$ (A). Comparison of *in vitro* free BMC$_{10}$ values for induction of Nrf2-mediated gene expression and predicted unbound plasma C$_{max}$ of EGCG equivalents from different dietary intake levels (B). Comparison of *in vitro* nominal BMC$_{10}$ values for induction of Nrf2-mediated gene expression and predicted large intestinal lumen concentrations of EGCG equivalents from a single dose at different dietary intake levels (C). Due to complexity of the content in the intestinal lumen, the fraction unbound values of model compounds in the large intestinal lumen are not available. Thus, instead of free BMC$_{10}$ values, nominal BMC$_{10}$ values were used for comparison in Figure 12C. GT, green tea; PE, Polyphenon E; Sp, EGCG supplement.

4. DISCUSSION

The aim of the present study was to develop a PBK model that includes the gut microbial metabolism compartment to predict both the blood and intestinal concentrations of the parent compound EGCG as well as the colonic metabolites (GA and PG) formed. Furthermore, the current study also aimed at predicting the EGCG dose dependent *in vivo* Nrf2 pathway activation, taking the activity of the colonic metabolites into account. This was done by combining concentration-response curves for the *in vitro* unbound EGCG induced Nrf2 induction quantified in the U2OS-Nrf2 CALUX reporter gene assay and PBK modeling-based reverse dosimetry based on the dose dependent unbound plasma C_{max} expressed in EGCG equivalents. Results obtained indicate that at daily consumption levels of green tea or EGCG supplements, the systemic concentrations reached are unlikely to result in Nrf2 pathway activation while the concentrations of EGCG reached in the intestinal lumen may potentially activate Nrf2 mediated gene expression in intestinal cells.

It has been reported that the majority of ingested EGCG could reach the colon as such where EGCG undergoes extensive microbial metabolism.[17, 53] Thus, the present PBK model integrated microbial EGCG metabolism by including two sub-models for the colonic metabolites GA and PG, respectively. These two microflora-derived metabolites were included since they were reported to be more potent in triggering Nrf2-mediated gene expression than the parent compound EGCG in our previous study.[19] Previous studies showed a proof-of-principle for the inclusion of gut microbial metabolism in PBK modeling using kinetic parameters derived from *in vitro* anaerobic fecal incubations.[25-26] The model predicted the C_{max} of GA and PG, after consumption of two capsules of EGCG supplement (the recommended daily intake), to be less than 1.5% of the blood C_{max} of EGCG and less than 14.1 % when expressed in unbound EGCG equivalents in plasma. The increase in the percentage is due to both the REP values for GA and PG that are higher than the REP value of 1.0 for EGCG and the fact that the plasma fraction unbound values of GA and PG are 1.8 and 4.5 times than that of EGCG, respectively. These percentages reveal that despite of the higher Nrf2 pathway activation ability of GA and PG their roles compared to the contribution of EGCG itself in Nrf2 activation appears to be limited due to their substantially lower systemic concentrations. The predicted low blood level of unconjugated GA is in line with results from an *in vivo* study where human volunteers who ingested green tea tablets and the time-dependent serum concentrations of unconjugated and conjugated GA were at non-detectable levels (detection limit: 2.4 nM).[54]

The estimated dose levels via consumption of either green tea or EGCG supplements were ranging between 1.57 to 28.57 mg/kg bw for a 70 kg man, which appeared to be at least 1.77-

fold lower than the BMDL$_{10}$ values derived from the predicted *in vivo* dose response curves for EGCG induced Nrf2 activation (**Figure 12A**). Similarly, the model predicted plasma unbound C$_{max}$ expressed in EGCG equivalents resulting from the different dietary exposure scenarios were ranging between 0.01 to 0.94 µM, being more than 1.76-fold lower than the unbound *in vitro* BMCL$_{10}$ value of EGCG for Nrf2 activation (**Figure 12B**). Moreover, the repeated dosing of EGCG at a daily base for four successive weeks did not increase the C$_{max}$ values expressed in EGCG equivalents significantly compared to a single oral dose of EGCG. This is due to the fact that EGCG is fully converted by intestinal microbiota or excreted to feces within 12 hours. Thus, these results indicate that it requires at least a 2-fold increase of the current maximum exposure levels to achieve a systemic C$_{max}$ expressed in EGCG equivalents that is able to induce a 10% Nrf2 activation *in vivo*. However, the consumption of such a high dose level of green tea or EGCG supplements is unrealistic and, more importantly, could cause adverse effects. For instance, certain adverse events, such as nausea, abdominal pain, headache, etc., were reported by volunteers taking high dose level, e.g., 17.14 mg/kg bw EGCG.[34] Moreover, high dose levels of green tea-containing dietary supplements (amounting to 10 – 29 mg/kg bw/day) have been reported to be hepatotoxic in humans.[55] In contrast to the systemic concentrations expressed in EGCG equivalents upon use of green tea or green tea containing dietary supplements that appear to be too low to result in activation of Nrf2 mediated gene expression. Concentrations of EGCG, GA and PG in the large intestinal lumen resulting from oral administration of two cups/capsules of green tea/EGCG supplements were predicted to amount to higher levels. For instance, after consumption of two cups of green tea, the maximum concentration expressed in EGCG equivalents was predicted to be 81.53 µM. This relatively high concentration is likely to exert certain local effects e.g., Nrf2 activation in exposed intestinal cells, antioxidant activity, prebiotic activity, etc.[56-57] Especially with respect to the prebiotic activity, it is of interest to note that Liu et al., observed that EGCG treatment was able to increase the relative abundance of beneficial bacteria such as *Christensenellaceae*, *Bacteroides*, and *Bifidobacterium* and inhibit the pathogenic bacteria *Enterobacteriaceae*, *Fusobacterium varium* and *Bilophila*.[56] Meanwhile, these changes in microbial composition could in turn alter the metabolic patterns of EGCG. The reciprocal interactions between EGCG and gut microbiota may thus contribute to the ultimate biological effects.[56, 58-59]

The current PBK model provides an alternative tool that includes microbial metabolism in an *in vitro - in silico* method to facilitate QIVIVE, which contributes to the 3Rs principle providing a NAM.[60] Nevertheless, it is important to note that some conditions that could affect EGCG

absorption, may influence the model predictions when they would be taken into account. For instance, the maximum free EGCG plasma concentrations in human increased 3.7 – 5.6 fold when the Polyphenon E capsules, containing 400 – 1200 mg EGCG, were taken under fasting conditions as compared to non-fasting conditions.[34] The model took this into account by using a modified value for the rate of EGCG uptake. Additionally, the bioavailability of EGCG taken without breakfast was 2.7 and 3.5 times higher than when taken with breakfast or strawberry sorbet,[35] a factor that can be taken into account by lowering the dose of EGCG actually being taken into account in the model calculations, assuming part of EGCG will be excreted in feces unmodified. Limited *in vivo* bioavailability may be related to the fact that food components reduced the dissolution of EGCG by increasing the viscosity of the digestive fluid or via increased bile secretion to facilitate excretion of EGCG into feces.[35, 37, 61]

Some of the parameters used in the developed PBK model were estimated values by assuming the parameter to be the same value as the parameter of a similar compound (e.g., $V_{max}LICt$, K_mLICt, CLintS9GA and CLintS9PG). The results of the sensitivity analysis revealed that all of these estimated parameters only had a very limited impact on the predictions for the systemic concentrations of EGCG (**Figure 8A**). Though these estimated parameters may affect the predictions of systemic concentrations of GA and PG (**Figure 8B-C**), it is not likely to change the fact that the very low systemic concentrations of these microbial metabolites are not enough to exert biological activities, e.g., Nrf2 activation. The results of the sensitivity analysis on the model predictions of the large intestinal concentrations of EGCG, GA and PG show that neither CLintS9GA nor CLintS9PG could affect the model predictions no matter what the exposure levels of EGCG were (data not shown). At a higher dose level, i.e., above 8.57 mg/kg bw, $V_{max}LICt$ and K_mLICt could affect the model predictions on the large intestinal concentrations of PG which may suggest a further refinement on this parameter to get a more accurate prediction for PG at higher dose levels of EGCG may be of interest. Generally, the current PBK models could adequately predict the *in vivo* kinetics of EGCG after oral administrations under different conditions.

In addition, it is relevant to note that the current PBK model is developed using parameter values for the average population, and thus does not take interindividual differences into account. For example, the P-glycoprotein (P-gp) transporter is a transporter of EGCG and its polymorphisms in humans has been associated with variations of C_{max} and bioavailability of EGCG.[62] Therefore, future models could include kinetics of this active transporter, and with the help of Monte Carlo modeling may provide insights on variabilities existing between

different individuals in *in vivo* studies. This also holds for interindividual differences in the gut microbial metabolism and hepatic metabolism of EGCG and its major metabolites. For instance, several studies have confirmed there are substantial interindividual differences in colonic microbial metabolism of green tea catechins, where potential fast and slow metabolisers may be characterized.[19, 63-64] By performing liver S9 incubations using liver S9 fractions of different individuals and fecal anaerobic incubations using the fecal suspension from individual volunteers, kinetic constants of different individuals could be obtained to enable PBK model predictions of potential interindividual variabilities in EGCG, GA and PG *in vivo* kinetics and define the distributions in PBK model parameters to be used in Monte Carlo simulations.

In conclusion, the newly developed PBK model was shown to be able to adequately predict blood concentrations of EGCG and to include gut microbial metabolism in the model. Although microbial metabolites GA and PG are more capable of inducing Nrf2 pathway activation than EGCG, their contributions to systemic induction of Nrf2 mediated gene expression were predicted to be limited due to their relatively lower systemic concentrations compared to EGCG. Besides, the dose-response curve derived by the PBK modeling facilitated reverse dosimetry approach indicates that daily intake of EGCG supplements or green tea is unlikely to result in enhanced systemic Nrf2-mediated gene expression. The potential Nrf2 mediated beneficial effects of EGCG, GA and PG might be limited to the intestinal tissue that is predicted to be exposed to substantially higher concentrations of EGCG and its active intestinal microbial metabolites. The present study illustrates a proof-of-principle on how to integrate *in vitro* data and *in silico* PBK modeling to predict *in vivo* kinetics of model compounds and characterise their dose levels needed to induce Nrf2 induction *in vivo* in humans, without the need for using laboratory animals or conducting a human intervention study.

AUTHOR INFORMATION

Corresponding Author

Chen Liu - Division of Toxicology, Wageningen University and Research, Wageningen, The Netherlands; orcid.org/0000-0002-7332-9304; Phone: +31633475749; E-mail: chen.liu@wur.nl. Fax: 0317-(4)84931; Fax: 0317-(4)84931

Authors

Jolijn van Mil - Division of Toxicology, Wageningen University and Research, Wageningen, The Netherlands

Annelies Noorlander - Division of Toxicology, Wageningen University and Research, Wageningen, The Netherlands

Ivonne M. C. M. Rietjens - Division of Toxicology, Wageningen University and Research, Wageningen, The Netherlands

Conflict of interest

The authors declare that there is no conflict of interest.

ABBREVIATIONS UESD

EGCG, (-)-epigallocatechin gallate; EGC, (-)-epigallocatechin; GA, gallic acid; PG, pyrogallol; PBK, physiologically based kinetic; NAM, new approach methodology; LC-TQ-MS, liquid chromatograph triple quadrupole mass spectrometry; Keap1/Nrf2, Kelch-like ECH-associated protein 1/NF-E2-related factor 2; IF, induction factor; BMD, benchmark dose modeling; POD, point of departure; EFSA, European Food Safety Authority; REP, relative potency; QIVIVE, the quantitative *in vitro* to *in vivo* extrapolation; DCC-FCS, dextran-coated charcoal-treated fetal calf serum

5. References

1.   Zhou, Y.; Huang, W.; Liu, X.; Cao, W.; Wang, D.; Liu, X.; Pang, Y.; Wen, S.; Zhang, X., Interannual variation and exposure risk assessment of lead in brick tea in Hubei, China. *Science of The Total Environment* **2020,** *745*, 141004.

2.   Reygaert, W. C., Green tea catechins: Their use in treating and preventing infectious diseases. *BioMed research international* **2018,** *2018*.

3.   Cabrera, C.; Artacho, R.; Giménez, R., Beneficial effects of green tea—a review. *Journal of the American College of Nutrition* **2006,** *25* (2), 79-99.

4.   Bernatoniene, J.; Kopustinskiene, D. M., The role of catechins in cellular responses to oxidative stress. *Molecules* **2018,** *23* (4), 965.

5.   Musial, C.; Kuban-Jankowska, A.; Gorska-Ponikowska, M., Beneficial properties of green tea catechins. *International journal of molecular sciences* **2020,** *21* (5), 1744.

6.   Xu, J.; Xu, Z.; Zheng, W., A review of the antiviral role of green tea catechins. *Molecules* **2017,** *22* (8), 1337.

7.   Butt, M. S.; Ahmad, R. S.; Sultan, M. T.; Qayyum, M. M. N.; Naz, A., Green tea and anticancer perspectives: updates from last decade. *Critical reviews in food science and nutrition* **2015,** *55* (6), 792-805.

8.   Velayutham, P.; Babu, A.; Liu, D., Green tea catechins and cardiovascular health: an update. *Current medicinal chemistry* **2008,** *15* (18), 1840.

9.   Onakpoya, I.; Spencer, E.; Heneghan, C.; Thompson, M., The effect of green tea on blood pressure and lipid profile: a systematic review and meta-analysis of randomized clinical trials. *Nutrition, Metabolism and Cardiovascular Diseases* **2014,** *24* (8), 823-836.

10.   Leung, C.-H.; Zhang, J.-T.; Yang, G.-J.; Liu, H.; Han, Q.-B.; Ma, D.-L., Emerging Screening Approaches in the development of Nrf2–Keap1 protein–protein interaction inhibitors. *International journal of molecular sciences* **2019,** *20* (18), 4445.

11.   He, F.; Ru, X.; Wen, T., NRF2, a transcription factor for stress response and beyond. *International journal of molecular sciences* **2020,** *21* (13), 4777.

12.   Yamamoto, M.; Kensler, T. W.; Motohashi, H., The KEAP1-NRF2 system: a thiol-based sensor-effector apparatus for maintaining redox homeostasis. *Physiological reviews* **2018,** *98* (3), 1169-1203.

13.   Grzesik, M.; Bartosz, G.; Stefaniuk, I.; Pichla, M.; Namieśnik, J.; Sadowska-Bartosz, I., Dietary antioxidants as a source of hydrogen peroxide. *Food chemistry* **2019,** *278*, 692-699.

14.   Muzolf-Panek, M.; Gliszczyńska-Świgło, A.; de Haan, L.; Aarts, J. M.; Szymusiak, H.; Vervoort, J. M.; Tyrakowska, B.; Rietjens, I. M. C. M., Role of catechin quinones in the induction of EpRE-mediated gene expression. *Chemical research in toxicology* **2008,** *21* (12), 2352-2360.

15.   Na, H.-K.; Surh, Y.-J., Modulation of Nrf2-mediated antioxidant and detoxifying enzyme induction by the green tea polyphenol EGCG. *Food and Chemical Toxicology* **2008,** *46* (4), 1271-1278.

16.   Liu, Z.; Bruins, M. E.; Ni, L.; Vincken, J.-P., Green and black tea phenolics: Bioavailability, transformation by colonic microbiota, and modulation of colonic microbiota. *Journal of Agricultural and Food Chemistry* **2018,** *66* (32), 8469-8477.

17.   Stalmach, A.; Mullen, W.; Steiling, H.; Williamson, G.; Lean, M. E.; Crozier, A., Absorption, metabolism, and excretion of green tea flavan-3-ols in humans with an ileostomy. *Molecular nutrition & food research* **2010,** *54* (3), 323-334.

18.   Monagas, M.; Urpi-Sarda, M.; Sánchez-Patán, F.; Llorach, R.; Garrido, I.; Gómez-Cordovés, C.; Andres-Lacueva, C.; Bartolomé, B., Insights into the metabolism and microbial biotransformation of dietary flavan-3-ols and the bioactivity of their metabolites. *Food & function* **2010,** *1* (3), 233-253.

19.   Liu, C.; Vervoort, J.; van den Elzen, J.; Beekmann, K.; Baccaro, M.; de Haan, L.; Rietjens, I. M. C. M., Interindividual Differences in Human In Vitro Intestinal Microbial Conversion of Green Tea (-)-Epigallocatechin-

3‑O‑Gallate and Consequences for Activation of Nrf2 Mediated Gene Expression. *Molecular Nutrition & Food Research* **2021,** *65* (2), 2000934.

20.   Pan, C.; Zhou, S.; Wu, J.; Liu, L.; Song, Y.; Li, T.; Ha, L.; Liu, X.; Wang, F.; Tian, J., NRF2 plays a critical role in both self and EGCG protection against diabetic testicular damage. *Oxidative Medicine and Cellular Longevity* **2017,** *2017*.

21.   Mi, Y.; Zhang, W.; Tian, H.; Li, R.; Huang, S.; Li, X.; Qi, G.; Liu, X., EGCG evokes Nrf2 nuclear translocation and dampens PTP1B expression to ameliorate metabolic misalignment under insulin resistance condition. *Food & function* **2018,** *9* (3), 1510-1523.

22.   Datta, S.; Sinha, D., EGCG maintained Nrf2-mediated redox homeostasis and minimized etoposide resistance in lung cancer cells. *Journal of Functional Foods* **2019,** *62*, 103553.

23.   Estudante, M.; Morais, J. G.; Soveral, G.; Benet, L. Z., Intestinal drug transporters: an overview. *Advanced drug delivery reviews* **2013,** *65* (10), 1340-1356.

24.   Louisse, J.; Beekmann, K.; Rietjens, I. M. C. M., Use of physiologically based kinetic modeling-based reverse dosimetry to predict in vivo toxicity from in vitro data. *Chemical research in toxicology* **2017,** *30* (1), 114-125.

25.   Wang, Q.; Spenkelink, B.; Boonpawa, R.; Rietjens, I. M. C. M.; Beekmann, K., Use of Physiologically Based Kinetic Modeling to Predict Rat Gut Microbial Metabolism of the Isoflavone Daidzein to S‑Equol and Its Consequences for ERα Activation. *Molecular nutrition & food research* **2020,** *64* (6), 1900912.

26.   Mendez‑Catala, D. M.; Wang, Q.; Rietjens, I. M. C. M., PBK Model‑Based Prediction of Intestinal Microbial and Host Metabolism of Zearalenone and Consequences for its Estrogenicity. *Molecular nutrition & food research* **2021**, 2100443.

27.   Wang, Q.; Spenkelink, B.; Boonpawa, R.; Rietjens, I. M. C. M., Use of Physiologically Based Pharmacokinetic Modeling to Predict Human Gut Microbial Conversion of Daidzein to S-Equol. *Journal of agricultural and food chemistry* **2021**.

28.   Davies, B.; Morris, T., Physiological parameters in laboratory animals and humans. *Pharmaceutical research* **1993,** *10* (7), 1093-1095.

29.   Gilbert‑Sandoval, I.; Wesseling, S.; Rietjens, I. M. C. M., Predicting the acute liver toxicity of aflatoxin B1 in rats and humans by an in vitro–in silico testing strategy. *Molecular nutrition & food research* **2020,** *64* (13), 2000063.

30.   Brown, R. P.; Delp, M. D.; Lindstedt, S. L.; Rhomberg, L. R.; Beliles, R. P., Physiological parameter values for physiologically based pharmacokinetic models. *Toxicology and industrial health* **1997,** *13* (4), 407-484.

31.   DeJongh, J.; Verhaar, H. J.; Hermens, J. L., A quantitative property-property relationship (QPPR) approach to estimate in vitro tissue-blood partition coefficients of organic chemicals in rats and humans. *Archives of Toxicology* **1997,** *72* (1), 17-25.

32.   Hou, T.; Zhang, W.; Xia, K.; Qiao, X.; Xu, X., ADME evaluation in drug discovery. 5. Correlation of Caco-2 permeation with simple molecular properties. *Journal of chemical information and computer sciences* **2004,** *44* (5), 1585-1600.

33.   Sun, D.; Lennernas, H.; Welage, L. S.; Barnett, J. L.; Landowski, C. P.; Foster, D.; Fleisher, D.; Lee, K.-D.; Amidon, G. L., Comparison of human duodenum and Caco-2 gene expression profiles for 12,000 gene sequences tags and correlation with permeability of 26 drugs. *Pharmaceutical research* **2002,** *19* (10), 1400-1416.

34.   Chow, H. S.; Hakim, I. A.; Vining, D. R.; Crowell, J. A.; Ranger-Moore, J.; Chew, W. M.; Celaya, C. A.; Rodney, S. R.; Hara, Y.; Alberts, D. S., Effects of dosing condition on the oral bioavailability of green tea catechins after single-dose administration of Polyphenon E in healthy individuals. *Clinical cancer research* **2005,** *11* (12), 4627-4633.

35.   Naumovski, N.; Blades, B. L.; Roach, P. D., Food inhibits the oral bioavailability of the major green tea antioxidant epigallocatechin gallate in humans. *Antioxidants* **2015,** *4* (2), 373-393.

36.   Zhang, M.; van Ravenzwaay, B.; Fabian, E.; Rietjens, I. M. C. M.; Louisse, J., Towards a generic physiologically based kinetic model to predict in vivo uterotrophic responses in rats by reverse dosimetry of in vitro estrogenicity data. *Archives of toxicology* **2018,** *92* (3), 1075-1088.

37.   Chu, K. O.; Pang, C. C., Pharmacokinetics and disposition of green tea catechins. *Pharmacokinetics and Adverse Effects of Drugs: Mechanisms and Risks Factors* **2018,** *17*.

38.   Chow, H. S.; Cai, Y.; Alberts, D. S.; Hakim, I.; Dorr, R.; Shahi, F.; Crowell, J. A.; Yang, C. S.; Hara, Y., Phase I pharmacokinetic study of tea polyphenols following single-dose administration of epigallocatechin gallate and polyphenon E. *Cancer Epidemiology and Prevention Biomarkers* **2001,** *10* (1), 53-58.

39.   Shahrzad, S.; Aoyagi, K.; Winter, A.; Koyama, A.; Bitsch, I., Pharmacokinetics of gallic acid and its relative bioavailability from tea in healthy humans. *The Journal of Nutrition* **2001,** *131* (4), 1207-1210.

40.   Ma, F.-W.; Deng, Q.-F.; Zhou, X.; Gong, X.-J.; Zhao, Y.; Chen, H.-G.; Zhao, C., The tissue distribution and urinary excretion study of gallic acid and protocatechuic acid after oral administration of Polygonum capitatum extract in rats. *Molecules* **2016,** *21* (4), 399.

41.   Rose, C.; Parker, A.; Jefferson, B.; Cartmell, E., The characterization of feces and urine: a review of the literature to inform advanced treatment technology. *Critical reviews in environmental science and technology* **2015,** *45* (17), 1827-1879.

42.   Zhang, M.; van Ravenzwaay, B.; Rietjens, I. M. C. M., Development of a generic physiologically based kinetic model to predict in vivo uterotrophic responses induced by estrogenic chemicals in rats based on in vitro bioassays. *Toxicological sciences* **2020,** *173* (1), 19-31.

43.   Lee, M.-J.; Maliakal, P.; Chen, L.; Meng, X.; Bondoc, F. Y.; Prabhu, S.; Lambert, G.; Mohr, S.; Yang, C. S., Pharmacokinetics of tea catechins after ingestion of green tea and (−)-epigallocatechin-3-gallate by humans: formation of different metabolites and individual variability. *Cancer Epidemiology and Prevention Biomarkers* **2002,** *11* (10), 1025-1032.

44.   Chow, H. S.; Cai, Y.; Hakim, I. A.; Crowell, J. A.; Shahi, F.; Brooks, C. A.; Dorr, R. T.; Hara, Y.; Alberts, D. S., Pharmacokinetics and safety of green tea polyphenols after multiple-dose administration of epigallocatechin gallate and polyphenon E in healthy individuals. *Clinical cancer research* **2003,** *9* (9), 3312-3319.

45.   Sohlenius-Sternbeck, A.-K.; Afzelius, L.; Prusis, P.; Neelissen, J.; Hoogstraate, J.; Johansson, J.; Floby, E.; Bengtsson, A.; Gissberg, O.; Sternbeck, J., Evaluation of the human prediction of clearance from hepatocyte and microsome intrinsic clearance for 52 drug compounds. *Xenobiotica* **2010,** *40* (9), 637-649.

46.   Law, F. C.; Yao, M.; Bi, H. C.; Lam, S., Physiologically based pharmacokinetic modeling of tea catechin mixture in rats and humans. *Pharmacology research & perspectives* **2017,** *5* (3), e00305.

47.   Evans, M. V.; Andersen, M. E., Sensitivity analysis of a physiological model for 2, 3, 7, 8-tetrachlorodibenzo-p-dioxin (TCDD): assessing the impact of specific model parameters on sequestration in liver and fat in the rat. *Toxicological sciences* **2000,** *54* (1), 71-80.

48.   van der Linden, S. C.; von Bergh, A. R.; van Vught-Lussenburg, B. M.; Jonker, L. R.; Teunis, M.; Krul, C. A.; van der Burg, B., Development of a panel of high-throughput reporter-gene assays to detect genotoxicity and oxidative stress. *Mutation Research/Genetic Toxicology and Environmental Mutagenesis* **2014,** *760*, 23-32.

49.   Lobell, M.; Sivarajah, V., In silico prediction of aqueous solubility, human plasma protein binding and volume of distribution of compounds from calculated pK a and AlogP98 values. *Molecular diversity* **2003,** *7* (1), 69-87.

50.   Punt, A.; Pinckaers, N.; Peijnenburg, A.; Louisse, J., Development of a Web-Based Toolbox to Support Quantitative In-Vitro-to-In-Vivo Extrapolations (QIVIVE) within Nonanimal Testing Strategies. *Chemical research in toxicology* **2020,** *34* (2), 460-472.

51.   van Tongeren, T. C.; Moxon, T. E.; Dent, M. P.; Li, H.; Carmichael, P. L.; Rietjens, I. M. C. M., Next generation risk assessment of human exposure to anti-androgens using newly defined comparator compound values. *Toxicology in Vitro* **2021,** *73*, 105132.

52.   Mathew, J.; Sankar, P.; Varacallo, M., Physiology, blood plasma. **2018**.

53.   Roowi, S.; Stalmach, A.; Mullen, W.; Lean, M. E.; Edwards, C. A.; Crozier, A., Green tea flavan-3-ols: colonic degradation and urinary excretion of catabolites by humans. *Journal of agricultural and food chemistry* **2010,** *58* (2), 1296-1304.

54.   Narumi, K.; Sonoda, J.-I.; Shiotani, K.; Shigeru, M.; Shibata, M.; Kawachi, A.; Tomishige, E.; Sato, K.; Motoya, T., Simultaneous detection of green tea catechins and gallic acid in human serum after ingestion of green tea tablets using ion-pair high-performance liquid chromatography with electrochemical detection. *Journal of Chromatography B* **2014,** *945*, 147-153.

55.   Mazzanti, G.; Menniti-Ippolito, F.; Moro, P. A.; Cassetti, F.; Raschetti, R.; Santuccio, C.; Mastrangelo, S., Hepatotoxicity from green tea: a review of the literature and two unpublished cases. *European journal of clinical pharmacology* **2009,** *65* (4), 331-341.

56.   Liu, Z.; de Bruijn, W. J.; Bruins, M. E.; Vincken, J.-P., Reciprocal interactions between epigallocatechin-3-gallate (EGCG) and human gut microbiota in vitro. *Journal of Agricultural and Food Chemistry* **2020,** *68* (36), 9804-9815.

57.   Badhani, B.; Sharma, N.; Kakkar, R., Gallic acid: a versatile antioxidant with promising therapeutic and industrial applications. *Rsc Advances* **2015,** *5* (35), 27540-27557.

58.   Cheng, M.; Zhang, X.; Guo, X. J.; Wu, Z. F.; Weng, P. F., The interaction effect and mechanism between tea polyphenols and intestinal microbiota: Role in human health. *Journal of Food Biochemistry* **2017,** *41* (6), e12415.

59.   Li, Q.; Van de Wiele, T., Gut microbiota as a driver of the interindividual variability of cardiometabolic effects from tea polyphenols. *Critical Reviews in Food Science and Nutrition* **2021**, 1-27.

60.   Olsson, I. A. S.; Franco, N. H.; Weary, D. M.; Sandøe, P., The 3Rs principle–mind the ethical gap. *ALTEX* **2012,** *1*, 333-336.

61.   Reppas, C.; Eleftheriou, G.; Macheras, P.; Symillides, M.; Dressman, J., Effect of elevated viscosity in the upper gastrointestinal tract on drug absorption in dogs. *European journal of pharmaceutical sciences* **1998,** *6* (2), 131-139.

62.   Hung, C.-C.; Chiou, M.-H.; Teng, Y.-N.; Hsieh, Y.-W.; Huang, C.-L.; Lane, H.-Y., Functional impact of ABCB1 variants on interactions between P-glycoprotein and methadone. *PloS one* **2013,** *8* (3), e59419.

63.   Liu, C.; Vervoort, J.; Beekmann, K.; Baccaro, M.; Kamelia, L.; Wesseling, S.; Rietjens, I. M. C. M., Interindividual Differences in Human Intestinal Microbial Conversion of (−)-Epicatechin to Bioactive Phenolic Compounds. *Journal of agricultural and food chemistry* **2020,** *68* (48), 14168-14181.

64.   Li, Q.; Van Herreweghen, F.; De Mey, M.; Goeminne, G.; Van de Wiele, T., The Donor-Dependent and Colon-Region-Dependent Metabolism of (+)-Catechin by Colonic Microbiota in the Simulator of the Human Intestinal Microbial Ecosystem. *Molecules* **2022,** *27* (1), 73.

Supporting Information

U2OS-Cytotox CALUX assay (Figure S1 in Supporting Information1). BMD analysis on the PBK model predicted dose-response curve of EGCG (Figure S2 in Supporting Information1). BMD analysis on the *in vitro* concentration-response curve of EGCG induced luciferase

expression in U2OS-Nrf2 CALUX reporter gene assay (Figure S3 in Supporting Information1). PBK model code (Supporting Information2).

Supporting Information 1
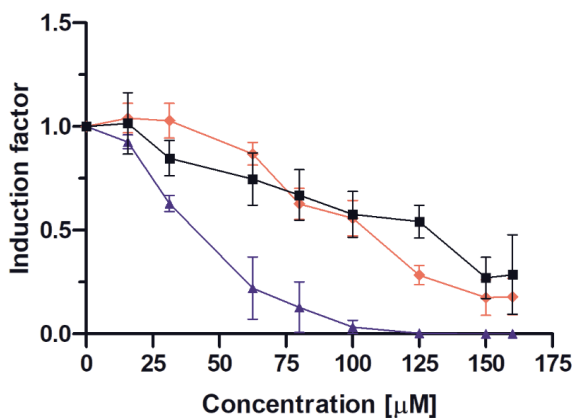
Figure S1. Induction of luciferase expression in U2OS-Cytotox CALUX reporter cells after 24 h exposure to EGCG (red line with diamond symbols), GA (blue line with triangle symbols) or PG (black line with square symbols). Results are presented as mean ± SEM compared with the solvent control, derived from three independent experiments.

<div style="float: right">**Chapter 6**</div>

B

**bootstrap curves
based on model averaging**

version: 70.0
model averaging results
dtype   10
selected   all
dose scaling: 1
conf level: 0.9
number of runs: 200
CES   0.1
BMD CI
 280 3830

C

**bootstrap curves
based on model averaging**

version: 70.0
model averaging results
dtype   10
selected   all
dose scaling: 1
conf level: 0.9
number of runs: 200
CES   0.1
BMD CI
 55 763
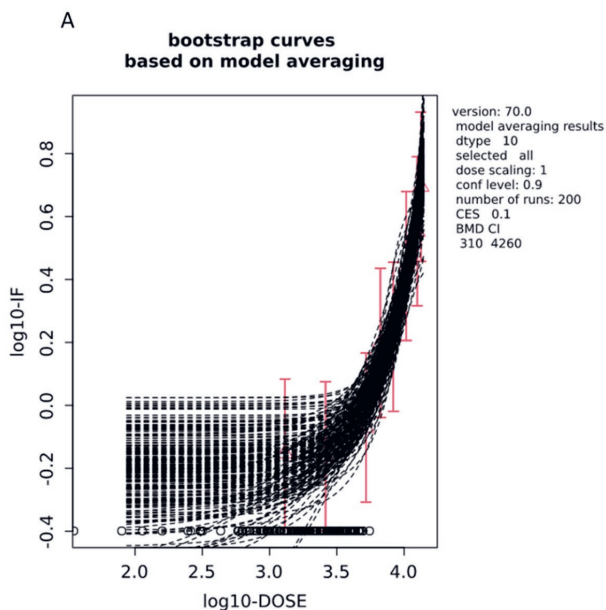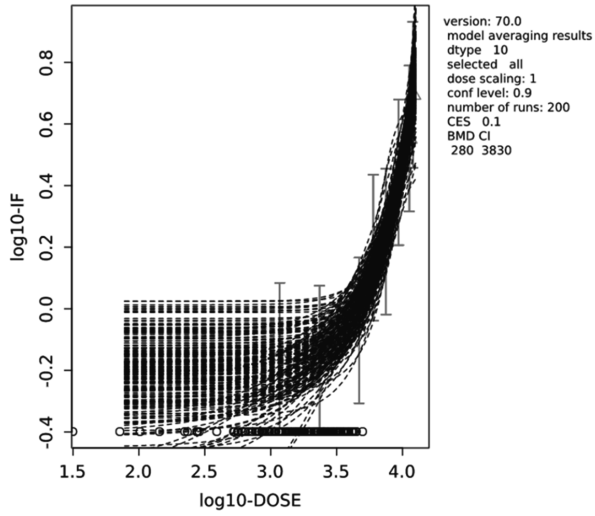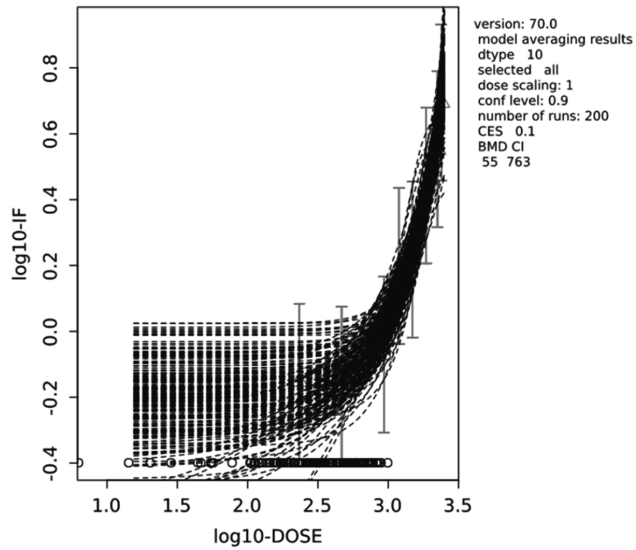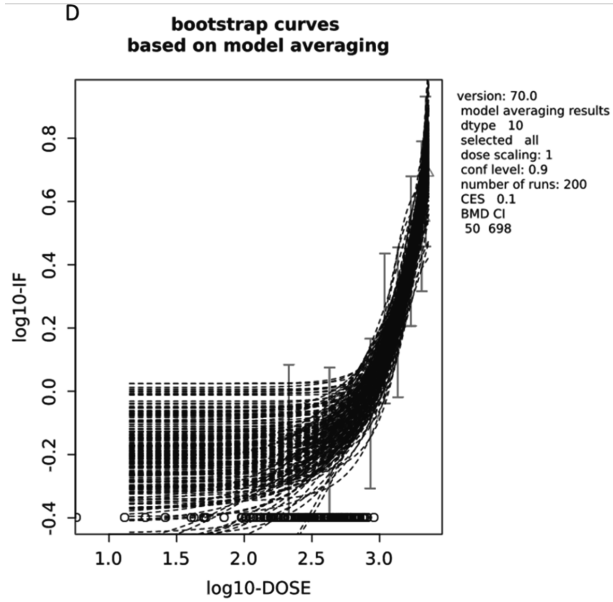
Figure S2. Benchmark dose modeling (BMD) analysis on the *in vivo* dose-response curve for Nrf2 induction by a single (A) or repeated (B) oral administration of EGCG in humans under non-fasting conditions and by a single(C) or repeated (D) oral administration of EGCG in humans under fasting conditions.
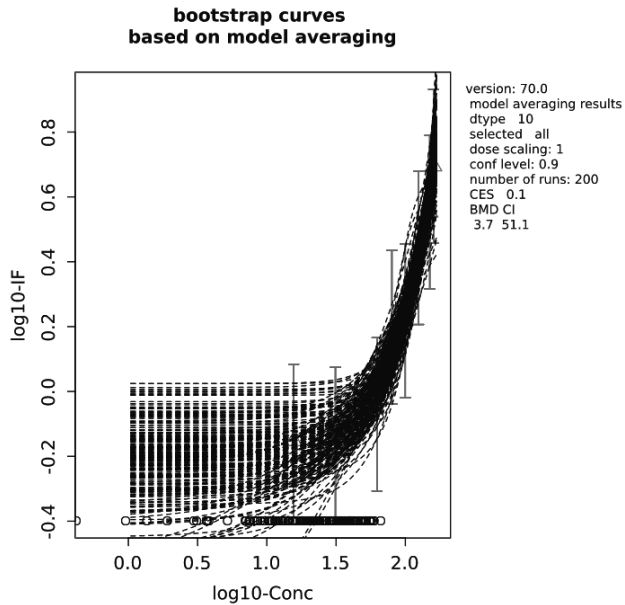
Figure S3. Benchmark dose modeling (BMD) analysis on the *in vitro* concentration-response curve of EGCG induced luciferase expression in U2OS-Nrf2 CALUX reporter gene assay.

Support Information 2

Model code: single/repeated does under fasting/non-fasting conditions

```
;============================================================
; Physiological parameters
;============================================================
; Tissue volumes
BW = 70  {Kg}              ; body weight human
VSIc = 0.0091                      ; fraction of small intestine[1]
VLIc =    0.0053                    ; fraction of large intestine[1]
VLc = 0.0257                        ; fraction of liver tissue[1]
VKc = 0.0044                        ; fraction of kidney tissue[1]
VRc = 0.0683                        ; fraction of rapidly perfused tissue[1]
VSc = 0.58                          ; fraction of slowly perfused tissue[1]
VFc = 0.2142                        ; fraction of fat tissue[1]
VBc = 0.079                         ; fraction of blood[1]
VGIc = 0.014                        ; fraction of GI tract contents[1]


VSI = VSIc*BW    {L or Kg}          ; volume of small intestine tissue (calculated)
VLI = VLIc*BW    {L or Kg}          ; volume of large intestine tissue (calculated)
VL = VLc*BW            {L or Kg}         ; volume of liver tissue (calculated)
VK = VKc*BW            {L or Kg}         ; volume of kidney tissue (calculated)
VR = VRc*BW            {L or Kg}         ; volume of rapidly perfused tissue (calculated)
VS = VSc*BW            {L or Kg}         ; volume of slowly perfused tissue (calculated)
VF = VFc*BW            {L or Kg}         ; volume of fat tissue (calculated)
VB = VBc*BW            {L or Kg}         ; volume of blood (calculated)
VLILu = 0.561         {L}                   ; volume of large intestine lumen[2]
;----------------------------------------------------------------------------------------------------------------
```

; Blood flow rates

QC = 347.9 {L/h} ; cardiac output:

QIc = 0.181 ; fraction of blood flow to small intestine[1]

QLc = 0.046 ; fraction of blood flow to liver[1]

QKc = 0.175 ; fraction of blood flow to kidney[1]

QRc = 0.255 ; fraction of blood flow to rapidly perfused tissue[1]

QSc = 0.291 ; fraction of blood flow to slowly perfused tissue[1]

QFc = 0.052 ; fraction of blood flow to fat[1]

QI = QIc*QC {L/h} ; blood flow to small intestine tissue (calculated)

QL = QLc*QC {L/h} ; blood flow to liver tissue (calculated)

QK = QKc*QC {L/h} ; blood flow to kidney tissue (calculated)

QR = QRc*QC {L/h} ; blood flow to rapidly perfused tissue (calculated)

QS = QSc*QC {L/h} ; blood flow to slowly perfused tissue (calculated)

QF = QFc*QC {L/h} ; blood flow to fat tissue (calculated)

;==

; Physicochemical parameters

;==

; partition coefficients, calculated using QPPR of DeJongh et al.[3]

; EGCG in main model

PIEGCG = 2.68 ; intestine/blood partition coefficient

PLEGCG = 2.68 ; liver/blood partition coefficient

PKEGCG = 1.49 ; kidney/blood partition coefficient

PREGCG = 2.68 ; rapidly perfused tissue/blood partition coefficient

PSEGCG = 1.94 ; slowly perfused tissue/blood partition coefficient

PFEGCG = 55.57 ; fat/blood partition coefficient

; Gallic acid in sub-model

PIGA = 0.72 ; intestine/blood partition coefficient

PLGA = 0.72 ; liver/blood partition coefficient

PKGA = 0.85   ; kidney/blood partition coefficient

PRGA = 0.72   ; rapidly perfused tissue/blood partition coefficient

PSGA = 0.82   ; slowly perfused tissue/blood partition coefficient

PFGA = 1.96   ; fat/blood partition coefficient

; Pyrogallol in sub-model

PIPG = 0.85   ; intestine/blood partition coefficient

PLPG = 0.85   ; liver/blood partition coefficient

PKPG = 0.91   ; kidney/blood partition coefficient

PRPG = 0.85   ; rapidly perfused tissue/blood partition coefficient

PSPG = 0.90   ; slowly perfused tissue/blood partition coefficient

PFPG = 5.18   ; fat/blood partition coefficient

;--;

; absorption/transfer rates

; intestinal absorption rate of EGCG

PappCaco2EGCG=10^(-4.36-0.01*197.37)   {cm/s}; quantitative structure–activity relationship (QSAR) method calculated in vitro apparent permeability coefficient (PappCaco2) of EGCG (non-fasting conditions)[4]; this value is adjusted to 0.0000099 when exposure under fasting conditions

PappEGCG=(10^(0.6836*LOG10(PappCaco2EGCG)-0.5579)) *3600/10   {dm/h} ; in vivo PappCaco2 of EGCG[5]

SAl=47.12   {dm^2}   ; surface area of large intestine[6]

ksto=2.8   {/h}   ; stomach emptying rate[6]

Vin=1.29 {L}   ; volume for each compartment of small intestines

SAin=10.3   {dm^2}   ; surface area of each compartment of small intestines[6]

kin=2.19   {/h}   ; transfer rate to next compartment within the small intestines[6]

kabin1=PappEGCG*SAin   {L/h}   ; absorption rate constant of EGCG

Vin1=Vin {L}   ; volume of compartment1 of small intestine

SAin1=SAin   {dm^2}   ; surface area of compartment1 of small intestine

kabin1=PappEGCG*SAin1   {L/h}   ; absorption rate constant of EGCG of small intestine comapartment1

kin1=kin   {/h}   ; transfer rate to compartment2 of the small intestine

Vin2=Vin {L}   ; volume of compartment2 of small intestine

SAin2=SAin   {dm^2}   ; surface area of compartment2 of small intestine

kabin2=PappEGCG*SAin2   {L/h}   ; absorption rate constant of EGCG of small intestine comapartment2

kin2=kin {/h}   ; transfer rate to compartment3 of the small intestine

Vin3=Vin {L}   ; volume of compartment3 of small intestine

SAin3=SAin   {dm^2}   ; surface area of compartment3 of small intestine

kabin3=PappEGCG*SAin3   {L/h}   ; absorption rate constant of EGCG of small intestine comapartment3

kin3=kin {/h}   ; transfer rate to compartment4 of the small intestine

Vin4=Vin {L}   ; volume of compartment4 of small intestine

SAin4=SAin   {dm^2}   ; surface area of compartment4 of small intestine

kabin4=PappEGCG*SAin4   {L/h}   ; absorption rate constant of EGCG of small intestine comapartment4

kin4=kin {/h}   ; transfer rate to compartment5 of the small intestine

Vin5=Vin {L}   ; volume of compartment5 of small intestine

SAin5=SAin   {dm^2}   ; surface area of compartment5 of small intestine

kabin5=PappEGCG*SAin5   {L/h}   ; absorption rate constant of EGCG of small intestine comapartment5

kin5=kin {/h}   ; transfer rate to compartment6 of the small intestine

Vin6=Vin {L}   ; volume of compartment6 of small intestine

SAin6=SAin   {dm^2}   ; surface area of compartment6 of small intestine

kabin6=PappEGCG*SAin6   {L/h}   ; absorption rate constant of EGCG of small intestine comapartment6

kin6=kin {/h}   ; transfer rate to compartment7 of the small intestine

Vin7=Vin {L}   ; volume of compartment7 of small intestine

SAin7=SAin   {dm^2}   ; surface area of compartment7 of small intestine

kabin7=PappEGCG*SAin3   {L/h}   ; absorption rate constant of EGCG of small intestine comapartment7

kin7=kin {/h}   ; transfer rate of EGCG from small intestine to the large intestine

kb=   0   {/h}   ; transfer rate of EGCG from large intestinal lumen to liver (EGCG is completely degraded
by colonic microbiota)

PappCaco2GA=10^(-4.36-0.01*97.99)   {cm/s}; QSAR method calculated in vitro PappCaco2 of GA[4]

PappGA=(10^(0.6836*LOG10(PappCaco2GA)-0.5579)) *3600/10   {dm/h}   ; in vivo PappCaco2 of GA[5]

Kgll =   PappGA*SAl   {L/h}   ; absorption rate constant of gallic acid from large intestinal lumen to liver

PappCaco2PG=10^(-4.36-0.01*60.69)   {cm/s}; QSAR method calculated in vitro PappCaco2 of PG[4]

PappPG=(10^(0.6836*LOG10(PappCaco2PG)-0.5579)) *3600/10   {dm/h}   ; in vivo PappCaco2 of PG[5]

Kpll =   PappPG*SAl   {L/h}   ; absorption rate constant pyrogallol from large intestinal lumen to liver

CLb =   50   {L/h}   ; biliary clearance of EGCG (model fitted)

CLr =   0   {L/h}   ; renal clearance of EGCG (extremely low, can be ignored)

CLrg =   8.4   {L/h}   ; renal clearance of GA[7]

CLrp =   8.4   {L/h}   ; renal clearance of PG (assume to be the same as GA)

Kf =   0.02   {L/h}   ; colon volume (0.561 L) dived by transit time (30 h)

Kfg =   0.02   {L/h}   ; colon volume (0.561 L) dived by transit time (30 h)

Kfp =   0.02   {L/h}   ; colon volume (0.561 L) dived by transit time (30 h)

;==

; Kinetic parameters

;==

; metabolism in large intestine lumen (microbiota compartment)

; scaling factors

VMB = 0.0018   ; fraction of faeces of BW[8]

; unscaled metabolites EGC, gallic acid and pyrogallol, catechol, maximum rates of metabolism, {µmol/h/g faeces}

VmaxLIEGCc= 3.07   ; experimental data derived from anaerobic human fecal incubations

VmaxLIGAc= 0.87 ; experimental data derived from anaerobic human fecal incubations

VmaxLIPGc= 2.43 ; experimental data derived from anaerobic human fecal incubations

VmaxLICtc= 2.43   ; assume to be the same as VmaxLIPGc

; metabolites EGC, gallic acid and pyrogallol, scaled maximum rates of metabolism, {µmol/h}

VmaxLIEGC= VmaxLIEGCc*1000 *VMB*BW

VmaxLIGA= VmaxLIGAc*1000 *VMB*BW

VmaxLIPG= VmaxLIPGc*1000 *VMB*BW

VmaxLICt= VmaxLICtc*1000 *VMB*BW

; metabolites EGC, gallic acid, pyrogallol and catechol, affinity constants, {μmol/L}

KmLIEGC =   41.61   ; experimental data derived from anaerobic human fecal incubations

KmLIGA =   11.13   ; experimental data derived from anaerobic human fecal incubations

KmLIPG =   68.70   ; experimental data derived from anaerobic human fecal incubations

KmLICt =   68.70   ; assume to be the same as KmLIPG

;--

; metabolism of liver

VLS9 = 120.7   {mg S9 protein/gram liver}   ; liver S9 protein yield   [9]

S9P=VLS9*1000   {mg S9 protein/kg liver}   ; liver S9 protein yield

CLintS9GA=300   {ul/min/mg protein}   ; Hepatic clearance of GA derived from S9 fraction, estimated value[10-11]

CLintGA=S9P*VL*(CLintS9GA*60/1000000)   {L/h}   ; Hepatic clearance of GA

CLintS9PG=300   {ul/min/mg protein}   ; Hepatic clearance of PG derived from S9 fraction, estimated value[10-11]

CLintPG=S9P*VL*(CLintS9PG*60/1000000)   {L/h}   ; Hepatic clearance of PG

;==

; Run settings

;==

; molecular weight

MWEGCG= 458.372   ; molecular weight EGCG

;--

Sigle dose:

; oral dose

ODOSEmg =   2.857   {mg/kg bw}   ; oral dose, variable

ODOSEumol= ODOSEmg*1000/MWEGCG*BW {μmol} ; unit change to μmol

; time

Starttime = 0   {hour}

Stoptime = 24   {hour}   ; variable

DTMIN = 1e-6

DTMAX = 1

DTOUT = 0

TOLERANCE = 0.000001

;---

Repeated dose:

ODOSEmg =   2.857   {mg/kg bw}   ; oral dose, variable

ODOSEumol= ODOSEmg*1000/MWEGCG*BW {μmol}   ; unit change to μmol

dose_int = 24   ; dosing interval in hours

; time

Starttime = 0   {hour}

Stoptime = 28*24   {hour}   ; days*hours in a day

DTMIN = 1e-6

DTMAX = 1

DTOUT = 0

TOLERANCE = 0.000001

;==

; Main model calculations/dynamics: EGCG

;==

Single dose:

; Stomach

; Ast=amount in stomach

Ast'=-ksto*Ast

Init Ast=ODOSEumol

;---

Repeated dose:

; Stomach

; Ast=amount in stomach

Ast'=pulse (ODOSEumol, 0, dose_int)-ksto*Ast

Init Ast=0

;--

; small intestine lumen compartment, divided in 7 compartments

; Ain1: amount of EGCG compartment1 of small intestinal lumen, {μmol}

Cin1=Ain1/Vin1

Ain1'=ksto*Ast-kin1*Ain1-kabin1*Cin1

Init Ain1=0

; Ain2: amount of EGCG compartment2 of small intestinal lumen, {μmol}

Cin2=Ain2/Vin2

Ain2'= kin1*Ain1-kin2*Ain2-kabin2*Cin2

Init Ain2=0

; Ain3: amount of EGCG compartment3 of small intestinal lumen, {μmol}

Cin3=Ain3/Vin3

Ain3'= kin2*Ain2-kin3*Ain3-kabin3*Cin3

Init Ain3=0

; Ain4: amount of EGCG compartment4 of small intestinal lumen, {μmol}

Cin4=Ain4/Vin4

Ain4'= kin3*Ain3-kin4*Ain4-kabin4*Cin4

Init Ain4=0

; Ain5: amount of EGCG compartment5 of small intestinal lumen, {μmol}

Cin5=Ain5/Vin5

Ain5'= kin4*Ain4-kin5*Ain5-kabin5*Cin5

Init Ain5=0

; Ain6: amount of EGCG compartment6 of small intestinal lumen, {μmol}

Cin6=Ain6/Vin6

Ain6'= kin5*Ain5-kin6*Ain6-kabin6*Cin6

Init Ain6=0

; Ain7: amount of EGCG compartment7 of small intestinal lumen, {μmol}

Cin7=Ain7/Vin7

Ain7'= kin6*Ain6-kin7*Ain7-kabin7*Cin7

Init Ain7=0

;---

; small intestine tissue compartment

; ASIEGCG: amount of EGCG in small intestinal tissue, {μmol}

ASIEGCG' = kabin1*Cin1+ kabin2*Cin2+ kabin3*Cin3+ kabin4*Cin4+ kabin5*Cin5+ kabin6*Cin6+ kabin7*Cin7+ QI*(CB - CVSIEGCG)

      Init ASIEGCG=0

      CSIEGCG = ASIEGCG/VSI

      CVSIEGCG = CSIEGCG/PIEGCG

;---

; large intestine lumen compartment: microbial activity

; ALIEGCG: amount of EGCG in large intestine lumen, {μmol}

      ALIEGCG' = kin7*Ain7 - ALIEGC' - Kb*ALIEGCG + CLb*CVLEGCG- Kf*CLIEGCG

      Init ALIEGCG = 0

      CLIEGCG = ALIEGCG/ VLILu

; ALIEGC: amount of EGC formed due to gut microbial activity, {μmol}

      ALIEGC'= VmaxLIEGC * CLIEGCG/(KmLIEGC + CLIEGCG)

      Init ALIEGC=0

; ALIGA: amount of gallic acid formed due to gut microbial activity, {μmol}

      ALIGA'= VmaxLIGA * CLIEGCG/(KmLIGA + CLIEGCG)

      Init ALIGA=0

; AfEGCG: excreted EGCG in feces, {μmol}

      AfEGCG'= Kf*CLIEGCG

      Init AfEGCG =0

;---

; liver compartment

; ALEGCG: amount of EGCG in liver, {µmol}

ALEGCG' = QL*CB + QI*CVSIEGCG - (QL+QI)*CVLEGCG + Kb* ALIEGCG -CLb*CVLEGCG

Init ALEGCG=0

CLEGCG = ALEGCG/VL

CVLEGCG = CLEGCG/PLEGCG

;--

; Kidney compartment

; AKEGCG: amount of EGCG in kidney, {µmol}

AKEGCG' = QK*(CB-CVKEGCG) - CLr*CVKEGCG

Init AKEGCG =0

CKEGCG = AKEGCG/VK

CVKEGCG = CKEGCG/PKEGCG

; AuEGCG: excreted EGCG in urine, {µmol}

AuEGCG'= CLr*CVKEGCG

Init AuEGCG =0

;--

; fat compartment

; AF = amount of EGCG in fat tissue, {µmol}

AF' = QF*(CB-CVF)

Init AF = 0

CF = AF/VF

CVF = CF/PFEGCG

;--

; rapidly perfused tissue

; AR = amount of EGCG in rapidly perfused tissue, {µmol}

AR' = QR*(CB-CVR)

Init AR = 0

CR = AR/VR

CVR = CR/PREGCG

;--

; slowly perfused tissue

; AS = amount of EGCG in slowly perfused tissue, {µmol}

AS' = QS*(CB-CVS)

Init AS = 0

CS = AS/VS

CVS = CS/PSEGCG

;--

; blood compartment

; AB: amount of EGCG in blood, {µmol}

AB' = (QI+QL)*CVLEGCG + QK*CVKEGCG +QF*CVF+QS*CVS+QR*CVR - QC*CB

Init AB = 0

CB = AB/VB

AUC'=AB

Init AUC=0

;==

; Sub-model 1 calculations/dynamics: gallic acid

;==

; large intestine lumen compartment

; ARLIGA = amount of gallic acid in large intestine lumen, {µmol}

      ARLIGA' = ALIGA' - Kgll*CLIGA-ALIPG'-Kfg*CLIGA

      init ARLIGA = 0

      CLIGA = ARLIGA/ VLILu

; CLIREPGA = concentration of large intestinal lumen GA in EGCG equivalents, {µmol}

      CLIREPGA = CLIGA*2.1

; ALIPG: amount of pyrogallol formed due to gut microbial activity, {µmol}

      ALIPG'= VmaxLIPG* CLIGA/(KmLIPG + CLIGA)

      Init ALIPG=0

    CLIGA = ARLIGA/ VLILu

; AfeGA: excreted GA in feces, {μmol}

        AfeGA'= Kfg*CLIGA

        Init AfeGA =0

;--

; liver compartment

; ALGA: amount of gallic acid in liver, {μmol}

ALGA' = Kgll*CLIGA + QL*(CBGA-CVLGA) - AMintGA'

Init ALGA =0

        CLGA = ALGA/VL

        CVLGA = CLGA/PLGA

; AMintGA: amount of GA metabolized

        AMintGA'= CLintGA*CVLGA

        Init AMintGA=0

;--

; Kidney compartment

; AKGA: amount of gallic acid in kidney, {μmol}

AKGA' = QK*(CBGA-CVKGA) - CLrg*CVKGA

Init AKGA =0

        CKGA = AKGA/VK

        CVKGA = CKGA/PKGA

; AuGA: excreted GA in urine, {μmol}

        AuGA'= CLrg*CVKGA

        Init AuGA =0

;--

; fat compartment

; AFGA: amount of gallic acid in fat tissue, {μmol}

AFGA' = QF*(CBGA-CVFGA)

Init AFGA = 0

        CFGA = AFGA/VF

        CVFGA = CFGA/PFGA

;---

; rapidly perfused tissue

; ARGA: amount of gallic acid in rapidly perfused tissue, {μmol}

    ARGA' = QR*(CBGA-CVRGA)

    Init ARGA = 0

    CRGA = ARGA/VR

    CVRGA = CRGA/PRGA

;---

; slowly perfused tissue

; ASGA: amount of gallic acid in slowly perfused tissue, {μmol}

    ASGA' = QS*(CBGA-CVSGA)

Init ASGA = 0

CSGA = ASGA/VS

CVSGA = CSGA/PSGA

;---

; blood compartment

; ABGA: amount of gallic acid in blood, {μmol}

ABGA' = QL*CVLGA +QK*CVKGA+ QF*CVFGA + QR*CVRGA + QS*CVSGA - (QL+QK+QF+QR+QS)*CBGA

Init ABGA= 0

CBGA = ABGA/VB

AUCGA'=ABGA

Init AUCGA=0

;==

; Sub-model 2 calculations/dynamics: pyrogallol

;==

; large intestine lumen compartment

; ARLIPG = amount of pyrogallol in large intestine lumen, {μmol}

ARLIPG' = ALIPG' - Kpll*CLIPG - ALICt'-Kfp*CLIPG

Init ARLIPG = 0

CLIPG = ARLIPG/ VLILu

; CLIREPPG = concentration of large intestinal lumen PG in EGCG equivalents, {μmol}

CLIREPPG = CLIPG*2.1

; ALICt: amount of catechol formed due to gut microbial activity, {μmol}

ALICt'= VmaxLICt* CLIPG/(KmLICt + CLIPG)

Init ALICt=0

CLIPG = ARLIPG/ VLILu

; AfePG: excreted PG in feces, {μmol}

AfePG'= Kfp*CLIPG

Init AfePG =0

;--

; liver compartment

; ALPG: amount of pyrogallol in liver, {μmol}

ALPG' = Kpll*CLIPG + QL*CBPG - QL*CVLPG - AMintPG'

Init ALPG =0

CLPG = ALPG/VL

CVLPG = CLPG/PLPG

; AMintPG: amount of PG metabolized

AMintPG'= CLintPG*CVLPG

Init AMintPG=0

;--

; Kidney compartment

; AKPG: amount of pyrogallol in kidney, {μmol}

AKPG' = QK*(CBPG-CVKPG) - CLrp*CVKPG

Init AKPG =0

CKPG = AKPG/VK

CVKPG = CKPG/PKPG

; AuPG: excreted PG in urine, {μmol}

AuPG'= CLrp*CVKPG

Init AuPG =0

;---

; fat compartment

; AFPG: amount of pyrogallol in fat tissue, {µmol}

AFPG' = QF*(CBPG-CVFPG)

Init AFPG = 0

CFPG = AFPG/VF

CVFPG = CFPG/PFPG

;---

; rapidly perfused tissue

; ARPG: amount of pyrogallol in rapidly perfused tissue, {µmol}

ARPG' = QR*(CBPG-CVRPG)

Init ARPG = 0

CRPG = ARPG/VR

CVRPG = CRPG/PRPG

;---

; slowly perfused tissue

; ASPG: amount of pyrogallol in slowly perfused tissue, {µmol}

ASPG' = QS*(CBPG-CVSPG)

Init ASPG = 0

CSPG = ASPG/VS

CVSPG = CSPG/PSPG

;---

; blood compartment

; ABPG: amount of pyrogallol in blood, {µmol}

ABPG' = QL*CVLPG +QK*CVKPG+ QF*CVFPG + QR*CVRPG + QS*CVSPG - (QL+QK+QF+QR+QS)*CBPG

Init ABPG= 0

CBPG = ABPG/VB

AUCPG'=ABPG

Init AUCPG=0

;---

; Plasma unbound fraction of EGCG equivalents: CBeqv {µmol/L}.

$$CBeqv = 0.13*CB+0.82*CBGA+2.1*CBPG$$; CBeqv is $C_{unbound, plasma, EGCG\ equivalents}$, which is calculated as $C_{unbound, plasma, EGCG\ equivalents} = C_{in\ vitro, EGCG} * f_{ub, in\ vitro, EGCG}$ where $C_{unbound, plasma, EGCG\ equivalents} = (C_{blood, EGCG} / BP_{EGCG}) * f_{ub, in\ vivo, EGCG} * REP_{EGCG} + (C_{blood, GA} / BP_{GA}) * f_{ub, in\ vivo, GA} * REP_{GA} + (C_{blood, PG} / BP_{PG}) * f_{ub, in\ vivo, PG} * REP_{PG}$, detailed explanations are in the main text.

; Large intestinal EGCG equivalents: CBeqvLI {µmol/L}.

$$CBeqvLI = CLIEGCG+CLIREPGA+CLIREPPG$$

;==

; Main model: mass balance calculation (Single dose)

;==

Totalm = ODOSEumol

Calculatedm = Ast+Ain1+ Ain2+ Ain3+ Ain4+ Ain5+ Ain6+ Ain7+ ASIEGCG + ALIEGCG + ALIEGC + AfEGCG + ALEGCG +AKEGCG+AuEGCG+ AF + AR + AS + AB

MASSBBALm=Totalm - Calculatedm + 1

Totalga = ALIGA

Calculatedga = ARLIGA + ALIPG + AfeGA + ALGA + AMintGA + AKGA + AuGA + AFGA + ARGA +ASGA + ABGA

MASSBBALga=Totalga - Calculatedga + 1

Totalpg = ALIPG

Calculatedpg = ARLIPG + ALICt + AfePG + ALPG + AMintPG + AKPG + AuPG +AFPG + ARPG + ASPG +ABPG

MASSBBALpg = Totalpg - Calculatedpg + 1

ERROR=((Totalm+ Totalga + Totalpg -Calculatedm- Calculatedga- Calculatedpg)/(Totalm+ Totalga+ Totalpg)+1E-30)*100

MASSBBAL = Totalm + Totalga + Totalpg - Calculatedm - Calculatedga - Calculatedpg +1

;==

; Main model: mass balance calculation (Repeated dose)

;==

Totalm' = pulse(ODOSEumol, 0, dose_int)

Init Totalm = 1E-50

Calculatedm = Ast+Ain1+ Ain2+ Ain3+ Ain4+ Ain5+ Ain6+ Ain7+ ASIEGCG + ALIEGCG + ALIEGC + AfEGCG + ALEGCG +AKEGCG+AuEGCG+ AF + AR + AS + AB

MASSBBALm=Totalm - Calculatedm + 1

Totalga = ALIGA

Calculatedga = ARLIGA + ALIPG + AfeGA + ALGA + AMintGA + AKGA + AuGA + AFGA + ARGA +ASGA + ABGA

MASSBBALga=Totalga - Calculatedga + 1

Totalpg = ALIPG

Calculatedpg = ARLIPG + ALICt + AfePG + ALPG + AMintPG + AKPG + AuPG +AFPG + ARPG + ASPG +ABPG

MASSBBALpg = Totalpg - Calculatedpg + 1

ERROR=((Totalm+Totalga+Totalpg-Calculatedm-Calculatedga-Calculatedpg)/(Totalm+ Totalga+Totalpg +1E-30))*100

MASSBBAL = Totalm + Totalga + Totalpg - Calculatedm - Calculatedga - Calculatedpg +1

References

1.   Brown, R. P.; Delp, M. D.; Lindstedt, S. L.; Rhomberg, L. R.; Beliles, R. P., Physiological parameter values for physiologically based pharmacokinetic models. *Toxicology and industrial health* **1997,** *13* (4), 407-484.

2.   Pritchard, S. E.; Marciani, L.; Garsed, K.; Hoad, C.; Thongborisute, W.; Roberts, E.; Gowland, P. A.; Spiller, R. C., Fasting and postprandial volumes of the undisturbed colon: normal values and changes in diarrhea-predominant irritable bowel syndrome measured using serial MRI. *Neurogastroenterology & Motility* **2014,** *26* (1), 124-130.

3.   DeJongh, J.; Verhaar, H. J.; Hermens, J. L., A quantitative property-property relationship (QPPR) approach to estimate in vitro tissue-blood partition coefficients of organic chemicals in rats and humans. *Archives of Toxicology* **1997,** *72* (1), 17-25.

4.   Hou, T.; Zhang, W.; Xia, K.; Qiao, X.; Xu, X., ADME evaluation in drug discovery. 5. Correlation of Caco-2 permeation with simple molecular properties. *Journal of chemical information and computer sciences* **2004,** *44* (5), 1585-1600.

5.   Sun, D.; Lennernas, H.; Welage, L. S.; Barnett, J. L.; Landowski, C. P.; Foster, D.; Fleisher, D.; Lee, K.-D.; Amidon, G. L., Comparison of human duodenum and Caco-2 gene expression profiles for 12,000 gene sequences tags and correlation with permeability of 26 drugs. *Pharmaceutical research* **2002,** *19* (10), 1400-1416.

6.   Mendez-Catala, D. M.; Wang, Q.; Rietjens, I. M. C. M., PBK Model-Based Prediction of Intestinal Microbial and Host Metabolism of Zearalenone and Consequences for its Estrogenicity. *Molecular nutrition & food research* **2021,** 2100443.

7.   Shahrzad, S.; Aoyagi, K.; Winter, A.; Koyama, A.; Bitsch, I., Pharmacokinetics of gallic acid and its relative bioavailability from tea in healthy humans. *The Journal of Nutrition* **2001,** *131* (4), 1207-1210.

8.   Rose, C.; Parker, A.; Jefferson, B.; Cartmell, E., The characterization of feces and urine: a review of the literature to inform advanced treatment technology. *Critical reviews in environmental science and technology* **2015,** *45* (17), 1827-1879.

9.   Cubitt, H. E.; Houston, J. B.; Galetin, A., Prediction of human drug clearance by multiple metabolic pathways: integration of hepatic and intestinal microsomal and cytosolic data. *Drug metabolism and disposition* **2011,** *39* (5), 864-873.

10.   Zhang, M.; van Ravenzwaay, B.; Fabian, E.; Rietjens, I. M. C. M.; Louisse, J., Towards a generic physiologically based kinetic model to predict in vivo uterotrophic responses in rats by reverse dosimetry of in vitro estrogenicity data. *Archives of toxicology* **2018,** *92* (3), 1075-1088.

11.   Zhang, M.; van Ravenzwaay, B.; Rietjens, I. M. C. M., Development of a generic physiologically based kinetic model to predict in vivo uterotrophic responses induced by estrogenic chemicals in rats based on in vitro bioassays. *Toxicological sciences* **2020,** *173* (1), 19-31.

Chapter 7

General discussion

1.1 Overview and main findings

Green tea is one of the most widely consumed healthful beverages around the world, second to water.[1-2] Catechins are the most abundant bioactive constituents in green teas, amounting to 30% of the total dry weight.[3-5] Among the catechins in green teas (-)-epigallocatechin gallate (EGCG), (-)-epigallocatechin (EGC), (-)-epicatechin gallate (ECG) and (-)-epicatechin (EC) are the four major ones.[5-6] The catechins are believed to be responsible for various beneficial health effects that have been ascribed to green tea consumption. Though the modes of action underlying those health-promoting effects can be complicated and have not been fully elucidated, the Kelch-like ECH-associated protein 1/Nuclear factor E2-related factor 2 (Keap1/Nrf2) regulatory network has been reported to play a role.[7-8] Only the bioavailable fraction of catechins has the chance to exert the systemic biological effects. However, like other polyphenols, the bioavailability of green tea catechins is generally considered to be poor.[9] After consumption of green tea or green tea supplements, only a small part of the tea catechins is absorbed and appears in the systemic circulation.[10-11] While the remaining majority reaches the colon where it undergoes extensive microbial metabolism, resulting in the formation of a diverse range of smaller molecular-weight polyphenols.[3] These colonic metabolites of green tea catechins can be reabsorbed and reach the systemic circulation, which not only improves the overall bioavailability but also potentially enriches the biological activities of green tea catechins.[12-14] So far, it remains to be elucidated to what extent these colonic metabolites are able to contribute to the bioactivities upon tea catechin administrations, and this also holds for their potential beneficial effects via activation of the Nrf2 pathway.

Moreover, current studies on the modes of actions underlying the beneficial health effects of tea catechins mostly rely on either *in vitro* cell-based models or *in vivo* laboratory animal studies.[15-16] The former are unable to include the important microbial metabolism that plays a role *in vivo* while the latter are considered costly, unethical and subject to potential interspecies differences.[17] Therefore, developing a combined *in vitro* and human physiologically based kinetic (PBK) modelling *in silico* approach, that includes gut microbial metabolism, could provide a new approach methodology (NAM) to characterize the microbial metabolism of tea catechins *in vivo*, and predict systemic exposure of the host to both the parent compound and its metabolites.[18]

The aim of the present thesis was to obtain better insights into the human intestinal microbiota-mediated conversion of model green tea catechins, including its intra- and inter-individual

variability, by using an *in vitro* anaerobic fecal incubation model, and to identify the bioactivity of the formed microbial metabolites in the activation of Nrf2-EpRE-mediated gene expression, a potential mode of action underlying the beneficial health effects. Furthermore, the thesis also aimed to build a human PBK model including gut microbial metabolism for the most abundant and bioactive green tea catechin, EGCG, and to use a PBK modeling-based reverse dosimetry approach to extrapolate the *in vitro* concentration-response curve for EGCG from the U2OS-Nrf2 CALUX reporter gene assay to an *in vivo* dose-response curve for Nrf2 activation in humans, taking the contribution of the gut microbial metabolites into account. This latter strategy will provide a NAM to evaluate whether at a realistic daily intake levels Nrf2-mediated health effects are to be expected without the use of laboratory animals and/or human intervention studies.

In **Chapter 2**, human fecal samples from 24 individuals were collected and used in an *in vitro* anaerobic incubation model to quantify interindividual differences in the human intestinal microbial metabolism of EC. EC derived colonic microbial metabolites were qualitatively and quantitively analyzed by liquid chromatography triple quadrupole mass spectrometry (LC-TQ-MS) and/or liquid chromatography time-of-flight mass spectrometry (LC-TOF-MS). Quantitative microbiota characterization was achieved by 16S rRNA analysis. Results obtained show 1-(3',4'-dihydroxyphenyl)-3-(2'',4'',6''-trihydroxyphenyl)-2-propanol (3,4-diHPP-2-ol) and 5-(3',4'-dihydroxyphenyl)-γ-valerolactone (3,4-diHPV) to be key intermediate microbial metabolites of EC and also revealed substantial interindividual differences in both the rate of EC conversion and the time-dependent EC metabolite pattern. Furthermore, substantial differences in microbiota composition among different individuals were detected. Correlations between specific microbial phylotypes and formation of certain metabolites were established. It is concluded in this chapter that interindividual differences in the intestinal microbial metabolism of EC may contribute to interindividual differences in potential health effects of EC-abundant dietary foods or drinks, including green tea.

In **Chapter 3**, this *in vitro* anaerobic fecal incubation model and a reporter gene assay were used to characterise interindividual differences in the gut microbial conversion of EGCG and its consequences for potential activation of Nrf2-mediated gene expression. To this end, fecal samples from 14 individuals were collected and used in anaerobic incubations to characterize the microbial metabolism of EGCG including interindividual variability. EGCG derived intestinal microbial metabolite patterns showed substantial interindividual differences that were correlated to relative microbial abundances determined by 16S rRNA sequencing. Results

obtained showed the time-dependent formation of gallic acid (GA), pyrogallol (PG), phenylpropane-2-ols, phenyl-γ-valerolactones and 5-(3',5'-dihydroxyphenyl)valeric acid (3,5-diHPVA) as the major metabolites, with substantial interindividual differences. The activity of the formed metabolites in the activation of Nrf2-EpRE-mediated gene expression was tested by the EpRE-LUX reporter gene assay. In contrast to EGCG, at low micromolar concentrations, especially GA, PG and catechol appeared able to induce significant activity in the EpRE-LUX assay. Given these results and taking the level of formation into account, this chapter concludes that especially GA and PG may contribute to the Nrf2-mediated beneficial effects of EGCG. The interindividual differences in the formation of these gut microbial metabolites may contribute to interindividual differences in the beneficial effects of EGCG and green tea consumption.

To further compare the potential intra- and inter-individual variabilities in the human gut microbial metabolism of tea catechins, in **Chapter 4**, intra- and inter-individual variations in the gut microbial conversion of EC and the concomitant formation of its major metabolites, including 3,4-diHPV, were identified and quantified via LC-TQ-MS in anaerobic fecal incubations. In addition, the bioactivity of EC and 3,4-diHPV in activating Nrf2-mediated gene expression was tested quantifying their effects in the U2OS-Nrf2 CALUX assay, and on the expression levels of Nrf2-related proteins in Hepa1c1c7 and Caco-2 cells via nanoLC-MSMS based label-free quantitative proteomics. RT-qPCR was carried out to confirm selected Nrf2-regulated gene expressions at the mRNA level. Results obtained show that both intra- and inter-individual differences exist in human gut microbial EC degradation and 3,4-diHPV formation, with inter-individual differences being more distinct than intra-individual differences. The metabolite, 3,4-diHPV, showed higher potency in the U2OS-Nrf2 CALUX assay than EC itself. Among the obviously altered Nrf2-related proteins, 14 and 10 Nrf2-associated proteins were upregulated to a higher extent upon 3,4-diHPV treatment than in the EC treated group for Hepa1c1c7 and Caco-2 cells, respectively. While only three and four of these Nrf2-associated proteins were induced at a higher level upon EC than upon 3,4-diHPV treatment for Hepa1c1c7 and Caco-2 cells, respectively. RT-qPCR results showed that indeed Nrf2-mediated genes (e.g., Nqo1 and Ugt1a) were only induced significantly in 3,4-diHPV treated and not in EC treated Hepa1c1c7 cells. Taken together, the results of this chapter suggest that the major colonic EC metabolite, 3,4-diHPV, was more capable of inducing Nrf2-mediated gene expression than its parent compound EC. This implies that the evident inter- and intra-individual differences in the

microbial conversion of EC to this major metabolite 3,4-diHPV may affect the overall health-promoting effects of EC consumption related to the Nrf2 pathway activation.

Based on the results from the previous chapter, in **Chapter 5**, Hepa1c1c7 cells were chosen as the *in vitro* cellular model to study the Nrf2-mediated genes after exposure to EGCG and its major microbial metabolites both at transcriptional and translational levels. To this end, a reporter gene bioassay, nanoLC-MSMS based label-free quantitative proteomics and RT-qPCR were combined to investigate the regulation of Nrf2-related gene expression after exposure to EGCG, or its gut microbial metabolites EGC, GA and PG. The results show that at micromolar concentrations PG displayed a more potent induction of the Nrf2 cascade than EGCG. The downstream bioinformatics analysis of the proteomics data suggested that Nrf2 pathway activation by PG was related to intermediary metabolisms, including especially Glutathione metabolism, Drug and/or xenobiotics metabolism, and the Pentose phosphate pathway as the major pathways. Taken together, findings in this chapter demonstrate that at lower concentrations, the microbial metabolites of EGCG including especially PG may contribute to the Nrf2 signalling activation upon exposure to the parent compound EGCG or green tea.

In order to investigate the contribution of the gut microbial metabolites of EGCG to induction of *in vivo* Nrf2 activation to a further extent, in **Chapter 6** a combined *in vitro – in silico* approach to predict Nrf2 activation by EGCG and its major colonic metabolites GA and PG in humans was developed. To this end a human PBK model for EGCG was developed, with sub-models for GA and PG and an intestinal compartment that included microbial metabolism to enable prediction of the kinetics of EGCG, GA and PG. The Nrf2 activation by these compounds was characterized using an U2OS-Nrf2 CALUX reporter gene assay and the resulting *in vitro* concentration-response curves were used to extrapolate the *in vitro* data to an *in vivo* dose-response curve for EGCG mediated Nrf2 induction in humans using PBK modeling-based reverse dosimetry. Results obtained show, by comparing to literature data, that the developed PBK model could adequately predict *in vivo* time-dependent blood concentrations of EGCG after either a single or repeated oral administration(s) of EGCG under both fasting and non-fasting conditions. The predicted *in vivo* dose response curve revealed that at daily intake levels of green tea or EGCG supplements, the resulting blood C_{max} of EGCG was in the sub-micromolar range, concentrations at which Nrf2 activation was shown to be limited. Moreover, blood C_{max} values of GA and PG upon intake of EGCG were predicted to be less than 1.5% of the C_{max} of EGCG, indicating that in spite of their higher potential for Nrf2 activation, their contribution to the overall systemic Nrf2 pathway induction upon EGCG

exposure is expected to be limited. In contrast, concentrations of these metabolites in the intestinal tract may reach levels that are, expressed in EGCG equivalents for Nrf2 induction, higher than that of EGCG, and also high enough to activate Nrf2 gene transcription. Taken together, combining *in vitro* data with a human PBK model allowed the prediction of a dose-response curve for EGCG induced Nrf2-mediated gene expression in humans, and provided insight into the contribution of gut microbial metabolites to this effect. It also provided a proof-of-principle for a novel approach methodology (NAM) to study the *in vivo* effects of bioactive phytochemicals without the need for human intervention studies.

In the following sections, the results of the present thesis, limitations, possible refinements of the current studies and some further future perspectives are discussed.

1.2 General discussion and future perspectives

The results obtained and approaches applied in the present thesis offer several topics that can be considered of relevance for further research on gut microbial metabolism of green tea catechins and on the use of NAMs in the study of *in vivo* biological activities of green tea polyphenols.

These topics include:

- Microbial metabolism of green tea catechins
- *In vitro* models to study gut microbial metabolism
- Modulatory effects of catechins and their microbial metabolites on human gut microbiota
- Biological activities of green tea catechins and their gut microbial metabolites
- Proteomics used in studies on the bioactivity of green tea catechins
- PBK modeling and quantitative *in vitro* to *in vivo* extrapolation (QIVIVE)

1.2.1 Microbial metabolism of green tea catechins

In the present thesis the metabolic fates of the representative catechins EC and EGCG upon human gut microbial metabolism were studied (**Chapter 2** and **Chapter 3**). EC and EGCG represent a galloylated and non-gallyoylated green tea catechin, respectively. Therefore, characterizing the gut microbial conversion of these two catechins could also provide insights that are relevant for other major green tea catechins, namely EGC and ECG. Results obtained indicate that the dominant microflora-derived metabolite of EC was 3,4-diHPV while 3,5-

diHPV was one of EGCG's dominant microbial metabolites. The trihydroxy group in the B ring of EGCG enables the formation of, among others, 5-(3',4',5'-trihydroxyphenyl)-γ-valerolactone (3,4,5-triHPV), 5-(3',4'-dihydroxyphenyl)-γ-valerolactone (3,4-diHPV) and 5-(3',5'-dihydroxyphenyl)-γ-valerolactone (3,5-diHPV) upon incubating with fecal samples. It is of interest to note that both 3,4,5-triHPV and 3,4-diHPV were detected at lower levels compared to 3,5-diHPV (**Chapter 3**), since this indicates a preference of the intestinal microbiota for performing 4'-dehydroxylation over 5'-dehydroxylation in the B-ring of the molecular skeleton. Wang and co-workers observed that the *Eubacterium* (*E*.) sp. strain SDG-2 was able to catalyse 4'-dehydroxylation activity in the B ring of several catechins including EGC and they proved that the presence of three vicinal hydroxy groups at 3', 4' and 5' in the B-ring is of importance for this 4'-dehydroxylation activity of this *E*. sp. strain SDG-2.[19] It is believed that the existence of ortho-hydroxy groups is crucial for the beneficial effects of polyphenols, e.g., radical scavenging ability, Nrf2 activation potency, etc.[20-22] Therefore, it can be expected that 3,4-diHPV will be able to show some superior bioactivities compared to its isomer 3,5-diHPV.

There are many reactions involved in the microbial degradation of catechins and some of these reactions are microbe-specific. Though many publications have explored microbial metabolites of catechins/dietary polyphenols, limited studies have focused on the actual metabolic pathways and underlying microbiota responsible for those reactions. For instance, to the best of our knowledge, *E.* sp. SDG-2, *Lactobacillus plantarum*, *Eggerthella lenta* and *Adlercreutzia equolifaciens* are the only bacteria reported so far to be capable of producing the metabolite diphenylpropan-2-ol from epicatechins (or catechins and epigallocatechin gallate),[19, 23-25] a reaction comparable to the formation of 1-(3',4'-dihydroxyphenyl)-3-(2'',4'',6''-trihydroxyphenyl)-2-propanol (3,4-diHPP-2-ol) from EC detected in the present study. Furthermore, the *Flavonifractor plautii*, which belongs to the class of *Clostridia*, was reported to be capable of the further metabolism of phenylpropan-2-ol into phenyl-γ-valerolactones.[23, 26] In the present study, microbial taxonomy and relative abundance of the fecal samples were characterized by 16S rRNA analysis and bacterial loads were quantified by qPCR, which allowed the identification of correlations between taxon abundances and formation of catechin gut microbial metabolites. For example, in addition to the already reported bacterial functionalities in catechin microbial conversions, we found statistically significant positive correlations between the relative abundance of *Lachnospiraceae NC2004 group* and the formation of 3,4-diHPP-2-ol, of *Phascolarctobacterium* and the concentration of 3,4-diHPV and statistically significant negative correlations between the quantity of residual EGCG and

the relative abundance of *Bilophila*. The established correlations between specific microbial phylotypes and formation of certain metabolites provide leading information for future studies on illustrating actual enzymes and pathways in the respective intestinal microbiota responsible for the tea catechin conversions. If we can know not only 'who is there' but also 'what they do' in the human intestines we would be able to predict the metabolic patterns based on the microbial compositions of individuals and, eventually, establish 'enterotypes'.[27] A well-investigated example is the microbial transformation of daidzein. Human subjects can be divided into equol- producers and nonequol-producers depending on whether they have equol-producing bateria.[28] In **Chapter 2**, two slow EC metabolizers were defined while their bacterial loads were not the lowest among all subjects, indicating it could be the relative microbial abundance that is underlying the difference in EC microbial clearance. However, due to the vast diversity of human microbial communities and possible involvements of several genera catalysing the EC degradation (functional redundancy) it still requires further investigations to fully identify the microbial strains and enzymes involved in the conversions observed in the current study.

The intestinal microbial degradation of catechins includes ester hydrolysis, A-ring and C-ring cleavages, dehydroxylation and continued loss of carbon atoms from aliphatic side chains via α-oxidations and β-oxidations, etc.[29] As a result of the many reactions involved, the microbial metabolic profiles of the catechins are complicated. In order to cover as many of the metabolites as possible, an optimized robust spectral chromatographic analysing method is required, which sometimes is quite challenging especially when the metabolic pathways are not fully elucidated and standard reference compounds are not available. In the present study, the molar mass recoveries for EC and its colonic metabolites ranged from 83.2 to 112.9% indicating the metabolites of EC were adequately covered by the current analytical method. The molar mass recoveries at 1, 2 and 3 h of fecal incubation were above 100% which were likely due to the lack of the standard references of diphenylpropan-2-ol causing some inaccuracy in the quantifications. Moreover, in the GA degradation route of EGCG, the total molar mass recovery started to decrease from 1 h onward, dropping from 99.8% at 1 h to 25.7% at 6 h and being almost undetectable at 24 h. This suggests that eventually PG is further degraded into metabolites that were not included in the present LC-TQ-MS measurements. This may be related to the fact that catechins or (one of) their metabolites could serve as carbon or energy source or act as a terminal electron acceptor in anaerobic respiration [30-31]. This proposal is in analogy to the observation reported by Walle and colleagues who discovered that after oral

dosing of isotope labelled quercetin, a substantial part (23.0–81.1%) of the radioactive quercetin was recovered as carbon dioxide, which may have come from quercetin or its microbial metabolites especially the phenolic carboxylic acids.[32]

1.2.2 *In vitro* models to study gut microbial metabolism

There are more than 100 trillions of microbes inhabiting the human intestine, 10 times higher than the number of cells in the human body with most of the microbiota living in the large intestine.[33] Despite the non-human nature, the highly diverse colonic microbial community contributes to the host's health in many ways, among others by metabolizing xenobiotic substances and thereby changing exposure of the host to those xenobiotics and their metabolites.[34] *In vitro* fermentation models using feces as the primary material are considered excellent tools to study the microbial conversion of a wide array of substances, including dietary ingredients, e.g., polysaccharides, polyphenols, dietary fibre, proteins, pathogen, pharmaceuticals and toxins, etc., without ethical constraints.[35-37] These models can also be used to study microbial modulation effects by food components, toxins and xenobiotics.[3, 38-40] Fecal samples have shown to be representative of the microbiota in the distal large intestine.[41] Lagkouvardos et al., who performed a thorough review on the cultivation of bacteria from the intestine of mammals, concluded that up to 65% of the molecular species detected by sequencing in pigs have corresponding strains in culture.[42] Another study that compared microbial-related *in vivo* metabolic changes in gut tissue, cecum content and feces of rats treated with antibiotics concluded that 'as a non-invasive sampling method, feces provides a suitable matrix for studies on metabolism by the gut microbiota'.[41] Thus fecal fermentation models appear to provide a useful approach to characterize intestinal microbial metabolism. These *in vitro* fecal fermentation models are mainly divided into two categories: (1) one compartment fermentation models and (2) dynamic fermentation models.[43] Based on different research purpures, researchers could select the appropriate fermentation model based on the advantages and limitations of the two types of models.

One compartment fermentation models are also known as batch (static) fermentation models which were chosen to study the gut microbial metabolism of representative green tea catechins EC and EGCG in the present thesis. These models are comparatively simple as compared to dynamic fermentation models, and normally consist of closed bottles/tubes or controlled reactors inoculated with fecal samples from the selected host.[44-45] These models are often used to conduct anaerobic incubations over short term periods (less than 72 h) as in longer

simulations the accumulation of the microbial metabolites may alter the conditions and the microbial composition compared to the conditions and the microbial composition at the initial stage. In the current thesis, the maximum incubation time was 24 h which can still be considered a short term incubation period for one compartment fermentation models. Moreover, these one compartment fermentation models are not only financially sustainable but also allow high-throughput studies. They provide an appropriate approach to study interindividual variabilities in gut microbial metabolism of food ingredients and other xenobiotics.[45] These models also require small quantities of chemicals of interest and are easy to operate. Besides these advantages certain limitations of one compartment fermentation models are worth to mention. For example, these models are not able to provide a constant refreshment of nutrients and removal of microbial metabolites. Also, they cannot mimic the dialysis and peristalsis of the intestines.[43] However, the main purpose of the present thesis was to unveil the metabolic pattern of EC and EGCG upon incubation with the human intestinal microbiota, including the intra- and inter-individual differences. The incubation results of both EC and EGCG revealed that the catechins were completely converted by fecal microbiota within 4 hours.[45-46] Therefore, for the studies of the present thesis a batch (static) fermentation model appeared suitable and of practical relevance.

It is also of interest to note that using anaerobic fecal incubations to characterize gut microbial metabolism, substantial differences were found in the level of deoxynivalenol conversion by the microbiota isolated from the different intestinal segments in chicken. Differences that were likely due the different composition of the microbiota in the different intestinal segments.[47] Thus, it may be interesting to investigate the metabolic patterns of tea catechins converted in anaerobic incubations with samples from different regions of the intestines.

In contrast to static fermentation models, a dynamic fermentation model enables the mimicking of the entire human gastrointestinal tract. One example of such a dynamic fermentation model is the human intestinal microbial ecosystem (SHIME) which consists of multi-compartment reactors to simulate the different conditions of the large intestine lumen, namely ascending colon, transverse colon and descending colon.[48-50] Besides SHIME, other representative dynamic fermentation models are the TNO computer-controlled, dynamic *in vitro* gastro-Intestinal Model of the colon (TIM-2) and SIMulator Gastro-Intestinal (SIMGI).[51-52] Generally, these dynamic fermentation models are considered to be able to maintain gut microbiota stability for longer timeframes and to simulate peristalsis and dialysis of the gut. The limitations of these dynamic models are also obvious, e.g., requiring large amounts of model compounds,

requiring experienced personnel, relatively expensive and time-consuming,[43] making them to offer no significant advantages over the batch (static) fermentation model for the aims of the studies of the present thesis. In addition, use of the batch (static) fermentation model to define PBK model kinetic constants V_{max} and K_m for gut microbial metabolism was previously shown to be valid for daidzein metabolism in rats, for which PBK model based predictions made were in line with experimental data on C_{max} levels for both daidzein and its gut microbial metabolite S-equol.[53]

1.2.3 Modulatory effects of catechins and their microbial metabolites on human gut microbiota

The results of **Chapter 2** and **3** show that the gut microbiota plays a crucial role in the degradation of green tea catechins and production of microbial metabolites. Meanwhile, recent studies have shown that the green tea catechins can, on the other hand, modulate the human intestinal microbial composition, which may also contribute to the improvement of hosts' health.[39, 54-55] In **Chapter 6**, the developed PBK model predicted, that after realistic dosing levels of green tea or EGCG supplements in humans, the concentrations of EGCG and its major metabolites may reach relatively high levels in especially the intestinal tract that may elicit Nrf2-mediated gene expression but also modulate the intestinal microbiome profile. For instance, green tea polyphenols and tea infusions have been reported to prevent the decrease in the α-diversity of the gut microbiota induced by high fat diet (HFD) as well as by selected xenobiotics.[56-59] Moreover, catechins are also able to modulate the relative microbial composition in the gut.[59] It has been reported that the tea polyphenols are able to inhibit the growth of pathogenic bacteria including *Bilophila*, *Enterobacteriaceae*, *Escherichia coli* O157:H7, *Fusobacterium varium*, *Helicobacter pylori*, *Pseudomonas aeruginosa*, *Staphylococcus aureus* and *Salmonella typhimurium* DT104, etc.[39, 60] Beneficial bacteria, such as *Bifidobacterium*, *Akkermansia muciniphila* and *Lactobacillus*, that could enhance intestinal barrier integrity, and counteract various pathogens were stimulated by tea ployphenols.[39, 45, 61-62] Zhang et al., observed selective prebiotic effects and anti-microbial activities of a catechin metabolite, namely (-)-epigallocatechin 3-*O*-(3-*O*-methyl) gallate (EGCG3''Me), showing a weight reducing effect in HFD-induced obesity in mice, which may be due to its ameliorating effect on the HFD-induced gut dysbiosis resulting in a decrease of the ratio of *Firmicutes*/*Bacteroidetes*.[60] The mechanisms underlying the microbial modulatory effects of tea polyphenols could be the result of a series of events, e.g., different sensitivity of bacteria toward polyphenols, a more anaerobic gut environment created by polyphenols, or a tea

polyphenol-altered nutrient environment in the gut.[59] However, as mentioned previously, green tea catechins are prone to intensive microbial metabolism in the large intestine, thus producing many metabolites. Therefore, it remains interesting to investigate on how those microbial metabolites could modulate the gut microecology.

1.2.4 Biological activities of green tea catechins and their gut microbial metabolites

In this thesis, we discovered that both EGCG and the microbial metabolites GA, PG, catechol and 3,4-diHPV were able to induce the Nrf2-EpRE-mediated gene expression, that may strengthen the cellular defence system (**Chapter 3**,**4** and **5**). Besides these Nrf2-dependent beneficial effects, other Nrf2-independent health-promoting effects of tea catechins also attract considerable attention from researchers worldwide. This section will discuss some of the most remarkable health effects of tea catechins.

1.2.4.1 Antimutagenic and Anticarcinogenic Potential

The function of green tea catechins in protection against cancers has been characterized in both studies using cell models and studies with laboratory animals. In animal studies, green tea catechins have been proved to inhibit the tumorigenesis of the skin, oral cavity, oesophagus, intestines, pancreas, liver, prostate, lung, etc.[63-64] The anticarcinogenic potential in internal organs of galloylated catechins, e.g., EGCG maybe limited due to its low systemic concentration. While the concentration of EGCG reached in the intestinal tract could be much higher than those in the systemic concentration, offering the opportunity for inhibiting carcinogenesis in the digestive tract.[63, 65] For example, Ju and co-workers reported that EGCG exerted a dose-dependent small intestinal tumour inhibition effect in $Apc^{min/+}$ mice, which was possibly through the aberration of nuclear β-catenin and activation of Akt and ERK signalling pathways.[66] Polyphenon E (consisting 65% of EGCG and 22% of other catechins) was found to be able to decrease the total number of aberrant crypt foci in a dose-dependent manner in an azoxymethane-induced rat colon cancer model. The inhibitory effect of Polyphenon E was associated with increased apoptosis, decreased nuclear expression levels of β-catenin and cyclin D1 and prevented loss of retinoid X receptor α in aberrant crypt foci with high-grade dysplasia.[67] EGCG was shown to increase the sensitivity of 5-fluorouracil-resistant (5-FUR) colorectal cancer cells to 5-fluorouracil and supress the proliferation in 5-FUR colorectal cancer cells through enhancement of apoptosis and cell cycle arrest. In line with the findings in the cell

model in that study, EGCG treatment inhibited the tumour growth in a spheroid-derived cancer stem cells xenograft murine model.[68]

In contrast to the strong evidence for the cancer-protective properties of green tea catechins in cell or animal models, studies in humans suggest the cancer preventive effect of tea is only mild and sometimes inconsistent. For instance, daily oral administration of 3 grams of mixed tea product to patients with oral mucosa leucoplakia for half a year was shown to significantly decrease the number and total volume of proliferation index and silver-stained nucleoli organizer regions.[69] While the subsequent phase 2 clinical trial on patients with pre-malignant lesions indicated only non-significant effects of green tea extract on ameliorating the pre-malignant lesions.[70] Similar results were obtained in human intervention studies investigating the anti-prostate cancer activity of tea catechins; Bettuzzi et al., claimed that green tea catechins are very effective for treating pre-malignant lesions before prostate cancer develops.[71] However, a later human trial conducted by Kumar and colleagues did not find a reduction in the number of prostate cancer cases between a Polyphenon E treated group and the placebo group.[72] The discrepancies between studies may be (partly) due to the differences in the genetic background and lifestyle of human subjects and also other confounding factors, such as for example smoking habits, which could substantially affect the study outcomes.[63]

The mode of action underlying the cancer preventive effects of green tea catechins may proceed through the regulation of genes and signalling pathways that are involved in the initiation, promotion and progression of cancer. Accumulation of reactive oxygen species (ROS) can cause irreversible DNA damage and may lead to cancer pathogenesis.[63] Catechins are capable of repressing cellular oxidative stress thus contributing to the inhibition of tumorigenesis. For instance, tea catechins can directly act as antioxidant that scavenge free radicals, including ROS. They can also play their protective role via inducing detoxifying enzymes, including for example glutathione S-transferases (GSTs), glutathione reductases (GRs) and UDP-glucuronosyltransferases (UGTs) and many others (**Chapter 5**). On the other hand, tea catechins ameliorate cellular and tissue oxidative status through down-regulating pro-oxidant enzymes such as xanthine oxidase and cyclooxygenase.

The ability of up-regulating or enhancing the stability of tumour suppressor genes is another mechanism underlying the inhibiting cancer progression and development by green tea catechins. For example, green tea polyphenols/EGCG treatment of LNCaP human prostate cancer cells resulted in acetylation of the tumour suppressor gene p53 which in turn enhanced the transcriptions of p53. The green tea polyphenols/EGCG-mediated p53 acetylation

facilitated its binding on the promoters of Bax and p21/waf1, which increased the number of cells in the G0/G1 phase of the cell cycle and promoted apoptosis.[73] EGCG has not only been reported to be able to increase the transcriptional activity of p53 but also to decrease the nuclear accumulation of E3 ubiquitin-protein ligase MDM2 thus increasing the stability of p53.[74] By performing a proteomics study on Caco-2 cells treated with green tea catechins and their colonic metabolites in this thesis (**Chapter 4**), we also discovered one potential tumour suppressor protein (Focadhesin) that was significantly up-regulated (data not shown). There is one study on the tumour suppressor function of Focadhesin in gliomas.[75] However, how catechins and their microbial metabolites could regulate Focadhesin expression and whether this regulation could contribute to the cancer-preventive effects of tea polyphenols *in vivo* remains interesting to be further unveiled in future studies.

Other mechanisms including anti-inflammatory effects, stimulation of apoptosis, anti-proliferative activity, inhibition of angiogenesis, modulation of cell signalling and interaction with 67-kDa Laminin receptor may also contribute to the observed cancer-preventive potency of green tea catechins.[6, 11, 63-65] However, in these studies the anti-cancer effects were always ascribed to the parent compound catechins, and therefore the role of the gut microbial metabolites in these effects remains to be investigated.

1.2.4.2 Other health-promoting effects of green tea polyphenols

Epidemiological studies have revealed that the consumption of green tea is associated with a reduced cardiovascular disease risk.[76-77] The mechanisms underlying this effect mainly include reducing ischemia/reperfusion injury, ameliorating oxidative stress, lowering blood lipid levels, attenuating inflammation, protecting cardiomyocyte function and improving endothelial function.[78-79] Green tea catechins have also been reported to display neuroprotective effects in humans and may have preventive effects for Parkinson and Alzheimer diseases.[80-82] The reduction of neurodegenerative disease risk by green tea catechins has been associated with the prevention of neuronal cell dysfunction and cell death in the cerebral cortex.[83] Moreover, it has been revealed that green tea catechins can prevent or delay the progression of inflammatory bowel disease (IBD), e.g., Crohn's disease (CD) and ulcerative colitis (UC), by their antioxidant and anti-inflammatory activities as well as via their modulatory effect on gut microbiota.[84-85] Additionally, anti-obesity is another attractive benefit of green tea consumption. The anti-obesity mechanisms of green tea catechins include prevention of absorption, inhibition of digestive enzymes, regulation of intestinal microbiota and activation of adenosine

monophosphate-activated protein kinase (AMPK) which suppresses adipogenesis and lipogenesis.[86-88] Besides, the anti-viral, anti-diabetic, osteoprotective and female reproductive disorder repairing effects are also valuable traits of green tea catechins.[6, 65, 89]

However, so far, to what extent these beneficial effects are due to the green tea catechins or their microbial metabolites is not clear. It is well-accepted that the tea polyphenols have a low bioavailability and thus the majority of the parent compounds are passed on to the large intestine where they are prone to intensive microbial conversion.[14, 59] Therefore, especially for *in vivo* studies investigating the mechanisms underlying the health-promoting properties of green tea catechins, it is advised to include the potential activities of major intestinal microbial metabolites of green tea catechins, as they may have higher potency than their parent compounds.

1.2.5 Proteomics used in studies on the bioactivity of green tea catechins

In this thesis, reporter gene assays and RT-qPCR were performed to characterize the Nrf2 activation by EGCG, EC and their microbial metabolites. However, these methods are not likely to effectively reflect a whole picture of the molecular functional network since Nrf2 is a master regulator that mediates more than 200 proteins.[90] Therefore, a label-free proteomics analysis was conducted to monitor the differences in the expression levels of a substantial amount of proteins between control and chemical (green tea catechins and their microflora-derived metabolites) exposed Caco-2 cells and/or Hepa1c1c7 cells. The results indicate that the gut microbial metabolites 3,4-diHPV and PG appeared able to induce changes in Nrf2-reglulated proteins more potently than their parent compounds EC and EGCG at equimolar concentrations (**Chapter 4** and **5**). Especially for the metabolite PG, the well-accepted Nrf2-mediated pathways, namely Glutathione metabolism, Metabolism of xenobiotics by cytochrome P450 and Drug metabolism-cytochrome P450, were the top three most significant altered signalling networks upon treatment of the Hepa1c1c7 cells with 30 µM PG. To further validate the results of these KEGG enrichments, the relative intracellular glutathione (GSH) levels between chemical-treated groups and the control group can be measured in future studies. Moreover, these Nrf2-associated bioinformatic terms were also significantly enriched upon exposure of cells to the reference compound t-BHQ. Therefore, the comparison indicates that PG and t-BHQ share some similar characteristics in regulating the Nrf2 pathway whose activation regulates a series of detoxification and antioxidant enzymes.[7-8, 90-91]

3,4-diHPV is definitely an important compound worth further investigations. It is the most abundant and stable gut microbial metabolites formed from several flavan-3-ols and is believed to be an important biomarker *in vivo* for catechin intake[45, 50, 92] Though the results of the U2OS-Nrf2 CALUX reporter gene assay and RT-qPCR both revealed that 3,4-diHPV was able to positively induce the Nrf2-mediated gene expression, it is worth noting that the Nrf2 signaling or Nrf2-regulated intermediary metabolism were not among the most significantly enriched pathways identified by the enrichment analysis of differentially expressed proteins (DEPs) which shows the translation related events that were likely to be affected most. Therefore, this also implies that future studies that aim to characterize the beneficial effects of 3,4-diHPV may better also explore Nrf2-independent mechanisms, e.g., studies on the pro- or anti-proliferative effects or the reciprocal interactions with gut microbiota.

The overall protein level changes in both Caco-2 and Hepa1c1c7 cells upon 30 µM PG or 3,4-diHPV treatments compared to untreated control cells were relatively mild, with fold changes smaller than 1.5. This may be due to the low cellular absorption of these polyphenols resulting in limited intracellular concentrations of the test compounds,[93-94] even though the exposure medium was supplemented with freshly made L-ascorbic acid which has been reported to be able to not only improve the stability but also inhibit the efflux transporters of green tea catechins.[95-96] On the other hand, it has been recognized that the formation of catechin quinone intermediates are underlying the mode of action of catechin-induced Nrf2 activation.[21, 97] Therefore, the supplemented L-ascorbic acid in the exposure medium may act as antioxidant and thus inhibit the pro-oxidative potential of green tea catechins and their microbial metabolites, ultimately leading to an only mild induction of the Nrf2 pathway. This may explain the discrepancy of GA in inducing Nrf2 activation in **Chapter 3** and **Chapter 5** of the present thesis. In **Chapter 3**, the reporter gene assay was performed with cells exposed to GA in the absence of L-ascorbic acid, while co-exposing to GA and L-ascorbic acid in the **Chapter 5**. As a result, GA was identified as an Nrf2 inducer in **Chapter 3** but not in the **Chapter 5**.

Other possible explanations for the general mild induction of Nrf2-mediated gene expression can be, e.g., saturation in mRNA translation efficiency and/or post-translational modifications via miRNAs. In the present thesis, though the proteomics results and RT-qPCR results share increased gene and protein expression characteristics, it is worth to mention that relative RNA levels (measured via RT-qPCR) of the selective Nrf2-associated genes were higher than the corresponding fold changes of proteins (detected via the proteomics). For example, the relative RNA levels of Gsta3 and Ugt1a6 were 10.2 and 3.6, respectively, while the fold changes of

glutathione S-transferase A3 and UDP-glucuronosyltransferase 1A6 (the corresponding proteins) amounted to 2.7 and 1.6, respectively. The comparatively lower fold changes are likely due to the post-translational regulations, indicating the relative transcriptional levels are not always exactly aligned with the respective translational levels from proteomics results in terms of the fold changes observed. Nevertheless, the reporter gene assay, RT-qPCR and proteomics results all corroborate the hypothesis that the microbial metabolites, 3,4-diHPV and PG, were more potent in inducing Nrf2 activation compared to their parent compounds EC and EGCG, respectively.

To further explore the induction of Nrf2-mediated protein expression by green tea catechins and their microbial metabolites, testing of low to high exposure concentrations are recommended for further proteomics experiments. Moreover, the exposure time period used in the experiments of the present thesis was 24 h. It is likely that the time course patterns for the expression of Nrf2-regualted proteins could be progressive or biphasic depending on the protein investigated.[98] For instance, Liu et al., observed the time-dependent elevation of catalase (Cat) and heme oxygenase 1 (Hmox1) but a biphasic time course pattern for induction of superoxide dismutase 1 (Sod1) in mouse bone marrow tissue in response to ionizing radiation. The biphasic response may reflect early and late responses to external stimuli that may be controlled by different mechanisms.[98-99] It is possible that biphasic time patterns could also occur for Nrf2-associated protein expression in cells exposed to green tea catechins or their microbial metabolites. Moreover, it is reported that the green tea catechins reach their maximum plasma concentrations in 2 hours and are eliminated within 12 hours while their microbial metabolites reach the maximum plasma concentrations in 6 hours and are cleared only after 24 h or even longer time periods.[13, 100-103] Therefore, to further explore these time dependent responses, further proteomics experiments could include more exposure time points, e.g., 4 h, 8h, 24 h, 48 h and 72 h. However, one should keep in mind that under the static exposure conditions, with increasing exposure time the conditions may change compared with shorter-time exposures. Therefore, the exposure medium should be refreshed at well-defined time points, especially for co-exposure with L-ascorbic acid that auto-oxidises quickly.[104] However one should also bear in mind that including more exposure concentrations and incubation time points will result in many more samples which may raise some financial pressure since doing a proteomics study is still relatively expensive.

As mentioned in the introduction, green tea infusions contain several green tea catechins and they can form many microbial metabolites *in vivo*. Moreover, other polyphenols can also be

present in the diet. Therefore, it may be necessary to take into account the combined biological responses mediated by the entire phenolic pool. For instance, co-exposure to curcumin improved the anti-proliferative effect of EGCG on prostate cancer cells (PC3) through synergistic up-regulation of p21-induced growth arrest.[105] EC showed a major synergistic effect on the induction of apoptosis in gastric carcinoma cells (MKN-45) treated with EGCG which may be due to the extracellular production of ROS under co-exposure conditions.[106] However, so far, there is no study investigating the potential synergistic effects of green tea catechins in combination with their microbial metabolites e.g., phenyl-γ-valerolactones, phenyl-γ-valeric acids, GA and PG, etc. Future research on establishing additional health benefits of combined exposure to catechins and their microbial metabolites, and the mechanistic pathways underlying potential synergistic beneficial effects is encouraged.

Additionally, for future studies it would be interesting to check whether the up-regulation of Nrf2-mediated protein expression levels could be of help in prevention or restoration of external stress factor stimulated adverse effects. For example, pretreatment of cells with hydrogen peroxide (H_2O_2) for a few hours to induce oxidative stress and subsequent exposure of the cells to green tea catechins and their microbial metabolites may be studied to elucidate whether there is a restorative effect of tea polyphenols on H_2O_2-induced oxidative stress. Similarly, one can also pretreat the cells with tea polyphenols during a certain amount of time and then expose the cells to H_2O_2 either in the absence or in the continued presence of the polyphenols to investigate whether there is a preventive effect of the tea polyphenols against this H_2O_2 induced oxidative stress. Importantly, further investigations on the mechanisms underlying the preventive/restorative effects of tea polyphenols will bring more insights in the health-promoting effects of green tea/supplements consumption. Moreover, it is of importance to consider what are realistic concentrations to test in *in vitro* studies as it has been reported that systemic concentrations of catechins and their microbial metabolites in humans are ranged between sub-micromolar to less than 10 µM upon intake of catechins or green tea.[107-111]

Some practical tips of the proteomics study can be useful to discuss to avoid batch effects and to reduce the impact of confounding factors, in order to provide stable/reliable results from different biological replicates in future experiments. For instance, one of the most crucial influencers is the cellular condition. It is suggested to use stably cultured cells and closely check the cell conditions before any further experiments. Discussion with experienced personnel/technicians is necessary to choose the optimal sample preparation method based on the proteins of interest (if possible). Moreover, as the sample preparation for a proteomics study

usually consists of more than 20 steps it is highly suggested to collect enough sample material for at least three biological replicates and then perform the processing together to reduce possible batch effects especially for situations where the changes in protein levels are mild as was the case in the proteomics studies of the present thesis. When target proteins are unstable certain protease/phosphatase inhibitors and processing under low temperature are also recommended.

1.2.6 PBK modeling and quantitative *in vitro* to *in vivo* extrapolation (QIVIVE)

To fulfil the 3Rs principle and also to develop a non-animal based novel method towards NAMs for characterizing the *in vivo* biological effects of phytochemicals, a PBK model for EGCG in humans was developed including a separate microbial metabolism compartment to predict *in vivo* kinetics of EGCG and to gain insight in the role of the gut microbiota and its EGCG metabolites in the *in vivo* effects observed upon oral exposure to EGCG (**Chapter 6**). The conceptual PBK model was designed according to the pharmacokinetics of EGCG following oral administration. After oral intake of EGCG, a very small portion is directly absorbed in the small intestine where the EGCG could be conjugated, resulting the formation of, e.g., 4″-O-methyl-EGCG, 4′,4″-O-dimethyl-EGCG and 4″-O-glucuronide-EGCG.[112-113] Similar conjugation reactions also occur in the liver. However, these conjugation reactions for EGCG are believed to contribute only to a limited extent since EGCG is found mostly in unmodified form in the plasma.[107, 114] The systemically absorbed EGCG is mainly excreted as such through the bile into the colon.[115] Moreover, active efflux of methylated EGCG conjugates by the multidrug resistance-associated protein 2 (MRP2) located on the apical surface of the intestinal cells further decreases the intracellular levels and systemic bioavailability of EGCG and its conjugates.[113] As a result, no conjugated metabolites of EGCG have been detected in biological fluids *in vivo*.[113, 115-116] Therefore, the conjugation of EGCG was assumed also in the present study to not affect the systemic circulation of EGCG and thus the current PBK model did not include these reactions in either the small intestine or liver compartment.

Upon oral exposure EGCG cannot be detected in urine, indicating its elimination is not renal, while its biliary excretion contributes to its transport to the colon where, together with the relatively high percentage of unabsorbed EGCG it becomes a substrate for gut microbial conversion.[115, 117-118] The major microbial metabolites formed include GA and PG which, upon their systemic absorption, are eliminated mainly through renal excretion. For instance,

Shahrzad et al. found that 36.4% of GA intake was excreted as GA and 4-O-methylgallic acid (4OMGA) in urine 12 h after oral administration of a GA tablet, indicating that GA is much more readily absorbed in the small intestine compared to EGCG and appears in higher proportion in the systemic circulation.[119] Similarly, sulfated and glucuronidated PG conjugates are also reported to be detected in human plasma and urine after a single dose of green or black tea extract consumptions.[120-121] Since the specific metabolic profile for GA and PG in the liver remains to be unveiled, their kinetics were described in the present PBK model by an overall clearance.

Though a number of studies have been devoted to developing proofs-of principle of the PBK modeling-based reverse dosimetry for the prediction of *in vivo* dose response curves for various biological endpoints, it is both time and resource consuming to develop a PBK model for each individual compound. Therefore, development of a simple and generic PBK model that requires a minimum number of *in vitro* and *in silico* determined parameter values to adequately describe the kinetics would be useful. The developed PBK model of the present thesis is able to adequately predict the *in vivo* kinetics of EGCG after oral administration under different conditions, serving as a starting point to develop a generic PBK modeling-based reverse dosimetry approach that can be used for *in vivo* bioactivity predictions of a battery of Nrf2-inducing phytochemicals including contributions of their respective microbial metabolites.

In addition, it is relevant to note that the current PBK model was developed using parameter values for the average population, and thus does not take interindividual differences into account. However, as shown in **Chapter 2** and **3**, substantial interindividual differences in the microbial compositions were observed among volunteers, which in turn could cause significant interindividual variabilities in microbial metabolic patterns of green tea catechins. Moreover, it is well known that most of the human hepatic genes can quantitatively vary substantially among human subjects, contributing to the strong interindividual difference in susceptibility to drugs or other external environmental factors.[122] Therefore, for further refinements of the PBK modeling, interindividual variations in human gut microbial metabolism and hepatic clearance of green tea catechins and their metabolites are encouraged to be studied to a further extent. These can be achieved by performing human liver S9 incubations using liver S9 fractions of different individuals and fecal anaerobic incubations using the fecal suspension from individual volunteers. Kinetic constants of different individuals thus obtained can be used to define individual PBK models and/or to define the distributions within the human population for the respective PBK model parameters to enable integration of the PBK model with Monte Carlo

simulations and the predictions of potential interindividual variabilities in EGCG, GA and PG *in vivo* kinetics.

Using the PBK modeling-based reverse dosimetry approach, it is concluded that the systemic concentrations expressed in EGCG equivalents upon exposure to green tea or green tea containing dietary supplements appear to be too low to result in induction of Nrf2-mediated gene expression in target organs different than the gastrointestinal tract. This may explain studies in humans that suggest the health effects of tea to be mild and sometimes inconsistent, limited or even absent (discussed in section 7.2.4.1). Alternatively, the systemic health benefits of EGCG may arise from Nrf2-independent modes of action. For instance, Li and colleagues conducted a study on protective effects of catechin-rich green tea extract (GTE) against high fat diet-induced nonalcoholic steatohepatitis in wild-type and Nrf2-null mice.[123] They showed that GTE reduced hepatic steatosis and injury and lowered mRNA expression of hepatic lipid uptake and lipogenic genes regardless of Nrf2 status. Additionally, GTE also lowered NFκB phosphorylation and TNF-α and MCP1 mRNA levels in Nrf2-null mice. Thus, they concluded that anti-inflammatory and hypolipidemic activities of GTE during nonalcoholic steatohepatitis likely occur largely through an Nrf2-independent mechanism.[123] In contrast, concentrations of EGCG, GA and PG in the large intestinal lumen resulting from oral administration of a realistic amount of green tea/EGCG supplements were predicted to amount to much higher levels, which are likely to exert certain local effects e.g., Nrf2 activation in exposed intestinal cells, antioxidant activity, modulation of the gastrointestinal enzyme activity, prebiotic activity, etc. For instance, Sukhthankar et al., found that 50 μM EGCG could significantly down-regulate the expression of basic fibroblast growth factor (bFGF) in colorectal cancer cell lines and subsequent experiments in *Apc*^min/+ mice treated with 0.01% EGCG drinking water showed that the suppression of intestinal tumorigenesis *in vivo* was associated with reduced bFGF expression.[124] The developed PBK model predicts that after consumption of two cups of green tea, the maximum concentration expressed in EGCG equivalents in the large intestine was predicted to be 81.53 μM, which is likely to be able to induce Nrf2 gene expression and to suppress growth and metastasis of colorectal cancer.

1.3 Conclusion

To conclude, the current thesis characterised the gut microbial metabolic fates of two representative green tea catechins, namely EC and EGCG, via performing *in vitro* anaerobic fecal incubations. Colonic metabolites of these tea catechins showed higher potency in

regulating Nrf2-mediated gene expression. The inter-individual and intra-individual differences found in the microbial conversions of tea catechins may thus affect the overall health-promoting effects of green tea consumption related to the Nrf2 signalling pathway activation. This thesis also generated a proof-of-principle on how to integrate *in vitro* data and *in silico* PBK modeling to predict *in vivo* kinetics of model compounds and characterise their dose levels needed to induce Nrf2 induction *in vivo* in humans. The inclusion of gut microbial metabolism in the PBK model enabled modeling of contributions of the colonic metabolites GA and PG to the overall Nrf2 activation upon EGCG exposure. The results reveal that although GA and PG are more capable of inducing Nrf2 pathway activation than EGCG, their contributions to systemic induction of Nrf2 mediated gene expression were predicted to be limited due to their substantial lower systemic concentrations compared to EGCG. In contrast, concentrations of the metabolites in the intestinal tract may reach levels that are high enough to activate Nrf2 gene transcription. Overall, the insights provided in the present thesis open a door for future studies on identification of catechin-converting gut microbiota, establishing metabotypes in humans regarding microbial degradation of green tea catechins and *in vivo* ADME of green tea catechins and their microbial metabolites focusing on target tissues where local effects may play an important role in the biological activity of the green tea catechins.

References

1.   Blumberg, J. B.; Bolling, B. W.; Chen, C. O.; Xiao, H., Review and perspective on the composition and safety of green tea extracts. *European Journal of Nutrition & Food Safety* **2015**, 1-31.

2.   Fallah, S.; Musa-Veloso, K.; Cao, J.; Venditti, C.; Lee, H. Y.; Hamamji, S.; Hu, J.; Appelhans, K.; Frankos, V., Liver biomarkers in adults: Evaluation of associations with reported green tea consumption and use of green tea supplements in US NHANES. *Regulatory Toxicology and Pharmacology* **2022,** *129*, 105087.

3.   Liu, Z.; Bruins, M. E.; Ni, L.; Vincken, J.-P., Green and black tea phenolics: Bioavailability, transformation by colonic microbiota, and modulation of colonic microbiota. *Journal of Agricultural and Food Chemistry* **2018,** *66* (32), 8469-8477.

4.   Graham, H. N., Green tea composition, consumption, and polyphenol chemistry. *Preventive medicine* **1992,** *21* (3), 334-350.

5.   Chacko, S. M.; Thambi, P. T.; Kuttan, R.; Nishigaki, I., Beneficial effects of green tea: a literature review. *Chinese medicine* **2010,** *5* (1), 1-9.

6.   Musial, C.; Kuban-Jankowska, A.; Gorska-Ponikowska, M., Beneficial properties of green tea catechins. *International journal of molecular sciences* **2020,** *21* (5), 1744.

7.   Tonelli, C.; Chio, I. I. C.; Tuveson, D. A., Transcriptional regulation by Nrf2. *Antioxidants & redox signaling* **2018,** *29* (17), 1727-1745.

8.   Yamamoto, M.; Kensler, T. W.; Motohashi, H., The KEAP1-NRF2 system: a thiol-based sensor-effector apparatus for maintaining redox homeostasis. *Physiological reviews* **2018,** *98* (3), 1169-1203.

9.   Cai, Z.-Y.; Li, X.-M.; Liang, J.-P.; Xiang, L.-P.; Wang, K.-R.; Shi, Y.-L.; Yang, R.; Shi, M.; Ye, J.-H.; Lu, J.-L., Bioavailability of tea catechins and its improvement. *Molecules* **2018,** *23* (9), 2346.

10.   van ͐t Slot, G.; Humpf, H.-U., Degradation and metabolism of catechin, epigallocatechin-3-gallate (EGCG), and related compounds by the intestinal microbiota in the pig cecum model. *Journal of agricultural and food chemistry* **2009,** *57* (17), 8041-8048.

11.   Alam, M.; Ali, S.; Ashraf, G. M.; Bilgrami, A. L.; Yadav, D. K.; Hassan, M. I., Epigallocatechin 3-Gallate: From Green Tea to Cancer Therapeutics. *Food Chemistry* **2022**, 132135.

12.   Del Rio, D.; Calani, L.; Cordero, C.; Salvatore, S.; Pellegrini, N.; Brighenti, F., Bioavailability and catabolism of green tea flavan-3-ols in humans. *Nutrition* **2010,** *26* (11-12), 1110-1116.

13.   Ottaviani, J. I.; Borges, G.; Momma, T. Y.; Spencer, J. P.; Keen, C. L.; Crozier, A.; Schroeter, H., The metabolome of [2-14 C](−)-epicatechin in humans: implications for the assessment of efficacy, safety and mechanisms of action of polyphenolic bioactives. *Scientific reports* **2016,** *6* (1), 1-10.

14.   Borges, G.; Ottaviani, J. I.; van der Hooft, J. J.; Schroeter, H.; Crozier, A., Absorption, metabolism, distribution and excretion of (−)-epicatechin: A review of recent findings. *Molecular Aspects of Medicine* **2018,** *61*, 18-30.

15.   Tang, G.; Xu, Y.; Zhang, C.; Wang, N.; Li, H.; Feng, Y., Green tea and epigallocatechin gallate (EGCG) for the management of nonalcoholic fatty liver diseases (NAFLD): Insights into the role of oxidative stress and antioxidant mechanism. *Antioxidants* **2021,** *10* (7), 1076.

16.   Kanner, J., Polyphenols by generating H2O2, affect cell redox signaling, inhibit PTPs and activate Nrf2 axis for adaptation and cell surviving: in vitro, in vivo and human health. *Antioxidants* **2020,** *9* (9), 797.

17.   Estudante, M.; Morais, J. G.; Soveral, G.; Benet, L. Z., Intestinal drug transporters: an overview. *Advanced drug delivery reviews* **2013,** *65* (10), 1340-1356.

18.   Louisse, J.; Beekmann, K.; Rietjens, I. M., Use of physiologically based kinetic modeling-based reverse dosimetry to predict in vivo toxicity from in vitro data. *Chemical research in toxicology* **2017,** *30* (1), 114-125.

19.   Wang, L.-Q.; Meselhy, M. R.; Li, Y.; Nakamura, N.; Min, B.-S.; Qin, G.-W.; Hattori, M., The heterocyclic ring fission and dehydroxylation of catechins and related compounds by Eubacterium sp. strain SDG-2, a human intestinal bacterium. *Chemical and pharmaceutical bulletin* **2001,** *49* (12), 1640-1643.

20.   Thavasi, V.; Leong, L. P.; Bettens, R. P. A., Investigation of the influence of hydroxy groups on the radical scavenging ability of polyphenols. *The journal of physical chemistry A* **2006,** *110* (14), 4918-4923.

21.   Muzolf-Panek, M.; Gliszczyńska-Świgło, A.; de Haan, L.; Aarts, J. M.; Szymusiak, H.; Vervoort, J. M.; Tyrakowska, B.; Rietjens, I. M., Role of catechin quinones in the induction of EpRE-mediated gene expression. *Chemical research in toxicology* **2008,** *21* (12), 2352-2360.

22.   Lee-Hilz, Y. Y.; Boerboom, A.-M. J.; Westphal, A. H.; van Berkel, W. J.; Aarts, J. M.; Rietjens, I. M., Pro-oxidant activity of flavonoids induces EpRE-mediated gene expression. *Chemical research in toxicology* **2006,** *19* (11), 1499-1505.

23.   Kutschera, M.; Engst, W.; Blaut, M.; Braune, A., Isolation of catechin‑converting human intestinal bacteria. *J. Appl. Microbiol.* **2011,** *111*, 165-175.

24.   Takagaki, A.; Nanjo, F., Bioconversion of (−)-epicatechin,(+)-epicatechin,(−)-catechin, and (+)-catechin by (−)-epigallocatechin-metabolizing bacteria. *Biol. Pharm. Bull.* **2015,** *38*, 789-794.

25.   Sánchez-Patán, F.; Tabasco, R.; Monagas, M.; Requena, T.; Peláez, C.; Moreno-Arribas, M. V.; Bartolomé, B. a., Capability of Lactobacillus plantarum IFPL935 to catabolize flavan-3-ol compounds and complex phenolic extracts. *J. Agric. Food. Chem.* **2012,** *60*, 7142-7151.

26.   Sánchez-Patán, F.; Tabasco, R.; Monagas, M.; Requena, T.; Peláez, C.; Moreno-Arribas, M. V.; Bartolomé, B. a., Capability of Lactobacillus plantarum IFPL935 to catabolize flavan-3-ol compounds and complex phenolic extracts. *J. Agric. Food Chem.* **2012,** *60*, 7142-7151.

27.   Stevens, J. F.; Maier, C. S., The chemistry of gut microbial metabolism of polyphenols. *Phytochemistry Reviews* **2016,** *15* (3), 425-444.

28.   van Duynhoven, J.; Vaughan, E. E.; Jacobs, D. M.; Kemperman, R. A.; van Velzen, E. J.; Gross, G.; Roger, L. C.; Possemiers, S.; Smilde, A. K.; Doré, J., Metabolic fate of polyphenols in the human superorganism. *Proceedings of the national academy of sciences* **2011,** *108* (Supplement 1), 4531-4538.

29.   Makarewicz, M.; Drożdż, I.; Tarko, T.; Duda-Chodak, A., The Interactions between polyphenols and microorganisms, especially gut microbiota. *Antioxidants* **2021,** *10* (2), 188.

30.   Da Silva, S. M.; Venceslau, S. S.; Fernandes, C. L.; Valente, F. M.; Pereira, I. A., Hydrogen as an energy source for the human pathogen Bilophila wadsworthia. *Antonie Van Leeuwenhoek* **2008,** *93*, 381-390.

31.   Kemperman, R. A.; Gross, G.; Mondot, S.; Possemiers, S.; Marzorati, M.; Van de Wiele, T.; Doré, J.; Vaughan, E. E., Impact of polyphenols from black tea and red wine/grape juice on a gut model microbiome. *Food Research International* **2013,** *53* (2), 659-669.

32.   Walle, T.; Walle, U. K.; Halushka, P. V., Carbon dioxide is the major metabolite of quercetin in humans. *The Journal of nutrition* **2001,** *131* (10), 2648-2652.

33.   Thursby, E.; Juge, N., Introduction to the human gut microbiota. *Biochemical Journal* **2017,** *474* (11), 1823-1836.

34.   Eckburg, P. B.; Bik, E. M.; Bernstein, C. N.; Purdom, E.; Dethlefsen, L.; Sargent, M.; Gill, S. R.; Nelson, K. E.; Relman, D. A., Diversity of the human intestinal microbial flora. *science* **2005,** *308* (5728), 1635-1638.

35.   Rowland, I.; Gibson, G.; Heinken, A.; Scott, K.; Swann, J.; Thiele, I.; Tuohy, K., Gut microbiota functions: metabolism of nutrients and other food components. *European journal of nutrition* **2018,** *57* (1), 1-24.

36.   Titgemeyer, E. C.; Bourquin, L. D.; Fahey Jr, G. C.; Garleb, K. A., Fermentability of various fiber sources by human fecal bacteria in vitro. *The American journal of clinical nutrition* **1991,** *53* (6), 1418-1424.

37.   Aura, A.-M.; O'leary, K.; Williamson, G.; Ojala, M.; Bailey, M.; Puupponen-Pimiä, R.; Nuutila, A.-M.; Oksman-Caldentey, K.-M.; Poutanen, K., Quercetin derivatives are deconjugated and converted to hydroxyphenylacetic acids but not methylated by human fecal flora in vitro. *Journal of agricultural and food chemistry* **2002,** *50* (6), 1725-1730.

38.   Fehlbaum, S.; Prudence, K.; Kieboom, J.; Heerikhuisen, M.; Van den Broek, T.; Schuren, F. H.; Steinert, R. E.; Raederstorff, D., In vitro fermentation of selected prebiotics and their effects on the

composition and activity of the adult gut microbiota. *International journal of molecular sciences* **2018,** *19* (10), 3097.

39.   Liu, Z.; de Bruijn, W. J.; Bruins, M. E.; Vincken, J.-P., Reciprocal interactions between epigallocatechin-3-gallate (EGCG) and human gut microbiota in vitro. *Journal of Agricultural and Food Chemistry* **2020,** *68* (36), 9804-9815.

40.   Liu, Z.; de Bruijn, W. J.; Bruins, M. E.; Vincken, J.-P., Microbial metabolism of theaflavin-3, 3′-digallate and its gut microbiota composition modulatory effects. *Journal of agricultural and food chemistry* **2020,** *69* (1), 232-245.

41.   Behr, C.; Sperber, S.; Jiang, X.; Strauss, V.; Kamp, H.; Walk, T.; Herold, M.; Beekmann, K.; Rietjens, I.; Van Ravenzwaay, B., Microbiome-related metabolite changes in gut tissue, cecum content and feces of rats treated with antibiotics. *Toxicology and applied pharmacology* **2018,** *355*, 198-210.

42.   Lagkouvardos, I.; Overmann, J.; Clavel, T., Cultured microbes represent a substantial fraction of the human and mouse gut microbiota. *Gut microbes* **2017,** *8* (5), 493-503.

43.   Verhoeckx, K.; Cotter, P.; López-Expósito, I.; Kleiveland, C.; Lea, T.; Mackie, A.; Requena, T.; Swiatecka, D.; Wichers, H., The impact of food bioactives on health: in vitro and ex vivo models. **2015**.

44.   Aura, A.-M.; Härkönen, H.; Fabritius, M.; Poutanen, K., Development of anIn VitroEnzymic Digestion Method for Removal of Starch and Protein and Assessment of its Performance Using Rye andWheat Breads. *Journal of Cereal Science* **1999,** *29* (2), 139-152.

45.   Ouyang, J.; Zhu, K.; Liu, Z.; Huang, J., Prooxidant effects of epigallocatechin-3-gallate in health benefits and potential adverse effect. *Oxidative Medicine and Cellular Longevity* **2020,** *2020*.

46.   Liu, C.; Vervoort, J.; van den Elzen, J.; Beekmann, K.; Baccaro, M.; de Haan, L.; Rietjens, I. M., Interindividual Differences in Human In Vitro Intestinal Microbial Conversion of Green Tea (-)-Epigallocatechin-3-O-Gallate and Consequences for Activation of Nrf2 Mediated Gene Expression. *Molecular Nutrition & Food Research* **2021,** *65* (2), 2000934.

47.   Jin, J.; Fall, M.; Liu, Q.; Rietjens, I. M.; Xing, F., Comparative Microbial Conversion of Deoxynivalenol and Acetylated Deoxynivalenol in Different Parts of the Chicken Intestine as Detected In Vitro and Translated to the In Vivo Situation. *Journal of agricultural and food chemistry* **2021,** *69* (50), 15384-15392.

48.   Wu, T.; Grootaert, C.; Pitart, J.; Vidovic, N. K.; Kamiloglu, S.; Possemiers, S.; Glibetic, M.; Smagghe, G.; Raes, K.; Van de Wiele, T., Aronia (Aronia melanocarpa) polyphenols modulate the microbial community in a Simulator of the Human Intestinal Microbial Ecosystem (SHIME) and decrease secretion of proinflammatory markers in a Caco-2/endothelial cell coculture model. *Molecular nutrition & food research* **2018,** *62* (22), 1800607.

49.   Koper, J. E.; Loonen, L. M.; Wells, J. M.; Troise, A. D.; Capuano, E.; Fogliano, V., Polyphenols and tryptophan metabolites activate the aryl hydrocarbon receptor in an in vitro model of colonic fermentation. *Molecular nutrition & food research* **2019,** *63* (3), 1800722.

50.   Li, Q.; Van Herreweghen, F.; De Mey, M.; Goeminne, G.; Van de Wiele, T., The Donor-Dependent and Colon-Region-Dependent Metabolism of (+)-Catechin by Colonic Microbiota in the Simulator of the Human Intestinal Microbial Ecosystem. *Molecules* **2022,** *27* (1), 73.

51.   Minekus, M.; Smeets-Peeters, M.; Bernalier, A.; Marol-Bonnin, S.; Havenaar, R.; Marteau, P.; Alric, M.; Fonty, G., A computer-controlled system to simulate conditions of the large intestine with peristaltic mixing, water absorption and absorption of fermentation products. *Applied microbiology and biotechnology* **1999,** *53* (1), 108-114.

52.   Barroso, E.; Cueva, C.; Peláez, C.; Martínez-Cuesta, M. C.; Requena, T., Development of human colonic microbiota in the computer-controlled dynamic SImulator of the GastroIntestinal tract SIMGI. *LWT-Food Science and Technology* **2015,** *61* (2), 283-289.

53.	Wang, Q.; Spenkelink, B.; Boonpawa, R.; Rietjens, I. M.; Beekmann, K., Use of Physiologically Based Kinetic Modeling to Predict Rat Gut Microbial Metabolism of the Isoflavone Daidzein to S-Equol and Its Consequences for ERα Activation. *Molecular nutrition & food research* **2020,** *64* (6), 1900912.

54.	Guo, T.; Song, D.; Cheng, L.; Zhang, X., Interactions of tea catechins with intestinal microbiota and their implication for human health. *Food science and biotechnology* **2019,** *28* (6), 1617-1625.

55.	Gowd, V.; Karim, N.; Shishir, M. R. I.; Xie, L.; Chen, W., Dietary polyphenols to combat the metabolic diseases via altering gut microbiota. *Trends in Food Science & Technology* **2019,** *93*, 81-93.

56.	Liu, Z.; Chen, Z.; Guo, H.; He, D.; Zhao, H.; Wang, Z.; Zhang, W.; Liao, L.; Zhang, C.; Ni, L., The modulatory effect of infusions of green tea, oolong tea, and black tea on gut microbiota in high-fat-induced obese mice. *Food & function* **2016,** *7* (12), 4869-4879.

57.	Wang, L.; Zeng, B.; Liu, Z.; Liao, Z.; Zhong, Q.; Gu, L.; Wei, H.; Fang, X., Green tea polyphenols modulate colonic microbiota diversity and lipid metabolism in high-fat diet treated HFA mice. *Journal of food science* **2018,** *83* (3), 864-873.

58.	Jung, E. S.; Park, H. M.; Hyun, S. M.; Shon, J. C.; Singh, D.; Liu, K.-H.; Whon, T. W.; Bae, J.-W.; Hwang, J. S.; Lee, C. H., The green tea modulates large intestinal microbiome and exo/endogenous metabolome altered through chronic UVB-exposure. *PLoS One* **2017,** *12* (11), e0187154.

59.	Chen, T.; Yang, C. S., Biological fates of tea polyphenols and their interactions with microbiota in the gastrointestinal tract: implications on health effects. *Critical reviews in food science and nutrition* **2020,** *60* (16), 2691-2709.

60.	Zhang, X.; Chen, Y.; Zhu, J.; Zhang, M.; Ho, C. T.; Huang, Q.; Cao, J., Metagenomics Analysis of Gut Microbiota in a High Fat Diet–Induced Obesity Mouse Model Fed with (−)-Epigallocatechin 3-O-(3-O-Methyl) Gallate (EGCG3 ″Me). *Molecular nutrition & food research* **2018,** *62* (13), 1800274.

61.	Liao, Z.-L.; Zeng, B.-H.; Wang, W.; Li, G.-H.; Wu, F.; Wang, L.; Zhong, Q.-P.; Wei, H.; Fang, X., Impact of the consumption of tea polyphenols on early atherosclerotic lesion formation and intestinal Bifidobacteria in high-fat-fed ApoE−/− mice. *Frontiers in nutrition* **2016,** *3*, 42.

62.	Jin, J. S.; Touyama, M.; Hisada, T.; Benno, Y., Effects of green tea consumption on human fecal microbiota with special reference to Bifidobacterium species. *Microbiology and immunology* **2012,** *56* (11), 729-739.

63.	Yang, C. S.; Wang, H., Cancer preventive activities of tea catechins. *Molecules* **2016,** *21* (12), 1679.

64.	Cabrera, C.; Artacho, R.; Giménez, R., Beneficial effects of green tea—a review. *Journal of the American College of Nutrition* **2006,** *25* (2), 79-99.

65.	Khan, N.; Mukhtar, H., Tea polyphenols in promotion of human health. *Nutrients* **2019,** *11* (1), 39.

66.	Ju, J.; Hong, J.; Zhou, J.-n.; Pan, Z.; Bose, M.; Liao, J.; Yang, G.-y.; Liu, Y. Y.; Hou, Z.; Lin, Y., Inhibition of intestinal tumorigenesis in Apcmin/+ mice by (−)-epigallocatechin-3-gallate, the major catechin in green tea. *Cancer research* **2005,** *65* (22), 10623-10631.

67.	Xiao, H.; Hao, X.; Simi, B.; Ju, J.; Jiang, H.; Reddy, B. S.; Yang, C. S., Green tea polyphenols inhibit colorectal aberrant crypt foci (ACF) formation and prevent oncogenic changes in dysplastic ACF in azoxymethane-treated F344 rats. *Carcinogenesis* **2008,** *29* (1), 113-119.

68.	Toden, S.; Tran, H.-M.; Tovar-Camargo, O. A.; Okugawa, Y.; Goel, A., Epigallocatechin-3-gallate targets cancer stem-like cells and enhances 5-fluorouracil chemosensitivity in colorectal cancer. *Oncotarget* **2016,** *7* (13), 16158.

69.	Li, N.; Sun, Z.; Han, C.; Chen, J., The chemopreventive effects of tea on human oral precancerous mucosa lesions. *Proceedings of the Society for Experimental Biology and Medicine* **1999,** *220* (4), 218-224.

70.	Tsao, A. S.; Liu, D.; Martin, J.; Tang, X.-m.; Lee, J. J.; El-Naggar, A. K.; Wistuba, I.; Culotta, K. S.; Mao, L.; Gillenwater, A., Phase II randomized, placebo-controlled trial of green tea extract in patients with high-risk oral premalignant lesions. *Cancer prevention research* **2009,** *2* (11), 931-941.

71.   Bettuzzi, S.; Brausi, M.; Rizzi, F.; Castagnetti, G.; Peracchia, G.; Corti, A., Chemoprevention of human prostate cancer by oral administration of green tea catechins in volunteers with high-grade prostate intraepithelial neoplasia: a preliminary report from a one-year proof-of-principle study. *Cancer research* **2006,** *66* (2), 1234-1240.

72.   Kumar, N. B.; Pow-Sang, J.; Egan, K. M.; Spiess, P. E.; Dickinson, S.; Salup, R.; Helal, M.; McLarty, J.; Williams, C. R.; Schreiber, F., Randomized, placebo-controlled trial of green tea catechins for prostate cancer prevention. *Cancer Prevention Research* **2015,** *8* (10), 879-887.

73.   Thakur, V. S.; Gupta, K.; Gupta, S., Green tea polyphenols increase p53 transcriptional activity and acetylation by suppressing class I histone deacetylases. *International journal of oncology* **2012,** *41* (1), 353-361.

74.   Jin, L.; Li, C.; Xu, Y.; Wang, L.; Liu, J.; Wang, D.; Hong, C.; Jiang, Z.; Ma, Y.; Chen, Q., Epigallocatechin gallate promotes p53 accumulation and activity via the inhibition of MDM2-mediated p53 ubiquitination in human lung cancer cells. *Oncology reports* **2013,** *29* (5), 1983-1990.

75.   Brockschmidt, A.; Trost, D.; Peterziel, H.; Zimmermann, K.; Ehrler, M.; Grassmann, H.; Pfenning, P.-N.; Waha, A.; Wohlleber, D.; Brockschmidt, F. F., KIAA1797/FOCAD encodes a novel focal adhesion protein with tumour suppressor function in gliomas. *Brain* **2012,** *135* (4), 1027-1041.

76.   Di Lorenzo, A.; Curti, V.; C Tenore, G.; M Nabavi, S.; Daglia, M., Effects of tea and coffee consumption on cardiovascular diseases and relative risk factors: an update. *Current pharmaceutical design* **2017,** *23* (17), 2474-2487.

77.   Kuriyama, S.; Shimazu, T.; Ohmori, K.; Kikuchi, N.; Nakaya, N.; Nishino, Y.; Tsubono, Y.; Tsuji, I., Green tea consumption and mortality due to cardiovascular disease, cancer, and all causes in Japan: the Ohsaki study. *Jama* **2006,** *296* (10), 1255-1265.

78.   Cao, S.-Y.; Zhao, C.-N.; Gan, R.-Y.; Xu, X.-Y.; Wei, X.-L.; Corke, H.; Atanasov, A. G.; Li, H.-B., Effects and mechanisms of tea and its bioactive compounds for the prevention and treatment of cardiovascular diseases: An updated review. *Antioxidants* **2019,** *8* (6), 166.

79.   Li, Q.; Van de Wiele, T., Gut microbiota as a driver of the interindividual variability of cardiometabolic effects from tea polyphenols. *Critical Reviews in Food Science and Nutrition* **2021**, 1-27.

80.   Gao, X.; Cassidy, A.; Schwarzschild, M.; Rimm, E. B.; Ascherio, A., Habitual intake of dietary flavonoids and risk of Parkinson disease. *Neurology* **2012,** *78* (15), 1138-1145.

81.   Yang, L.; Jin, X.; Yan, J.; Jin, Y.; Yu, W.; Wu, H.; Xu, S., Prevalence of dementia, cognitive status and associated risk factors among elderly of Zhejiang province, China in 2014. *Age and ageing* **2016,** *45* (5), 708-712.

82.   Ide, K.; Matsuoka, N.; Yamada, H.; Furushima, D.; Kawakami, K., Effects of tea catechins on Alzheimer's disease: Recent updates and perspectives. *Molecules* **2018,** *23* (9), 2357.

83.   Pervin, M.; Unno, K.; Ohishi, T.; Tanabe, H.; Miyoshi, N.; Nakamura, Y., Beneficial effects of green tea catechins on neurodegenerative diseases. *Molecules* **2018,** *23* (6), 1297.

84.   Kaulmann, A.; Bohn, T., Bioactivity of polyphenols: preventive and adjuvant strategies toward reducing inflammatory bowel diseases—promises, perspectives, and pitfalls. *Oxidative medicine and cellular longevity* **2016,** *2016*.

85.   Huang, Y.; Xing, K.; Qiu, L.; Wu, Q.; Wei, H., Therapeutic implications of functional tea ingredients for ameliorating inflammatory bowel disease: a focused review. *Critical Reviews in Food Science and Nutrition* **2021**, 1-15.

86.   Yang, C. S.; Zhang, J.; Zhang, L.; Huang, J.; Wang, Y., Mechanisms of body weight reduction and metabolic syndrome alleviation by tea. *Molecular nutrition & food research* **2016,** *60* (1), 160-174.

87.   Suzuki, T.; Pervin, M.; Goto, S.; Isemura, M.; Nakamura, Y., Beneficial effects of tea and the green tea catechin epigallocatechin-3-gallate on obesity. *Molecules* **2016,** *21* (10), 1305.

Chapter 7

88.   Liu, Z.; Chen, Q.; Zhang, C.; Ni, L., Comparative study of the anti-obesity and gut microbiota modulation effects of green tea phenolics and their oxidation products in high-fat-induced obese mice. *Food Chemistry* **2022,** *367*, 130735.

89.   Kamal, D. A. M.; Salamt, N.; Zaid, S. S. M.; Mokhtar, M. H., Beneficial Effects of Green Tea Catechins on Female Reproductive Disorders: A Review. *Molecules* **2021,** *26* (9), 2675.

90.   Hayes, J. D.; Dinkova-Kostova, A. T., The Nrf2 regulatory network provides an interface between redox and intermediary metabolism. *Trends in biochemical sciences* **2014,** *39* (4), 199-218.

91.   He, F.; Ru, X.; Wen, T., NRF2, a transcription factor for stress response and beyond. *International journal of molecular sciences* **2020,** *21* (13), 4777.

92.   Ottaviani, J. I.; Fong, R.; Kimball, J.; Ensunsa, J. L.; Britten, A.; Lucarelli, D.; Luben, R.; Grace, P. B.; Mawson, D. H.; Tym, A., Evaluation at scale of microbiome-derived metabolites as biomarker of flavan-3-ol intake in epidemiological studies. *Scientific Reports* **2018,** *8* (1), 1-11.

93.   Dube, A.; Nicolazzo, J. A.; Larson, I., Chitosan nanoparticles enhance the plasma exposure of (−)-epigallocatechin gallate in mice through an enhancement in intestinal stability. *European Journal of Pharmaceutical Sciences* **2011,** *44* (3), 422-426.

94.   Liang, J.; Yan, H.; Puligundla, P.; Gao, X.; Zhou, Y.; Wan, X., Applications of chitosan nanoparticles to enhance absorption and bioavailability of tea polyphenols: A review. *Food Hydrocolloids* **2017,** *69*, 286-292.

95.   Shim, S.-M.; Yoo, S.-H.; Ra, C.-S.; Kim, Y.-K.; Chung, J.-O.; Lee, S.-J., Digestive stability and absorption of green tea polyphenols: Influence of acid and xylitol addition. *Food Research International* **2012,** *45* (1), 204-210.

96.   Chen, L.; Wang, W.; Zhang, J.; Cui, H.; Ni, D.; Jiang, H., Dual effects of ascorbic acid on the stability of EGCG by the oxidation product dehydroascorbic acid promoting the oxidation and inhibiting the hydrolysis pathway. *Food Chemistry* **2021,** *337*, 127639.

97.   Na, H.-K.; Surh, Y.-J., Modulation of Nrf2-mediated antioxidant and detoxifying enzyme induction by the green tea polyphenol EGCG. *Food and Chemical Toxicology* **2008,** *46* (4), 1271-1278.

98.   Liu, K.; Singer, E.; Cohn, W.; Micewicz, E. D.; McBride, W. H.; Whitelegge, J. P.; Loo, J. A., Time-Dependent Measurement of Nrf2-Regulated Antioxidant Response to Ionizing Radiation Toward Identifying Potential Protein Biomarkers for Acute Radiation Injury. *PROTEOMICS–Clinical Applications* **2019,** *13* (6), 1900035.

99.   Murray, D.; Mirzayans, R.; McBride, W. H., Defenses against pro-oxidant forces-Maintenance of cellular and genomic integrity and longevity. *Radiation research* **2018,** *190* (4), 331-349.

100.   Roowi, S.; Stalmach, A.; Mullen, W.; Lean, M. E.; Edwards, C. A.; Crozier, A., Green tea flavan-3-ols: colonic degradation and urinary excretion of catabolites by humans. *Journal of agricultural and food chemistry* **2010,** *58* (2), 1296-1304.

101.   Kohri, T.; Suzuki, M.; Nanjo, F., Identification of metabolites of (−)-epicatechin gallate and their metabolic fate in the rat. *Journal of agricultural and food chemistry* **2003,** *51* (18), 5561-5566.

102.   Urpi-Sarda, M.; Garrido, I.; Monagas, M.; Gomez-Cordoves, C.; Medina-Remon, A.; Andres-Lacueva, C.; Bartolome, B., Profile of Plasma and Urine Metabolites after the Intake of Almond [Prunus dulcis (Mill.) D.A. Webb] Polyphenols in Humans. *Journal of agricultural and food chemistry* **2009,** *57* (21), 10134-10142.

103.   González-Sarrías, A.; Espín, J. C.; Tomás-Barberán, F. A., Non-extractable polyphenols produce gut microbiota metabolites that persist in circulation and show anti-inflammatory and free radical-scavenging effects. *Trends in Food Science & Technology* **2017,** *69*, 281-288.

104.   Eison-Perchonok, M.; Downes, T., Kinetics of ascorbic acid autoxidation as a function of dissolved oxygen concentration and temperature. *Journal of Food Science* **1982,** *47* (3), 765-767.

105.   Eom, D.-W.; Lee, J. H.; Kim, Y.-J.; Hwang, G. S.; Kim, S.-N.; Kwak, J. H.; Cheon, G. J.; Kim, K. H.; Jang, H.-J.; Ham, J., Synergistic effect of curcumin on epigallocatechin gallate-induced anticancer action in PC3 prostate cancer cells. *BMB reports* **2015,** *48* (8), 461.

106.   Horie, N.; Hirabayashi, N.; Takahashi, Y.; Miyauchi, Y.; Taguchi, H.; Takeishi, K., Synergistic effect of green tea catechins on cell growth and apoptosis induction in gastric carcinoma cells. *Biological and Pharmaceutical Bulletin* **2005,** *28* (4), 574-579.

107.   Chow, H. S.; Cai, Y.; Alberts, D. S.; Hakim, I.; Dorr, R.; Shahi, F.; Crowell, J. A.; Yang, C. S.; Hara, Y., Phase I pharmacokinetic study of tea polyphenols following single-dose administration of epigallocatechin gallate and polyphenon E. *Cancer Epidemiology and Prevention Biomarkers* **2001,** *10* (1), 53-58.

108.   Naumovski, N.; Blades, B. L.; Roach, P. D., Food inhibits the oral bioavailability of the major green tea antioxidant epigallocatechin gallate in humans. *Antioxidants* **2015,** *4* (2), 373-393.

109.   Chow, H. S.; Cai, Y.; Hakim, I. A.; Crowell, J. A.; Shahi, F.; Brooks, C. A.; Dorr, R. T.; Hara, Y.; Alberts, D. S., Pharmacokinetics and safety of green tea polyphenols after multiple-dose administration of epigallocatechin gallate and polyphenon E in healthy individuals. *Clinical cancer research* **2003,** *9* (9), 3312-3319.

110.   Chow, H. S.; Hakim, I. A.; Vining, D. R.; Crowell, J. A.; Ranger-Moore, J.; Chew, W. M.; Celaya, C. A.; Rodney, S. R.; Hara, Y.; Alberts, D. S., Effects of dosing condition on the oral bioavailability of green tea catechins after single-dose administration of Polyphenon E in healthy individuals. *Clinical cancer research* **2005,** *11* (12), 4627-4633.

111.   van der Linden, S. C.; von Bergh, A. R.; van Vught-Lussenburg, B. M.; Jonker, L. R.; Teunis, M.; Krul, C. A.; van der Burg, B., Development of a panel of high-throughput reporter-gene assays to detect genotoxicity and oxidative stress. *Mutation Research/Genetic Toxicology and Environmental Mutagenesis* **2014,** *760*, 23-32.

112.   Monagas, M.; Urpi-Sarda, M.; Sánchez-Patán, F.; Llorach, R.; Garrido, I.; Gómez-Cordovés, C.; Andres-Lacueva, C.; Bartolomé, B., Insights into the metabolism and microbial biotransformation of dietary flavan-3-ols and the bioactivity of their metabolites. *Food & function* **2010,** *1* (3), 233-253.

113.   Lambert, J. D.; Sang, S.; Yang, C. S., Biotransformation of green tea polyphenols and the biological activities of those metabolites. *Molecular pharmaceutics* **2007,** *4* (6), 819-825.

114.   Narumi, K.; Sonoda, J.-I.; Shiotani, K.; Shigeru, M.; Shibata, M.; Kawachi, A.; Tomishige, E.; Sato, K.; Motoya, T., Simultaneous detection of green tea catechins and gallic acid in human serum after ingestion of green tea tablets using ion-pair high-performance liquid chromatography with electrochemical detection. *Journal of Chromatography B* **2014,** *945*, 147-153.

115.   Chu, K. O.; Pang, C. C., Pharmacokinetics and disposition of green tea catechins. *Pharmacokinetics and Adverse Effects of Drugs: Mechanisms and Risks Factors* **2018,** *17*.

116.   Reygaert, W. C., Green tea catechins: Their use in treating and preventing infectious diseases. *BioMed research international* **2018,** *2018*.

117.   Nakagawa, K.; Miyazawa, T., Absorption and distribution of tea catechin,(-)-epigallocatechin-3-gallate, in the rat. *Journal of nutritional science and vitaminology* **1997,** *43* (6), 679-684.

118.   Zhu, M.; Chen, Y.; Li, R. C., Oral absorption and bioavailability of tea catechins. *Planta medica* **2000,** *66* (05), 444-447.

119.   Shahrzad, S.; Aoyagi, K.; Winter, A.; Koyama, A.; Bitsch, I., Pharmacokinetics of gallic acid and its relative bioavailability from tea in healthy humans. *The Journal of Nutrition* **2001,** *131* (4), 1207-1210.

120.   van Duynhoven, J.; van der Hooft, J. J.; van Dorsten, F. A.; Peters, S.; Foltz, M.; Gomez-Roldan, V.; Vervoort, J.; de Vos, R. C.; Jacobs, D. M., Rapid and sustained systemic circulation of conjugated gut microbial catabolites after single-dose black tea extract consumption. *Journal of proteome research* **2014,** *13* (5), 2668-2678.

121.   van der Hooft, J. J.; de Vos, R. C.; Mihaleva, V.; Bino, R. J.; Ridder, L.; de Roo, N.; Jacobs, D. M.; van Duynhoven, J. P.; Vervoort, J., Structural elucidation and quantification of phenolic conjugates present in human urine after tea intake. *Analytical chemistry* **2012,** *84* (16), 7263-7271.

122.   Rogue, A.; Lambert, C.; Spire, C.; Claude, N.; Guillouzo, A., Interindividual variability in gene expression profiles in human hepatocytes and comparison with HepaRG cells. *Drug Metabolism and Disposition* **2012,** *40* (1), 151-158.

123.   Li, J.; Sapper, T. N.; Mah, E.; Rudraiah, S.; Schill, K. E.; Chitchumroonchokchai, C.; Moller, M. V.; McDonald, J. D.; Rohrer, P. R.; Manautou, J. E., Green tea extract provides extensive Nrf2-independent protection against lipid accumulation and NF$_\kappa$B pro-inflammatory responses during nonalcoholic steatohepatitis in mice fed a high-fat diet. *Molecular nutrition & food research* **2016,** *60* (4), 858-870.

124.   Sukhthankar, M.; Yamaguchi, K.; Lee, S. H.; McEntee, M. F.; Eling, T. E.; Hara, Y.; Baek, S. J., A green tea component suppresses posttranslational expression of basic fibroblast growth factor in colorectal cancer. *Gastroenterology* **2008,** *134* (7), 1972-1980.

8

Chapter 8

Summary

Summary

Green tea, which is mainly manufactured from buds and leaves of *Camellia sinensis*, is one of the most widely consumed beverages around the world. Catechins are the most abundant bioactive constituents in green teas, amounting up to 30% of the total dry weight. (-)-Epigallocatechin gallate (EGCG), (-)-epigallocatechin (EGC), (-)-epicatechin gallate (ECG) and (-)-epicatechin (EC) are the four major catechins among others. These catechins are believed to be responsible for various beneficial health effects that have been ascribed to green tea consumption. Though the modes of action underlying these health-promoting effects can be complicated and have not been fully understood, the Kelch-like ECH-associated protein 1/Nuclear factor E2-related factor 2 (Keap1/Nrf2) regulatory network has been reported to play a role. The aim of the present thesis was to obtain better insights into human intestinal microbiota-mediated conversion of model green tea catechins, including the intra- and inter-individual variability, and to characterise the consequences of this conversion for the potential activation of Nrf2-EpRE-mediated gene expression, all using new approach methodologies (NAMs).

Chapter 1 started with a brief introduction of the background and aims of the present thesis followed by an overview of the major green tea catechins. It then introduced the beneficial effects of green tea catechins focusing on the activation of the Keap1/Nrf2 signalling pathway. The structure of the Keap1/Nrf2 system was described and the potential consequences of its activation were also illustrated. Subsequently, the metabolism of green tea catechins was described, including especially the role of the colonic microbial metabolism, and the potential intra- and inter-individual variations in this metabolism. Furthermore, the proteomics technologies that were used in the present thesis were introduced. Finally, the chapter introduced the physiologically based kinetic (PBK) modelling and how to use it for reverse dosimetry in a NAM to translate *in vitro* concentration response curves into *in vivo* dose response curves.

In **Chapter 2**, the time-dependent microbial conversion of the green tea catechin EC was characterized using an *in vitro* anaerobic fecal incubation model. Moreover, the potential inter-individual differences in the human intestinal microbial metabolism of EC were studied using fecal inocula from 24 healthy donors. Results obtained show 1-(3',4'-dihydroxyphenyl)-3-(2'',4'',6''-trihydroxyphenyl)-2-propanol (3,4-diHPP-2-ol) and 5-(3',4'-dihydroxyphenyl)-γ-valerolactone (3,4-diHPV) to be key intermediate microbial metabolites of EC and also

revealed substantial interindividual differences in both the rate of EC conversion and the time-dependent EC metabolite pattern. Furthermore, quantitative microbiota characterization in the fecal samples, achieved by 16S rRNA, revealed substantial differences in microbiota composition among different individuals. Correlations between specific microbial phylotypes and formation of certain metabolites were established. It was concluded that interindividual differences in the intestinal microbial metabolism of EC may contribute to interindividual differences in potential health effects of EC-abundant dietary foods or drinks, including green tea.

In **Chapter 3**, anaerobic human fecal incubations were performed to characterize the microbial metabolism of the most abundant green tea catechin, EGCG, including inter-individual variability in the metabolic profiles. Results obtained showed the time-dependent formation of gallic acid (GA), pyrogallol (PG), phenylpropane-2-ols, phenyl-γ-valerolactones and 5-(3',5'-dihydroxyphenyl)valeric acid (3,5-diHPVA) as the major metabolites, with substantial interindividual differences. Spearman correlations between specific microbial genera types/phylotypes and formation of major metabolites were established. The activity of the formed colonic metabolites in the activation of Nrf2-EpRE-mediated gene expression was tested using the EpRE-LUX reporter gene assay. In contrast to EGCG, at low micromolar concentrations, especially GA, PG and catechol appeared able to induce significant activity in the EpRE-LUX assay. Given these results and taking the level of formation into account, this chapter concluded that especially GA and PG may contribute to the Nrf2-mediated beneficial effects of EGCG. The interindividual differences in the formation of these gut microbial metabolites may contribute to interindividual differences in the beneficial effects of EGCG and green tea consumption.

In **Chapter 4**, the intra- and inter-individual differences in the gut microbial metabolism of EC were characterized and compared by using anaerobic human fecal incubations. The Nrf2 signalling pathway activation by EC and its major colonic metabolite, 3,4-diHPV, was studied using the U2OS-Nrf2 CALUX reporter gene assay. Subsequently, the protein expression profiles of EC or 3,4-diHPV treated Caco-2 and Hepa1c1c7 cells were studied with the help of label-free proteomics. Bioinformatical analysis was carried out to interpret the biological consequences after exposure. Finally, RT-qPCR was performed to corroborate the results of the proteomics data. Results obtained show that both intra- and inter-individual differences exist in human gut microbial EC degradation and 3,4-diHPV formation, with inter-individual differences being more distinct than intra-individual differences. The metabolite, 3,4-diHPV,

showed higher potency in the U2OS-Nrf2 CALUX assay than EC itself. Among the obviously altered Nrf2-related proteins, 14 and 10 Nrf2-associated proteins were upregulated to a higher extent upon 3,4-diHPV treatment than in the EC treated group for Hepa1c1c7 and Caco-2 cells, respectively. While only three and four of these Nrf2-associated proteins were induced at a higher level upon EC than upon 3,4-diHPV treatment for Hepa1c1c7 and Caco-2 cells, respectively. RT-qPCR results showed that Nrf2-mediated genes (e.g., Nqo1 and Ugt1a) were only induced significantly in 3,4-diHPV treated and not in EC treated Hepa1c1c7 cells. Taken together, the results of this chapter suggest that the major colonic EC metabolite, 3,4-diHPV, was more capable of inducing Nrf2-mediated gene expression than its parent compound EC. This implies that the evident inter- and intra-individual differences in the microbial conversion of EC to this major metabolite 3,4-diHPV may affect the overall health-promoting effects of EC consumption related to the Nrf2 pathway activation.

In **Chapter 5**, the ability to activate the Nrf2-mediated gene expression was tested for EGCG, and its major colonic metabolites EGC, GA and PG using the U2OS-Nrf2 CALUX reporter gene assay, nanoLC-MSMS based label-free quantitative proteomics and RT-qPCR. The results obtained reveal that at micromolar concentrations PG displayed a more potent induction of the Nrf2 cascade than EGCG, which is in line with the results from Chapter 3 for EGCG. The downstream bioinformatical analysis of the proteomics data suggested that Nrf2 pathway activation by PG was related to intermediary metabolisms, including especially Glutathione metabolism, Drug and/or xenobiotics metabolism, and the Pentose phosphate pathway as the major pathways. Taken together, findings in this chapter demonstrate that the microbial metabolites of EGCG including especially PG may contribute to the Nrf2 signalling activation upon exposure to the parent compound EGCG or green tea.

In **Chapter 6**, a human PBK model was developed for EGCG, with sub-models for its major microbial metabolites GA and PG. The model enabled prediction of *in vivo* kinetics of EGCG, GA and PG which allowed the translation of the obtained *in vitro* concentration-response curves from the U2OS-Nrf2 CALUX reporter gene assay to *in vivo* dose-response curves for Nrf2 activation, and comparison of these data to estimated daily intake levels. Results obtained reveal, by comparison to literature data on EGCG kinetics, that the developed PBK model could adequately predict *in vivo* time-dependent blood concentrations of EGCG after either a single or repeated oral administration(s) of EGCG under both fasting and non-fasting conditions. The predicted *in vivo* dose response curve revealed that at daily intake levels of green tea or EGCG supplements, the resulting blood C_{max} of EGCG was in the sub-micromolar range,

concentrations at which Nrf2 activation was shown to be limited. Moreover, blood C_{max} values of GA and PG upon intake of EGCG were predicted to be less than 1.5% of the C_{max} of EGCG, indicating that in spite of their higher potential for Nrf2 activation, their contribution to the overall systemic Nrf2 pathway induction upon EGCG exposure is expected to be limited. In contrast, concentrations of these metabolites in the intestinal tract may reach levels that are, expressed in EGCG equivalents for Nrf2 induction, higher than that of EGCG, and also high enough to activate Nrf2 gene transcription. Taken together, combining *in vitro* data with a human PBK model allowed the prediction of a dose-response curve for EGCG induced Nrf2-mediated gene expression in humans, and provided insight into the contribution of gut microbial metabolites to this effect. It also provided a proof-of-principle for a NAM to study the *in vivo* effects of bioactive phytochemicals without the need for human intervention studies.

In **Chapter 7**, the main findings of the previous chapters were put together in an integrated discussion, and further recommendations/possibilities for future research were explored. It was concluded that the present thesis characterised the human gut microbial metabolic fates of the catechins EC and EGCG, including the inter- and/or intra-individual differences, and consequences of the gut microbial conversion for the potential activation of Nrf2-EpRE-mediated gene expression, all using NAMs. This work contributes to the implementation of the 3Rs (replacement, reduction and refinement) of experimental animal studies. The insights provided in the present thesis open a door for future studies on identification of catechin-converting gut microbiota, establishing metabotypes in humans regarding microbial degradation of green tea catechins and *in vivo* ADME of green tea catechins and their microbial metabolites focusing on target tissues where local effects may play an important role in the biological activity of the green tea catechins.

Annex

Acknowledgements

List of publications

Curriculum Vitae

Overview of completed training activities

Acknowledgements

There is a joke saying that only two days of the PhD journey are enjoyable. The first day is the day of getting accepted as a PhD candidate and the second day is the day of getting your doctoral degree. Apparently, it is joking about the constant challenging and pressure during the road of pursuing the doctoral degree. On the other hand, this journey is also full of excitements, joy, supports and achievements. I would like to express my sincere gratitude to all people who have helped and encouraged me during my PhD journey.

First and foremost, I would like to thank my promotor Prof. Dr. Ivonne Rietjens for your professional supervision. I could learn a lot of merits from you, such as how to be efficient, how to make good plans and how to critically think my issues, etc. Many memorable pictures pumping into my head. It still provides me a smile when I think of all the useful meetings with you to solve various problems we met in the project. You are a role model of what a brilliant researcher should act as in the scientific world. Your way of working in the academia makes me become determinant of how I should be in the future. Most importantly, I understand the importance of being proactive and devoted in doing research. I would also express my sincere gratitude to my co-promotor Pr. Dr. Jacques Vervoort for the help both in life and at work. You were always busy in the lab for helping with different students, including me. Thanks for the essential inputs in my project which definitely improved the quality of the current thesis. I am very grateful for your positive feedback and compliments whenever I made progress which were quite important as they did make me become more confident but also stimulate me to push my boundaries. Unfortunately, I cannot have your presence in my defense as your sudden decease in the summer of 2021. May you rest in peace and hope you can still enjoy a wonderful life in the other world.

I would like to extend my sincere thanks to the "Peop team" (Karsten, Bert, Katja, Qianrui, Diana and me). Although the fecal sample collection was quite tedious and sometimes smelly but now the memory is precious to me. We grew as friends more than merely colleagues in the end. Also, the valuable fecal samples enabled all of us to do our research in the following years.

My special thanks go all my co-authors during my PhD journey: Ivonne Rietjens, Jacques Veroort, Karsten Beekmann, Marta Baccaro, Lenny Kamelia, Sebas Wesseling, Joris van den Elzen, Laura de Haan, Sjef Boeren, Ignacio Miro Estruch, Jolijn van Mil and Annelies Noorlander. Especially thanks to Karsten for guiding me to the new filed when I joined TOX at the very beginning. Hope we will have another chance to cooperate in the future.

I would like to take the opportunity to thank all the staff at TOX: Hans, Nico, Nynke, Laura, Sebas, Wouter, Ignacio, Bert, Gerda, Carla and Lidy for creating a nice research environment. Thanks Hans for interviewing me and giving me the offer when I applied for the opportunity to study at TOX. Thanks Bert for interesting talks in the lab and also for the ordering of various chemicals for me. Although you retired two years ago but you still send me emails from time to time which makes happy and relaxed. I hope you can enjoy your life after retirement and have lots of happy moments with your family.

Thank you my friendly officemates Mengying, Annelies, Orsi, Yasser and Frances for creating such a lovely working vibe also many interesting conversations that were enjoyed among us. Special thanks to Annelies, you are such a kind person that makes me feel warm in heart. Thank you for the carpool, Christmas card, brainstorm, etc. Wish you can always follow your heart and do what you like. Many thanks also go to all the colleagues at TOX, Diego, Aziza, Mebrahtom, Artem, Shuo, Shensheng, Felicia, Isaac, Bohan, Miaoying, Biyao, Weija, Jing, Merel, Veronique, Edith, Maartje, Nina, Jingxuan, Yiming, Qiuhui, Jiaqi, Liang, Xiyu, Xukun, Hugo, Ixchel, Tessa, Ghalia, Shivani and Katharina, thanks for the good times, e.g., nice talks, coffee, parties, seminars and so on. To Miaoying, Shuo, Shensheng, Jingxuan and Jing, thanks for the suggestions which helped me to solve problems appeared when doing my project. To Menno, Biyao, Akanksha, Aafke, Qiong, Qian, Qi, Xiaofei and Chunzhe for the friendship. It was really enjoyable to hang out with you no matter if it was biking, drinking, training, playing basketball, or cooking, they all made me happy and relaxing. You made my personal life colourful during my PhD journey.

I would like also to express my gratitude to my MSc students, Kathy, Joris, Jolijn and Olaf who contributed to my project. It was rewarding to teach you to do the experiments, analysis, writing, etc. Working with you improved my educational ability and sometimes you may also provide wonderful idea which had a high value to the project. I hope all of you could make huge achievements in your career.

To my paranymphs, Akanksha and Aafke, thank you so much for the supports and helping with my defence. Akanksha, we started almost at the same time, and we shared joys and pains. It is good to talk with you both in the lab and gym. It was fun to "make fun" with each other. I hope you can also graduate soon and find a job you like. Aafke, we knew each other since the first day I came into the lab. At that moment, you were still a MSc student and we were doing similar cell assays. You are always a kind and polite person which sometimes make it difficult to relate you as a semi-professional soccer player. I wish you can enjoy playing soccer as long as you

want to. And I am sure you will manage your PhD life in the near future. Again, thank you both for being my paranymphs. I do appreciate.

Finally, my deepest gratitude goes to my family. As a student from a poor family, it was almost impossible to dream about studying abroad. Thanks to my greatest parents, you always give me enough freedom to do the things I need to do. You always support me even though it means endless hardworking and exhaustion to you. Without your sacrifices I could never achieve what I have today. I also would like to extend my greatest gratitude to my wife Pengyao, and my parents in law. Thanks for the tremendous understanding, trusting and supporting during my PhD pursuing. Also, thanks a lot for your meticulous care of my young boy Duoduo, I wish to go back to reunite with you soon.

List of publications

Chen Liu*, Jacques Vervoort, Karsten Beekmann, Marta Baccaro, Lenny Kamelia, Sebas Wesseling, Ivonne M. C. M. Rietjens (2020). Interindividual differences in human intestinal microbial conversion of (-)-epicatechin to bioactive phenolic compounds. *Journal of Agricultural and Food Chemistry.*

Chen Liu*, Jacques Vervoort, Joris van den Elzen, Karsten Beekmann, Marta Baccaro, Laura de Haan, Ivonne M. C. M. Rietjens (2021). Interindividual differences in human in vitro intestinal microbial conversion of green tea (-)-epigallocatechin-3-O-gallate and consequences for activation of Nrf2 mediated gene expression. *Molecular Nutrition and Food Research*.

Chen Liu*, Sjef Boeren, Ignacio Miro Estruch, Ivonne M.C.M. Rietjens. The gut microbial metabolite pyrogallol is a more potent regulator of Nrf2-associated gene expression than its parent compound green tea (-)-epigallocatechin gallate in in vitro cell models *Under review*.

Chen Liu*, Sjef Boeren, Ivonne M.C.M. Rietjens. Intra- and inter-individual differences in human intestinal microbial conversion of (-)-epicatechin and bioactivity of its major colonic metabolite 5-(3',4'-dihydroxyphenyl)-γ-valerolactone in regulating Nrf2-mediated gene expression. *Under review*.

Chen Liu*, Jolijn van Mil, Annelies Noorlander, Ivonne M.C.M. Rietjens. Use of physiologically based kinetic modeling-based reverse dosimetry to predict in vivo Nrf2 pathway activation by EGCG and its colonic metabolites in humans. *To be submitted*.

Chen Liu*, Ivonne M.C.M. Rietjens. Effects and mechanisms of tea catechins and their gut microbial metabolites in cancer. *In preparation*.

Curriculum Vitae

Chen Liu was born on 20th November 1991 in Ma Anshan city, Anhui Province, China. He studied Forest Resources Conservation & Recreation at Northwest A&F University. After obtaining his BSc degree in 2015, Chen Liu continued his MSc study in Agricultural Entomology and Pest Control at the Institute of Plant Protection, Chinese Academy of Agricultural Sciences with focus on Insect Toxicology. After receiving his MSc degree in 2018, Chen Liu decided to move to the Netherlands to do his PhD research at the Division of Toxicology at Wageningen University and Research with the financial support from Chinese Scholarship Council. During the PhD study, he was supervised by Prof. dr. ir. Ivonne Rietjens and Prof. dr. ir. Jacques Vervoort to do investigations on the project titled "Influence of human intestinal microbial metabolism on the biological activity of green tea catechins". The results of the research program are presented in this dissertation. During his PhD, he followed a postgraduate education in Toxicology (PET) as part of the training required for the registration as European Toxicologist.

Overview of completed training activities

Discipline specific activities

Molecular Toxicology	PET	2019
Laboratory Animal Science	PET	2019
Organ Toxicology	PET	2020
Pathobiology	PET	2020
Epidemiology	PET	2021
Immunotoxicology	PET	2021
Toxicogenomics	PET	2021

Conferences

14th World Congress on Polyphenols Applications, poster, online, 2021

61st Annual Meeting and ToxExpo, poster, San Diego and online, 2022

General courses

VLAG PhD week	VLAG	2019
Philosophy and Ethics of Food Science and Technology	WGS	2019
Risk Assessment	PET	2019
Critical thinking and argumentation	WGS	2020
Big Data Analysis in the Life Sciences	VLAG	2021
Scientific Publishing	WGS	2021

Other activities

Preparation Research proposal	TOX	2018
Environmental toxicology	TOX	2020
Food Toxicology	TOX	2020
General Toxicology	TOX	2021
Scientific presentations	TOX	2018 – 2022

Approved by VLAG graduate school

茶